Analysis of the roles of *Pax6* in development of the cerebral cortex

Helen Pearson

Ph.D.
The University of Edinburgh
1999

Declaration

I declare that this thesis has been composed by myself and that all the work is my own unless otherwise stated.

Helen Pearson

October 1999

'The *mu* answer is an important one.'

Robert M. Pirsig
Zen and the Art of Motorcycle Maintenance

Acknowledgements

First, thankyou to my various supervisors:
Veronica van Heyningen for support, David Price for guidance and especially Penny Rashbass for eccentricity and everything else.

Second, I would like to acknowledgement and thank the other people who contributed to the work in this thesis: Julie Moss for a valuable lab apprenticeship, Paul Perry for imaging, Andrew Carothers and Peter Teague for statistics, Natasha Warren for DiI labelling, Judy Fletcher for *in situs*, Stewart McKay for sequencing, Isabel Hanson for sequence analysis, Allyson Ross for all wax sectioning, Sandy Bruce for help with thesis figures, and Paul and Shelagh for tea.

Outside science, thankyou to Rent-A-Crowd for dancing, Tania and Dom for good times in St Alban's Rd, Nyla for long haul destinations and Peter for distraction.

Table of Contents

List of figures

List of tables

Abstract

The mammalian cerebral cortex develops from the dorsal telencephalon, an expansion of the anterior neural tube. During embryonic development, cortical neurons are generated by dividing progenitors in the inner cortical wall (ventricular zone, VZ) and migrate outwards to settle and differentiate in the cortical plate. The transcription factor *Pax6* is essential in development of the eye and regions of the CNS including the cortex. *Pax6* is highly expressed in the cortical VZ and in *Pax6* null mice (*Sey* homozygotes) late-born cortical neurons are unable to complete their migration, instead accumulating to create an expanded VZ.

Here, cellular and molecular techniques were employed to elucidate the function of *Pax6* in cortical development. It has been proposed that cell division within the VZ may be either symmetric, generating two progenitor cells, or asymmetric, generating a progenitor and a migratory neuron. An analysis of progenitor cleavage orientation revealed an increase in asymmetric division in the *Sey/Sey* cortex. In addition, interkinetic nuclear migration during the cell cycle is disrupted. I propose that these defects are most consistent with a role for *Pax6* in regulating progression through the cell cycle.

DiI labelling revealed a complete absence of innervation from thalamus to cortex in the *Sey* homozygote which may play a role in the cortical phenotype. To address this possibility an explant system was established to study cortical migration *in vitro*. The analysis showed that neurons migrating from the mutant cortex show a tendency to clump together indicative of alterations in their adhesive properties. These defects are not rescued by co-culture with wildtype diencephalon, suggesting that the absence of thalamocortical innervation does not contribute to the *Sey/Sey* cortical phenotype *in vivo*.

On the basis of these findings combined with others, I hypothesise that the loss of *Pax6* function results in increased proliferation and altered neuronal adhesion. These abnormalities account for the gradual accumulation of neurons in the *Sey/Sey* VZ during later cortical development.

In order to identify molecular differences between wildtype and *Sey/Sey* underlying these defects, candidate and differential gene expression analyses were performed. The former revealed altered expression patterns of putative cell fate determination molecules Numb and Prox1 and cell adhesion molecules L1 and TAG1. The latter involved construction and

analysis of a subtracted telencephalon cDNA library from which two molecules were identified which mediate protein interactions in transcriptional complexes. Expression of these genes is absent from the *Sey/Sey* cortex and thus they represent exciting candidate genes acting downstream of *Pax6*.

Abbreviations

+/+	wildtype
-/-	*Small eye* homozygote
A	anterior
AA	amygdaloid area
ACX	archicortex
AEP	anterior entopeduncular area
AH	anterior hypothalamus
ap	alar plate
at	amygdaloid tracts
BCIP	5-Bromo-4-chloro-3-indolyl phosphate
bp	basal plate
BrdU	bromodeoxyuridine
BSA	bovine serum albumin
C	caudal
C-terminal	carboxy-terminal
Cb	cerebellum
C.elegans	*Caenorhabitis elegans*
cDNA	complementary deoxyribonucleic acid
CGE	caudal ganglionic eminence
CO_2	carbon dioxide
CP	cortical plate
cpe	cerebral peduncle
CRTX or Ctx	cortex
D	dorsal
DAPI	4,6-diamidino-2-phenylindole
dATP	deoxyadenosine triphosphate
DB	diagonal band
dCTP	deoxycytosine triphosphate
dGTP	deoxyguanosine triphosphate
DIG	digoxigenin
DiI	1,1′-dioctadecyl-3,3,3′,3′-tetramethylindo-carbocyanin perchlorate
dH_2O	distilled water
di	diencephalon
DNA	deoxyribonucleic acid
dNTPs	deoxynucleotide triphosphates
DT	dorsal thalamus
dTTP	deoxythymine triphosphate
dUTP	doeoxyuridine triphophosphate
E	embryonic day
ECM	extracellular matrix
E. coli	*Escherischia coli*
EDTA	ethylenediamine tetra-acetic acid disodium salt
EMT	eminentia thalami
EST	expressed sequence tag
ET	epithalamus
fp	floor plate
GMC	ganglion mother cell
HCC	hypothalamic cell cord
HCl	hydrocloric acid
IPTG	isopropylthio-β-D- galactosidase
is	isthmus
IZ	intermediate zone
kb	kilobase
KCl	potassium chloride
LGE	lateral ganglionic eminence
LiCl	lithium chloride
LIM	limbic system
m or me	mesencephalon
M	molar
MA	mammilary area
ma	mammilary hypothalamus
$MgCl_2$	magnesium chloride
MGE	medial ganglionic eminence
$MgSO_4$	magnesium sulphate
MRC	Medical Research Council
mRNA	messenger ribonucleic acid
MZ	marginal zone
NCX	neocortex
N-terminal	amino-terminal
NaAc	sodium acetate
NaCl	sodium chloride
NaH_2PO_4	sodium dihydrogen orthophosphate
Na_2HPO_4	di-sodium hydrogen orthophosphate
NaOH	sodium hydroxide
NB	neuroblast
NBT	4-Nitro blue tetrazolium chloride
NH_4OAc	ammonium acetate
np	nasal placode
nr	neural retina
OB	olfactory bulb
oc	optic cup
OD	optical density
ov	optic vesicle

p	prosomere
P	posterior
PALL	pallidum
PBS	phosphate buffered saline
PCR	polymerase chain reaction
pe	pigemented retinal epithelium
ped	peduncular area of the hypothalamus
PEG	polyethylene glycol
PEP	posterior entopeduncular area
PFA	paraformaldehyde
Pfu	plaque forming units
po	preoptic area
POA	anterior preoptic area
POP	posterior preoptic area
PPL	preplate layer
PT	pretectum
r	rhombomere
R	rostral
RCH	retrochiasmatic area
rh	rhombencephalon
RNA	ribonucleic acid
rp	roof plate
rpm	revolutions per minute
sc	spinal cord
SCH	suprachiasmatic area
sm	stria medullaris
SDS	sodium dodecyl sulphate
SE or SEPT	septum
Sey	*Small eye*
SP	subplate
spv	supraoptic paraventricular area
ssDNA	single stranded deoyribonucleic acid
STR or St	striatum
SVZ	subventricular zone
TCA	thalamocortical axon
TE	Tris:EDTA
TESPA	3-aminuteopropyl-triethoxysilane
tpoc	tract of the postoptic commissure
tRNA	transfer ribonucleic acid
tu	tuberal hypothalamus
UV	ultraviolet
V	ventral
VDi	ventral diencephalon
VT	ventral thalamus
VTel	ventral telencephalon
VZ	ventricular zone
X-gal	5-Bromo-4-Chloro-3-Indolyl β-D-Galactopyranoside
Zl	zona limitans intrathalamica

All units are standard international (SI) units.

CHAPTER 1

Introduction

The transcription factor *Pax6* first became prominent due to its key role in the developing eye. *Pax6* genes from various organisms are able to induce ectopic eye formation in *Drosophila* (reviewed in Gehring & Ikeo, 1999), leading to the proposal that *Pax6* is a master control gene for eye development. However, *Pax6* is also expressed in the developing central nervous system and in organisms which do not possess eyes. Moreover, absence of *Pax6* function in humans and mice results in severe brain abnormalities as well as arrested eye development (Glaser *et al.*, 1994; Schmahl *et al.*, 1993; Stoykova *et al.*, 1996), suggesting that the gene is widely required for nervous system development. This thesis examines the role of *Pax6* in development of the cerebral neocortex. In order to put this in context I will first describe the process of mammalian cortical development, followed by a summary of the *Pax6* gene with particular emphasis on its putative roles in the developing eye and nervous system. In view of this I propose several hypotheses of how *Pax6* may function in cortical development, which are addressed by the experiments in my thesis.

1.1 Cortical development

The mammalian cerebral cortex develops from the dorsal telencephalon, an expansion of the anterior neural tube. The cerebral cortex consists of the paleocortex, archicortex and neocortex. The phylogenetically old paleocortex and archicortex comprise the olfactory areas and the limbic system (including the hippocampus) respectively. The neocortex, which comprises the vast majority of the mammalian cerebral cortex (90% in humans), is the subject of this thesis and shall herein be referred to as the 'cortex'.

The adult cortex is composed of six radial layers of neurons, each defined by cellular morphology, cell density and the formation of distinct axonal connections (Fig. 1.1A). It is also organised into domains along a dimension tangential to its surface. These form connections with other parts of the central nervous system, including midbrain, hindbrain and thalamic nuclei and serve different functions, for example in sensory processing and motor control (Fig 1.1B). In humans the cortex also performs higher mental processes such as thought and memory.

1.1.1 Specification of the telencephalon and cortex

The vertebrate central nervous system (CNS) arises from the neural plate, a sheet of epithelial cells which forms in the midline ectoderm on the dorsal surface of the mouse embryo at E8.0 (Fig1.2A,B). The neural plate rolls up along its rostrocaudal axis to form the

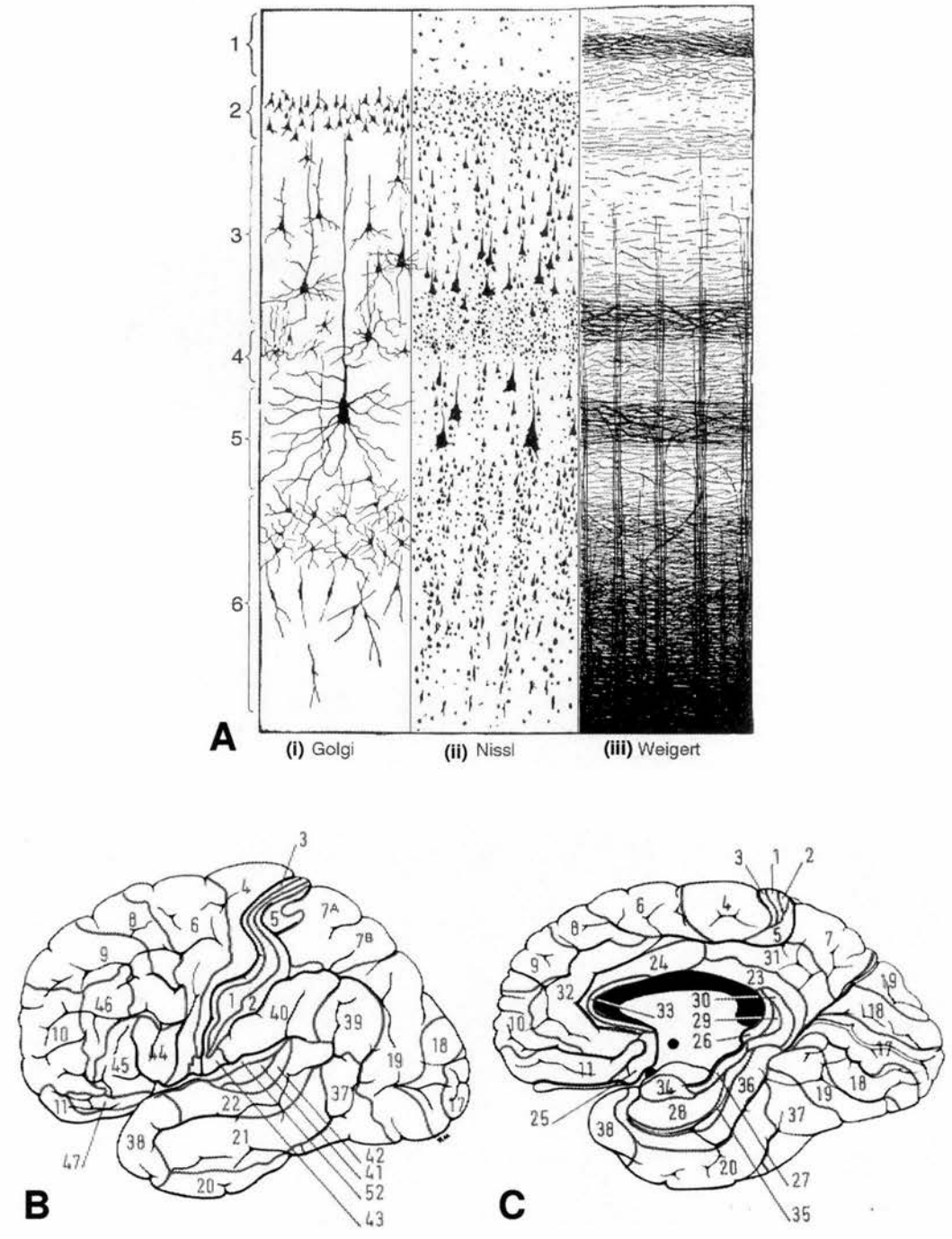

Figure 1.1 Structure of the adult human cortex

A. Histological sections through the adult cerebral neocortex using different staining techniques to demonstrate the differences in the 6 layers:

(i) Golgi stain: identifies a subset of neurons and their processes;

(ii) Nissl technique: identifies nucelic acids and distinguishes individual cell bodies;

(iii) Weigert technique: stains myelin sheaths.

1. Molecular layer; 2. External granular layer; 3. External pyramidal layer; 4. Internal granular layer; 5. Internal pyramidal layer; 6. Multiform layer.

B,C. The lateral (B) and medial (C) surfaces of the human cerebral cortex showing cytoarchitectural areas defined by Brodmann (1909); different areas are associated with different functions in sensory processing, motor control, language and spatial awareness (from Williams, 1995).

neural tube in a process known as neurulation (Fig. 1.2C). The caudal part of the neural tube will form the spinal cord, whilst the rostral portion will both expand and flex to form the early brain compartments.

The earliest gross morphological division of the developing brain along the rostrocaudal axis is apparent as a series of bulges in the rostral neural plate, which, on neural tube closure, are identifiable as three vesicles: the prosencephalon (forebrain), mesencephalon (midbrain) and rhombencephalon (hindbrain) (Fig. 1.3A). Subsequent subdivisions divide the forebrain into the telencephalon and diencephalon and the hindbrain into metencephalon and myelencephalon (Fig. 1.3B). The dorsal telencephalon ultimately gives rise to the cerebral cortex, and ventral telencephalon to the striatum, pallidum and septum (Fig. 1.3C).

Specification of cortical tissue therefore requires patterning on several levels:

- dorsoventrally (DV) to specify dorsal from ventral forebrain;
- anteroposteriorly (AP, or rostrocaudally) to define telencephalon from diencephalon;
- locally to specify subdivisions of the telencephalon.

The molecular mechanisms leading to the establishment of these regions are beginning to be elucidated. It has been established that the expression patterns of certain genes in the developing forebrain correlate with specific morphological and anatomical boundaries, and that these molecules may play important roles in defining region-specific identity (reviewed by Rubenstein & Shimamura, 1997; Fishell, 1997; Rubenstein & Beachy, 1998).

Along the dorsoventral axis (corresponding to the lateral-medial axis of the neural plate), the secreted molecules Sonic hedgehog (Shh) and bone morphogenetic proteins (BMPs) play key roles in early patterning (Fig. 1.4 and Table 1.1; Shimamura & Rubenstein, 1997; Dale *et al.*, 1997; Furuta *et al.*, 1997). *Shh* is expressed throughout the AP axial tissue beneath the neural plate - in the mesodermally derived notochord posteriorly and in the prechordal plate anteriorly (Echelard *et al.*, 1993; Shimamura & Rubenstein, 1997). In posterior regions of the neural tube (the presumptive spinal cord, hind- and mid-brain), Shh, secreted from the notochord, induces the neural ventral midline cells to differentiate into floorplate cells (Roelink *et al.*, 1994; Roelink *et al.*, 1995; Ericson *et al.*, 1996). The floorplate cells then also secrete Shh which is required to induce ventral neuronal fates (Tanabe & Jessell, 1996). *BMP*s expressed in the dorsal neural tube are able to induce dorsal neuronal fates (Liem *et al.*, 1995).

Anterior neural tube cells that overlie the prechordal plate express different cell markers compared with the posterior regions of the spinal cord and hindbrain. However, it appears

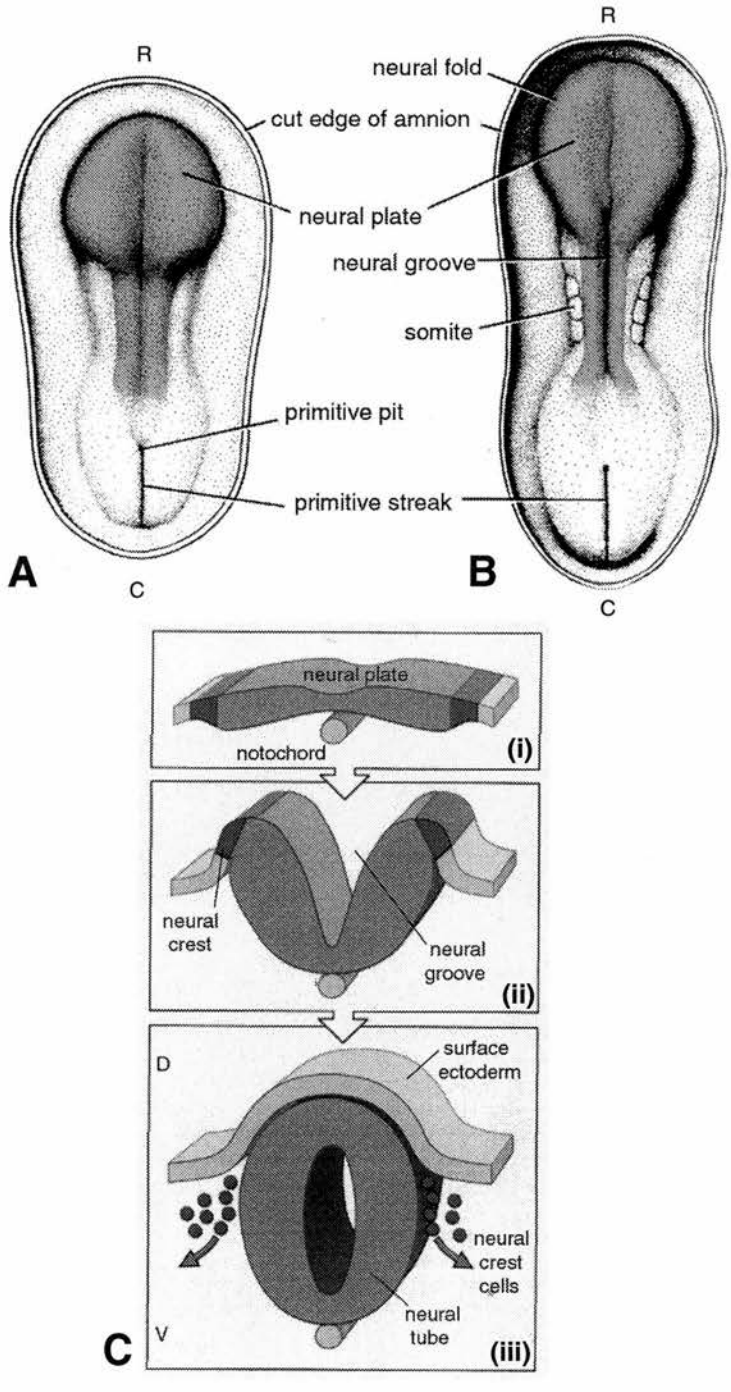

Figure 1.2 Vertebrate neurulation

A. Dorsal view of a neural plate stage embryo (corresponding to mouse E8.0).

B. Dorsal view of a 3 somite embryo (corresponding to mouse E8.25) showing the neural plate starting to roll up in the region overlying the first somites to form the neural tube. Closure of the neural tube proceeds from this point both rostrally (R) and caudally (C).

C. Transverse sections showing different stages of neural tube formation:

(i) The neural plate (corresponding to mouse E8.0) is a thickening of the surface ectodermin the midline over the notochord;

(ii) The neural plate rolls up over the first formed somites (corresponding to mouse E8.25-E8.5);

(iii) Aposition of the neural folds to form the neural tube. Neural crest cells of ectodermal origin migrate to the dorsolateral aspect of the neural tube where they give rise to the ganglia of the spinal and cranial nerves.

C, caudal; R, rostral; D, dorsal;V, ventral (from Sadler, 1985 and Wolpert *et al.*,1998)

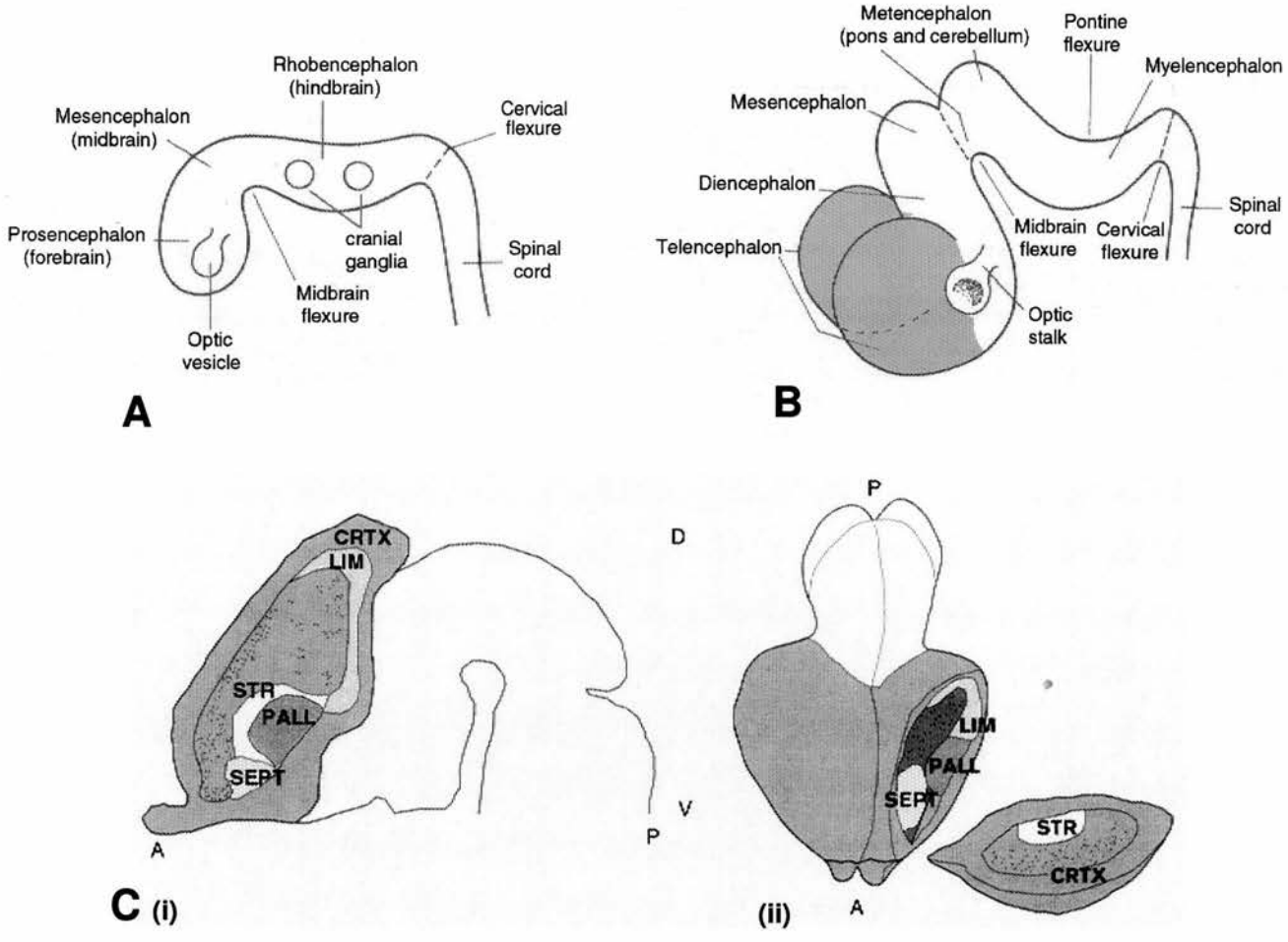

Figure 1.3 Schematic showing gross morphological development of the developing vertebrate brain

A. Lateral view of a vertebrate embryo corresponding to E9.5 in mouse. Soon after closure of the rostral neural tube, the lumen in the region of the future brain starts to dilate, particularly in the prosencephalon (future forebrain). Two folds become evident, the midbrain flexure between the primitive mesencephalon (midbrain) and rhombencephalon (hindbrain) and the cervical flexure at the juction between the primitive rhombencephalon and the rostral part of the future spinal cord. The optic vesicles grow out from the diencephalic region of the forebrain; two cranial neural crest aggregations associated with the rhombencephalon form the pre-ganglia of the cranial nerves.

B. Lateral view of a vertebrate embryo correspnding to E11.0 in mouse. The primitive forebrain is now partitioned into the telencephalon (shaded grey) and diencephalon. The telencephalon gives rise to the telencephalic vesicles and its component structures shown in (C) and the diencephalon to the remainder of the forebrain including the thalamus (see figure 1.5). The mesencephalon differentiates into the midbrain. The hindbrain is indented by the pontine flexure and is partitioned into the metencephalalon, which will form the cerebellum (dorsally) and pons (ventrally), and the myelencephalon which differentiates into the medulla oblongata.

C. Sagittal view (i) and dorsal perspective (ii) of an E15.5 mouse brain showing major structures of the telencephalon (shaded). (ii) shows a region of the telencephalon cut away to reveal the underlying organisation. The dorsal telencephalon gives rise to the cerebral cortex (CRTX) and limbic system(LIM), which includes the archicortex. The ventral telencephalon gives rise to subcortical regions: striatum (STR), pallidum (PALL) and septum (SEPT). The striatum and pallidum are generally referred to as the lateral and medial ganglionic eminences (LGE and MGE) respectively.

A, anterior; P, posterior; D, dorsal; V, ventral (from Kaufmann & Bard, 1999 (A,B) and Fishell, 1997 (C,D))

that the same signals are important to specify these cells (Barth & Wilson, 1995; Ericson *et al.*, 1995; Dale *et al.*, 1997). Thus, anterior to the mid-diencephalon, *BMP7* is coexpressed with *Shh* in the axial prechordal plate and the two proteins act coordinately to induce anterior ventral midline cells (Fig. 1.4 and Table 1.1; Dale *et al.*, 1997;). BMP-7 appears to lower the response threshold of neural tissue explants to Shh signaling, such that low levels of Shh, which normally induce differentiation of posterior floor plate, instead induce anterior neuronal fates defined by the expression of *Nkx2.1* (Dale *et al.*, 1997). BMPs are also implicated in regulating dorsal fate specification in the anterior neural tube. *BMP*s are expressed in the anterior non-neural ectoderm flanking the neural plate and in the roof of the forebrain and BMP-2, -4 and -7 can induce expression of the dorsal midline marker *Msx1* in neural plate explants (Fig. 1.4; Shimamura & Rubenstein, 1997; Furuta *et al.*, 1997).

Along the anteroposterior axis, fibroblast growth factor-8 (Fgf8) produced from the anterior neural ridge is important in early patterning (Shimamura & Rubenstein, 1997); Fgf8 applied to neural plate tissue which has not yet been specified induces expression of the transcription factor *Brain factor*-1 (*BF1*), a marker of early telencephalic tissue. Together, these early signaling molecules act to regulate the expression of specific transcription factors involved in locally specifying AP subdivisions of the telencephalon (Ericson *et al.*, 1995; Kohtz *et al.*, 1998; Shimamura & Rubenstein, 1997; Ye *et al.*, 1998). These include *BF1*, members of the *Dlx, Emx, Otx, Nkx* and *Pax* homeobox gene families and the zinc finger transcription factor *Gli3*. All have specific temporal and regional expression patterns in the prospective telencephalon and mice mutant for these genes exhibit specific defects of telencephalic patterning - these are summarised in Table 1.1 and Figure 1.5 (and reviewed by Fishell, 1997; Rubenstein & Shimamura, 1997). However, it remains to be established exactly what role each of these genes is playing on a cellular level: for example, whether they are required to regulate cell proliferation or to specify cell fate.

The combination of morphological and expression boundaries have been used to propose prosomeric models of forebrain organisation. These postulate that the forebrain is subdivided into a grid-like pattern of neuromeric domains by longitudinal (AP) and transverse (DV) boundaries (Fig. 1.5; Bulfone, *et al.*, 1993; Figdor & Stern, 1993; Puelles & Rubenstein,1993; Rubenstein *et al.*, 1994; Shimamura *et al.*, 1995; Shimamura *et al.*, 1997 and reviewed by Rubenstein & Shimamura, 1997). In the prosomeric model the dorsal domains of the most anterior prosomeres (p3-p6) are postulated to give rise to the telencephalon (Fig. 1.5).

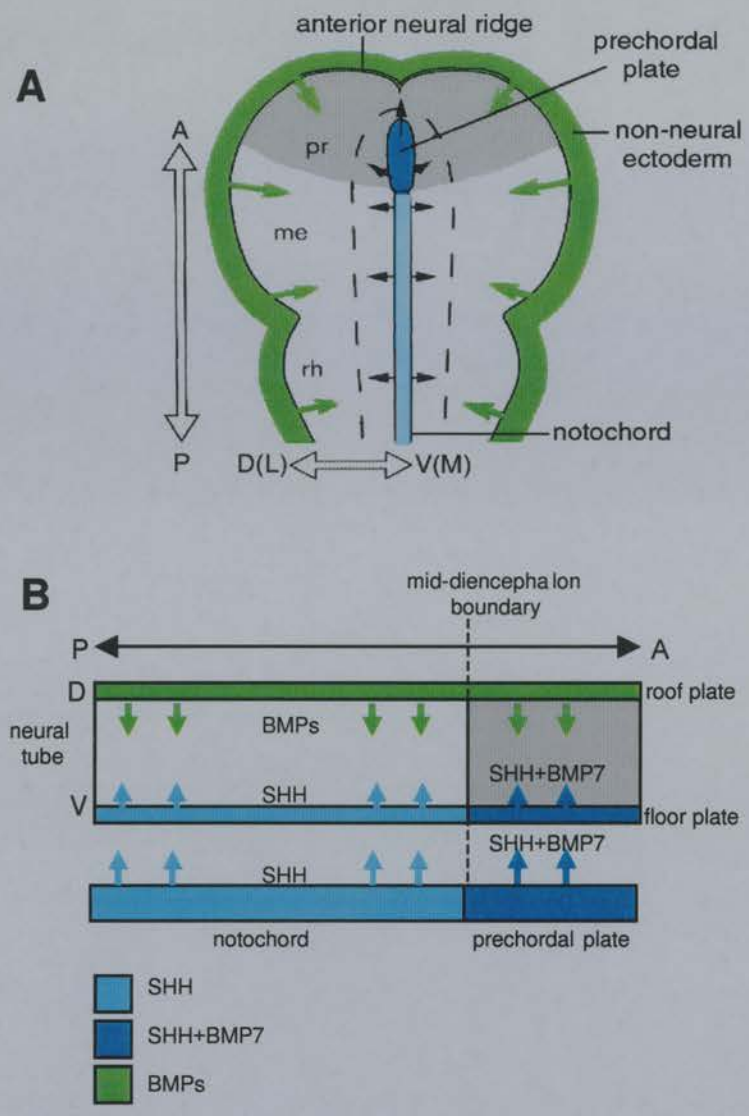

Figure 1.4 Schematic showing the different tissues and molecules thought to pattern the vertebrate neural plate and neural tube.

A. Dorsal view of the anterior part of the neural plate. Shh emanates from the prechordal plate beneath the prosencephalon primordium (pr) and the notochord under the mesencephalon (me) and rhombencephalon (rh) primordia. *BMPs* are expressed in the non-neural ectoderm around the neural plate. A model for their action in neural tube patterning is described below.

B. Sagittal section through the midline of the anterior part of the neural tube. Shh and BMPs specify cells along the dorsoventral (DV) axis of the neural tube. Posterior to the mid-diencephalon, notochord-derived Shh signals differentiation of ventral midline floorplate cells in the overlying neural tube. Anterior to the mid-diencephalon, *BMP7* is co-expressed with *Shh* in the prechordal plate and acts coordinately with Shh to induce anterior ventral midline cells. Anterior ventral midline cells also express *Shh* and *BMP7*; it is not known if this expression is necessary for subsequent neural tube patterning in this anterior domain. Dorsally, *BMPs* expressed in the non-neural ectoderm and later in the dorsal neural tube induce dorsal neuronal fates.

A, anterior; P, posterior; D(L), dorsal (lateral); V(M), ventral (medial); me, mesencephalon primordium; pr, prosencephalon primordium; rh, rhombencephalon primordium [adapted from Rubenstein & Beachy, 1998 (A) and Dale *et al.*, 1997 (B)].

Figure 1.5 Schemata showing gene expression patterns and theoretical organisation of the mouse forebrain

A,B. Schemata showing gene expression patterns of *BF1, Pax6, Nkx2.1, Nkx2.2, Otx1, Emx1* and *Dlx2* in the E10.5 mouse brain. Expression patterns are mapped on the E10.5 neuromeric model of forebrain patterning (Bulfone *et al.*, 1993; Puelles & Rubenstein, 1993; Rubenstein *et al.*, 1994). In this model the forebrain is proposed to be divided into six transverse neuromeric regions (prosomeres, p), similar to division of the hindbrain into rhombomeres (r). Transverse boundaries are indicated by slashed lines. The *BF1* positive domain in the dorsal regions of p3-p6 and marks the presumptive telencephalon. Within this region, the anterior expression boundary of *Otx1* and *Pax6* corresponds to the boundary between the future cortical (p3/4) and subcortical (p5/6) domains of the telencephalon (Rubenstein & Shimamura,1997). The derivative structures of these domains are shown in (C). Gene expression boundaries of *Nkx2.2* (and *Shh* which is also expressed in the basal plate of the mesencephalon (me), p1 and p2 but is omitted for simplicity) suggest the forebrain is also organised into longitudinal domains: floor plate (fp), basal plate (bp), alar plate (ap) and roof plate (rp) (Shimamura *et al.*, 1995).

C. Schema of the E12.5 mouse brain showing longitudinal and transverse subdivisions adapted from neuromeric models of forebrain patterning. The forebrain structures derived from the theoretical prosomeres are labelled.
Prosomeres p1, p2 and ventral p3-p6 form the diencephalon (pale purple): p1, p2 and ventral p3 give rise to the pretectum, dorsal thalamus and ventral thalamus respectively. Ventral p4, p5 and p6 give rise to ventral regions of the diencephalon including hypothalamic areas (po, ped, spv, tu, ma) and optic stalk. Dorsal p3-p6 form the telencephalon (dark purple). p3/4 give rise to the cortex which is divided into the neocortex, archicortex (including the hippocampus) and paleocortex (olfactory bulb and olfactory cortex). p5/6 give rise to the subcortical areas: the striatum (lateral ganglionic eminence, LGE) and the pallidum (medial ganglionic eminence , MGE).
Rhombomeres (r) r1-7 form the rhomebencephalon (hindbrain). The isthumus (is) is a specialised region between the rhombencephalon and mesencephalon (m, midbrain) that is a source of signals involved in midbrain/hindbrain patterning.

Abbreviations: ap, alar plate; bp, basal plate; fp, floor plate; is, isthmus; LGE, lateral ganglionic eminence; m or me, mesencephalon; ma, mammilary hypothalamus; MGE, medial ganglionic eminence; p1-p6, prosomeres; ped, peduncular area of the hypothalamus including the anterior hypothalamus; po, preoptic area; r1-r7, rhombomeres; rp, roof plate; spv, supraoptic paraventricular area; tu, tuberal hypothalamus; zl, zona limitans intrathalamica separating ventral and dorsal thalamus (adapted from Rubenstein & Shimamura, 1997).

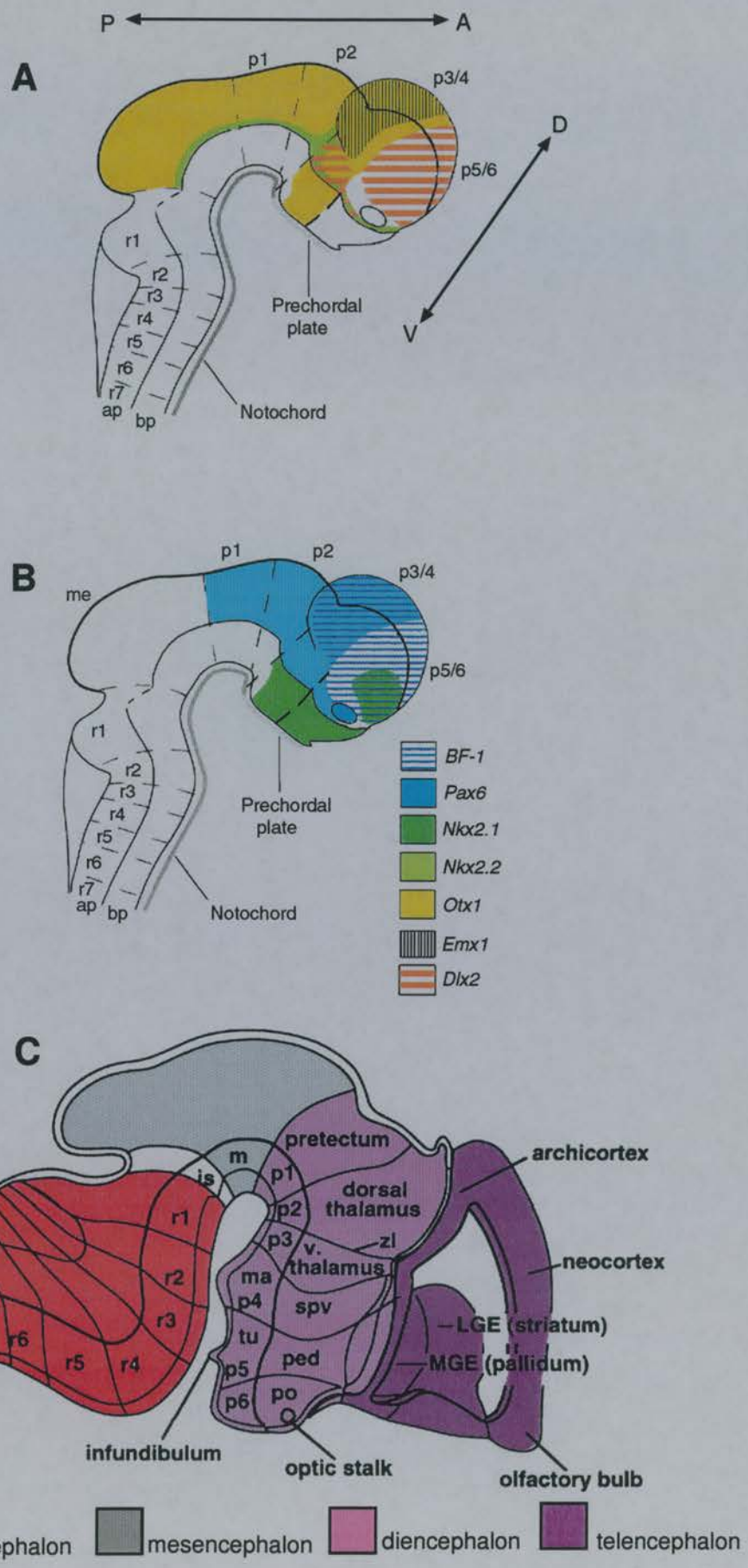
A
P
A
p1
p2
p3/4
p5/6
D
V
r1
r2
r3
r4
r5
r6
r7
ap
bp
Prechordal plate
Notochord
B
me
p1
p2
p3/4
p5/6
r1
r2
r3
r4
r5
r6
r7
ap
bp
Prechordal plate
Notochord
BF-1
Pax6
Nkx2.1
Nkx2.2
Otx1
Emx1
Dlx2
C
pretectum
m
is
p1
p2
dorsal thalamus
p3
v. thalamus
zl
ma
p4
spv
tu
p5
ped
p6
po
r1
r2
r3
r4
r5
r6
r7
archicortex
neocortex
LGE (striatum)
MGE (pallidum)
rp
ap
bp
fp
infundibulum
optic stalk
olfactory bulb
rhombencephalon
mesencephalon
diencephalon
telencephalon

Gene	Expression pattern	Forebrain phenotype in mutant	Function	References
Shh	Notochord and prechordal plate	Holoprosencephaly, cyclopia, lack of ventral forebrain structures (medial ganglionic eminence, MGE)	Induces differentiation of early ventral midline neuronal cell fates; also required for later telencephalic regionalisation - inducing ventral telencephalic fates (MGE and LGE)	Echelard *et al.*, 1993 Ericson *et al.*, 1995 Barth & Wilson, 1995 Chiang *et al.*, 1996 Kohtz *et al.*, 1998
BMPs (bone morphogenetic proteins) e.g. *BMP2,4,7*	Overlapping expression patterns in anterior non-neural ectoderm, anterior neural plate and later, the dorsal neural tube and roof of the forebrain	No obvious abnormalities; possibly due to functional redundancy	DV neural tube patterning - induces dorsal neuronal cell fates (inhibits *BF1*/induces *Msx1* expression in neuroectoderm explants) ; and in anterior neural tube acts coordinately with Shh to induce anterior ventral midline fates.	Liem *et al.*, 1995 Furata *et al.*, 1997 Shimamura & Rubenstein,1997 Dale *et al.*, 1997
Hepatic nuclear factor-3β (HNF3β) and *goosecoid*	Notochord and prechordal plate	*HNF3β -/-* mutants exhibit neural tube patterning defects; goosecoid mutants exhibit craniofacial abnormalities; double mutants lack Shh expression in notochord and exhibit forebrain growth defects	Regulate *Shh* expression and DV patterning of neural tube	Ang & Rossant, 1994 Weinstein *et al.*, 1994 Rivera-Perez, 1995 Yamada *et al.*, 1995 Filosa *et al.*, 1997
Fgf8	Anterior neural ridge	Early lethality	Induces *BF1* expression in neural explants	Shimamura *et al.*, 1995 Meyers *et al.*, 1998
BF1	Prospective telencephalon from E8.0	Reduced telencephalon size; lack basal ganglia	Putative role in regulating progenitor proliferation	Shimamura *et al.*, 1995 Xuan *et al.*, 1995.
Otx1	Forebrain and midbrain neuroepithelium	No major defects; *Otx1/Otx2* double heterozygotes exhibit defects in rostral brain indicative of co-operative action.		Simeone *et al.*, 1992a Acampora *et al.*, 1996 Suda *et al.*, 1997 Simeone, 1998
Otx2	Anterior endoderm and neuroectoderm; later in dorsal tel- di- and mesencephalon	Loss of neural tissue anterior to rhombomere 3	Chimeric embryos show a requirement for *Otx2* early for induction of forebrain/midbrain and later for forebrain regionalisation	Simeone *et al.*, 1992a Acampora *et al.*, 1995 Matsuo *et al.*, 1995 Ang *et al.*, 1996 Simeone, 1998 Rhinn *et al.*, 1998
Emx1	Dorsal telencephalon	Subtle forebrain defects including disorganised fasciculation of anterior commissure and corpus callosum and reduced cortical plate	Putative function in defining pallio-choroidal boundary in dorsal telencephalon and in later regional specification	Simeone *et al.*, 1992a Simeone *et al.*, 1992b Qiu *et al.*, 1996 Yoshida *et al.*, 1997
Emx2	Dorsal telencephalon and diencephalon	Dorsal telencephalic defects: reduced cerebral size, reduced hippocampus and medial limbic cortex; lack dentate gyrus	Putative functions in early patterning and later proliferation/specification of dentate gyrus and archicortex	Simeone *et al.*, 1992a Simeone *et al.*, 1992b Pellegrini *et al.*, 1996 Yoshida *et al.*, 1997
Pax6	Telencephalon and diencephalon	Early loss of prosomere distinction; later di- and telencephalic patterning defects and abnormal lamination of cortex	Putative roles in early forebrain patterning and later regulating cortical proliferation, cell adhesion and cell fate specification (section 1.2.5)	Stoykova *et al.*, 1996 Warren & Price, 1997 Gotz *et al.*, 1998

Table 1.1 A few of the key genes involved in specification and patterning of the telencephalon. A comprehensive list of genes expressed in the embryonic brain and a review of their function is given by Rubenstein & Shimamura (1997)

Gene	Expression pattern	Forebrain phenotype in mutant	Function	References
Nkx2.1, Nkx2.2	*Nkx2.1*: initial expression in anterior neural plate induced by Shh; later in ventral telencephalon; *Nkx2.2*: length of ventral neural tube	*Nkx2.1*:ventral telencephalic defects: septum and basal ganglia *Nk2.2*: forebrain phenotype not published (loss of ventral neurons in spinal cord)	Specification of ventral telencephalic cell fates	Price *et al.*, 1992 Barth & Wilson, 1995 Shimamura *et al.*, 1995 Kimura *et al.*, 1996 Sussel *et al.*, 1999 Briscoe *et al.*, 1999
Dlx1, Dlx2	Domains of diencephalon and ventral telencephalon	No major patterning defects in single mutants; *Dlx1/Dlx2* double homozygote mutants exhibit abnormal proliferation and differentiation of basal telencephalic regions including the striatum	Differentiation and migration of striatal neurons	Bulfone *et al.*, 1993 Qiu *et al.*, 1995 Qiu *et al.*, 1997 Anderson *et al.*, 1997
Lhx2	Developing cerebral cortex and diencephalon	Reduced cerebral cortex and hippocampus	Required for cortical proliferation	Xu *et al.*, 1993 Porter *et al.*, 1997
Gli3	Telencephalon, dorsal mid- and hindbrain	Loss of definition of the diencephalic/telencephalic boundary; defects in structures derived from the dorsal telencephalon including reduction of cortex	Specification of dorsal telencephalon; required for *Emx* gene expression in dorsal telencephalon and *Wnt* expression in hem of cerebral cortex	Hill *et al.*, 1989 Franz, 1994 Platt *et al.*, 1997 Grove *et al.*, 1998 Theil *et al.*, 1999

Table 1.1 (continued)

1.1.2 Generation of cortical cell types

Cortical cells are generated in the ventricular zone (VZ), a layer of dividing progenitor cells on the inner edge of the cortical wall. Nuclei of ventricular progenitor cells undergo dynamic intracellular migration during the cell cycle: nuclei move away from the apical surface during G1, occupy the outer half of the VZ during S phase and return apically in G2 so that mitosis occurs at the ventricular surface (Sauer, 1935; Fig. 2.1).

The progenitor population gives rise to diverse neural and glial cell types at specific times of cortical development. During the earliest phase, progenitors divide to expand the proliferative population. The second phase is neurogenesis, the production of specified postmitotic cortical neurons which occurs over a period of six days in the mouse (embryonic days E10.5-16.5; Takahashi *et al.*, 1995a; Caviness, 1982; Fig1.10). Radial glia are also produced in this phase and newborn neurons migrate outwards on radial glia to the cortical plate. In the third phase, VZ progenitors give rise to a second proliferative population of subventricular zone (SVZ) cells (Bayer & Altman, 1991; Takahashi *et al.*, 1995b) where gliogenesis predominantly occurs from E15.5 to postnatal ages. At the end of neuronal migration, bipolar radial glia transform into mature multipolar astrocytes (Misson *et al.*, 1991; Edwards *et al.*, 1990).

1.1.2.1 Cortical progenitors

It is thought that, during cortical development, the ventricular zone consists of a heterogeneous population of cell types, including:

- multipotential progenitors capable of giving rise to all neuronal and glial (radial, oligodendrocyte and astrocyte) cell types;
- lineage-restricted progenitors which give rise to specific neural or glial cell types;
- specified daughter cells, whose neural or glial cell fate is determined and which later manifest features of their neural or glial phenotype during differentiation (Fig. 1.6A).

Experiments using retroviral lineage tracing to mark daughter cells arising from a single precursor revealed the existence of multipotent progenitors in the mammalian VZ (Luskin *et al.*, 1988; Price & Thurlow,1988; Walsh & Cepko, 1992; Grove *et al.*, 1993). At least some multipotent progenitors are thought to be self renewing stem cells (Davis & Temple, 1994; Reid *et al.*, 1995; Williams & Price, 1995; Qian *et al.*, 1998). These predominate early in development (Williams & Price,1995) and can subsequently give rise to progenitors of more restricted lineage *in vitro* (Davis & Temple, 1994). Lineage restricted progenitors, whose fate cannot be altered, are present as early as E12, and by E16 the majority of progenitors appear to be specified (Williams & Price, 1995).

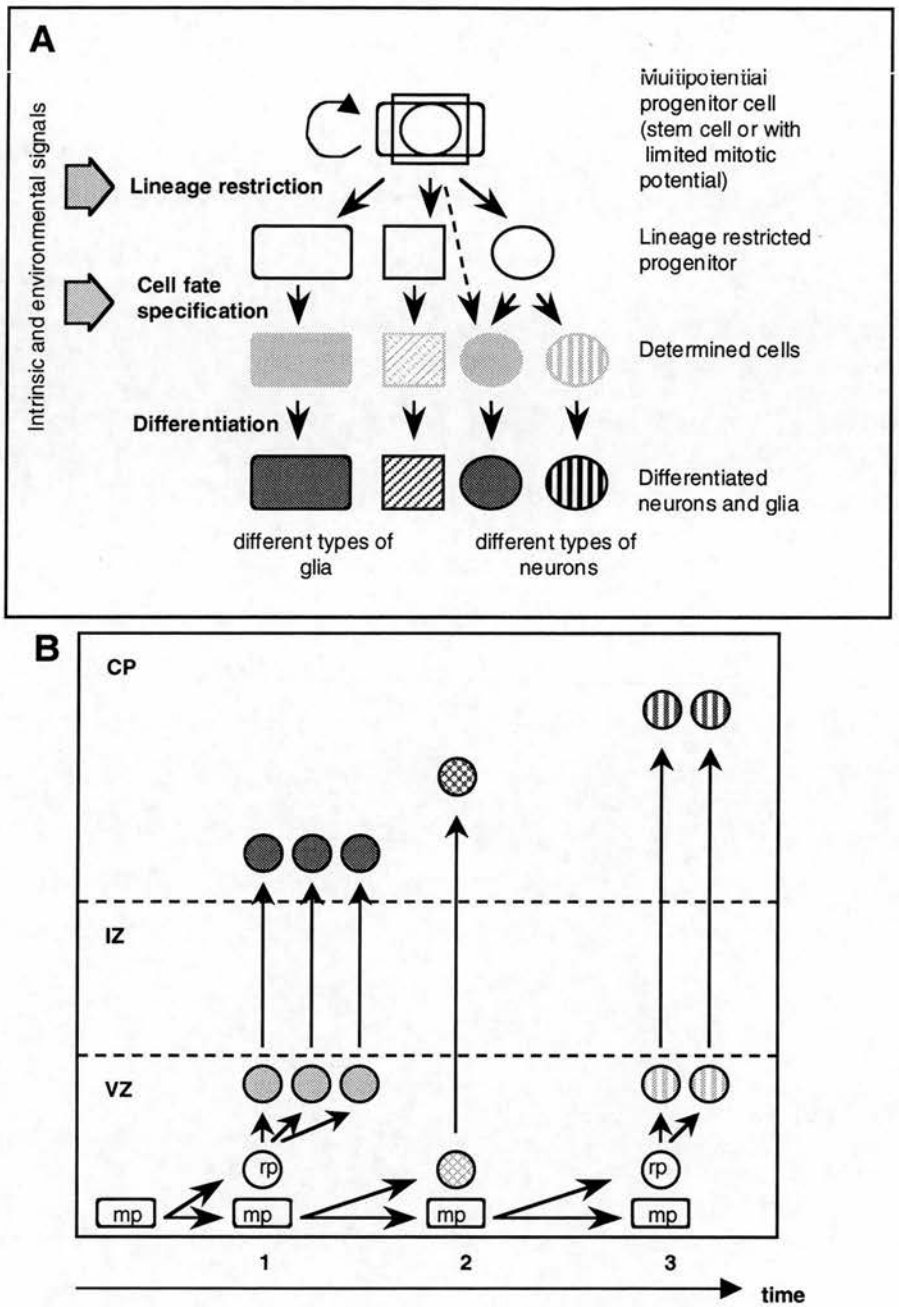

Figure 1.6 Lineage restriction of cortical progenitors

A. The possible hierarchy of multipotential progenitor cells (which have the potential to give rise to all cell types), lineage restricted progenitors (which give rise to specific neural or glial lineages) and determined cells (whose cell fate has been specified and which manifest features of their neuronal or glial fate upon differentiation). Multipotential progenitors may be self-renewing stem cells or have limited mitotic potential. The dotted arrow indicates that a multipotential progenitor may give rise directly to a specified cell type without going through an intermediate lineage restricted progenitor stage. Intrinsic changes in gene expression and external signals together regulate progenitor development.

B. Model for the behaviour of multipotential progenitor cells (mp) in the cortex based on clonal analysis (Reid *et al.*, 1995). A multipotential progenitor in the ventricular zone (VZ) divides asymmetrically, at regular time intervals, giving rise to another mp and either a lineage restricted progenitor [rp, which generates a cluster of neurons of similar type (divisions 1 and 3)] or directly to a specified neuron (division 2). Specified neurons produced by mps or rps migrate into the cortical plate (CP) and differentiate. Early born neurons migrate to form the deeper layers of the cortical plate; later born neurons form more superficial layers.

mp, multipotential progenitor; rp, lineage restricted progenitor; CP, cortical plate; IZ, intermediate zone; VZ ventricular zone [adapted from Lillien, 1998 (A) and Reid *et al.*, 1995 (B)].

In vivo, the behaviour of multipotent cells has been examined by infection of progenitors with a retroviral library and identification of sibling cells by PCR amplification of retrovirally encoded tags (Fig. 1.6B; Reid *et al.*, 1995). Cortical clones were either clustered, consisting of one or more neurons of similar cell type, or widespread, consisting of several clustered clones of different laminar fates, spaced at even intervals. These observations support a model in which multipotential cells divide asymmetrically (see below), at regular time intervals, giving rise either to a lineage restricted progenitor (creating clusters) or to a single cell which differentiates (Fig. 1.6B).

1.1.2.2 Factors regulating progenitor proliferation and lineage

A combination of intracellular and external environmental signals are thought to regulate progenitor cell development (reviewed in Lillien, 1998; Temple & Qian, 1996; Shen *et al.*, 1998). These act (1) to regulate progenitor proliferation, (2) to restrict a progenitor to producing a neuronal or glial lineage, (3) to specify the fate of daughter cells. The first two will be discussed in this section and the third in section 1.1.2.3.

Little is known about mechanisms that switch a multipotent stem cell to become a restricted potential progenitor, although recent experiments have suggested a role for the transcription factors *Mash1*, *Prox1* and *Pax6*. *In vitro*, *Mash1* and *Prox1* expression in E11.5 neuroepithelial cells correlates with the transition of stem cells to progenitors of limited mitotic potential (Torii *et al.*, 1999) and ectopic expression of Mash-1 leads to a down-regulation of nestin, a marker for undifferentiated progenitor cells. However, neuronal defects in the *Mash1* null mouse are predominantly confined to ventral telencephalic regions rather than the dorsal telencephalon-derived cortex (Casarosa *et al.*, 1999). Altered ratios of cell types generated by *Pax6* null multipotential progenitors *in vitro* suggests that this gene may have a role in specifying cortical cell fates (Gotz *et al.*, 1998); this will be discussed in more detail in section 1.2.5.

Both cell-intrinsic and environmental factors are also implicated in regulating progenitor proliferation. *BF1* is a candidate intrinsic regulator of the cell cycle expressed throughout the prospective telencephalon in mice from E8.0 (Shimamura *et al.*, 1995). Mice lacking *BF1* exhibit reduced telencephalic size (Xuan *et al.*, 1995) although the telencephalon appears to be correctly specified by expression of markers *Emx1*, *Emx2* and *Pax6*. However, from the onset of neurogenesis at E10.5 the number of proliferating progenitor cells in the cortical VZ is reduced and the number expressing *microtubule- associated protein-2* (*MAP-2*), a marker of early postmitotic neurons, increased. This suggests that cortical progenitors progress

through a reduced number of cell cycles and differentiate prematurely, leading to early reduction in the proliferative population (Xuan *et al.*, 1995). This hypothesis could be tested by examining whether *BF1*$^{-/-}$ neurons only differentiate into early-generated neurons that are usually present in the deep cortical layers. It is also unknown how *BF1* may act to regulate the number of cell cycles that progenitors undergo. It could act either indirectly, by regulating the cellular response to secreted factors such as FGF2 (discussed below) and thus facilitating cell cycle progression, or directly by regulating expression of cell-cycle components (Xuan *et al.*, 1995).

Several environmental factors have been identified which, when applied to cortical progenitors *in vitro*, stimulate proliferation and accelerated differentiation of neurons or glia. These include fibroblast growth factor-2 (FGF2), neurotrophin-3 (NT-3; Ghosh & Greenberg, 1995), platelet derived growth factor (PDGF; Williams *et al.*, 1997; Johe *et al.*, 1996), epidermal growth factor (EGF; Kilpatrick& Bartlett, 1995; Burrows *et al.*, 1997) and ciliary neurotrophic factor (CNTF; Bonni *et al.*, 1997; Johe *et al.*, 1996).

In addition to regulating the *rate* of proliferation, some of these factors are also implicated in regulating the cell *lineage* (neurons or glia) generated by multipotent cortical progenitors. For example, early (E10) cortical stem cells generate a varying number of neuronal progeny by default, however treatment with FGF2 stimulates a switch to glial (oligodendrocyte) cell fate (Qian *et al.*, 1997). This data supports a hypothesis in which intrinsic factors lead to neuronal generation and extrinsic factors are required to switch the progenitors to generate glia later in cortical development. However, it is probable that *in vivo* a combination of both are required throughout progenitor development. Recent reports have suggested that different multipotent and restricted lineage progenitor cell types themselves exhibit differential responsiveness to mitogens (Kilpatrick & Bartlett, 1995; Burrows *et al.*, 1997; Marmur *et al.*, 1998; Tropepe *et al.*, 1999; reviewed in Lillien, 1998), which could lead to selective expansion of neuronal then glial lineages. For example, cortical progenitors show an increased response to EGF coincident with an increase in gliogenesis (Kilpatrick& Bartlett, 1995). Retroviral overexpression of the *EGF* receptor in progenitors also stimulates a switch to glial (astrocyte) cell fate (Burrows *et al.*, 1997), suggesting that changes in EGF responsiveness contribute towards the neuronal/glial switch. However, the latter study did not convincingly distinguish between the effects of EGF on accelerated stem cell proliferation and maturation as opposed to cell fate selection. Evidence also suggests that a considerable amount of cell death occurs in proliferative areas during progenitor proliferation (Blaschke *et al.*, 1996; Thomaidou *et al.*, 1997); the selective role of cell death in generation of cell lineage has not yet been assessed.

1.1.2.3 Cortical cell fate specification

1.1.2.3.1 Asymmetric division

Current evidence suggests that one way in which cortical progenitors generate diverse cell types is by asymmetric division: one which results in the specification of different cell fates in the daughter cells (Horvitz & Herskowitz, 1992). Asymmetric division is a process involving:

- polarised localisation of cell fate determinants (cytoplasmic, nuclear or membrane molecules) within the parent cell;
- orientation of cleavage such that the polarised determinants will be distributed differentially to the daughter cells.

Recent work has suggested that the molecular mechanisms underlying asymmetric division in the mammalian cortex are similar to those regulating neurogenic divisions in the *Drosophila* CNS. Therefore I will first discuss a few of the molecules required for *Drosophila* neurogenesis as a foundation to considering asymmetrical division in cortical development.

Drosophila neurogenesis

During *Drosophila* neurogenesis stem cell neuroblasts (NBs) undergo repeated asymmetric division giving rise to a series of ganglion mother cells (GMCs); GMCs then undergo a terminal asymmetric division to produce a pair of postmitotic neurons or glia (Goodman & Doe, 1993; Fig. 1.7A). During these divisions the membrane associated protein Numb and the homeodomain transcription factor Prospero are asymmetrically localised to the basal pole of the cell and are inherited by the basal daughter cell only (Knoblich *et al.*, 1995; Spana & Doe, 1995; Fig. 1.7B). Prospero acts as a cell fate determinant in daughter cells of the NB, where it promotes expression of GMC-specific genes (Doe *et al.*, 1991; Vaessin *et al.*, 1991); Numb is required for cell fate determination in GMC divisions (Buescher *et al.*, 1998; Skeath & Doe, 1998), possibly by inhibition of Notch signalling (Frise *et al.*, 1996).

In order for asymmetrically localised cell fate determinants to be segregated correctly during division, the orientation of the mitotic spindle has to be co-ordinated with protein localisation. Two apically localised *Drosophila* proteins involved in this process have been identified, Bazooka and Inscuteable (Kraut & Campus-Ortega, 1996; Kuchinke *et al.*, 1998). Bazooka is required to coordinate apico-basal polarity of neuroblasts with that of the embryo (Kuchinke *et al.*, 1998). NBs lacking Bazooka have intrinsic cellular polarity, maintain spindle orientation and Prospero localisation but fail to co-ordinate this with the rest of the embryo (Fig. 1.7C). Thus in *bazooka* mutants Prospero is correctly segregated and GMCs are

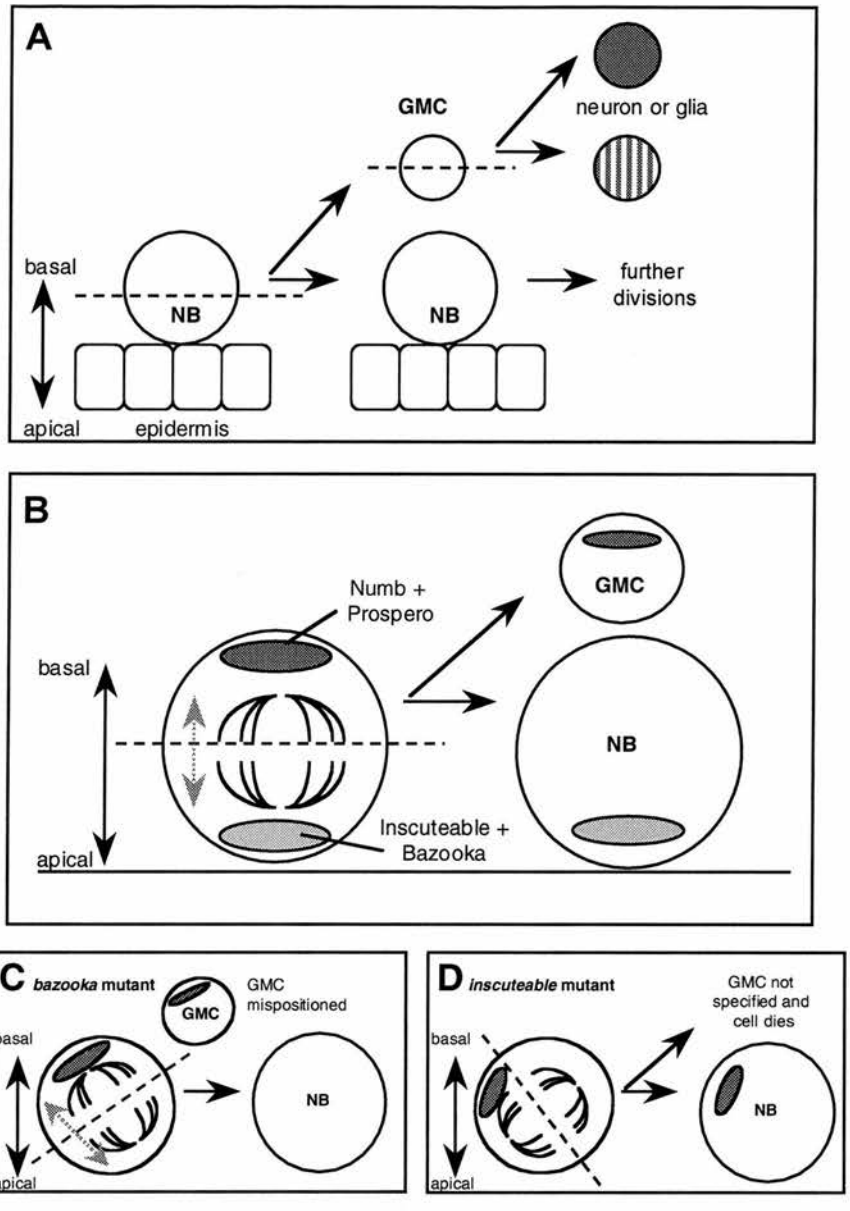

Figure 1.7 Asymmetric cell division in *Drosophila* neurogenesis

A. *Drosophila* neuroblasts (NBs) arise from epithelial cells and segregate basally from the epithelial cell layer. NBs divide asymmetrically with a cleavage plane parallel to the epidermal surface, giving rise to a larger apical daughter cell and a smaller basal ganglion mother cell (GMC). GMCs undergo a terminal asymmetric division to produce a pair of postmitotic neurons or glia. The apical daughter cell retains neuroblast charcteristics and continues to divide.

B. During NB asymmetric division cell fate determinant molecules Numb and Prospero are localised to the basal pole of the cell, and Inscuteable and Bazooka proteins are localised to the apical pole. Cell division segregates Numb and Prospero to the basal daughter cell only, in which Prospero promotes expression of GMC-specific genes. Asymmetric division requires (1) polarised localisation of cell determination molecules and (2) appropriate spindle and cleavage orientation relative to these molecules to distribute them to the daughter cells. Correct positioning of the daughter cells also requires the apico-basal polarity of the cell (represented by the dotted grey arrow) to be co-ordinated with that of the embryo (black arrow). These processes involve Inscuteable and Bazooka proteins and are disrupted in *inscuteable* and *bazooka* mutants (C and D).

C. In *bazooka* mutants intrinsic apico-basal polarity of the NB is not co-ordinated with that of the embryo. Prospero localisation and spindle orientation are maintained such that Prospero is correctly segregated and GMCs are specified, but GMCs are mispositioned in the embryo.

D. In *inscuteable* mutants different aspects of cellular polarity are not co-ordinated. Prospero localisation and spindle orientation are randomised so many GMCs fail to inherit Prospero, are not specified and die.

specified, but they are mispositioned. The second protein, Inscuteable, is required for both the localisation of Numb and Prospero and orientation of the mitotic spindle (Kraut *et al.*, 1996). In *inscuteable* mutants, NB spindle axis and Prospero localisation are randomised, so many GMCs fail to inherit Prospero and hence fail to develop (Kraut *et al.*, 1996; Fig. 1.7D). This suggests a function for *inscuteable* in coordinating different aspects of cellular polarity.

Cortical neurogenesis

Retroviral lineage tracing experiments first indicated that mammalian cortical progenitors undergo asymmetric division. Labelled progenitor cells give rise to neurons which occupy several layers of the cortex (Walsh & Cepko, 1988; 1992; Luskin *et al.*, 1988; Price & Thurlow, 1988; Reid *et al.*, 1995; Kornack & Rakic, 1995; Reid *et al.*, 1997) suggesting that a single progenitor undergoes multiple asymmetric divisions over time, each division generating a progenitor and a neuron. A recent study by Chenn & McConnell (1995) provided direct evidence for the concept of asymmetric division during cortical neurogenesis, using time lapse imaging of dividing cells in cortical slices. They demonstrated that vertical cleavage of precursors, with a plane perpendicular to the ventricular surface, gives rise symmetrically to two identical daughter cells which remain within the VZ (Fig. 1.8A). Horizontal cleavage, with a cleavage plane parallel to the ventricular surface, gives rise asymmetrically to one cell which remains in the VZ and one which migrates out towards the cortical plate. Chenn & McConnell proposed that early in development, during expansion and maintenance of the progenitor population, symmetric divisions predominate within the VZ. With the onset and progression of neurogenesis asymmetric divisions increase in frequency (Chenn & McConnell, 1995) corresponding to the increasing rate of neuronal production during neurogenesis (Miller, 1985; Caviness *et al.*, 1995). However, they did not show that the different daughter cells go on to divide or differentiate, respectively.

Ultimately, conclusive evidence for asymmetric division in cortical development requires the isolation of molecular cell fate determinants and ascertaining their subcellular localisation during cell division. Remarkably, vertebrate homologues of *Drosophila numb* have recently been isolated in mouse (Zhong *et al.*, 1996), rat (Verdi *et al.*, 1996) and chick (Wakamatsu *et al.*, 1999) and have been shown to localise asymmetrically in mitotic cortical cells. Symmetric division distributes the protein equally between daughter cells whereas an asymmetric division partitions all the protein to one cell. However, whilst Numb localises to the apical membrane of cortical progenitors in mouse, it has been reported to show basal localisation in chick. The disparity in Numb localisation suggest the two groups may have detected different Numb isoforms (Verdi *et al.*, 1999) or have isolated different members of the *Numb* gene family.

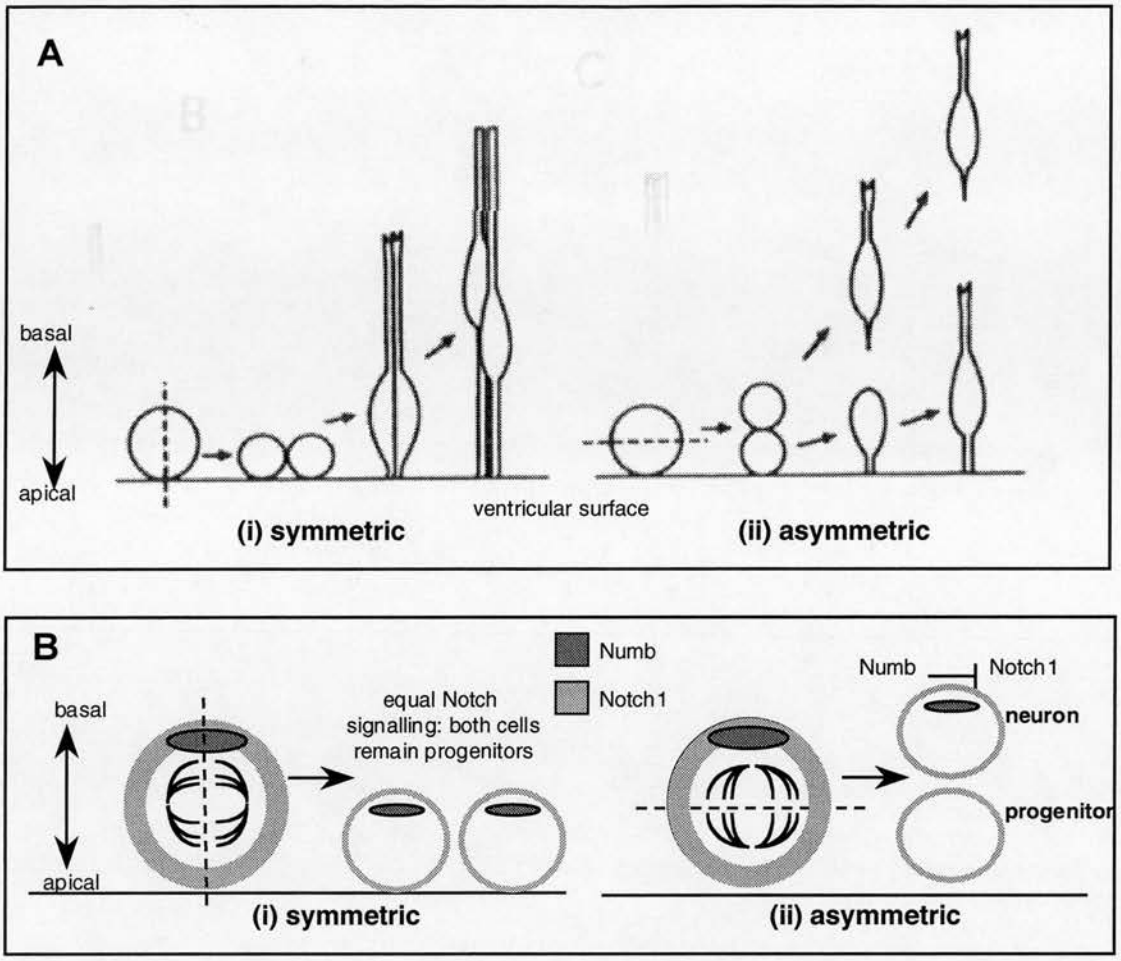

Figure 1.8 Symmetric and asymmetric division of mammalian cortical progenitors

A. Cortical progenitors divide at the inner surface of the ventricular zone (VZ).

(i) Symmetric division occurs when there is vertical cleavage of progenitors (with a plane perpendicular to the ventricular surface) giving rise to two identical daughter cells. These cells remain within the VZ and, on entry into G1 phase of the next cell cycle, undergo basal directed interkinetic nuclear migration.

(ii) Asymmetric division occurs when there is horizontal cleavage (with a plane parallel to the ventricular surface) giving rise to one cell which remains in the VZ and one which migrates out towards the cortical plate like a postmitotic neuron (from Chenn & McConell, 1995).

B. Model for mNumb and Notch1 protein function in generating cell fate during cortical symmetric and asymmetric division. mNumb is localised to the basal pole of the dividing progenitor and Notch1 is distributed evenly around the cell membrane in both forms of division.

(i) During symmetric division mNumb and Notch1 are inherited equally and, in the absence of sufficient repression by mNumb, Notch signalling maintains a progenitor fate in both cells.

(ii) During asymmetric division the basal daughter cell inherits the majority of mNumb where it is sufficient to inhibit Notch1 acitivity and permit neuronal differentiation.

Conflicting results have also been presented on the localisation of a second protein, the receptor Notch1. Notch1 becomes localised to the basal membrane of cortical progenitors in the ferret (Chenn & McConnell, 1995), but asymmetric localisation has not been found in either mouse or chick (Zhong *et al.*, 1996; Wakamatsu *et al.*, 1999). Differences in Notch1 localisation may be attributable to difficulties detecting small quantitative differences in protein localisation or by cross reaction of Notch antibodies between different Notch family members, to as yet unidentified members of the Notch family or to another protein.

Although debate exists over the exact localisation and role of these proteins in vertebrate systems, their involvement in neuronal cell fate determination is an attractive idea. Misexpression of mouse *Numb* (*mNumb*) can rescue neuronal loss in the *Drosophila numb* mutant. Furthermore, mouse and chick Numb proteins can physically interact with the intracellular domain of Notch1 (Zhong *et al.*, 1996; Wakamatsu *et al.*, 1999) and, in chick, can inhibit Notch1-mediated suppression of neuronal differentiation(Wakamatsu *et al.*, 1999). The most parsimonious model for mNumb and Notch1 function in generating cell fate during cortical asymmetric divisions is shown in Figure 1.8B. mNumb is localised to the basal daughter cell where it inhibits Notch1 activity and permits neuronal differentiation; in the apical cell, mNumb is absent and Notch1 signalling maintains a progenitor cell fate. This is also in agreement with evidence that Notch1 activation is associated with the suppression of neuronal cell fate (reviewed by Artavanis-Tsakonis *et al.*, 1999). However, it remains possible that other Numb and Notch family members are segregated to the apical cell where they promote a progenitor cell fate.

A second mammalian gene has been cloned by sequence similarity to *Drosophila numb*, called *Numblike* (*Nbl*; Zhong *et al.*, 1997). Like mNumb, Nbl can bind Notch1 and misexpression of *Nbl* rescues the *Drosophila numb* mutant, suggesting that it too can direct cells toward a neuronal cell fate. However, Numblike is cytoplasmically distributed and its expression appears to be limited to differentiating cells of the cortical plate (Zhong *et al.*, 1997). *Prox-1*, a vertebrate homologue of *Drosophila prospero*, has also been isolated (Oliver *et al.*, 1993). Asymmetrical localisation of neither Nbl nor Prox-1 has been detected and their roles in cortical cell fate determination remain obscure.

It will be interesting to establish whether polar localisation of other, as yet unidentified, proteins regulate spindle orientation in mammalian neurogenesis, or whether they employ a different mechanism (reviewed in Rhyu & Knoblich, 1995). The polarised distribution of a variety of proteins including cadherins and cytoskeletal elements in VZ cells has highlighted their intrinsic apico-basal polarity (Chenn *et al.*, 1998). In contrast to the situation in

Drosophila in which asymmetric localisation of Numb and Prospero occurs only during asymmetric divisions, in the vertebrate cortex Notch1 and Numb protein polarisation occurs in both symmetric and asymmetric divisions. This suggests that the mechanisms determining protein localisation and spindle orientation are independent of each other (although both use the same positional information within the cell).

A second intriguing issue concerning spindle orientation in cortical neurogenesis has yet to be addressed: how a progenitor switches from proliferative (symmetric) to neurogenic (asymmetric) division. *In vitro*, continuous time-lapse monitoring of isolate E10.5 neural progenitor cells revealed that they undergo stereotyped patterns of symmetric and asymmetric division during the neurogenic period (Qian *et al.*, 1998). This suggests they follow cell intrinsic programs of division, and that the mechanisms controlling cell cycle progression and spindle orientation may be very closely linked.

1.1.2.3.2 Specification of neuronal cell type

The previous section suggested that the fate of cortical cells is partly determined by the symmetry of the progenitor division which generates them: either giving rise to two progenitors or to a progenitor and a neuron. At the same time a second aspect of cell fate - neuronal cell type - is specified. Postmitotic neurons acquire a specific fate within the cortex, reflected by the position they take up in a particular layer of the cortical plate. Layers can be distinguished by their neuronal density, morphology and gene expression. Neuronal phenotype is also reflected in long-distance axonal connections and neurotransmitter type (reviewed in Chenn *et al.*, 1997). Studies in the ferret cortex have gone some way towards understanding how neuronal cell fate is specified (Fig.1.9), suggesting that:

1. *Environmental factors act on early progenitors to determine laminar fate.* Young (E29) precursors normally generate neurons early in development destined for deep layers of the cortex. However, young progenitors transplanted into an older (postnatal) brain can become respecified to produce daughters destined for upper layers, appropriate to the host (McConnell & Kaznowski, 1991; Fig.1.9A). It appears that environmental signals act during the G2 phase of the mitotic division that generates the neuron. Young progenitors transplanted into an older host brain during S-phase become respecified, whereas progenitors transplanted during G2 do not (McConnell & Kaznowski, 1991). Some evidence suggests that these environmental signals are short range or contact-mediated: young progenitors cultured together before transplantation into an older host mostly maintain the laminar fate appropriate to the donor, whereas cells cultured alone become respecified by the host (Bohner *et al.*, 1997). However, culture experiments such as these do not necessarily reflect cell behaviour *in vivo*.

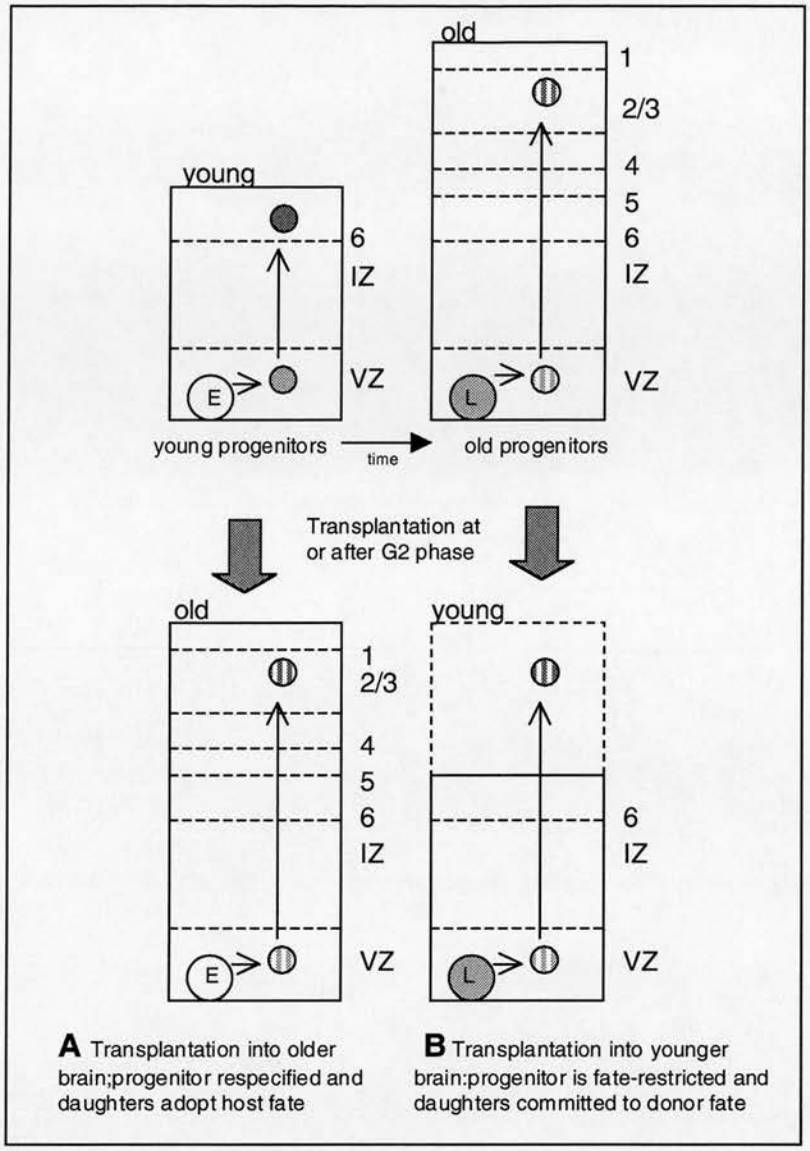

Figure 1.9 Outcomes of cortical progenitor transplantation experiments in the ferret cortex

A. Early (E29) cortical progenitor cells (E) in the ventricular zone (VZ) normally generate neurons which migrate to layer 6 of the cortical plate (upper panel). Early progenitors transplanted into older host brains (lower panel) become respecified by environmental factors and produce daughter cells destined for upper layers 2/3 appropriate to the host. However, during development the potential of neuronal progenitors becomes progressively restricted to that shown in (B).

B. Late (postnatal) progenitors (L) normally generate neurons destined for upper layers 2/3 of the cortical plate (upper panel). Late progenitors transplanted into a younger host brain maintain their specification and generate neurons which continue to migrate to upper layers.

E, early progenitors; L, late progenitors; 1-6, layers 1-6 of the cortical plate; IZ, intermediate zone; VZ ventricular zone

2. *The developmental potential of neuronal progenitors becomes progressively restricted with time.* Progenitors transplanted from older to younger brains maintain their specification and generate neurons which migrate only to upper layers appropriate to the donor (Frantz & McConnell, 1996; Fig.1.9B),. Cell intrinsic mechanisms may be involved in the narrowing of developmental potential. For example, during the neurogenic period, cortical progenitors undergo a maximum of 11 cell cycles during neurogenesis (Takahashi *et al.*, 1995a) and the laminar identity of cortical neurons is closely correlated to the cell cycle in which the cell is born: neurons of layers 6 and 5 arise from cycles 1-8 in mice, whilst neurons destined for layers 4 and 3/2 are born in cycles 9-11 (Takahashi *et al.*, 1996). This suggests that an internal mechanism linked to cell cycle progression may be operating. Ventricular zone progenitors also exhibit intrinsic molecular differences that alter with time. The transcription factor *Otx1* is highly expressed in neurons of layers 5 and 6 and in their ventricular precursors whilst they are being generated, after which it is downregulated in the VZ (Frantz *et al.*, 1994). Expression of specific regulatory genes at different times during neurogenesis may regulate the competence of a progenitor to generate neurons of a certain fate. It will be interesting to examine mutants of such genes for the absence of specific neuronal cell types.

Thus it seems that both intrinsic changes in gene expression and external environmental cues act on the cortical neural progenitor population during cell division to specify neuronal fate. It remains unclear exactly how these different factors interact.

1.1.3 Neuronal migration

Newborn neurons migrate outwards into the cortical plate where they settle and differentiate in a highly ordered pattern of layers (Fig. 1.10). The first born postmitotic neurons form the preplate layer (PPL), and subsequent cortical plate neurons migrate into the preplate, splitting it into the marginal zone (MZ) above the CP and the subplate (SP) below (reviewed in Marin-Padilla, 1998). CP layers are laid down in an inside first, outside last manner; cells born early in development form the deepest layers of the cortex while cells born at later stages migrate past early-born neurons to generate outer layers (Angevine & Sidman, 1961; Berry & Rogers, 1965; Rakic, 1974). The majority of neurons migrate on radial glia (Angevine & Sidman, 1961; Rakic, 1972; Edmondson & Hatten, 1987; Hatten, 1990).

Early generated cortical layers appear essential for radial migration of later-born CP neurons. For example, injection of a mitotic inhibitor during formation of the subplate leads to radial glial defects and abnormal lamination in the ferret cortex (Noctor *et al.*, 1999).

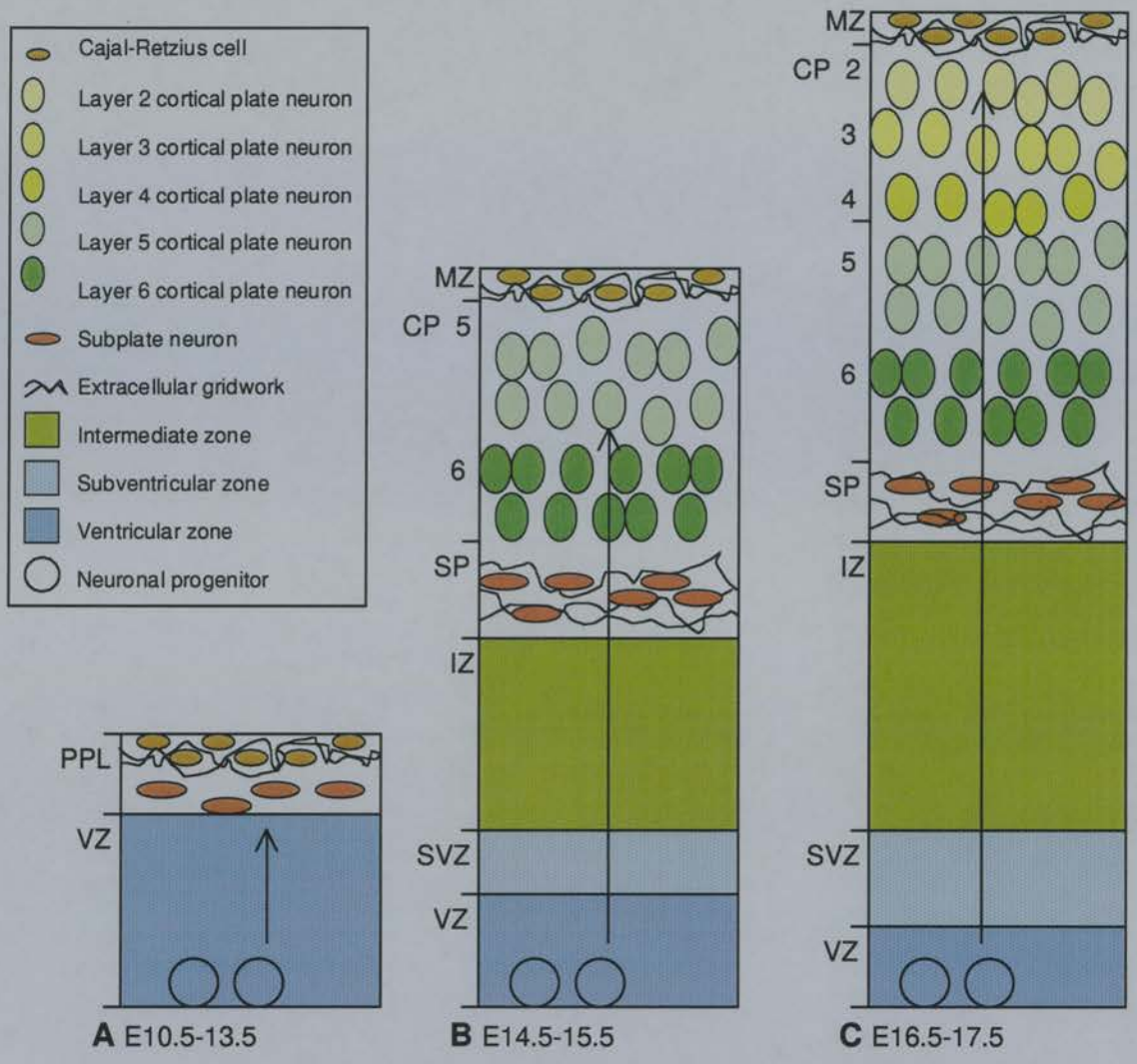

Figure 1.10 Schematic showing the sequence of events during murine cortical neurogenesis

Figures represent sagittal sections through the ventrolateral neocortex at stages of cortical neurogenesis. Prior to the onset of neurogenesis at E10.5 the ventricular neuroepithelium is the only constituent of the cortical primordium.

A. In the early stages of cortical neurogenesis (E10.5 - E13.5) the ventricular zone (VZ) is the sole region of cell division. During this stage the first born postmitotic neurons (presumptive subplate (SP) neruons and Cajal-Retzius cells) are born in the ventricular zone (VZ) and migrate outwards. These cells, together with an extracellular gridwork, comprise the the primordial plexiform or preplate layer (PPL).

B. In the middle stage (E14.5-15.5) there are two germinal zones: a large VZ where neurogenesis occurs and a smaller layer derived from the VZ, the subventricular zone (SVZ), where gliogenesis predominantly occurs. With the increasing production of postmitotic neurons the number of neuronal progenitors in the VZ decreases, and the number of glial progenitors in the SVZ proportionately increases. Neurons destined for cortical plate (CP) layers 6 and 5 are mainly produced in the VZ during this stage and migrate into the preplate, splitting it into the marginal zone (MZ) above the CP and the subplate below. Layer 5 neurons migrate past layer 6 neurons to form a more superficial layer. The intermediate zone (IZ) also emerges at this stage - a transitional field comprised of neurons migrating radially to the CP and tangentially to lateral and ventrolateral parts of the neocortex and regions outside the neocortex. Afferent axons from subcortical regions and efferent axons from the CP extend in the PPL, SP and IZ.

C. In the late stage (E16.5-E17.5) the VZ shrinks as progenitors undergo terminal neurogenic divisions and the SVZ expands. CP neurons destined for layers 4, 3 and 2 are mainly born during this stage, and migrate past early-born neurons.

1-6, layers 1-6 of the cortical plate; IZ, intermediate zone; MZ, marginal zone; PPL, preplate; SP, subplate; SVZ, subventricular zone; VZ, ventricular zone (adapted from Bayer & Altman,1991).

In addition, studies on the mouse mutant *reeler* have highlighted a role for Cajal-Retzius (CR) cells in radial migration. CR cells are a transient neuronal population in the MZ which mostly die postnatally (reviewed in Frotscher, 1998).The *reeler* mutant exhibits altered cortical and cerebellar radial migration and the defective gene, *reelin* is expressed in CR cells (D'Arcangelo *et al.*,1995; Hirotsune *et al.*, 1995 and reviewed in Goffinet, 1995). Grafting and co-culture experiments have shown that diffusible signals released from CR cells can both induce adult cerebellar glia to adopt a radial glia phenotype and attract migrating neurons (Soriano *et al.*, 1997). It is possible that these cells play a similar role in the cortex.

Once initiated, radial glial-guided migration of a neuron to its correct position in the cortical plate involves recognition and adhesion to radial glia, initiation of cell movement, active migration through a diverse cellular environment, arrest and detachment at the appropriate position in the cortical plate (Rakic, 1972; Hatten & Mason, 1990; Anton,1996; reviewed in Rakic *et al.*, 1994; Rakic & Caviness, 1995) This process requires dynamic regulation of molecules involved in cell-cell recognition, signalling, adhesion, and cell motility. Molecules implicated in steps of the migration process have been identified by *in vitro* studies of tissue slices or dissociated glia, and by analysis of mouse mutants with disrupted cortical laminar organisation. These are reviewed in Lambert & Goffinet (1998) and summarised in Table 1.2.

There is now considerable evidence suggesting that a proportion of cortical cells also undergo non-radial, or tangential, migration parallel to the ventricular surface. The occurrence of tangential migration was first suggested by the wide-spread dispersion of clonally-related cells labelled by retrovirus (Walsh & Cepko, 1992; 1993) or a *lac-Z* transgene incorporated into early cortical progenitors(Tan & Breen, 1993; Tan *et al.*, 1995). Focal DiI injections into the ferret cortical VZ labelled tangentially oriented cells in the VZ/SVZ and demonstrated their gradual dispersion over considerable distances (O'Rourke *et al.*, 1997); these cells were mainly postmitotic according to expression of the early neuron-specific marker *TuJ1* and absence of BrdU incorporation. In the mouse, evidence for tangential migration of progenitors has also been suggested by time lapse imaging of cells at the ventricular surface, some of which divide as they migrate (Fishell *et al.*, 1993). Furthermore, at least some MZ neurons are thought to originate in subcortical regions and migrate tangentially into the cortex (De Carlos *et al.*, 1996; Anderson *et al.*, 1997).

Little is known about molecular cues guiding non-radial migration, although two recent studies of mice mutant for specific transcription factors have highlighted defects in tangential migration. *Dlx-1/Dlx-2* homozygous double mutants lack neuronal migration from ventral telencephalic striatum into the cortex (Anderson *et al.*, 1997) and disruption of

precerebellar nuclei in *Pax6* null mutants has been attributed to defects in non-glial guided migration (Engelkamp *et al.*, 1999).

Type of molecule	Molecule	Function	Reference
Extracellular matrix (ECM) molecules	Reelin	Secreted ECM-like protein expressed by CR cells and mutated in *reeler* mice. Mutants exhibit cortical lamination defects; late born neurons fail to migrate past preplate and radial glia are abnormal.	D'Arcangelo *et al.*, 1995 Ogawa *et al.*, 1995 Hirotsune *et al.*, 1995
	Laminin	Required for cerebellar granule cell migration *in vitro*	Liesi, *et al.*, 1992
Receptors for ECM components	$\alpha_3\alpha_v$ and α_6 integrins	Cell surface receptors for ECM which mediate cell-ECM and cell-cell interactions; α_v required for cortical neuron-glia interaction *in vitro*, α_3 for neuron-neuron interactions; α_6 null mice exhibit ectopic clumps of cortical plate neurons.	Georges-Labouesse *et al.*, 1998 Zhang & Galileo, 1998 Anton *et al.*, 1999
Signalling molecules/ pathways	Mouse disabled 1 (mdab1)	Cytoplasmic protein expressed throughout cortex. *Mdab1*$^{-/-}$ (*scrambler*) mice similar to *reeler*; putative role in transduction of reelin signal.	Howell *et al.*, 1997 Sheldon *et al.*, 1997 Goffinet *et al.*, 1997
	VLDL receptor/ apolipoprotein E receptor 2 (ApoR2)	Both receptors bind mdab1; null mice exhibit *reeler* phenotype - probable involvement in same signalling pathway	Trommsdorff *et al.*, 1999
	Neuregulins (NRGs) and erbB receptors	NRGs are members of EGF family expressed by cerebellar granule cells and cortical neurons; NRG promotes cortical glial migration and promotes radial glial elongation. NRG signalling required to induce cerebellar radial glia formation and neuronal migration.	Rio *et al.*, 1997 Anton, *et al.*, 1997
	Brain lipid binding protein (BLBP)	Expression correlated with neuronal glial migration; required to maintain differentiation of neurons on radial glia	Feng *et al.*, 1994 Feng & Heintz, 1995
Cell adhesion molecule	Astrotactin	Cell adhesion molecule expressed in cortical neurons; required for neuron-glia binding and cerebellar glial migration *in vitro*	Zheng *et al.*, 1996
Ion channels	K channel	Mutated in the *weaver* mutant; required for cerebellar granule cell differentiation and radial-glial guided migration	Patil *et al.*, 1995
	N-type Ca^{2+} channels and NMDA glutamate receptors	*In vitro* inhibition of Ca^{2+} influx/intracellular Ca^{2+} fluctuations blocks cerebellar migration. Possibly involved in regulating cytoskeletal assembly or conformation of cell adhesion molecules	Komoru & Rakic, 1992 Komoru & Rakic, 1996
Cytoskeletal or cytoskeletal regulation	Doublecortin	Expressed in migrating and differentiating cortical neurons in association with microtubules; mutations cause disrupted cortical lamination in human X-linked lissencephaly	Gleeson *et al.*, 1998 Francis *et al.*, 1999
Cytoskeletal regulation	Cyclin-dependent kinase 5 (cdk5) and its activator p35	Expressed in postmitotic cortical neurons; cdk5 phosphorylates cytosekeletal proteins. *Cdk5*$^{-/-}$ mice lack cortical lamination; neurons migrate into preplate but late born neurons fail to migrate past earlier established layers.	Ohshima *et al.*, 1996 Chae *et al.*, 1997
	Filamin1	Actin-crosslinking protein expressed in developing cortex; mutations cause cortical migratory defects in human periventricular heterotopia	Fox *et al.*, 1998

Table 1.2 Some of the molecules involved in radial glial-guided migration

1.1.4 Thalamocortical innervation and regional specification

Normal cortical development occurs under the influence of other areas of the brain. In particular the thalamus, a region of the dorsal diencephalon, relays sensory information to the cortex via the extensive projection of thalamocortical axons (TCAs). The timing of thalamocortical projection is summarised in Table 1.3. Neurons which will produce TCAs are born in the dorsal thalamus between E10.5 and E13.5 in mice (Angevine, 1970). The axons from these cells extend through the ventral diencephalon and ventral telencephalon into the cortex; the first axons arriving in the cortex by E13.5 (Bicknese *et al.*, 1994; Fig. 1.11). TCAs extend tangentially within the subplate layer to their target cortical area (Ghosh & Shatz, 1992; Miller *et al.*, 1993; Bicknese *et al.*, 1994) guided by subplate cells (Molnar *et al.*, 1998b). Axons then pause for a period that varies depending on the species (imperceptible in rodents but up to two weeks in cats) in the subplate before extending branches into the cortical plate (Erzurumulu & Shaveri, 1990; Catalano *et al.*, 1991; Ghosh & Shatz, 1992; Molnar *et al.*, 1998a).

Evidence suggests that thalamocortical innervation plays at least three roles in cortical development: in cortical cell survival, neurite outgrowth and determining regional identity. The first two roles were suggested by *in vitro* studies, showing that diffusible factors released from the thalamus promote survival of subplate cells (Price & Lotto, 1996) and non-directional neurite outgrowth from cortical layers (Lotto & Price, 1996; Lotto *et al.*, 1999) at mid-late stages of development (E15-E19).

Specification of transverse cortical domains (Fig. 1.1B) appears to involve both early and late cues (reviewed in Levitt *et al.*, 1997):

- early: progenitors in the VZ contain positional information (a 'protomap') inherited by the cells they generate;
- late: extrinsic cues, including thalamocortical innervation, act on cortical tissue after neurons settle in the cortical plate.

Early regionalisation is supported by evidence showing region-specific expression of molecular markers prior to thalamocortical innervation (reviewed in Levitt, *et al.*, 1997; Rubenstein *et al.*, 1999), such as the cell adhesion molecule limbic-system-associated membrane protein (LAMP; Barbe & Levitt, 1991; Eagleson *et al.*, 1997), latexin (Arimatsu *et al.*, 1992; Arimatsu *et al.*, 1999) and T-brain-1 (Bulfone *et al.*, 1995) and regional differences in rates of proliferation (Dehay *et al.*, 1993; Polleux *et al.*, 1997). However, the occurrence of non-radial migration is difficult to reconcile with an early regionalisation hypothesis, as non-radial migration fails to transfer positional information in the VZ to neurons of the CP.

Thalamocortical innervation is thought to be a critical late determinant of regional identity. Firstly, thalamocortical projections are organised such that specific thalamic nuclei project to precisely targeted cortical areas (Hohl-Abrahao & Creutzfeldt, 1991; Braisted & O'Leary,1995; DeCarlos & O'Leary, 1992). Secondly, transplant experiments suggest that thalamocortical input can directly alter regional identity. Afferents from the ventroposterior (VP) thalamic nucleus, which normally innervate only somatosensory cortex, will invade visual cortex transplanted into newborn somatosensory cortex and cause the transplanted tissue to differentiate with architecture characteristic of somatosensory cortex (Schlagger & O'Leary, 1991). This may partly explain why rat cortical transplants to different areas of older cortex develop structure and projections appropriate to the host tissue (O'Leary *et al.*, 1992). However, *Gbx-2* null embryos, which lack thalamocortical innervation, express cortical region-specific genes normally (Miyashita-Lin *et al.*, 1999), suggesting that thalamocortical innervation alone cannot account for cortical regionalisation.

One hypothesis reconciling early and late determinants of regional identity suggests that early patterning is confined to cells of the preplate and subplate (O'Leary, 1989; O'Leary *et al.*, 1995). Positional information in the VZ could be conserved in the preplate and used by thalamic efferents growing in the subplate for cortical targeting. TCA innervation and local cell-cell interactions within a region together create region-specific functional identity.

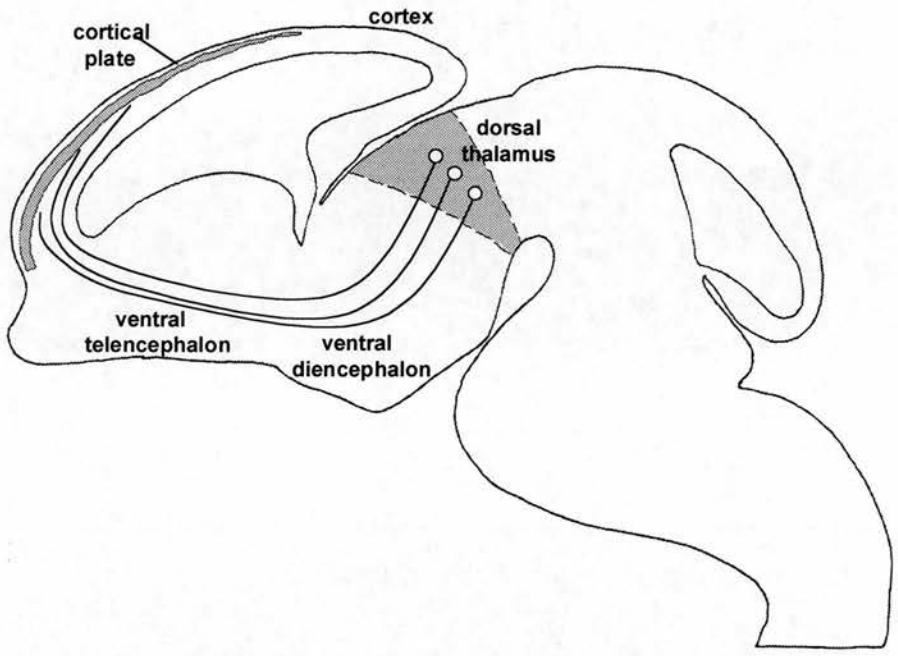

Figure 1.11 Pathway of thalamocortical axons

Drawing representing a parasagittal view of an E15.5 wildtype brain illustrating the pathway of thalamocortical axons from dorsal thalamus through the ventral diencephalon and ventral telencephalon to the cortex. Axons grow to their target cortical area in the subplate before extending branches into the overlying cortical plate.

Age	Events
E10.5	Birth of first prospective TCAs in dorsal thalamus and start of neurogenesis in the cortex
E12.5	Commencement of thalamocortical axonal outgrowth from thalamus and corticothalamic outgrowth from cortical preplate
early E13.5	Corticothalamic and thalamocortical axons meet in basal telencephalon
E13.5	Arrival of first thalamic axons in cortex; first cortical neurons settle in the cortical plate
E14.5-16.5	Majority of thalamic axons arrive under the cortex
E16.5-17.5	Major invasion of the cortical plate by TCAs begins
P0	Arrival of thalamic axons in cortical plate layer 4

Table 1.3 Chronology of thalamocortical innervation in the mouse (adapted from Molnar & Blakemore, 1995)

1.2 *Pax6*

As apparent from the previous section, cortical development is a highly co-ordinated process, requiring correct tissue patterning, proliferation and cell fate specification. An important step in understanding these processes is elucidating their underlying molecular mechanisms. However, our current knowledge in this area is very limited. In this next section I will go on to discuss why the transcription factor *Pax6* is a key candidate gene for regulation of a number of different aspects of cortical development, having first discussed the *Pax* gene family in general.

1.2.1 The *Pax* gene family

The identification of genes involved in early patterning in *Drosophila* has had a profound impact on our understanding of vertebrate development. The high degree of conservation between *Drosophila* and vertebrate genes has allowed developmental gene families to be identified by means of sequence homology. One such family is the *Pax* genes (Walther *et al.*, 1991) which exhibit homology to a DNA-binding motif present in the *Drosophila* genes *paired* and *gooseberry* (Bopp *et al.*, 1986).

The murine Pax family consists of nine members which all contain a 128 amino acid paired domain at the amino terminal end. Sequence comparison places the *Pax* genes into four distinct subgroups (Fig. 1.12) defined by the presence or absence of two other conserved regions, an octapeptide and a paired-type homeobox (Walther *et al.*, 1991). Genes within a group also share intron/exon boundaries and a higher degree of coding sequence similarity than with other *Pax* genes, suggesting that the subgroups may reflect the evolutionary history of the family via gene duplication and divergence. Sequence-specific DNA binding activity of the paired domain and homeodomain intimate the Pax proteins act as transcription factors (Chalepakis *et al.*, 1991). The crystal structure of the paired domain of *Drosophila paired* reveals distinct N- and C-terminal subdomains of which the highly conserved N-terminal domain makes DNA contacts and confers the different DNA binding specificities of Pax proteins (Xu *et al.*, 1995; Czerny & Busslinger, 1995).

The *Pax* family members show dynamic expression patterns during development; with the exception of *Pax1* and *Pax9* all are expressed in specific domains along the DV axis of the spinal cord and in the developing brain (Stoykova & Gruss, 1994; summarised in Figure 1.13). Of these, *Pax6* alone is a candidate regulator of telencephalic development. On a cellular level *Pax* genes appear to function in cell proliferation, differentiation and migration (reviewed in Mansouri *et al.*, 1996).

Pax gene	Conserved domains N — Paired domain — Octapeptide — Paired-type homeobox — C	Chromosomal location Mouse	Human
Group1			
Pax1		2	20p11
Pax9		12	14q12-q13
Group 2			
Pax2		19	10q25
Pax5		4	9p13
Pax8		2	2q12-q14
Group3			
Pax3		1	2q35
Pax7		4	1p36
Group 4			
Pax4		6	7
Pax6		2	11p13

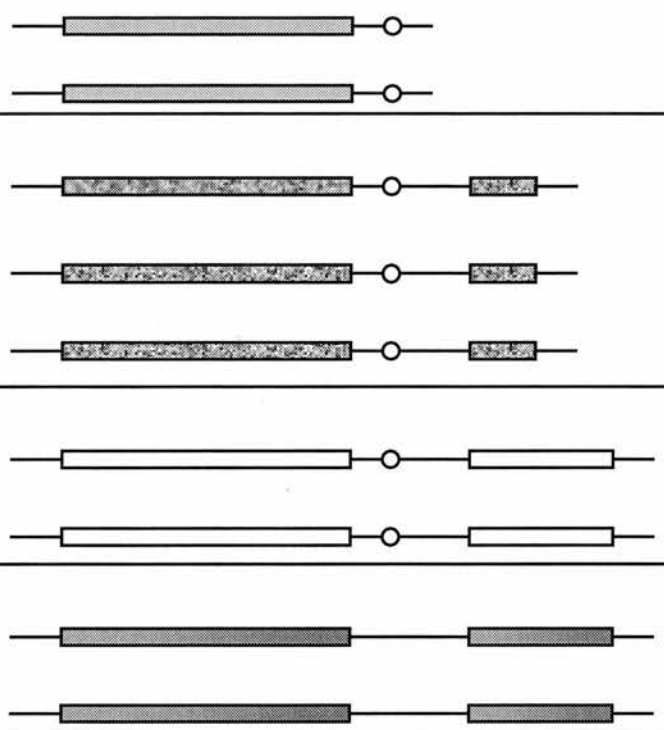

Figure 1.12 Structure and chromosomal location of the Pax proteins.

All the proteins contain a conserved paired domain at the amino terminal end. Related genes are placed into subgroups (shown by the same shading) defined by the presence or absence of two additional conserved domains: an octapeptide and a paired-type homeodomain. The paired domain and homeodomain exhibit sequence-specific DNA binding activity (adapted from Mansouri *et al.*, 1996).

Gene	Expression pattern								Vertebrate mutants (and affected structures)		References
	CNS					Mesoderm					
	Forebrain Tel	Forebrain Di	Midbrain	Hindbrain	Spinal cord	Neural crest	Somite Scler	Somite Derm	Kidney	Other	mouse	human	
Group 1										pharyngeal pouches, thymus	*Undulated* (axial skeletal and thymus defects)		Balling et al.,1988 Wallin, et al.,1994 Helwig et al.,1995
Pax1													
Pax9										pharyngeal pouches, thymus	Targeted mutant (pharyngeal pouch derivatives, craniofacial and limb skeleton)		Peters et al., 1998
Group 2	proximal eye structures: optic stalk			medial									
Pax2											*Mouse krd* (*kidney and retinal defects)* and targeted mutant (eye and urogenital system)	Renal-coloboma syndrome	Dressler et al., 1990 Nornes et al., 1990 Torres et al., 1995 Favor et al., 1996
Pax5				medial						B cell lineage	Targeted mutant (B cell differentiation and midbrain patterning		Urbanek et al., 1994
Pax8				medial						thyroid	Targeted mutant (thyroid)		Plachov et al., 1990
Group 3				dorsal									
Pax3											*Splotch* (neural crest derivatives, limb myoblast)	Waardenburg syndrome	Epstein et al., 1991 Tassabehji et al., 1993
Pax7				dorsal							Targeted mutant (neural crest derivatives)		Mansouri, et al., 1996
Group 4				ventral						pancreas	Targeted mutant (pancreas)		Sosa-Pineda, et al., 1997
Pax4													
Pax6	distal eye structures;optic vesicle, lens placode; nasal placodes			ventral						pancreas	*Small eye (*eye, brain and pancreas)	Aniridia and other eye defects	Hogan et al., 1986 Freund et al., 1996(Stoykova et al., 1996

Figure 1.13 Summary of the expression patterns and mouse and human mutant syndromes caused by mutation of Pax genes. Tel, telencephalon; di, diencephalon; scler, sclerotome; derm, dermomyotome (adapted from Mansouri *et al.*, 1996)

1.2.2 *Pax6*: General background

1.2.2.1 Pax6 gene *Pax6* encodes a 422 amino acid protein containing two known DNA-binding domains, a paired domain of 128 amino acids and a paired-type homeodomain of 61 amino acids (Ton *et al.*, 1992). A C-terminal transcriptional activation domain has also been identified (Glaser *et al.*, 1994). The gene encodes two proteins with different DNA-binding properties produced by alternative splicing of a 14 amino acid exon (exon 5a) in the paired domain. Eye defects in a family with an exon 5a splice acceptor site mutation suggest that the ratio of alternative spliced products may be important in gene function (Epstein *et al.*, 1994). The expression pattern of *Pax6* in the developing CNS, eye, nasal epithelium and pancreas will be described in detail below.

1.2.2.2 Pax6 function and haploinsufficiency

The role of *Pax6* in eye development has been extensively studied (reviewed in Hanson & van Heyningen, 1995; Gehring & Ikeo, 1999). In humans, heterozygous mutations in *PAX6* are responsible for aniridia (Glaser *et al.*, 1992; Jordan *et al.*, 1992) and a range of other eye phenotypes without aniridia (reviewed in Freund *et al.*, 1996). Mice heterozygous for mutations in *Pax6* exhibit the *Small eye* (*Sey*) phenotype (Hill *et al.*, 1991), which is characterised by reduced eye size, lens and iris defects and cataracts (Hogan *et al.*, 1986). Homozygous *Sey* mice fail to develop eyes and nasal cavities, exhibit brain abnormalities and die soon after birth. A rare human case of a baby with compound heterozygote mutations for *PAX6* exhibited a similar phenotype (Glaser *et al.*, 1994). A rat *Sey* phenotype has also been described (Matsuo *et al.*, 1993). The phenotypic similarity between *Sey* mice and humans with *PAX6* mutations supports the use of the mouse mutant as a model for the human disorder.

The increased severity of eye defects in *Sey* homozygotes compared to heterozygotes provides evidence that the level of *Pax6* expression is critical in eye development. This has been supported by transgenic experiments in which expression of human *PAX6* rescued the *Sey* mutant phenotype, but overexpression caused different developmental abnormalities of the eye (Schedl *et al.*, 1996). The role of *Pax6* dosage in brain development is less clear: although minor defects have been reported in the cortex and olfactory bulbs of *Sey* heterozygotes (Schmahl *et al.*, 1993; Dellovade, *et al.*, 1998), *Pax6* expressing tissues other than the eye were grossly unaffected by increased gene dosage (Schedl *et al.*, 1996).

1.2.2.3 Conservation of Pax6

The Pax6 protein, its expression pattern and function are highly conserved throughout

evolution. Isolation of the *Drosophila* homologue of *Pax6* revealed it to be responsible for the *eyeless* (*ey*) fly (Quiring *et al.*, 1994), and highly conserved *Pax6* homologues have now been found in most animal groups studied so far (reviewed in Callaerts *et al.*, 1997). These include a wide range of vertebrates: rat (Matsuo *et al.*, 1993), chicken (Li *et al.*, 1994), quail (Plaza *et al.*, 1993), zebrafish (Krauss *et al.*, 1991; Nornes *et al.*, 1998), and invertebrates: sea urchin (Czerny & Busslinger, 1995), squid (Tomarev *et al.*, 1997), ribbonworm (Loosli *et al.*, 1996), nematodes (Chisholm & Horwitz, 1995; Zhang & Emmons, 1995), amphioxus (Glardon *et al.*, 1998), planarian (Callaerts *et al.*, 1999) and ascidian (Glardon *et al.*, 1997).

Mouse and rat Pax6 proteins are identical (Matsuo *et al.*, 1993) and show 94% identity to *Drosophila* Pax6 in the paired domain (Quiring *et al.*, 1994). The planarian Pax6 is the most diverged found to date, yet still shows 73% identity to the vertebrate gene in the paired domain (Callarets *et al.*, 1999). The remarkably high degree of gene conservation suggests that strong selection pressure has acted against mutations arising in *Pax6*. Targeted ectopic expression of both mammalian and invertebrate *Pax6* has been shown to induce the formation of ectopic eyes in *Drosophila* imaginal discs (Halder *et al.*, 1995; Loosli *et al.*, 1996). Injection of *Pax6* RNA can induce ectopic eyes in *Xenopus* (Chow *et al.*, 1999), further demonstrating their high degree of functional conservation and the essential role played by *Pax6* in eye formation. It has been suggested that *Pax6* may function as a master control gene in a common genetic programme, triggering eye development in both vertebrates and invertebrates. *Pax6* expression, however, is not limited to eye structures or to species with eyes, and in all species investigated so far, *Pax6* is also expressed in other parts of the CNS. Conserved expression in the developing nervous system implies a fundamental role in neural development. In *C. elegans*, which lacks eyes, homologues of *Pax6* are involved in head patterning (Chisholm & Horwitz, 1995) and sense organ identity (Zhang & Emmons, 1995). These findings suggest the ancestral *Pax6* gene may have been involved in anterior neural tissue specification and its presence was a prerequisite for eye development during elaboration of the nervous system (Gehring & Ikeo, 1999).

1.2.2.4 Regulators and targets of Pax6

Recent experiments have demonstrated that conservation of *Pax6* extends to its regulatory regions; insertion of the enhancer region of the *Drosophila eyeless* gene upstream of mouse *Pax6* directs normal eye and CNS expression (Xu *et al.*, 1999). Analyses of the structure of *Pax6* genes suggests its expression in different tissues is regulated by several proteins and differential use of regulatory promoters, enhancers and repressors. Conserved regulatory elements have been identified in mouse and human *Pax6* which, when used in *lacZ* reporter constructs, result in expression in distinct domains of the developing eye, pancreas and CNS

(Xu & Saunders, 1997; Williams *et al.*, 1998; Kammandel *et al.*, 1999; Xu *et al.*, 1999). However, little is known about the genes involved in directing *Pax6* expression.

Downstream, current evidence suggests that *Pax6* regulates expression of a range of functionally dissimilar target genes. Ultimately, it is necessary to confirm direct interactions of *Pax6* with putative target elements using biochemical screens such as electromobility shift assays and cellular transfection experiments. Candidate regulators and targets of *Pax6* are summarised in Tables 1.4 and 1.5 respectively, and some are discussed where appropriate in the following sections.

Molecule	Evidence	Role	References
Shh	Treatment of neural plate explants with Shh represses *Pax6* expression; Shh signalling from the notochord and floor plate creates a dorsal high-ventral low gradient of Pax6 in the ventral neural tube. Role of Shh in the eye is described below.	Indirect repressor of *Pax6* expression	Goulding *et al.*, 1993 Ekker *et al.*, 1995 Macdonald *et al.*, 1995 Burrill *et al.*, 1997 Osumi *et al.*, 1997 Ericson *et al.*, 1997
Pax2, protein kinase A (PKA)	In the zebrafish *Shh* $^{-/-}$ (cyclops) mutant *Pax2* expression in the eye is lost and *Pax6* expression expanded; conversely, ectopic *Shh* expression induces *Pax2* and inhibits *Pax6*. *Pax2* $^{-/-}$ mouse mutant exhibits expanded *Pax6* expression domains in the eye. *PKA* injection mimics the *Shh* overexpression phenotype and rescues optic stalk defects in cyclops mutant.	*Pax2* and *PKA* thought to act downstream of Shh-mediated pathway- restrict *Pax6* expression to lateral optic vesicle and optic cup.	Torres, *et al.*, 1996 Hammerschmidt, *et al.*, 1996 reviewed in Macdonald & Wilson, 1996
Activin A	Expressed in the dorsal neural tube, abolishes *Pax6* expression in chick neural plate explants correlating with impaired motor neuron differentiation	Indirect downregulator of *Pax6* expression in dorsal neural tube	Pituello *et al.*, 1995 Liem *et al.*, 1997
Pax6	Quail *Pax6* directly upregulates its own transcription via binding sites in its promoter In the *Sey/Sey* mouse onset of expression of the mutant form of *Pax6* in the surface ectoderm at E8 is normal. By E9.5, when expression normally becomes restricted to lens and nasal placodes, expression in surface ectoderm is completely lost. Boundaries of *Pax6* expression are also altered in the *Sey/Sey* brain	Autoregulation	Plaza *et al.*, 1993 Grindley *et al.*, 1995 Mastick *et al.*, 1997
c-myb (transcriptional regulator)	*c-myb* expression coincident with quail *Pax6-QNR* in neuroretina; transactivates the *Pax6-QNR* promoter, directly by DNA binding in promoter regions, and indirectly	Putative neuroretinal regulator:	Plaza *et al.*, 1995
Brn-3b	Interacts with quail *Pax6* promoter and activates *Pax6* expression in neuroretina cells *in vitro*	Putative neuroretinal regulator	Plaza *et al.*,,1999

Table 1.4 Putative regulators of *Pax6* expression

Region	Gene	Evidence	Reference
Eye	Crystallins	*Pax6* binding sites in the control regions of several lens crystallin genes are necessary for lens-specific expression	reviewed in Cvekl & Piatigorsky, 1996
	Eye developmental genes: *sine oculis, eyes absent dachsund, teashirt* and *eyegone*	Series of genes which, like Pax6, can drive ectopic eye formation in *Drosophila;* thought to function in a complex regulatory network regulating *Drosophila* eye development Mouse homologs of *sine oculis* (*Six* gene family) and *eyes absent* (*Eya* gene family) have been identified - possible that regulatory interactions with *Pax6* could be conserved.	Bonini *et al.*, 1993 Cheyette, *et al.*, 1994 Mardon, *et al.*, 1994 Serikaku & O'Tousa, 1994 Bonini *et al.*, 1997 Shen & Mardon, 1997 Pan & Rubin, 1998 Jang, Development, in press Oliver, *et al.*, 1995 Xu *et al.*, 1997
	Msx1	Loss of expression from nasal placode in *Sey/Sey*	Grindley *et al.*, 1995
Spinal cord and hindbrain	Spinal cord: *Pax2, Nkx2.2, En1,Chx10,* LIM domain proteins Islet1/2,Lim3 Hindbrain: *Islet-2, Wnt-7b*	Altered expression domains in ventral spinal cord or hindbrain in *Sey/Sey* corresponding to altered cell fates	Ericson *et al.*, 1997 Burrill *et al.*, 1997 Osumi, *et al.*, 1997
Cerebellum	Netrin receptor *Unc5h3*	Expression lost from external granule cells in cerebellum	Engelkamp, *et al.*, 1999
Forebrain	Patterning molecules including Shh, HNF3β; members of *Dlx, Otx, Wnt, Dbx* gene families, *Patched, Prox1, Mash1, Gli3, Lim1, Gsh1, Tcf-4.* Cell adhesion molecules *R-cadherin;* ECM molecule *tenascin-C*	Regionally expressed patterning genes exhibiting altered or absent expression domains or boundaries in the forebrain of *Sey/Sey* mice	Stoykova *et al.*, 1996 Grindley *et al.*, 1997 Stoykova *et al.*, 1997 Mastick, *et al.*, 1997 Warren & Price, 1997 Cho & Dressler, 1998
Cortex	Neural cell adhesion molecule *L1* *TuJ1, Sox11,* neurotrophin receptors *trkB, trkC* *tenascin-C*	*Pax6* binds regions of L1 promoter region *in vitro;* altered pattern of *L1* expression in *Sey/Sey* cortex Altered expression patterns in *Sey/Sey*	Chalepakis *et al.*, 1994 Caric *et al.*, 1997 Meech *et al.*, 1999 Gotz *et al.*, 1998 Warren *et al.*, 1999

Table 1.5 Candidate targets and downstream genes of *Pax6* in development

1.2.3 *Pax6* expression pattern

Pax6 expression in the mouse embryo begins at E8.0 in the anterior surface ectoderm and neuroepithelium of the closing neural tube in the presumptive spinal cord, fore- and hindbrain (Fig 1.14). This pattern is largely maintained throughout development.

In the developing spinal cord, early widespread expression across the DV axis of the neural tube becomes gradually restricted from E9.5 to the ventral region excluding the floor plate or cells adjacent to the floor plate. As the neural tube becomes stratified from E11.5, *Pax6* is expressed predominantly in the ventricular zone (VZ) around the lumen. This declines as the VZ regresses with the end of neurogenesis although expression is maintained in a subset of postmitotic cells (Walther & Gruss, 1991; Stoykova & Gruss, 1994). In the hindbrain *Pax6* is highly expressed in the rhombic lip at E12.5 (Engelkamp *et al.*, 1999) and in structures derived from it: rostrally, the cerebellar granule cell precursors, and caudally, the precerebellar neuroepithelium from which *Pax6* positive cells migrate to form the precerebellar nuclei.

In the forebrain, *Pax6* expression throughout the prosencephalic neuroepithelium at E9.5 (Fig.1.14; Mastick *et al.*, 1997) gradually becomes restricted to the developing cortex and regions of the dorsal diencephalon (Walther and Gruss, 1991; Stoykova & Gruss, 1994; Grindley *et al.*, 1995; Grindley *et al.*, 1997; Stoykova *et al.*, 1996; Mastick *et al.*, 1997; Warren & Price, 1997). As in the spinal cord, expression occurs chiefly in the mitotically active regions: in the telencephalon, *Pax6* is expressed in the ventricular zone at E13.5 and by E16.5 extends into the subventricular zone (Caric *et al.*, 1997). The optic vesicle, which buds from the neural ectoderm of the ventral prosencephalon, and the olfactory bulb, which develops from the rostral telencephalon, also express *Pax6*. Expression in the anterior surface ectoderm becomes restricted to the eye and nasal placodes by E9 (Walther & Gruss, 1991; Stoykova & Gruss, 1994; Grindley *et al.*, 1995).

Pax6 is also expressed in the developing pancreas (Turque *et al.*, 1994; St-Onge *et al.*, 1997), and in the adult, *Pax6* is still present in postmitotic cells of the ventral thalamus, olfactory epithelium, olfactory bulb (Stoykova & Gruss, 1994) and internal granule cells of the cerebellum (Dieter Engelkamp and Penny Rashbass, personal communication).

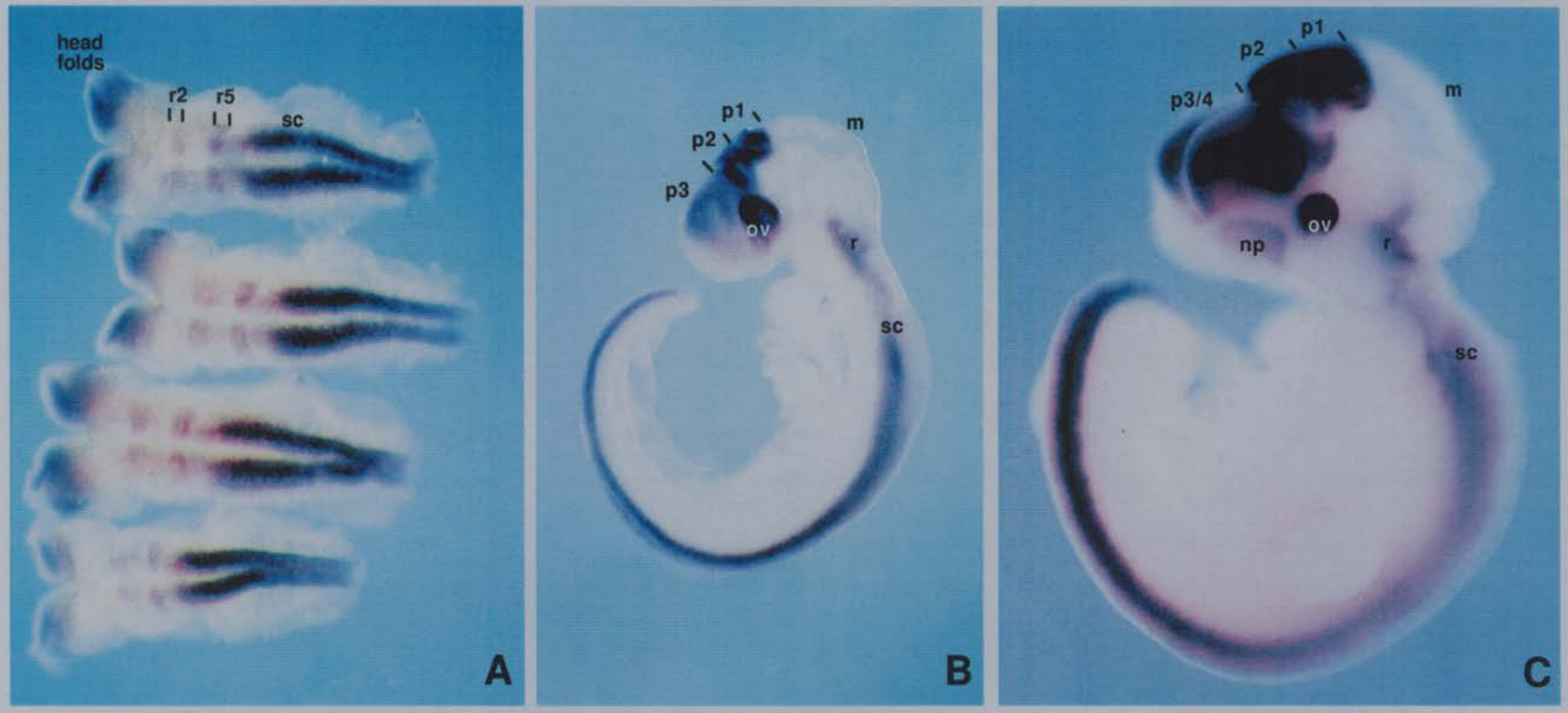

Figure 1.14 Wholemount *in-situ* hybridisation of *Pax6* during mouse embryogenesis

A. Dorsal view of E8.5 mouse embryos, showing expression in the developing head folds, rhombomeres 2 and 5 (r2, r5) and the presumptive spinal cord (sc).

B. Lateral view of E9.5 mouse embryo; *Pax6* is expressed in the lens placode, the dorsal prosencephalon including prosomeres 1-3 (p1-3), optic vesicle (ov), rhombencephalon (r) and presumptive spinal cord. Further prosomeric subdivisions cannot be distinguished at this stage.

C. Lateral view of E10.5 mouse embryo; *Pax6* is expressed in the nasal placodes (np), lens placode, optic vesicle (ov), developing telencephalon and diencephalon (prosomeres 1-4), rhombencephalon and spinal cord.

m, mesencephalon; np, nasal placode; oc, optic cup; ov, optic vesicle; p1-4, prosomeres 1-4; r, rhombencephalon; sc spinal cord (from P. Rahsbass).

1.2.4 Roles of *Pax6* in development

The defects in *Pax6* expressing tissues in the *Sey* homozygote mouse have given insights into the different roles that Pax6 may play throughout development. In this section I will outline the evidence for roles in the eye, spinal cord, hindbrain and forebrain.

1.2.4.1 Eye and nasal development

During normal eye development the optic vesicle contacts the overlying surface ectoderm, causing it to thicken into the lens placode; optic vesicle and lens placode then invaginate to form the optic cup and lens (Fig. 1.15A). In the *Sey/Sey* embryo, although initial contact between optic vesicle and surface ectoderm occurs, the lens placode does not form and the optic vesicle subsequently degenerates (Hogan *et al.*, 1986; Fujiwara *et al.*, 1994; Grindley *et al.*, 1995). Similarly, contact of the neuroepithelium with the surface ectoderm fails to initiate nasal placode formation and invagination of nasal pits (Hogan *et al.*, 1986; Grindley *et al.*, 1995). In addition, neurons of the rostral migratory stream, which are born in the SVZ of the anterior cortex and normally migrate into the olfactory bulb, fail to invade the olfactory bulb in *Sey/Sey* (Stoykova *et al.*, 1997).

Construction of chimeric mouse embryos from wildtype and *Sey/Sey* cells suggest that Pax6 acts cell autonomously in surface ectoderm and optic vesicle (Quinn *et al.*, 1996). Mutant cells are excluded from lens and nasal epithelium, suggesting that *Pax6* is required to specify cell fate in surface ectoderm regions which give rise to the lens and nasal placodes. In addition, wildtype and mutant cells do not mix in tissues derived from the optic vesicle, suggesting that Pax6 may play a role in regulating cell adhesion.

1.2.4.2 Spinal cord and hindbrain development

A role for Pax6 in cell fate specification has been established in the developing spinal cord. Here, graded Shh signalling from the notochord and floor plate represses *Pax6* expression, creating a dorsal high-ventral low gradient of Pax6 in progenitor cells across the ventral neural tube (Goulding *et al.*, 1993; Burrill *et al.*, 1997; Osumi *et al.*, 1997). Pax6 acts to repress *Nkx2.2* expression; the combination of *Pax6* and *Nkx2.2* defines populations of progenitors and the neuronal cell types they produce (Fig. 1.16A). Absence of *Pax6* from the spinal cord or hindbrain results in loss or dorsal-ventral transformation of ventrally located neuron populations (Ericson *et al.*, 1997; Osumi *et al.*, 1997; Fig.1.16B) and a dorsal shift in glial cell fates (Sun *et al.*, 1998). These findings demonstrate that *Pax6* expression in the neural tube is required in progenitor cells for the specification of neural and glial cell fate. As discussed earlier (section 1.1.1), Shh is also a key pattering signal in the developing forebrain, and has been shown to regulate expression of *Pax6*, *Nkx2.1* and *Nkx2.2* (Macdonald *et al.*, 1995; Barth

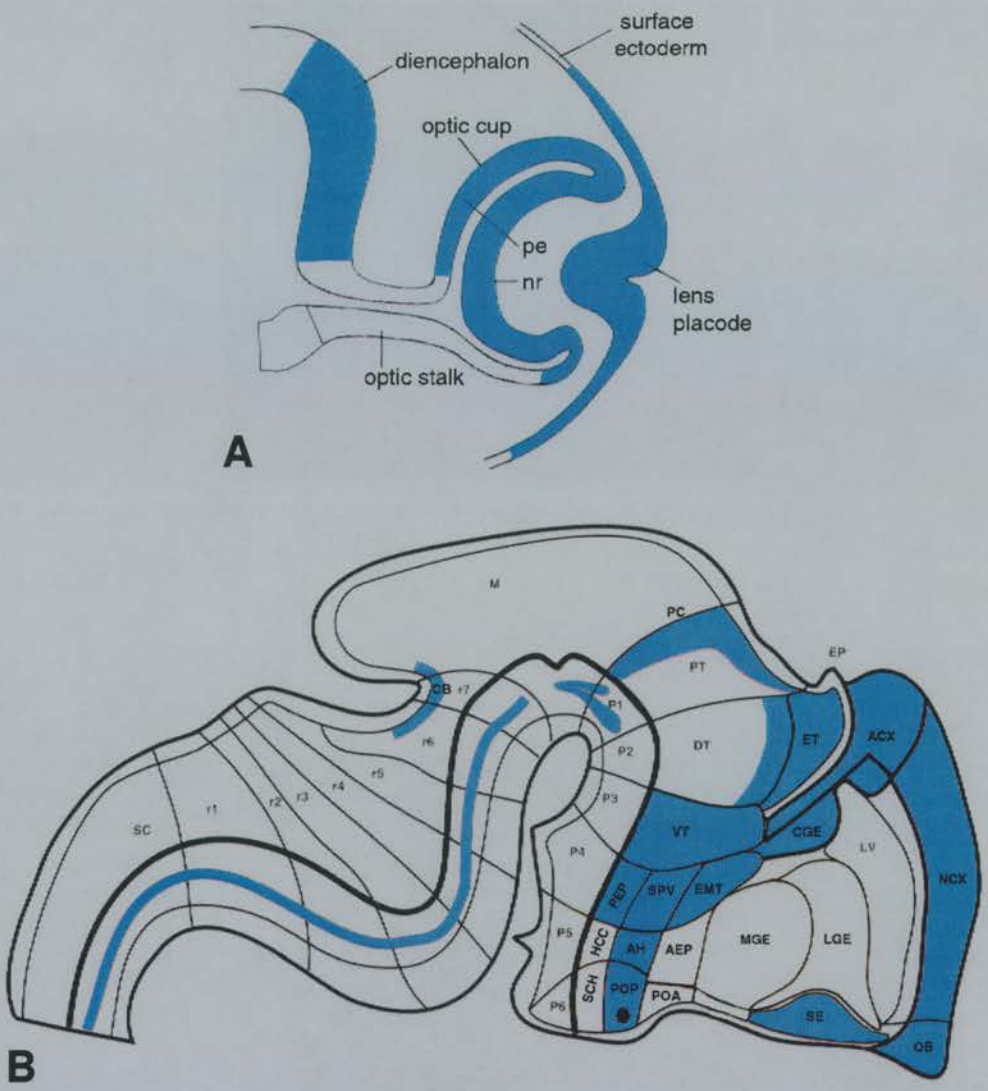

Figure 1.15 Diagrams of Pax6 expression in the developing eye and brain

A. A transverse section through the devloping prosencephalon and eye corresonding to mouse E10.5. *Pax6* (blue) is expressed in both inner and outer layers of the optic cup (pigement epithelium, pe and neural retina, nr) and in the overlying surface ectoderm.

B. *Pax6* expression (blue) mapped on the mouse E12.5 prosomeric model of forebrain patterning (Puelles & Rubenstein, 1993; described in figure 1.5). The forebrain structure derived from each region is labelled. *Pax6* is expressed in the telencephalon in the presumptive neocortex (NCX), archicortex (ACX), olfactory bulb (OB), septum (SE) and caudal ganglionic eminence (CGE). In the diencephalon *Pax6* is expressed in the dorsal midline of the presumtive pretectum (PT) and dorsal thalamus (DT), the presumptive ventral thalamus (VT), eipthalamus (ET) and regions of the hypothalamus (PEP, SPV, EMT, AH and POP). Expression is also shown in the rhombencephalon (cerebellum, CB and ventral rhombomeres (r)1-7) and the ventral spinal cord (SC).

ACX, archicortex; AEP, anterior entopeduncular area; AH, anterior hypothalamus; Cb, cerebellum; CGE, caudal ganglionic eminence; DB, diagonal band; DT, dorsal thalamus; EMT, eminentia thalami; ET, epithalamus; HCC, hypothalamic cell cord; LGE, lateral ganglionic eminence; M, mesencephalon; MA, mammilary area; MGE, medial ganglionic eminence; NCX, neocortex; nr, neural retina; OB, olfactory bulb; pe, pigmented epithelium; P1-P6, prosomeres 1-6; PEP, posterior preoptic area; POA, anterior preoptic area; POP, posterior preoptic area; PT, pretectum; r1-7, rhombomeres 1-7; RCH, retrochiasmatic area; SC, spinal cord; SCH, suprachiasmatic area; SE, septum; SPV, supraoptic/paraventricular area; TU, tuberal hypothalamus, VT, ventral thalamus [adapted from Macdonald & Wilson, 1996 (A) and Stoykova *et al.*, 1996 (B)].

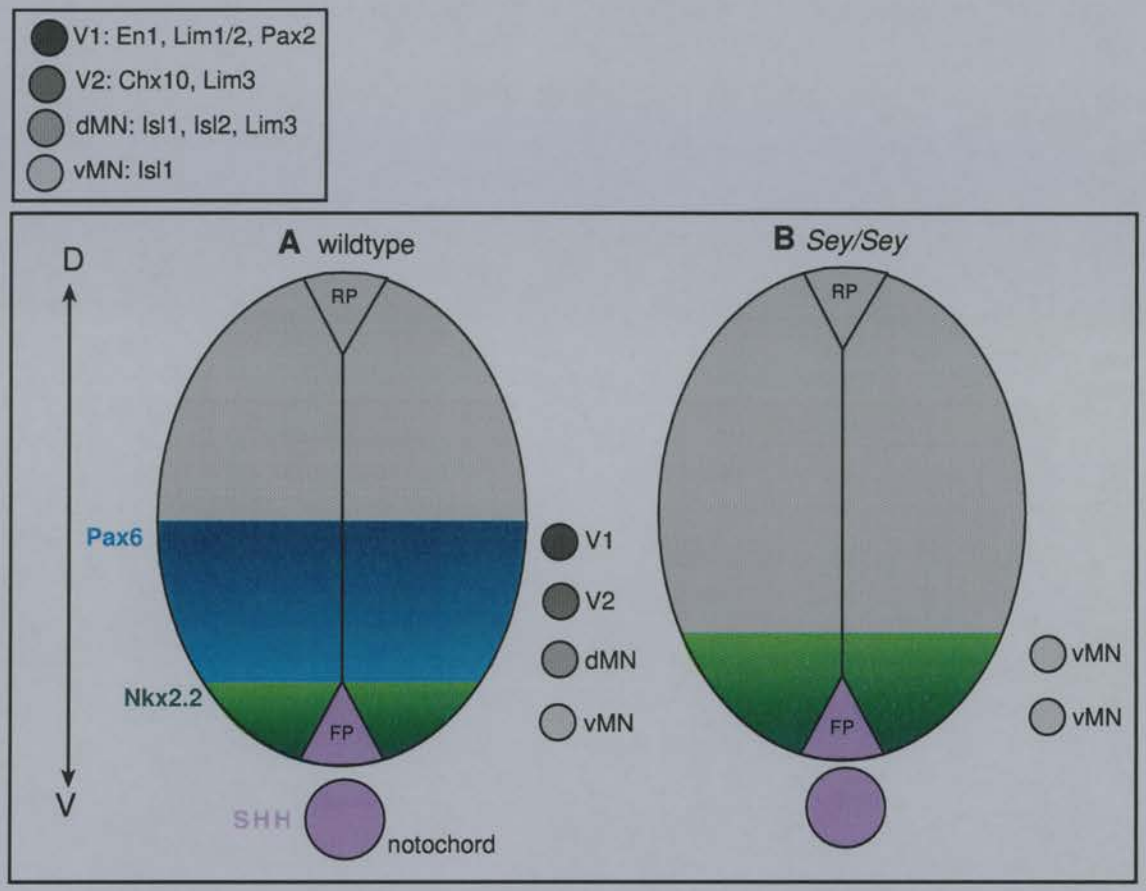

Figure 1.16 The role of *Pax6* in ventral neuronal cell fate determination in the spinal cord

A. Wildtype spinal cord. Graded Shh signalling from the notochord and floor plate creates a dorsal (D) high-ventral (V) low gradient of *Pax6* expression in progenitor cells across the ventral neural tube. Pax6 represses *Nkx2.2* expression to a ventral domain adjacent to the floor plate (FP). *Pax6* and *Nkx2.2* expression defines populations of neuronal progenitors. Different types of neurons produced by these progenitors (indicated by grey shading) can be recognised by expression of different homeodomain genes. *Nkx2.2* positive progenitors give rise to ventral motor neurons (vMN) which express *Isl1*. The ventral-most population of *Pax6* positive progenitors give rise to dorsal motor neurons (dMN) expressing *Isl1*, *Isl2* and *Lim3* whereas more dorsal *Pax6* positive progenitors give rise to ventral internuerons 1 (V1) which express Chx10 and Lim3, and ventral interneurons 2 (V2) which express *En1*, *Lim1/2* and *Pax2*.

B. Changes in progenitor cell domains and neuronal identity in the *Sey/Sey* mutant. Absence of *Pax6* expression creates a dorsal expansion of the *Nkx2.2* expression domain, loss of V1 and V2 interneurons and transformation of dMNs into vMNs.

D; dorsal; FP, floor plate; RP, roof plate; V1, ventral interneurons 1; V2, ventral interneurons 2; dMN, dorsal motor neurons; V, ventral; vMN, ventral motor neurons.

& Wilson, 1995; Ekker *et al.*, 1995; Ericson *et al.*, 1995), raising the possibility that Shh and Pax6 may be involved in cell type specification in more rostral regions of the brain.

Recently, grafting experiments in chick demonstrated that *Pax6* expression is induced in the neural plate by a somite graft, and this activity is not abolished by pre-incubation with Shh antibodies. This suggests that initial activation of *Pax6*, prior to neural tube closure, may be regulated by another signal, independent of Shh, which is released by somites as they differentiate from the paraxial mesoderm beneath the neural plate (Pituello *et al.*, 1999). The nature of such signals has yet to be determined.

A recent study of cerebellar development in *Sey/Sey* embryos highlighted a role for Pax6 in cell migration (Engelkamp *et al.*, 1999). Development of precerebellar nuclei is disrupted - proliferation is unaffected and cell fate markers are expressed normally, yet enlargement of the precursor nuclei suggest cells are born but fail to undergo tangential migration. In addition, cerebellar foliation is absent and granule cell migration is disorganised *in vivo* and *in vitro*. These defects are attributed to a failure in neurite extension (Engelkamp *et al.*, 1999), although they could also be accounted for by altered cell adhesive properties.

1.2.4.3 Forebrain development

In the developing forebrain *Pax6* exhibits a region-specific expression pattern which corresponds to the Puelles & Rubenstein (1993) model of neuromeric segmentation (Fig. 1.15B). Developmental analyses of the *Sey/Sey* forebrain reveal morphological and gene expression defects in regions of *Pax6* expression which suggest the gene may play a key role in forebrain patterning (Stoykova *et al.*, 1996; Stoykova *et al.*, 1996; Warren & Price,1997; Grindley *et al.*, 1997; Mastick *et al.*, 1997). Broad patterning abnormalities arise as early as E9.5, when the caudal prosencephalon, which gives rise to the cerebral vesicles, shows altered morphology (Mastick *et al.*, 1997) and may be compounded by local patterning defects later in development.

Studies in the developing diencephalon have established several different roles for Pax6 in regulating proliferation, cell fate and cell adhesion which may contribute to early patterning defects. First, diencephalic proliferative rates are decreased in the mutant at E10.5 (Warren & Price, 1997). Second, ventral diencephalic cell fates exhibit partial transformation to dorsal fates (Grindley *et al.*, 1997; Mastick *et al.*, 1997; Warren & Price, 1997). Third, E10.5 axons comprising the tract of the postoptic commissure (tpoc) exhibit aberrant pathfinding over

Pax6 expression domains and boundaries in the ventral diencephalon (Mastick *et al.*, 1997).

In addition to patterning defects early in forebrain development, there are late-onset abnormalities in *Sey/Sey* cortical development which become apparent from E14.5. The *Sey/Sey* cortex has a thinner cortical plate, expanded VZ and SVZ and ectopic clusters of cells characteristic of SVZ cells extend into the IZ (Schamhl *et al.*, 1993; Caric *et al.*, 1997). These defects becomes more pronounced with time; the *Sey/Sey* cortical phenotype at E17.5 is shown in Figure 1.17. BrdU labelling studies have shown that whereas early born neurons migrate to their normal position in the overlying cortical plate, late-born (E16.5) neurons fail to migrate past earlier established cortical layers, and instead accumulate within the ventricular layers (Caric *et al.*, 1997). Expression of the early neuronal markers *TuJ1* and *Sox11* by these ectopic cells suggests they are undergoing early stages of neuronal differentiation (Caric *et al.*, 1997; Warren *et al.*, 1999). It is possible that early functions of Pax6 in forebrain patterning make a secondary contribution to the development of late-onset cortical defects. However, the compounding accumulation of cells in the VZ suggests that the gene performs additional functions in cortical progenitors throughout development.

1.2.5 Functions of Pax6

It is clear from the previous section that it is difficult to reconcile the diverse defects observed in the *Sey/Sey* mouse to a single underlying function of Pax6. Pax6 is a transcription factor, and by regulating transcription of more than one gene (or by interaction with other modulatory proteins), it could control different processes at different times, in different cells, or even simultaneously within the same cell. My thesis aims to elucidate the roles of *Pax6* in cortical development.

One way to understand Pax6 function is to directly identify the genetic pathways it is acts in. I employed candidate gene and differential gene expression analyses to identify genes acting downstream of Pax6; these results are presented in Chapters 5 and 6. Alternatively, detailed analyses of cortical development in the *Sey/Sey* mouse can extend our understanding of the cellular roles of Pax6. For the remainder of this section I will discuss my hypotheses for how Pax6 could influence cortical development, and how I have addressed some of them in my experiments.

1. *Cell fate specification*

Pax6 is highly expressed in cortical progenitors, and recent evidence suggests it may play a role in the specification of cortical cell types. Gotz *et al.* (1998) found an increase in radial glial progenitors (RC2 /nestin positive) in the *Sey/Sey* cortex. They examined the cell types

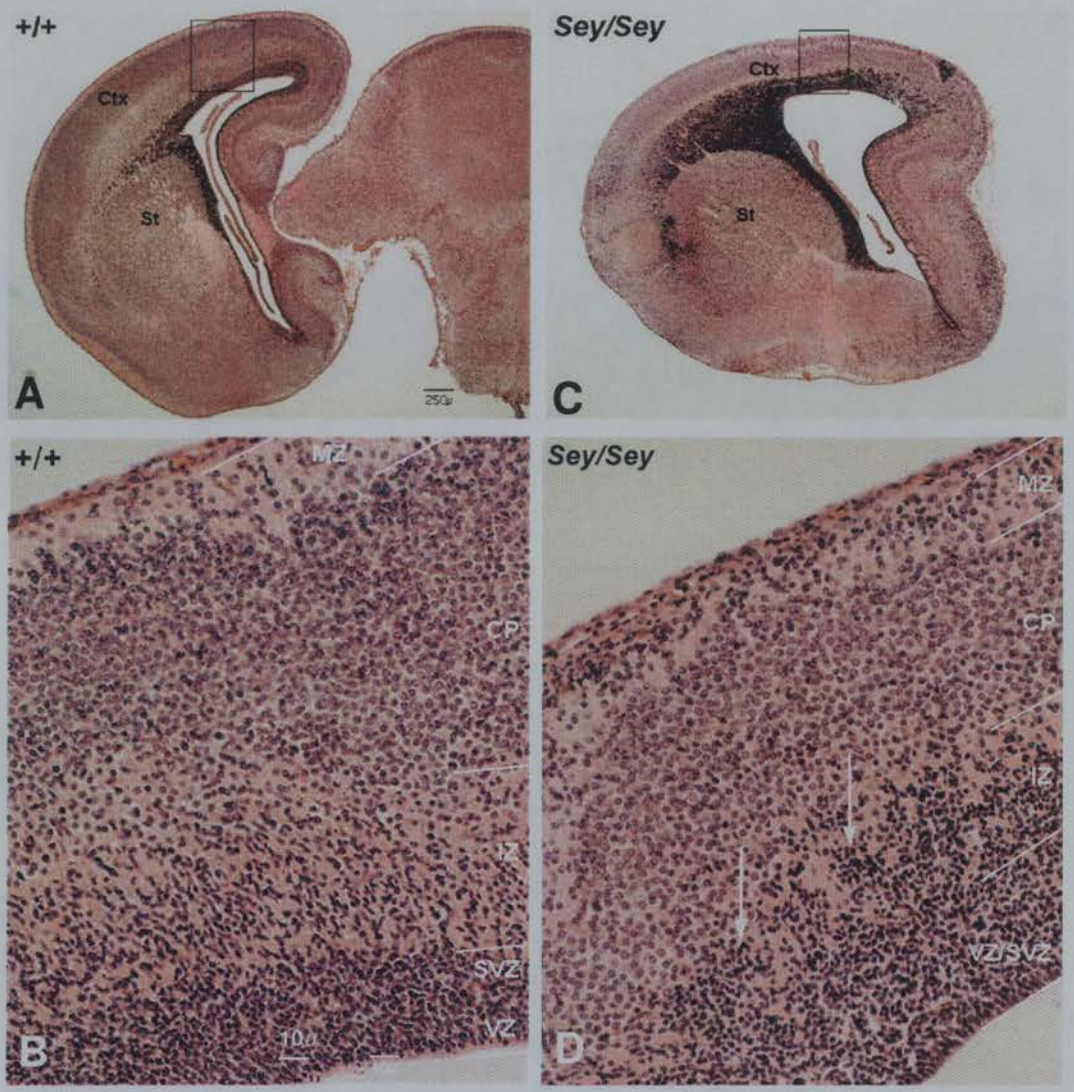

Figure 1.17 Cortical histology in the E17.5 wildtype and *Sey/Sey* brain

H&E stained parasagittal sections of mouse E17.5 telencephalon. In all sections rostral is to the left and dorsal is up.

A. Wildtype telencephalon showing structure of the cortex (Ctx) and striatum (St).

B. High power magnification of the boxed region in (A) showing layers of the embryonic cortex: ventricular zone (VZ), subventricular zone (SVZ), intemediate zone (IZ), cortical plate (CP) and marginal zone (MZ).

C. *Sey/Sey* mutant telencephalon reveals increased width of the ventricular zone (stained dark brown).

D. High power magnification of the boxed region in (C). The *Sey/Sey* cortex has a thinner CP and expanded VZ and SVZ compared to wildtype. Ectopic clusters of SVZ cells extend into the IZ (arrows).

CP, cortical plate; Ctx, cortex, IZ, intemediate zone; MZ marginal zone; St, striatum; SVZ subventricular zone; VZ ventricular zone. Scale bars: A, 250μm and applies to C; B, 10μm and applies to D.

generated by dissociated cortical cells *in vitro* and found that clones generated by *Pax6* null cells contained an excess of RC2 /nestin positive progenitors over other progenitor cell types or neurons. This suggests that cell fate specification in the progeny of *Sey/Sey* multipotential progenitors is aberrant. The neuronal/glial composition of *Sey/Sey* clones is rescued by co-culture with wildtype cells (Gotz *et al.*, 1998), suggesting that Pax6 acts non-autonomously in these cells to regulate release of environmental factors which control progenitor development, and cause a switch to a lineage-restricted or determined cell state.

These findings lead to the suggestion that other cell fates may also be altered in the *Sey/Sey* cortex. I discussed in section 1.1.3 that production of diverse cell types by progenitors is thought to occur by asymmetric division. To address the hypothesis that Pax6 plays a role in this process, an analysis of progenitor cleavage orientation was carried out (Chapter 2) and the distribution of putative cell fate determinants analysed (Chapter 5) in the *Sey/Sey* cortex.

2.*Cell cycle regulation*

BrdU labelling studies have revealed defects in the *Sey/Sey* cortical cell cycle. Firstly, proliferative rates are increased from as early as E10.5 until mid- to late neurogenesis (E15.-5-E17.5; Gotz *et al.*, 1998; Warren *et al.*, 1999). Secondly, progenitor nuclei exhibit differences in distribution within the *Sey/Sey* VZ (Gotz *et al.*, 1998; Warren, *et al.*, 1999). Wildtype nuclei labelled by BrdU incorporation at S-phase, and allowed sufficient time for progression into M-phase, have moved to the ventricular surface, whereas in the *Sey/Sey* cortex, nuclei remain positioned in the basal VZ due to a failure or delay in interkinetic nuclear migration. Taken together this evidence strongly supports a role for Pax6 in regulation of the cell cycle - either in progression through the cell cycle, or in co-ordination of cell cycle kinetics with interkinetic nuclear migration. To explore this possibility the distribution of mitotic cells was analysed in the *Sey/Sey* cortex during neurogenesis (Chapter 2).

3. *Cell adhesion*

There is also evidence that *Pax6* is required to specify the adhesive properties of cortical cells. In *Sey/Sey* mutants the expression domain of *Dlx1* in the lateral ganglionic eminence extends ectopically into the cortex (Stoykova *et al.*, 1996), and corresponds to a loss of regional differences in expression of the cell adhesion molecule *R-cadherin* (Stoykova *et al.*, 1997). *In vitro*, cell aggregation studies on dissociated cortical cells reveal that *Sey/Sey* cells show greater homophilic adhesion than wildtype cells (Stoykova,1997). The neural cell adhesion molecule *L1* has been identified as a putative *Pax6* target: *in vitro* binding and transfection assays suggest that regions in the promoter region of the *L1* gene are bound by *Pax6* and required for *Pax6* mediated activation (Chalepakis *et al.*, 1994; Meech *et al.*, 1999).

Together, this evidence suggests that *Pax6* regulates expression of cortical cell adhesion molecules, and that this might contribute towards defects in radial or tangential migration. To test this, the expression of two cell adhesion molecules, *L1* and *TAG1* was examined in the *Sey/Sey* cortex (Chapter 5) and the behaviour of migrating neurons was observed in a cortical explant system (Chapter 4).

4. *Thalamocortical innervation*

I described in section 1.1.4 evidence that thalamocortical innervation influences the survival and neurite outgrowth of cortical cells. Defects in the *Sey/Sey* diencephalon, which gives rise to TCAs, could therefore affect *Sey/Sey* cortical development. Experiments to examine the role, if any, of thalamocortical innervation in the *Sey/Sey* cortical phenotype are described in Chapters 3 and 4.

CHAPTER 2

An analysis of cell division patterns in the *Sey/Sey* cortex

2.1 Introduction

The *Sey* homozygote cerebral cortex develops in a structurally abnormal manner (Schmahl *et al.*, 1993; Caric *et al.*, 1997; Gotz *et al.*, 1998) and to date, little is known about the principal cellular functions of Pax6 which underlie these abnormalities. However, previous work has suggested its functions may include regulation of the cell cycle and specification of cell fate and, in this chapter, these possibilities were addressed by the analysis of a cell cycle-related process (interkinetic nuclear migration) and cell-fate related process (cleavage orientation) in the *Sey/Sey* cortex.

BrdU labelling studies have shown an increase in proliferation in the *Sey/Sey* cortex (Gotz *et al.*, 1998; Warren *et al.*, 1999). In addition, BrdU labelled nuclei exhibit differences in distribution within the *Sey/Sey* ventricular zone (VZ) which represent a failure or delay in nuclear migration towards the ventricular surface (Gotz *et al.*, 1998; Warren *et al.*, 1999). This observation is compatible with two explanations, there is either:

- a lengthened S-phase/failure in cell cycle progression into M-phase, or;
- a defect in interkinetic nuclear migration (Fig 2.1A), such that cells enter M-phase before nuclei have migrated to the ventricular surface.

To address this issue, a comparison of the position of M-phase cells was made between wildtype and *Sey/Sey* cortex.

Pax6 has also been implicated in the regulation of cell fate specification by multipotential progenitors in the cortex (Gotz *et al.*, 1998). This led to the hypothesis that other cell fate decisions might be altered in the *Sey/Sey* cortex, in particular that proliferative defects during neurogenesis might be accompanied by a disruption in the switch from proliferative to neurogenic division. As outlined in the introduction, cortical neurons are thought to be generated by asymmetric division, a process which partly depends on two events:

- polarised localisation of cell fate determinants such as Numb (Fig. 1.8B);
- orientation of cleavage such that the cell fate determinants are distributed symmetrically or asymmetrically to daughter cells (Chenn & McConnell, 1995).

Pax6 may function in either of these pathways; here, the second was analysed by comparing the distribution of mitotic cleavage orientations between wild type and *Sey/Sey* cortex. The question of altered expression of cell fate determinants in the mutant brain is addressed separately in Chapter 5.

2.2 Results

The experiments described in this chapter were performed at three ages: E10.5, E12.5 and E15.5. These stages correlate with the onset of neurogenesis, early neurogenesis and mid-neurogenesis (Caviness *et al.*, 1995) where neurogenesis is defined as the period of production of committed postmitotic neurons destined for the cortical plate.

A preliminary analysis of the distribution of mitotic cells was performed by immunohistochemistry in wildtype and *Sey/Sey* cortex. Cells in metaphase were visualised using an antibody directed against phosphorylated histone H3. This antibody is cell cycle-specific, reacting initially within pericentromeric heterochromatin during G2 and then spreading in an ordered fashion coincident with mitotic chromosome condensation so that it is most strongly expressed during metaphase (Hendzel *et al.*, 1997; Hendzel *et al.*, 1998). As expected, in both wild type and *Sey/Sey* cortex at E10.5 and E12.5 metaphase cells were largely restricted to the ventricular surface. However, at E15.5 there appeared to be a significant proportion of metaphase cells located away from the ventricle in the mutant cortex (Fig. 2.1B,C)

To obtain a complete representation of cell division patterns throughout the developing cortex a comprehensive count of cells in telophase was undertaken. At each stage (E10.5, E12.5 and E15.5) coronal 10μm sections were cut through the telencephalon of two wildtype and two *Sey/Sey* embryos. Sections were stained with DAPI, which clearly identifies cells in late anaphase and telophase when condensed chromosomes are separating (Fig. 2.3B,C), and the numbers of cells in these stages were counted. The cortex exhibits positional gradients of development; anterior to posterior and dorso-lateral to ventro-medial (Bayer & Altman, 1991). To test whether cell division patterns were influenced by the anterior-posterior gradient of development, counts were carried out at three different anterior-posterior positions in the cortex. Thus, cells were counted in 5 adjacent sections which were 25%, 50% and 75% through the telencephalon (where 0% is the most rostral part and 100% is the most caudal part, Fig2.2A). However, position was found to have no significant effect on either ectopic or asymmetric division therefore these numbers were combined in the final analysis. Preliminary counts showed that a single dividing cell was not represented in adjacent sections and therefore cells were unlikely to be counted twice. At least 180 cells were counted in each brain, and divisions of the secondary proliferative population in the intermediate zone (IZ) were excluded on the basis of laminar cell morphology.

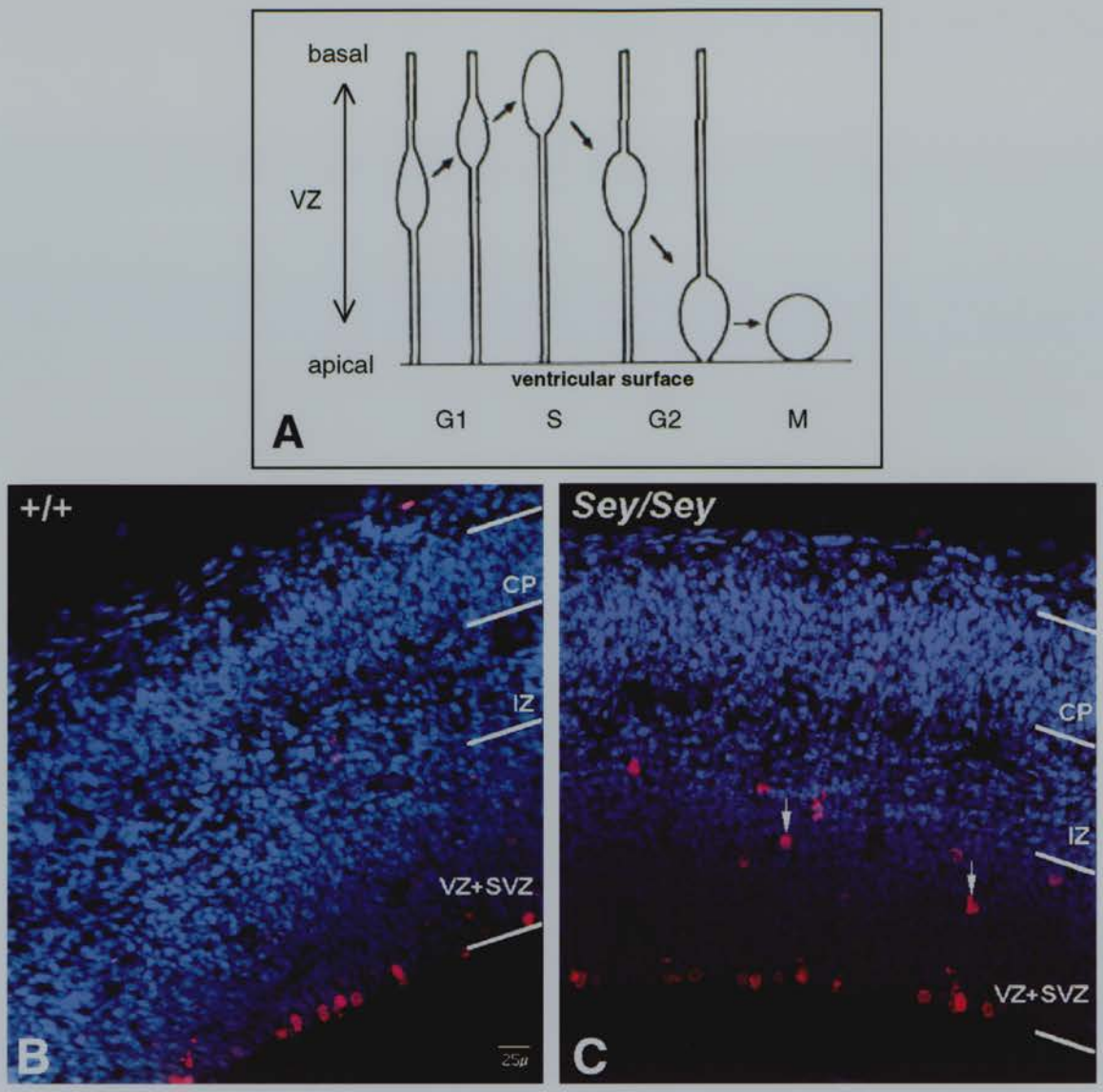

Figure 2.1 Ectopic cell division in wildtype and *Sey/Sey* cortex

A. Diagram of a cortical progenitor cell in the ventricular zone undergoing intracellular nuclear migration during the cell cycle. The nucleus ascends away from the apical ventricular surface during G1, is located in the basal third of the ventricular zone during S phase and translocates apically during G2. Mitosis (M) normally occurs at the ventricular surface (from Chenn & McConnell, 1995).

B,C. Mitotic cells in (B) wildtype and (C) *Sey/Sey* E15.5 cortex identified with an antibody against phosphorylated histone H3 which labels metaphase chromosomes.

B. In the wildtype cortex the majority of dividing cells are located at the ventricular surface.

C. In the *Sey/Sey* cortex some dividing cells are located ectopically (away from the ventricular surface, arrows).

CP, cortical plate; IZ, intermediate zone; MZ, marginal zone; SVZ, subventricular zone; VZ, ventricular zone.

For each section, cells throughout the cortical VZ were simultaneously classified in two ways:

- Position: either at the ventricular surface or ectopic (within the VZ but more than three cell diameters from the ventricular surface);
- Orientation of division (Fig. 2.3A): either dividing symmetrically (plane of division 60-90° relative to the ventricular surface; Fig. 2.3B), asymmetrically (0-30°; Fig.2.3C) or intermediate (30-60°).

The spindles of cortical progenitors rotate throughout metaphase but stop at the start of anaphase (Adams, 1996) therefore this method provides a good approximation of the plane of division. Furthermore, it has been shown that the distributions of cleavage orientations observed by staining fixed sections are identical to those of living cells viewed by DiI in cortical slices (Chenn & McConnell, 1995). Therefore the counts provide a representative picture of the pattern of cleavage seen *in vivo*. An analysis of variance (ANOVA) was carried out on the resulting data. Each data set (numbers undergoing ectopic division, symmetric division, asymmetric division or intermediate division) was shown to comply with the assumptions necessary for an ANOVA.

In confirmation of the preliminary observations, the ANOVA revealed a significant increase in ectopic division in the *Sey/Sey* cortex specifically at E15.5. Averaged values for the proportion of ectopic telophase cells (all ± S.E. of 2%) are shown in Figure 2.2C. At E10.5, 3% of wildtype and 7% of *Sey/Sey* divisions are ectopic, and this proportion rises slightly at E12.5 to 12% in wild type and 17% in *Sey/Sey*. By contrast, at E15.5, 13% of division is occurring ectopically in wildtype compared to 47% in *Sey/Sey* ($p=0.00006$). The data strongly suggest that interkinetic nuclear migration is disrupted during mid-neurogenesis, causing cells to enter mitosis before nuclei undergo apical relocation to the ventricular surface.

The cell division analysis also revealed a significant increase in the proportion of cells undergoing asymmetric division in the *Sey/Sey* cortex. Averaged values for the proportions of symmetric, asymmetric and intermediate divisions (± S.E.) are shown in Figure 2.3D,E. In the E10.5 wild type cortex (Fig. 2.3D), at the onset of neurogenesis, the majority of divisions (79±2 %) were symmetric (11±2 % asymmetric, 10±1 % intermediate). The same pattern is maintained during early neurogenesis at E12.5 (80±2 % symmetric, 8±2 % asymmetric and 12±1 % intermediate). By E15.5, in mid neurogenesis, the proportion of symmetric divisions has fallen to 69±2 % and asymmetric divisions have risen to 17±2 %. The data are consistent with a predicted increase in asymmetric divisions as neurogenesis progresses and are very similar to that observed by Chenn & McConnell (1995) at equivalent developmental stages in the ferret.

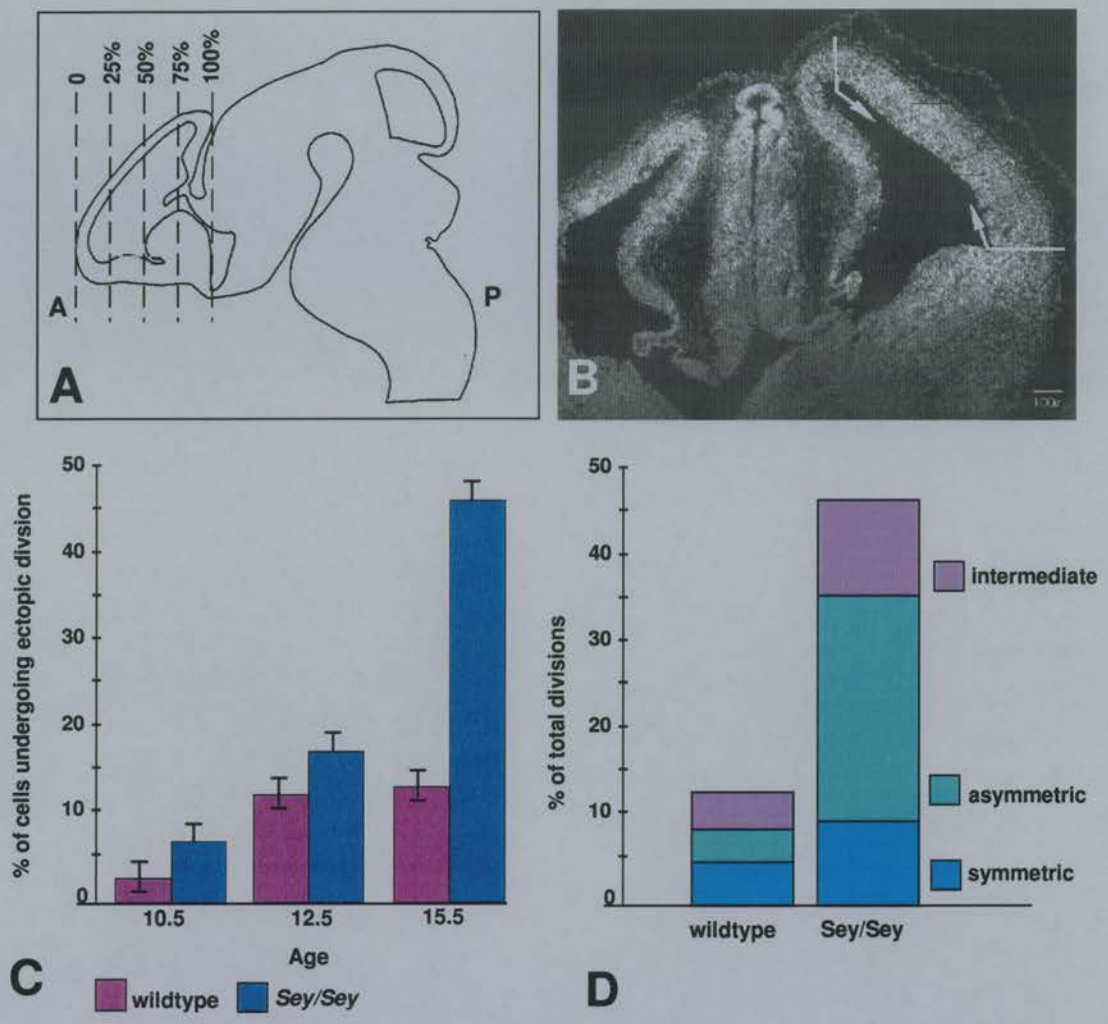

Figure 2.2 Analysis of ectopic cell division in the wildtype and *Sey/Sey* cortex

A. Drawing of a parasagittal view of an E12.5 wildtype forebrain to show the planes of section in which cell divisions were counted. Cells were counted in 5 adjacent sections at 25%, 50% and 75% through the telencephalon (dashed lines), where 0% is the most anterior (A) part and 100% is the most posterior (P) part.

B. Coronal section through an E12.5 wildtype embryo at a position that is 50% through the telencephalon in (A). Dorsal is upwards. Cell nuclei are stained with DAPI. Cell counts were made in the ventricular zone of the cortex between the two lines.

C. Histogram showing the percentage of late anaphase and telophase cells that are dividing in an ectopic position (away from the ventricular surface) at E10.5, E12.5 and E15.5 in wildtype and *Sey/Sey* brains. Bars show standard error. There is a increase in ectopic division in the *Sey/Sey* cortex at E15.5 ($p=0.00006$).

D. Histogram showing the percentage of cells that are dividing in an ectopic position in E15.5 wildtype and *Sey/Sey* brains. The components contributed by symmetric, asymmetric and intermediate division are shown. Symmetric, asymmetric and intermediate cell division all occur in ectopically positioned cells and are increased in the *Sey/Sey* mutant but asymmetric divisions make the biggest contribution. All percentages are +/- standard error of 2%.

Two wildtype and two *Sey/Sey* brains were counted at each age and at least 180 cells were counted in each brain.

A, anterior; P, posterior. Scale bar in A, 100μm.

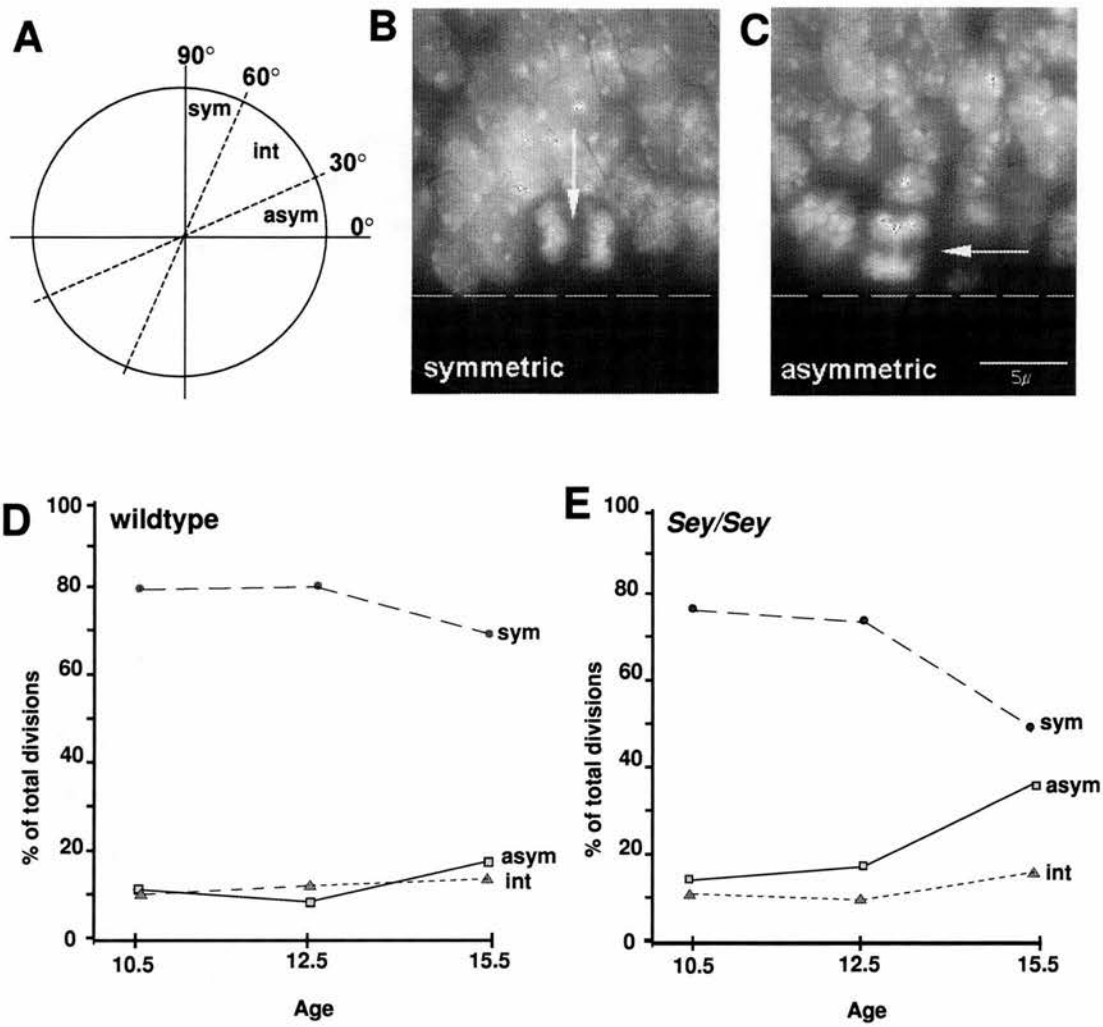

Figure 2.3 Analysis of the distribution of cleavage orientation in wildtype and *Sey/Sey* cortex

A. Diagram showing how late anaphase and telophase cells were classified by their plane of division relative to the ventricular surface. 0-30°, asymmetric division; 30-60°, intermediate division; 60-90°, symmetric division

B,C. DAPI labelled chromosomes to show symmetric (B) and asymmetric (C) cell division. Dashed line indicates the plane of the ventricular surface and the arrow indicates the plane of cell division.

D,E. Graphs comparing the percentage of dividing cells in wildtype (D) and *Sey/Sey* (E) undergoing symmetric (dashed line, circles), asymmetric (continuous line, squares) and intermediate (dotted line, triangles) divisions at E10.5, E12.5 and E15.5. All data points are +/- standard error of 2%.

D. In the wildtype cortex there is a gradual increase in asymmetric division and a decrease in symmetric division with time.

E. In the *Sey/Sey* cortex there is an accelerated increase in symmetric divsion and decrease in asymmetric division with time compared to wildtype. At E12.5 the proportion of asymmetric division in *Sey/ Sey* is 17% compared to 8% in wildtype ($p=0.03$); at E15.5 the proportion of asymmetric division in *Sey/Sey* is 36% compared to 17% in wildtype ($p=0.0003$).

Two wildtype and two *Sey/Sey* brains were counted at each age and at least 180 cells were counted in each brain. asym, asymmetric; int, intermediate; sym, symmetric. Scale bar in C, 5μm and applies to B.

In the *Sey/Sey* cortex at E10.5 the distribution of cleavage orientations is comparable to that observed in wild type (75±2% symmetric, 14±2% asymmetric and 11±1 % intermediate) (Fig. 2.3E). However, in contrast to wild type, by E12.5 the proportion of symmetric divisions in *Sey/Sey* has fallen to 73±2 % and asymmetric divisions have risen to 17±2% (compared to 8±2% asymmetric in wildtype, p=0.03). This trend continues at E15.5, when only 48±2% of divisions are occurring symmetrically and 36±2% asymmetrically (compared to 17±2 % asymmetric in wildtype, p=0.0003). Taken together, the data reveal that there is an accelerated decrease in symmetric division and increase in asymmetric division in the *Sey/Sey* cortex as neurogenesis progresses.

Based on the finding that both ectopic and asymmetric division are significantly increased in the *Sey/Sey* cortex by mid-neurogenesis, the cell division data was analysed to examine whether there was any correlation between the two observations. Without undertaking a complex multivariate analysis, this can be done by breaking down the proportion of cells dividing ectopically into the components contributed by symmetric, asymmetric and intermediate division. This would indicate if, for example, all the ectopic divisions are also asymmetric.

The results of this breakdown are shown in Table 2.1 and Figure 2.2D. At E15.5, 13±2% of total wildtype divisions are ectopic. Of these ectopic divisions, 5% are symmetric, 4% asymmetric and 4% intermediate. In contrast, 47±2% of total *Sey/Sey* divisions are ectopic and of these, 10% are symmetric, 26% asymmetric and 11% intermediate. This suggests that in both wildtype and *Sey/Sey* all three orientations of division occur in ectopically positioned dividing cells, however, those undergoing asymmetric division make a larger contribution in the mutant.

Age	Strain	% of cells undergoing ectopic division (±S.E.)	Breakdown of % ectopic divisions (±S.E.)		
			symmetric	asymmetric	intermediate
E10.5	+/+	3.5 (±2.45)	1.5 (±0.9)	1.3 (± 1.6)	0.7 (± 1.1)
	Sey/Sey	7.3 (±2.45)	2.3 (±0.9)	4.4 (± 1.6)	0.6 (± 1.1)
E12.5	+/+	11.7 (±2.45)	3.3 (±0.9)	5.5 (± 1.6)	2.9 (± 1.1)
	Sey/Sey	17.1 (±2.45)	5.8 (±0.9)	7.9 (± 1.6)	3.4 (± 1.1)
E15.5	+/+	13.4 (±2.45)	5.4 (±0.9)	4.4 (± 1.6)	3.6 (± 1.1)
	Sey/Sey	47.1 (±2.45)	10.4 (±0.9)	26.1 (± 1.6)	10.6 (± 1.1)

Table 2.1. Ectopic ell division in the wildtype and *Sey/Sey* cortex. Breakdown of the proportion of cells dividing ectopically at each age and for each strain (wildtype and *Sey/Sey*) into the components contributed by symmetric, asymmetric and intermediate division.

2.3 Discussion

The cell division analysis presented in this chapter provides evidence that in the cortex *Pax6* is involved in both interkinetic nuclear migration and regulation of cleavage orientation. I will discuss how these results relate to previous work in the *Sey/Sey* cortex and the possible underlying functions of *Pax6*, leading to the proposal that both defects could arise from a primary function in regulating progression through the neurogenic cell cycle.

As outlined in Chapter 1, it is thought that during cortical neurogenesis the founder progenitor population undergoes a set number of cell divisions (Takahashi *et al.*, 1995a), during which there is a gradual switch from proliferative (symmetric) to neurogenic (asymmetric) division (Chenn & McConell, 1995; Takahashi, *et al.*, 1996). In agreement with this idea, my analysis of cortical precursor cleavage orientation in the wildtype cortex revealed a gradual increase in asymmetric division with the onset and progression of neurogenesis.

It was proposed in the introduction to this chapter that Pax6 might have a role in regulating the decision that switches a progenitor cell from symmetric divisions to asymmetric divisions during neurogenesis and that this would be reflected in an altered distribution of cleavage orientations. Indeed, in the *Sey/Sey* cortex my results show an increase in asymmetric division, suggesting that neurogenic divisions are favoured over proliferative divisions. One explanation for this could be a breakdown in the mechanisms controlling cleavage orientation. For example, the intrinsic apical-basal polarity of the cell required for spindle orientation may not be established correctly, as seen in *Drosophila inscuteable* and *bazooka* mutants (Kraut *et al.*, 1996; Kuchinke *et al.*, 1998). However, if control of cleavage orientation had broken down we would predict cleavage to occur at random orientations and the distribution of symmetric, asymmetric and intermediate divisions to be equal.

Instead, the pattern of cleavage orientation in *Sey/Sey* mirrors that of wildtype, but occurs earlier during development. At the onset of neurogenesis the ratios of division in *Sey/Sey* are approximately equal to wild type, and by E15.5 (mid-neurogenesis) the distribution in *Sey/Sey* is comparable to that observed during late neurogenesis in the ferret cortex (Chenn & McConnell, 1995). This trend strongly suggests that control over cleavage orientation is maintained but that cells are cycling through divisions at an accelerated rate due to a shortened cell cycle. Therefore, the data does support a role for Pax6 in regulating progenitor cell fate via control of cleavage orientation, but I propose that this is secondary to regulation of cell cycle progression.

In further agreement with this idea are previous findings of increased proliferation in the *Sey/Sey* cortex. BrdU labelling studies have shown an increase in the proportion of cells in S phase, rather than an overall increase in the number of precursor cells (Gotz *et al.*, 1998; Warren *et al.*, 1999), which is compatible with a shortened cell cycle length and earlier progression into neurogenic division.

The same BrdU labelling studies revealed that the nuclei of *Sey/Sey* cortical precursors fail to undergo apical relocation to the ventricular surface during the cell cycle (Gotz *et al.*, 1998; Warren *et al.*, 1999). This is compatible with either:

- a delay in M-phase due to lengthened S-phase/failure to progress into M-phase, or;
- a failure in interkinetic nuclear migration (either in the ability to undergo migration or the co-ordination of migration with the cell cycle), such that cells enter M-phase before migration to the ventricular surface.

My results now reveal increased numbers of M-phase cells located ectopically within the cortical VZ at E15.5. This demonstrates that cells are able to progress through the cell cycle into M-phase, but that nuclei do not migrate to the ventricular surface before they begin mitosis and thus favour the latter explanation.

It is possible that the increase in ectopic division may be partly accounted for by an increase in division of the secondary proliferative population (SPP). This population of mainly glial progenitors arises from the VZ from E12.5 and is distributed diffusely through the SVZ and IZ in a region overlapping with ventricular progenitors (Takahashi *et al.*, 1995b). However, in the E15.5 wildtype cortex, the expected proportion of SPP division is much greater than the proportion of ectopic division I observed (Takahashi *et al.*, 1995b). This suggests that SPP divisions were mainly excluded from my counts and do not account for the increased ectopic mitoses seen in *Sey/Sey*. The inclusion of SPP divisions in the cell counts might, however, mask small differences in ectopic ventricular divisions between wildtype and *Sey/Sey*. This may partly explain a difference between my results and previous observations: whereas I observed an increase in *Sey/Sey* ectopic mitosis only at E15.5, the BrdU labelling study by Warren *et al.*, (1999) suggested that fragmented BrdU labelled cells, which are probably M-phase cells, are absent from the ventricular surface earlier in development at E10.5 (Warren *et al.*, 1999). However, in the Warren *et al.* study a quantitative analysis of the observation was not carried out.

The failure in interkinetic migration might be explained if Pax6 regulates the transcription of genes involved in cytoskeletal interactions. Nuclear migration within a cell requires dynamic intracellular organisation including construction of a cytoskeletal scaffold and transport of

nuclei along it; a breakdown in these processes could account for defects in the *Sey/Sey* cortex. In support of this idea, recent observations in the *Sey/Sey* cerebellum showed that *Pax6* expressing granule cells appear to possess cytoskeletal deficiencies which prevent neurite extension (Engelkamp *et al.*, 1999). However, the normal pattern of nuclear distribution observed during early neurogenesis suggests that cells are intrinsically capable of nuclear migration. Furthermore, data presented in Chapter 4 shows that mutant cortical cells are able to undergo neurite extension and radial migration, suggesting that cytoskeletal organisation is not a primary function of *Pax6* in the cortex.

I would argue instead that, like cleavage orientation, the nuclear migratory defect can also be explained by a shortened cell cycle. Interkinetic nuclear migration is tightly linked to cell cycle progression, such that nuclei migrate away from the ventricular surface during G1, are located in the basal third of the ventricular zone during S phase, and migrate back during G2 to undergo mitosis at the ventricular surface (Sauer, 1935; Fig 2.1A). The fact that *Sey/Sey* cells are entering into M-phase ectopically suggests that they are cycling through these stages before nuclei have had time to complete the return migration due to a shortening in cell cycle length.

On the basis of these results, I therefore postulate that a primary function of Pax6 in the cortex is the regulation of progression through the cell cycle during neurogenesis; Pax6 normally acts at a key checkpoint to delay cell cycle progression and in the absence of Pax6 function:

- the length of the cell cycle is shortened from the onset of neurogenesis at E10.5 (and possibly earlier);
- cells undergo accelerated progression through neurogenesis;
- there is an associated loss of control over interkinetic nuclear migration.

This hypothesis may account for two paradoxical observations in the *Sey/Sey* brain: that proliferation is increased compared to wildtype (Gotz *et al.*, 1998)(Warren *et al.*, 1999), yet overall, the *Sey/Sey* telencephalon is reduced in size. A preliminary analysis of cortical cell death suggests that apoptosis is comparable between wildtype and mutant (Gotz *et al.*, 1998). If increased proliferation corresponds to accelerated progression through neurogenesis then this suggests that overall there will be no increase in cell number by the end of neurogenesis at E16.5. I suggest the smaller size of the *Sey/Sey* cortex could be explained by the failure of cells to acquire their normal position and spacing in the CP, instead remaining packed together in the cell dense VZ/SVZ (Schmahl *et al.*, 1993; Caric *et al.*, 1997); this leads to the

prediction of increased cell density in the *Sey/Sey* cortex during mid-neurogenesis, which could easily be tested in future work.

The hypothesis also leads to speculation about where in the cell cycle *Pax6* might act. The G1 checkpoint is an obvious candidate: during neurogenesis there is a systematic increase in the duration of G1 phase, whereas S, G2 and M phases remain of constant length (Takahashi *et al.*, 1995a) suggesting that checkpoints in G1 are likely to be key regulators of cell cycle progression (Caviness *et al.*, 1999). A defect in G1 checkpoint control would account for both a shortened cell cycle length and an increasing divergence between the length of wildtype and *Sey/Sey* cell cycle. This could explain the increasing severity of cell cycle-related defects (increased asymmetric division and the disruption of interkinetic migration only by E15.5) as neurogenesis proceeds.

However, an argument can also be made for *Pax6* function during G2, as current evidence suggests that cortical cell fate is determined during G2 (McConnell & Kaznowski, 1991; McConnell, 1998). *Pax6* has been implicated in the control of cortical cell fate: in determining whether progenitor cells generate glial or neuronal lineages (Gotz *et al.*, 1998) as well as the specification of neuron type (Chapter 6). Therefore the most parsimonious explanation for roles in cell cycle and cell fate would be a function for Pax6 in regulating exit from G2. In order to determine which, if either, of these two explanations could be true, further investigations are needed into the length of the component phases of the cell cycle. For example, the length of time spent in each phase could be assessed by a live cell imaging study using phase-specific markers, or by crossing a line ubiquitously expressing a histone green fluorescent protein (Hadjantonakis *et al.*, 1998) onto *Sey* to visualise chromosome movements.

It is also important to investigate in more detail the relationship between interkinetic nuclear migration and cleavage orientation. A preliminary breakdown of my data suggests that there is some correlation between ectopic and asymmetric division in the *Sey/Sey* cortex, which could be accounted for by two possible explanations:

- cells dividing asymmetrically in *Sey/Sey* are more likely to undergo ectopic division: if, for example, these cells have progressed through more cell cycles during neurogenesis and are more likely to have lost control over interkinetic nuclear migration;
- cells dividing ectopically are more likely to undergo asymmetric division.

My data suggests that asymmetric division increases in *Sey/Sey* at E12.5 prior to the increase in ectopic division, favouring the former explanation. However, this awaits confirmation by extended cell counts and statistical analysis.

How might Pax6 regulate the rate of progression through the cell cycle? It remains to be tested whether the role for Pax6 in cell cycle regulation is cell autonomous or not. Previous work (Gotz *et al.*, 1998) suggests that increased proliferation of disaggregated *Sey/Sey* cortical precursors can be rescued by secreted factors from wildtype cortex, favouring a non-autonomous role. External growth factors such as FGF2 have been shown to influence the rate of progression through cortical cell cycles (reviewed in Temple & Qian, 1995) and Pax6 may act to regulate the release of such factors.

Finally, although it is tempting to speculate on a single primary function for Pax6 in the cortex which can account for all the *Sey/Sey* cortical defects, in all probability Pax6 plays multiple roles. As a transcription factor, Pax6 may have distinct functions in different cells and at different times during development. Therefore, although my data strongly suggests a cell cycle related function, it remains feasible that it has separate roles in regulating the cell cycle, cell fate, cell adhesion and possibly other processes. This issue will be discussed further in the following chapters.

CHAPTER 3

Thalamocortical innervation in the *Sey/Sey* brain

3.1 Introduction

In the previous chapter I presented evidence that *Pax6* is required within the cortex for normal cell cycle progression. This suggests that, in the absence of *Pax6*, intracortical defects lead to aberrant cortical development. However, in a broader context, telencephalic development occurs under the influence of interactions with other regions of the brain. A second possibility therefore exists: that extracortical defects in the *Sey/Sey* brain contribute to the cortical phenotype.

I discussed evidence in Chapter 1 that thalamocortical innervation has a broad influence on cortical development. *Pax6* is expressed in the dorsal thalamus throughout the period of thalamocortical axon (TCA) generation and in ventral thalamic domains along the TCA pathway (Stoykova *et al.*, 1996; Warren & Price, 1997). In the absence of Pax6 function diencephalic proliferation is reduced and boundaries of regulatory gene expression are altered (Stoykova *et al.*, 1996; Warren & Price, 1997). Furthermore, pathfinding defects have formerly been identified in the diencephalic tract of the post optic commissure during early *Sey/Sey* development corresponding to disrupted forebrain patterning (Mastick *et al.*, 1997). Together, these previous observations led me to hypothesise that:

- thalamocortical innervation may show defects in *Sey/Sey* mice: in their generation, pathfinding, or both;
- that defects in TCA innervation might contribute to the *Sey/Sey* cortical phenotype.

To address the former hypothesis, TCA tracts were analysed in wild type and *Sey/Sey* mice.

3.2 Results

To study TCA projection in *Sey/Sey* mutants anterograde DiI labelling was carried out by insertion of DiI crystals into a range of positions in the thalamus. Subsequent analysis showed the crystals were large enough to label TCAs regardless of their insertion position. Labelling was carried out at E13.5, E15.5 and E17.5, corresponding to key time points in TCA innervation: early axon outgrowth from thalamus to telencephalon, arrival of the majority of TCAs in the cortex and major cortical plate invasion, respectively (Molnar & Blakemore, 1995; Table 1.3).

In E13.5 sagittal sections of wildtype brains (n=5), early TCAs form a thin tightly fasciculated tract extending through the rostral ventral thalamus, turning sharply into the ventral

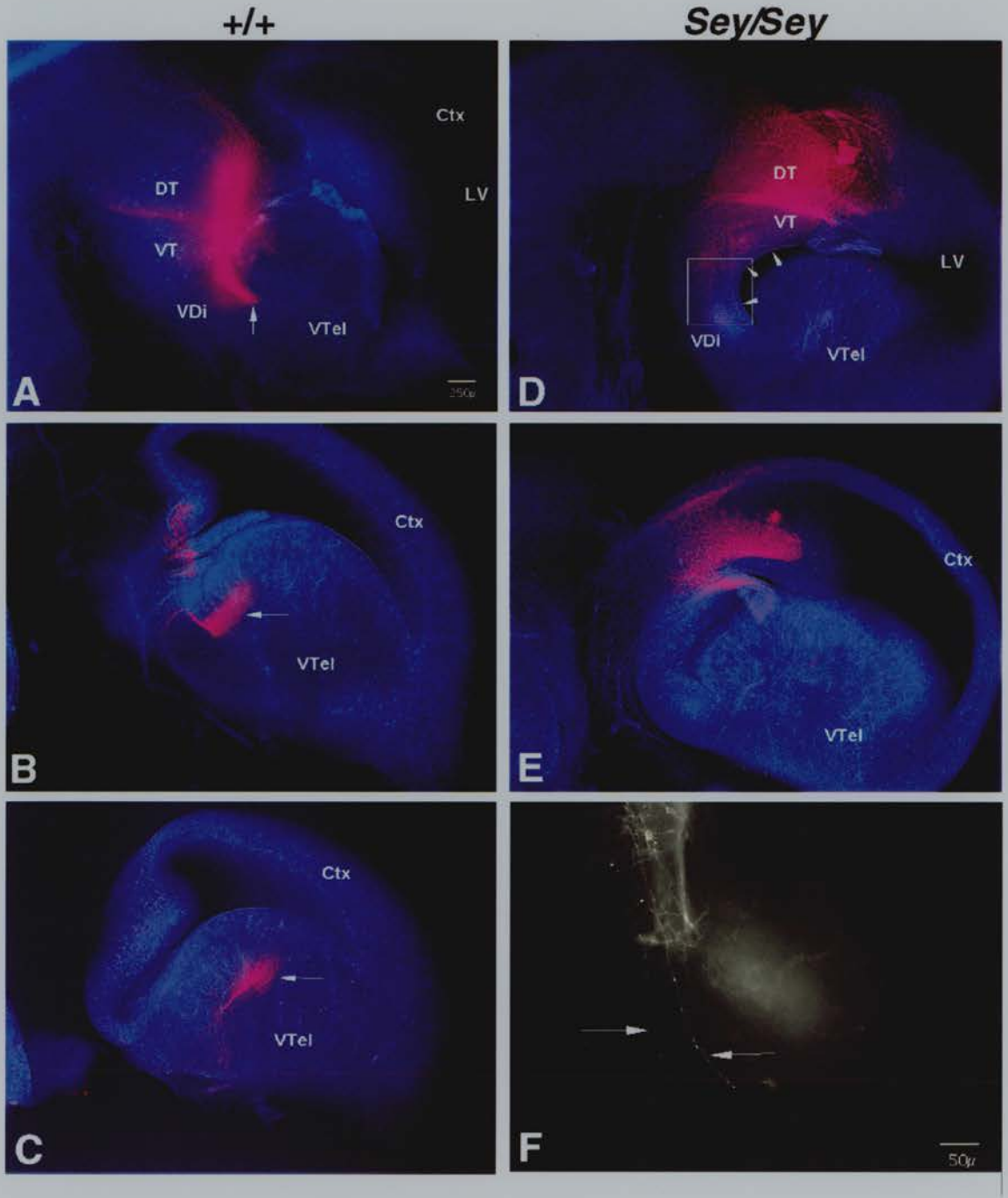

Figure 3.1 Thalamocortical axons in E13.5 wildtype and *Sey/Sey* mice

250µm vibrotome sagittal sections cut through E13.5 wildtype (A-C) and *Sey/Sey* (D-F) brain showing thalamocortical axons (TCAs) labelled by a DiI crystal placed in the dorsal thalamus (DT). For all sections rostral is to the right and dorsal is up. (A-C) are a medial to lateral series of sections. (D,E) are adjacent sections at the same level as (A,B).

A. Wildtype. TCAs (arrows) extend from the dorsal thalamus through the ventral thalamus (VT) and ventral diencephalon (VDi), turning sharply into the ventral telencephalon (VTel).

B,C. TCAs curve steeply dorsolaterally towards the dorsal telencephalon but do not reach the cortex (Ctx) at this age.

D. *Sey/Sey*. A few TCAs project from the dorsal thalamus into the ventral diencephalon but do not progress into the ventral telencephalon. Arrowheads indicate the altered morphology of the ventral diencephalon in the *Sey/Sey* brain in which the dorsal surface of the diencephalon is concave and the lateral ventricle (LV) extended dorsally and caudally.

E. TCAs do not extend into the *Sey/Sey* latero-ventral telencephalon.

F. Higher magnification of the boxed region in (D) showing a few sparse TCAs (arrows) projecting into the *Sey/Sey* ventral diencephalon.

DT, dorsal thalamus; Ctx, cortex; VDi, ventral diencephalon; VT ventral thalamus; VTel, ventral telencephalon. Scale bars: A, 250µm and applies to B-E; F, 50µm.

telencephalon and curving steeply dorsolaterally (and less rostrally than at later stages) towards the dorsal telencephalon (Fig. 3.1A-C). As expected, no cortical labelling is apparent at this stage. In contrast, in *Sey/Sey* E13.5 brains (n=3), fewer axons in each brain project from the dorsal to the ventral thalamus and they do not progress any further into the ventral diencephalon or beyond into the telencephalon (Fig.3.1D-F). Therefore at E13.5, thalamocortical tracts are already developmentally delayed in the *Sey/Sey* brain.

At E15.5 wildtype TCAs appear as a wide, even array of fibres extending ventrally from the dorsal thalamus through the ventral thalamus, turning at the diencephalic-telencephalic boundary and projecting rostrally and dorsolaterally through the ventral telencephalon into the ventro-medial cortex (Fig. 3.2A). Cortical labelling was seen in all brains examined (n=7). Again, the *Sey/Sey* E15.5 brain revealed a very different pattern of axonal tracts (n=6): TCAs extend from the dorsal into the ventral thalamus, however comparatively few axons proceed through the ventral thalamus (Fig. 3.2C). Those that do, extend more deeply ventrally compared to wildtype and do not turn to project across the diencephalic/telencephalic boundary into the telencephalon. In contrast to wild type, no labelled tracts extended into the cortex in any brain examined. High power examination of thalamocortical tracts revealed straight bundles of axons in wildtype brains (Fig. 3.2B). In contrast, *Sey/Sey* tracts have a meandering, disorganised arrangement and individual axons can be distinguished due to a loss of fasciculation (Fig. 3.2D).

Immunohistochemical analysis has shown neural cell adhesion molecule L1 localises to TCAs in rat (Fukuda *et al.*, 1997). A preliminary inspection of L1 distribution in the *Sey/Sey* cortex revealed, in contrast to wildtype, the absence of straight fibres penetrating the ventrolateral cortex (see Chapter 5, Fig). These probably represent TCAs and confirm the DiI results.

To determine whether *Sey/Sey* thalamic tracts are delayed in progression to the cortex, but eventually reach their target, TCA DiI labelling was repeated at E17.5. In E17.5 wildtype brains wide smooth tracts of TCAs are now seen to have extended far into the dorsal cortex (Fig 3.3A-C). High power magnification shows individual axons projecting tangentially along the subplate and branching into the overlying cortical plate (Fig. 3.3D). Extensive cortical innervation was apparent in all brains examined (n=7). In contrast, the E17.5 *Sey/Sey* axonal projections are similar to those observed at E15.5 (n=5). The vast majority of thalamic axons leading through the ventral diencephalon stall at the diencephalic/telencephalic boundary (Fig. 3.3 E-G). Closer inspection of this region in 2/5 brains revealed a few axons extending into the ventral telencephalon, however none extended far beyond this point or reached the ventral cortex (Fig. 3.3H).

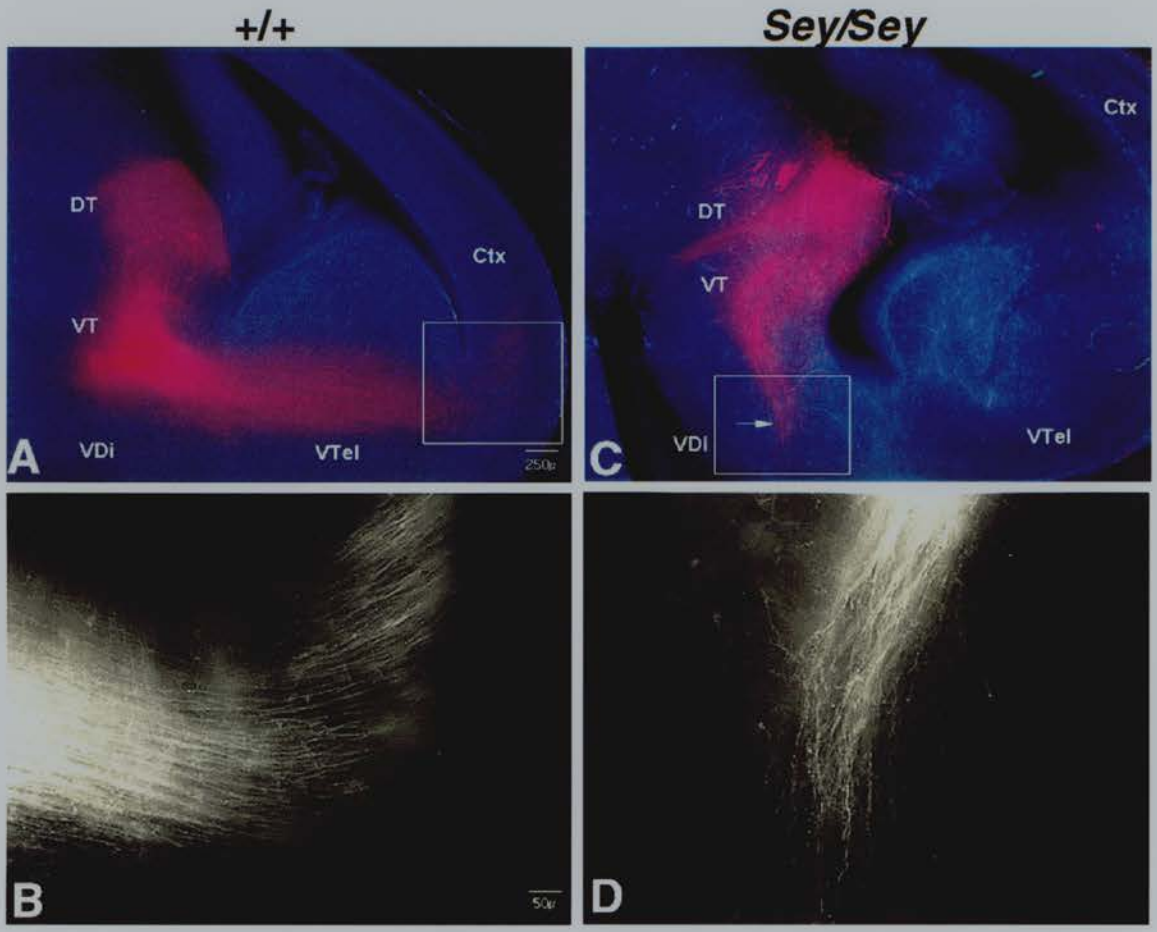

Figure 3.2 Thalamocortical axons in E15.5 wildtype and *Sey/Sey* mice

250µm vibrotome sagittal sections of E15.5 wildtype (A,B) and *Sey/Sey* (C,D) brain showing thalamocortical axon (TCA) tracts labelled by a DiI crystal inserted in the dorsal thalamus (DT). For all sections rostral is to the right and dorsal is up.

A. Wildtype. TCAs extend ventrally from the dorsal thalamus (DT) through the ventral thalamus (VT), turning at the diencephalic-telencephalic boundary and projecting rostrally and dorsolaterally through the ventral telencephalon (VTel) into the ventro-medial cortex (Ctx).

B. Higher magnification of boxed region in (A) showing straight tracts of fasciculated thalamocortical axons extending into the ventro-medial cortex.

C. *Sey/Sey*. TCAs extend from the dorsal into the ventral thalamus, but few axons proceed through the ventral diencephalon. Those that do extend more deeply ventrally compared to wildtype (arrow), do not turn to project across the diencephalic/telencephalic boundary into the ventral telencephalon and do not reach the cortex.

D. Higher magnification of boxed region in (C) revealing disorganised pathway and loss of fasciculation in *Sey/Sey* TCAs.

DT, dorsal thalamus; Ctx, cortex; VDi, ventral diencephalon; VT ventral thalamus; VTel, ventral telencephalon.

Scale bars: A, 250µm and also applies to C; B, 50µm and also applies to D.

Figure 3.3 Thalamocortical axons in E17.5 wildtype and *Sey/Sey* mice

250μm vibrotome sagittal sections cut through the brain of a single E17.5 wildtype (A-D) and *Sey/Sey* (E-H)) brain showing thalamocortical axon (TCA) tracts labelled by a DiI crystal inserted in the ventral thalamus (VT). For all sections rostral is to the right and dorsal is up.

A-C. A medial to lateral series of sections through the wildtype brain. Wide, straight TCA tracts extend from the dorsal thalamus (DT) through the ventral thalamus (VT), ventral telencephalon (VTel) into the dorsal cortex (Ctx).

D. Higher magnification of the boxed region in (A) revealing individual axons (arrows) projecting tangentially along the cortex and brancing upwards into the cortical plate.

E-G. A medial to lateral series of sections through the *Sey/Sey* brain at the same level as (A-C). TCAs extend from the dorsal into the ventral thalamus, but the majority of TCAs do not extend beyond the diencephalic/telencephalic boundary.

H. Higher magnification of boxed region in (G) revealing a few axons extending into the *Sey/Sey* ventral telencephalon but not as far as the cortex.

DT, dorsal thalamus; Ctx, cortex; VDi, ventral diencephalon; VT ventral thalamus; VTel, ventral telencephalon. Scale bars: A, 250μm and also applies to A-C,E-G; D, 25μm; H, 50μm.

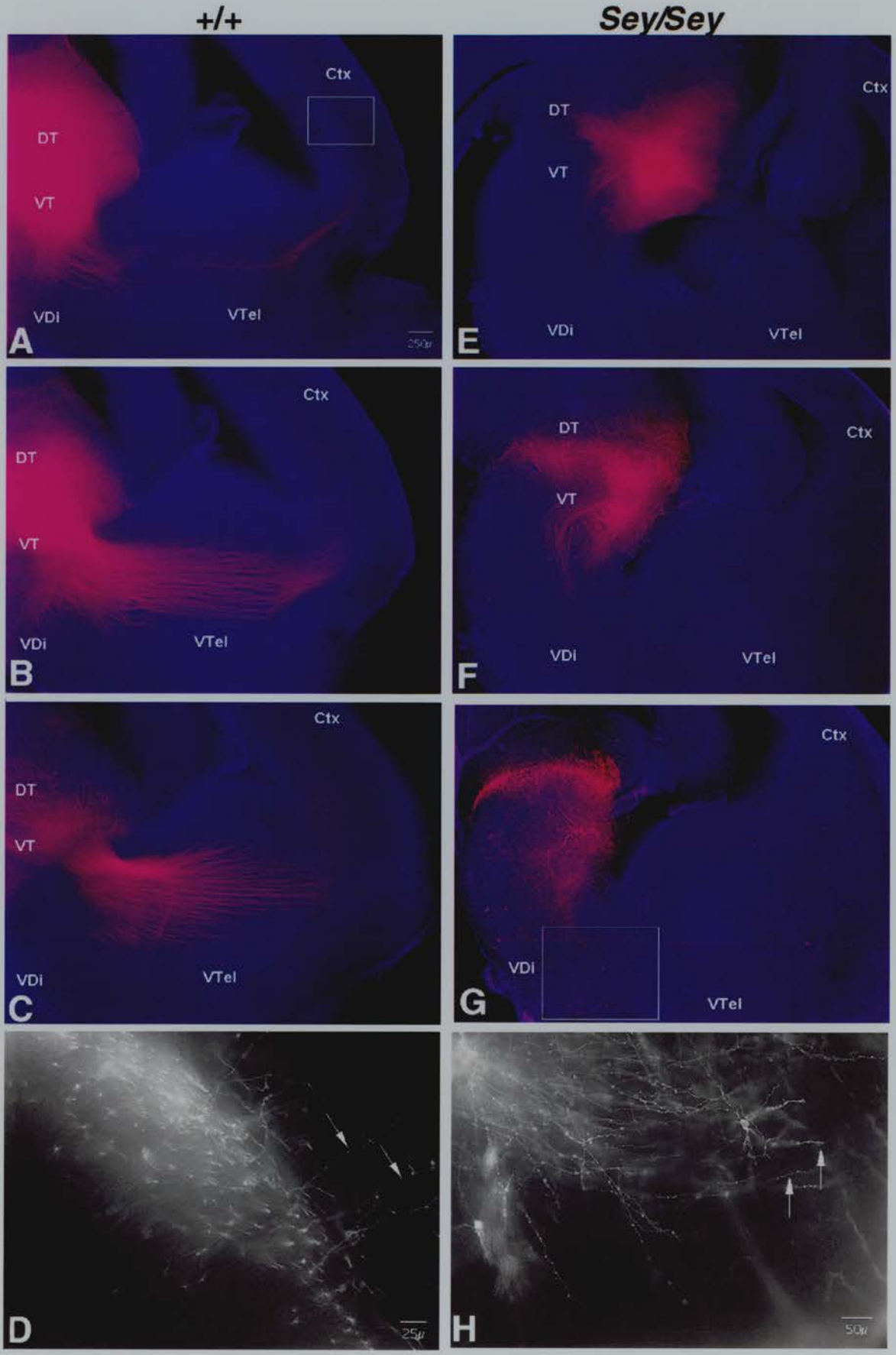
+/+
Sey/Sey
Ctx
DT
VT
VDi
VTel
A
E
B
F
C
G
D
H

To prove the tracts I observed in *Sey/Sey* are indeed aberrant TCA tracts and not another, retrogradely labelled tract projecting into or through the thalamus (Jones, 1985; Molnar *et al.*, 1998a; Braisted *et al.*, 1999), DiI crystals were inserted into the preoptic and amygdaloid areas of E17.5 brains. In both wild type and *Sey/Sey* brains the tract of the post optic commissure (tpoc) and tracts projecting from the amygdaloid region are labelled in lateral sections (Fig. 3.4B,D,F,H). However, in medial sections of these brains, in which TCA tracts are present, no retrograde labelling of thalamic tracts or nuclei was seen (Fig. 3.4A,C,E,G; n=2 brains for both wild type and *Sey/Sey*). This suggests the tracts anterogradely labelled from the thalamus in *Sey/Sey* are indeed TCA projections.

At both E15.5 and E17.5 the *Sey/Sey* thalamic tracts were greatly reduced in width compared to those seen in control brains suggesting that reduced numbers of TCAs leave the dorsal thalamus (Fig.3.2A,C; Fig.3.3 B,F). This could be the result of altered cell proliferation or differentiation defects within the thalamus. These options were not further assessed as my thesis is primarily concerned with the role of *Pax6* in the developing cortex and not in the thalamus *per se*.

Figure 3.4 DiI labelling of preoptic and amygdaloid tracts in E17.5 wildtype and *Sey/Sey* mice

250µm vibrotome sagittal sections of E17.5 wildtype (A-D) and *Sey/Sey* (E-H) brain showing axon tracts labelled by DiI. For all sections rostral is to the right and dorsal is up.

A.B. Wildtype. A and B are sections from the same brain; A is more medial than B. Tracts labelled by insertion of a DiI crystal in the preoptic area (POA).

A. Fibre tracts skirting the dorsal thalamus (DT) - the stria meduallaris (sm) rostrally and the cerebral peduncle (cpe) caudally - are labelled. There is no retrograde labelling of thalamocortical axons (TCAs) originating from the DT.

B. The tract of the postoptic commissure (tpoc) which projects from the POA is anterogradely labelled in the ventrolateral telencephalon.

C,D. Wildtype. C and D are adjacent sections; C is more medial than D. Tracts labelled by insertion of a DiI crystal into the anygdaloid area (AA).

C. Axonal tracts projecting through the AA are labelled but TCA tracts or cell bodies in the thalamus (T) are not retrogradely labelled.

D. Tracts in the amygdaloid region (at) are anterogradely labelled in the ventrolateral telencephalon.

E,F. *Sey/Sey*. E and F are sections from the same brain at the same level as (A,B); E is more medial than F. Tracts labelled by insertion of a DiI crystal in the preoptic area (POA).

E. In the *Sey/Sey* brain the cpe projecting through the ventral thalamus and tracts projecting through the dorsal thalamus (arrowhead) are labelled, but thalamocortical cell bodies in the dorsal thalamus are not retrogradely labelled.

F. As in the wildtype brain, the tpoc is anterogradely labelled in the ventrolateral telencephalon.

G,H. *Sey/Sey*. G and H are adjacent sections at the same level as (C,D); G is more medial than H. Tracts labelled by insertion of a DiI crystal into the amygdaloid area (AA)

G. As in the wildtype brain, axonal tracts projecting through the AA are labelled in the mutant, but TCA tracts or cell bodies are not retrogradely labelled.

H. Tracts projecting from the amygdaloid region are anterogradely labelled.

AA, amygdaloid area; at, amygdaloid tracts; cpe, cerebral peduncle; Ctx, cortex; DT, dorsal thalamus; POA; preoptic area; tpoc, tract of the postoptic commissure; sm, stria medullaris; VT ventral thalamus; VTel, ventral telencephalon. Scale bar in A, 250µm and applies to all images.

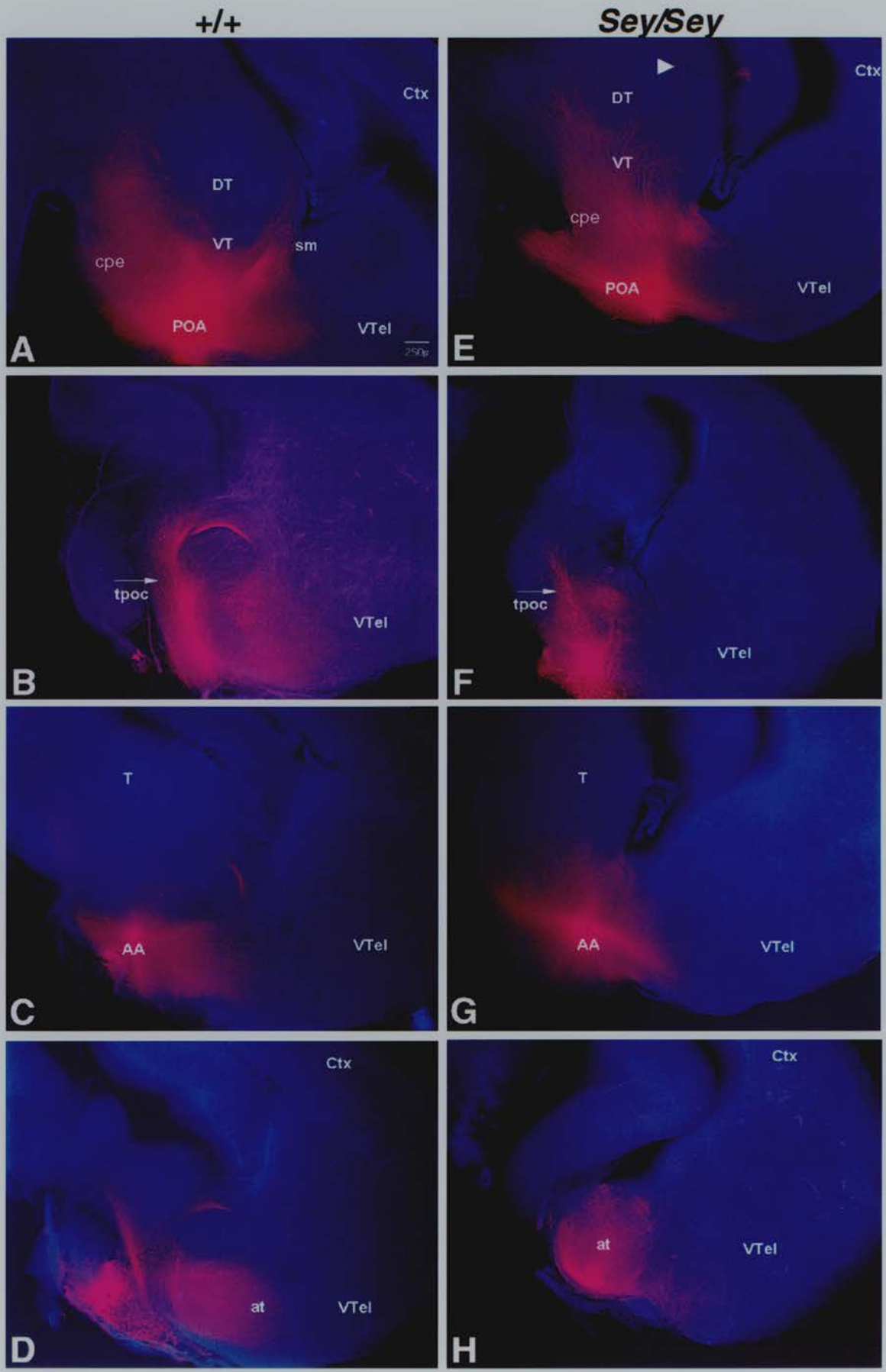
+/+
Sey/Sey
Ctx
DT
VT
sm
cpe
POA
VTel
A
E
tpoc
B
F
T
AA
C
G
at
D
H

3.3 Discussion

The data presented in this chapter reveal that *Sey/Sey* homozygote mice lack thalamocortical innervation; the number of TCAs extending from the thalamus is reduced, their projection developmentally delayed and almost all fail to cross the diencephalic/telencephalic boundary. These findings imply that *Pax6* is required for normal TCA generation and pathfinding.

3.3.1 A role for TCA innervation in the *Sey/Sey* cortical phenotype

The failure in thalamocortical innervation has implications for cortical development in the *Sey/Sey* mouse. Thalamic explant studies carried out at mid-late stages of cortical development (E15-E19) have suggested that diffusible factors provided by thalamocortical innervation are essential for survival and neurite outgrowth of cortical cells (Lotto & Price,1996; Lotto *et al.*, 1998; Price & Lotto, 1996). Interestingly, the onset of several aspects of the *Sey/Sey* cortical phenotype coincides with the expected arrival of the majority of thalamocortical axons in the cortex around mid-neurogenesis (E14.5-16.5) (Bicknese *et al.*, 1994; Metin & Godemont, 1996). Expansion of the ventricular zone in the *Sey/Sey* cortex becomes apparent from E14.5 (Schmahl *et al.*, 1993), and late-born (E16.5) neurons are unable to undergo migration out of the ventricular zone (Caric *et al.*, 1997), whereas earlier born neurons (E13.5) migrate normally. This raises the possibility that the absence of thalamocortical innervation in *Sey/Sey* could play a contributory role to the late onset of the *Sey/Sey* cortical phenotype. Experiments to test this hypothesis using an explant culture system are described in Chapter 4.

3.3.2 Possible causes of thalamocortical defects in the *Sey/Sey* brain

Orderly formation of thalamocortical connections requires: proliferation and specification of TCAs, axonal extension, axonal navigation from thalamus to cortex and targeting of the appropriate cortical area. In the *Sey/Sey* brain, my data reveal four main defects of TCA development:

1. *Numbers of TCAs extending out of the thalamus may be reduced*

Pax6 is expressed in the ventricular zone of the dorsal thalamus at early stages of development at a time when thalamocortical axons are generated (Stoykova *et al.*, 1996; Warren & Price, 1997). Reduced numbers of TCAs exiting the thalamus could be a consequence of either decreased neuronal proliferation in the dorsal thalamus, a defect in TCA fate specification or a failure in axon outgrowth. In favour of the first explanation, proliferative rates are reduced in the *Sey/Sey* diencephalon at E10.5, creating a reduced

precursor cell population at later stages (Warren & Price, 1997). This could result in a paucity of TCAs. Although expression boundaries are disrupted in the mutant diencephalon throughout development (Stoykova *et al.*, 1996; Grindley *et al.*, 1997; Warren & Price, 1997) they generally suggest a ventral shift in domains but maintenance of regional cellular identity, suggesting that TCAs probably are correctly specified. The third explanation, that factors contributing to axon outgrowth are disrupted in the *Sey/Sey* brain, is discussed below.

2. *Progression of thalamocortical outgrowth is delayed*

Delayed progression of TCAs through the *Sey/Sey* diencephalon is apparent from the earliest stages of TCA development, and might be accounted for by delayed neuronal differentiation. However, expression of regulatory genes in the *Sey/Sey* thalamus at the appropriate times during embryonic development do not support a general developmental delay in thalamic differentiation (Stoykova *et al.*, 1996; Warren & Price, 1997).

Alternatively, growth-promoting or growth-permissive factors could be altered in the *Sey/Sey* brain. Several studies have established that the developing cortex releases diffusible factors which promote non-directional dorsal thalamic neurite outgrowth *in vitro* (Blakemore & Molnar, 1990; Rennie *et al.*, 1994; Lotto & Price, 1995; Molnar & Blakemore, 1999 and reviewed in Molnar & Blakemore, 1995). Fibroblast growth factors (FGFs) and nerve growth factor (NGF) also stimulate thalamic outgrowth and therefore represent candidate molecules for this activity (Lotto & Price, 1995). Altered release of such factors from the *Sey/Sey* cortex might contribute to delayed TCA growth. It seems probable that locally growth-promoting or growth-permissive factors in the diencephalon could also contribute to thalamocortical axonal outgrowth and that these might be affected in the mutant.

3. *TCAs exhibit aberrant pathfinding and are unable to navigate past the diencephalic/ telencephalic boundary.*

During brain development, axons such as TCAs navigate long distances over specific pathways to their target areas. Neuronal growth cones appear to be guided by a combination of attractive and repulsive cues, both long-range (diffusible molecules) and short range (contact-mediated mechanisms involving cell surface and extracellular matrix molecules; reviewed in Tessier-Lavigne & Goodman, 1996). Indeed, current evidence suggests that TCAs use an array of pathfinding cues including an axonal scaffold, long-distance and local diffusible signals. Correct targeting is probably achieved by a balance of growth-permissive, attractive and repulsive cues.

Recent evidence that TCA pathfinding is dependent on axonal guidance molecules has been provided by co-culture experiments showing that dorsal thalamic axons are repelled by diffusible activity released from the hypothalamus and attracted by ventral telencephalic tissue (Braisted *et al.*, 1999). *Pax6*, and other regulatory genes, are thought to pattern the forebrain partly by controlling expression of axon guidance molecules and thus directing axon pathways (for example Macdonald *et al.*, 1994; Figdor & Stern, 1993; Shimamura *et al.*, 1995; Ba-Charvet *et al.*, 1998). Two lines of evidence support this idea in relation to *Pax6*. Firstly, during early brain development, the ventral diencephalic tract of the postoptic commissure (tpoc) exhibits pathfinding errors in regions of the diencephalon where *Pax6* is normally expressed (Mastick *et al.*, 1997). Secondly, alterations in ventral thalamic domains expressing *Pax6* correlate with aberrant TCA navigation in mice deficient for the transcription factor *Mash1* (Tuttle *et al.*, 1999).

At E12.5, when the first TCAs are migrating through the diencephalon towards the cortex, the *Sey/Sey* brain already shows severe morphological and patterning abnormalities in regions of the dorsal thalamus, ventral thalamus, hypothalamus and nuclei of the dorsal diencephalon (Stoykova *et al.*, 1997; Warren *et al.*, 1997). Patterning defects continue later in development in diencephalic structures derived from these areas. If critical contact-mediated cues or diffusible signals are abolished or altered by disruptions in diencephalic patterning, this might account for aberrant TCA pathfinding in the *Sey/Sey* brain.

In the future, it will be important to establish the nature of putative guidance molecules regulated by *Pax6* and required for TCA pathfinding. The neural cell adhesion molecule *L1* is a good candidate; *L1* is highly expressed by TCAs (Fukuda *et al.*, 1997) and evidence that Pax6 can bind and drive expression from *L1* promoter regions *in vitro* suggests it is a direct downstream target of Pax6 in the forebrain (Chalepakis *et al.*, 1994; Meech *et al.*, 1999) and see Chapter 5). In the *Mash-1* null mutant, a ventral medial telencephalic domain of *Nkx2.1* and *Netrin1* expression is absent, which extends to the diencephalic-telencephalic border (where TCAs normally enter the ventral telencephalon) and correlates with a failure of TCAs to cross this boundary (Tuttle *et al.*, 1999). It is proposed that this domain is required to allow crossing and extension into the ventral telencephalon. *Netrin1* and *Nkx2.1* therefore represent excellent candidates for investigating the nature of the diencephalic/telencephalic stalling of TCAs in the *Sey/Sey* brain. However, TCAs appear to turn normally at the diencephalic/telencephalic boundary in both *Netrin1* and *DCC* (a *Netrin1* receptor) deficient mice (Braistead *et al.*, 1999). Other candidate extracellular matrix (ECM) and cell surface molecules implicated in thalamocortical axonal guidance are listed in Table 3.1.

Sey/Sey TCA pathfinding defects might also be explained by a morphological, rather than a molecular, barrier. Axonal projections from the ventral telencephalon into the dorsal thalamus have been identified before or near the time at which the first TCAs extend into the ventral thalamus. It has been proposed that these form part of an axonal scaffold to guide initial thalamocortical projections (Metin & Godemont, 1996; Molnar *et al.*, 1998a; Braisted *et al.*, 1999). Further along the TCA pathway, thalamocortical and corticothalamic tracts meet in the internal capsule and might guide each other (the 'handshake hypothesis'; Molnar & Blakemore, 1995; Molnar *et al.*, 1998a). Amongst patterning defects in the *Sey/Sey* diencephalon, there is a failure of the ventral thalamus and eminentia thalami to fuse with the basal forebrain except at the most rostral levels (Stoykova *et al.*, 1996; Warren & Price, 1997). This creates dramatically altered morphology of the hypothalamic-telencephalic transition region (apparent in Fig. 3.1D) in which the dorsal surface of the diencephalon is compacted ventrally and the lateral ventricle extended dorsally and caudally. The lack of tissue in this region could create a barrier to the growth of early guidance axons comprising the axonal scaffold, and prevent progression of later TCAs into the ventral telencephalon.

4. *Loss of axon fasciculation*

Loss of axon fasciculation in *Sey/Sey* TCAs might be the result of altered axonal adhesive properties (mediated by inter-axon attractive or repulsive molecules), or again, of altered local environmental cues. For example, a more permissive growth substrate might be less restrictive to axons (reviewed in Tessier-Lavigne & Goodman,1996). It would be interesting to examine whether the effects of *Pax6* on TCA pathfinding are cell autonomous, by thalamic transplants from mutant to wildtype.

Since this study was carried out the findings of a similar investigation of cortical efferent and afferent pathways in rat *Small eye* (*rSey/rSey*) have been reported (Kawano *et al.*, 1999). In agreement with results reported here, pathfinding defects were found in the trajectory of dorsal thalamic axons in *rSey/rSey*. These are partly attributed to loss of a ventral thalamic *Pax6* expression domain bordering the hypothalamus, above which normal TCAs change course to enter the telencephalon. In contrast to the findings in this investigation TCAs are reported to show limited extension into the ventral telencephalon over the lateral amygdaloid region. However, the possibility that this represents ectopic labelling of tracts of amygdaloid origin in the mutant was not excluded.

Molecule	Function	Reference
Fibroblast growth factors (FGFs) and nerve growth factor (NGF)	Stimulate thalamic outgrowth *in vitro*; expressed in cortex and in diencephalon (NGF)	Lotto & Price, 1995
Netrin1	Well characterised chemoattractant expressed in ventral telencephalon during TCA navigation; ventral telencephalon explants also attract cortical neurite outgrowth. Response of growth cones to netrin1 may be modified by ECM molecules.	Serafini *et al.*, 1996 Metin *et al.*, 1997 Richards *et al.*, 1997 Braisted *et al.*, 1999 Hopker, *et al.*, 1999
Semaphorin III/D/collapsin1	Axonal chemorepellant expressed in ventral diencephalon (although TCA projections are normal in semaphorin $III^{-/-}$ mice).	Bagnard *et al.*, 1996 Puschel *et al.*, 1996 Catalano *et al.*, 1998
Slit1	Diffusible chemorepellant for neurons migrating from lateral geniculate nucleus to cortex.	Zhu *et al.*, 1999
Ephrin-A5 and receptor Eph5	Members of well characterised family of ligands and receptor tyrosine kinases involved in axonal guidance and targeting; ephrin A5 regulates thalamic neurite outgrowth *in vitro*	reviewed in O'Leary & Wilkinson, 1999 Gao *et al.*, 1998
Chondroitin sulfate proteoglycans (CSPGs) including neurocan, which interacts with tenascin-C	ECM components enriched along TCA pathway in cortex and responsible for layer-specific thalamocortical outgrowth in cortex; *neurocan* and *tenascin-C* are expressed in developing diencephalon.	Bicknese *et al.*, 1994 Emerling & Lander, 1996 Oohira *et al.*, 1994 Grumet *et al.*, 1985
Heparin-binding growth associated molecule (HB-GAM) and its receptor N-syndecan (heparan sulphate proteoglycan)	ECM molecules associated with TCA pathway: N-*syndecan* expressed by TCA axons; preferential thalamic outgrowth on HB-GAM	Kinnunen *et al.*, 1999
L1	Neural cell adhesion molecule localised to TCAs	Fukuda *et al.*, 1997

Table 3.1 Molecules with a putative role in thalamocortical axonal growth and pathfinding. Axonal navigation involves a combination of multiple guidance cues.

CHAPTER 4

In vitro analysis of cortical cell migration in the wildtype and *Sey/Sey* brain

4.1 Introduction

I have shown in the previous chapter that thalamic innervation to the cortex is absent from the *Sey/Sey* brain and proposed that this may contribute to *Sey/Sey* cortical defects. In this chapter, I tested this hypothesis *in vitro* by establishment of a cortical explant system. The system was designed to observe differences in the behaviour of cells migrating from wildtype and *Sey/Sey* cortical explants. I then tested whether co-culture of cortical explants with wildtype or *Sey/Sey* diencephalic tissue could rescue *Sey/Sey* migratory defects.

4.2 Results

4.2.1 An analysis of cortical cell behaviour

The experimental system set up to culture cortical explants is illustrated in Figure 4.1. E15.5 or E13.5 wildtype and *Sey/Sey* cortex was divided into anterior, middle and posterior thirds. Anterior (A) and posterior (P) thirds were cut into pieces (0.1-0.2mm in diameter) and placed in 9x9mm wells on chambered coverglass slides coated with poly(L)-lysine and laminin in serum free medium. Wildtype and *Sey/Sey* diencephalon from brains of the same age were dissected out and added to the wells such that tissue was co-cultured in the following combinations:

Co-culture treatment	Genotype (and A/P position) of cortex	
alone	+/+ (A)	Sey/Sey (A)
alone	+/+ (P)	Sey/Sey (P)
+/+ diencephalon	+/+ (A)	Sey/Sey (A)
+/+ diencephalon	+/+ (P)	Sey/Sey (P)
Sey/Sey diencephalon	+/+ (A)	Sey/Sey (A)
Sey/Sey diencephalon	+/+ (P)	Sey/Sey (P)

The cortical explants were co-cultured at varying distances from the diencephalic tissue in the wells. However, explants in contact with diencephalic tissue, or which became innervated by processes which grew from the diencephalon, were excluded from the analyses. Preliminary experiments suggested that cortical explants co-cultured with diencephalic tissue showed increased survival (Table 4.1), process outgrowth and increased cell migration, in agreement with previous explant analyses (Lotto & Price, 1996; Lotto *et al.*,

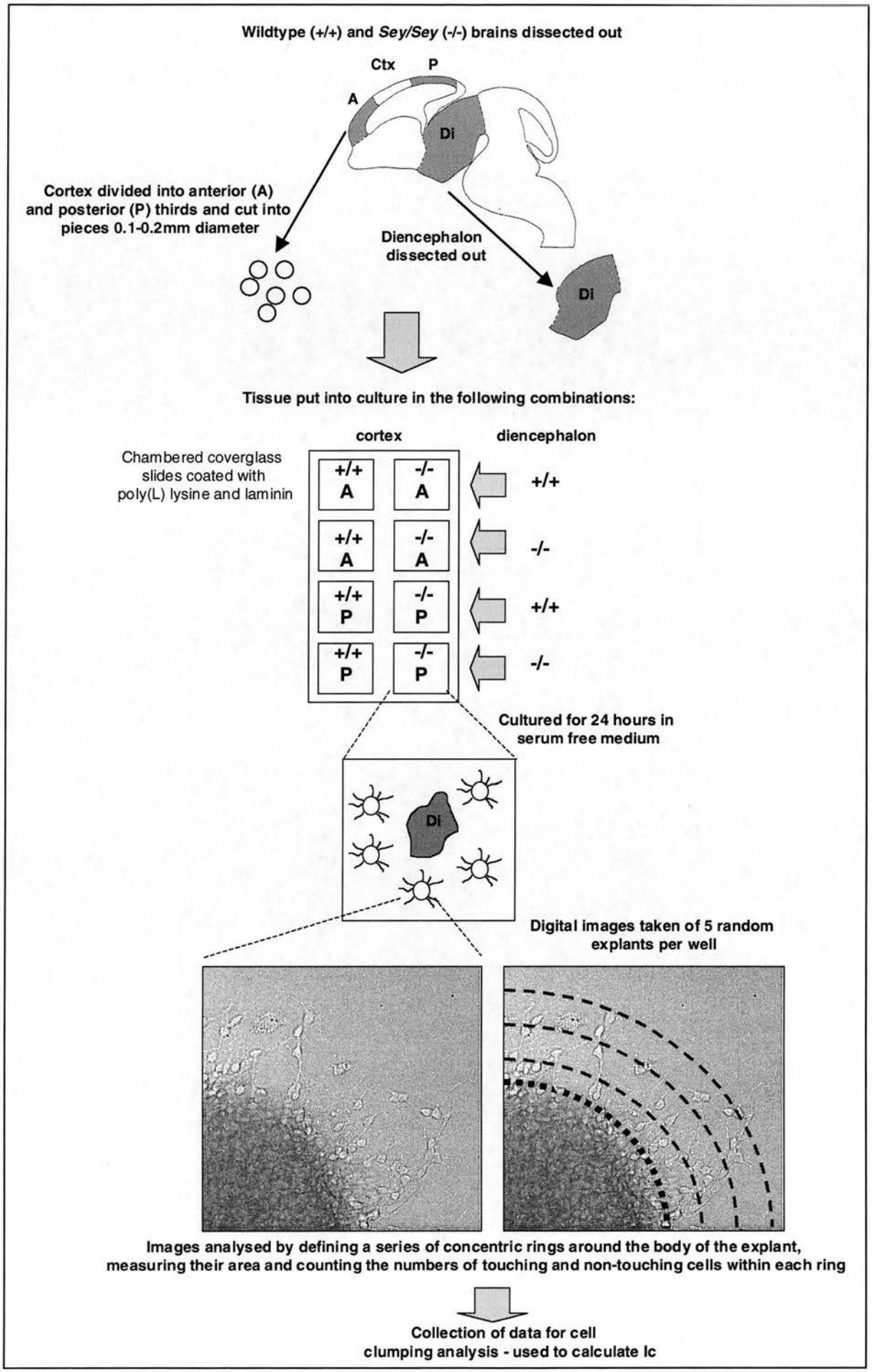

Figure 4.1 Flow diagram illustrating the cortical explant system and cell clumping analysis

The same procedure was followed for both E13.5 and E15.5 tissue.

+/+, wildtype; -/-, *Sey/Sey*; A, anterior; Ctx, cortex; Di, diencephalon; P, posterior.

1999). Therefore all the studies described in this chapter were limited to explants co-cultured with wildtype or *Sey/Sey* diencephalon.

After 24 hours in culture, both wildtype and *Sey/Sey* cortical explants had extended numerous processes and cells had migrated out from the explant body (Fig.4.2A,B). However, a striking difference in cell behaviour between the wildtype and *Sey/Sey* tissue was observed: whereas wildtype cells migrate out on processes individually or in association with one or two other cells (Fig.4.2A), many *Sey/Sey* cells migrate together in streams and form distinct clusters away from the explant body (Fig.4.2B). On the basis of this observation, an experimental system was designed to examine cellular clumping.

The explant system (shown in Figure 4.1) was set up to test differences in:

- strain (between wildtype and *Sey/Sey* tissue);
- treatment (co-culture with either wildtype or *Sey/Sey* diencephalon);
- position (explants taken from the anterior or posterior cortex);
- age (E13.5 and E15.5 cortex).

For each age, the explant cultures were set up using three separate wildtype and *Sey/Sey* brains (in three independent experiments). After 24 hours in culture, digital images of 5 randomly selected explants in each culture well were recorded.

To quantify cellular clumping and allow differences between wildtype and *Sey/Sey* tissues to be tested statistically, a model for measuring clumping was designed by Andrew Carothers at the MRC Human Genetics Unit (described in detail in the Appendix). The model gives a measurement of the degree to which cells clump together, I_C , independent of cell density. I_C is calculated based on the expected proportion of isolated cells (cells not touching another cell) under the null hypothesis that cells are randomly distributed around an explant. A scale of clumping is produced where $I_C = 0$ if all cells are isolated (not touching another cell), $I_C = \infty$ if all cells are touching one or more other cells, and $I_C = 1$ if the proportion of isolated cells is equal to that expected under the null hypothesis that cells are randomly distributed. The model was subjected to tests for validity and shown to produce a measure of clumping which fulfilled the criteria for analysis of variance (ANOVA). Further details of the model and the validation tests are contained in the Appendix.

Explant images were analysed using an IPLab script (Scanalytics Inc.) written by Paul Perry at the MRC Human Genetics Unit. Measurements were made by defining a series of concentric rings of equal width surrounding the explant, measuring their area and counting the numbers of touching and non-touching cells within each ring; these figures were used to

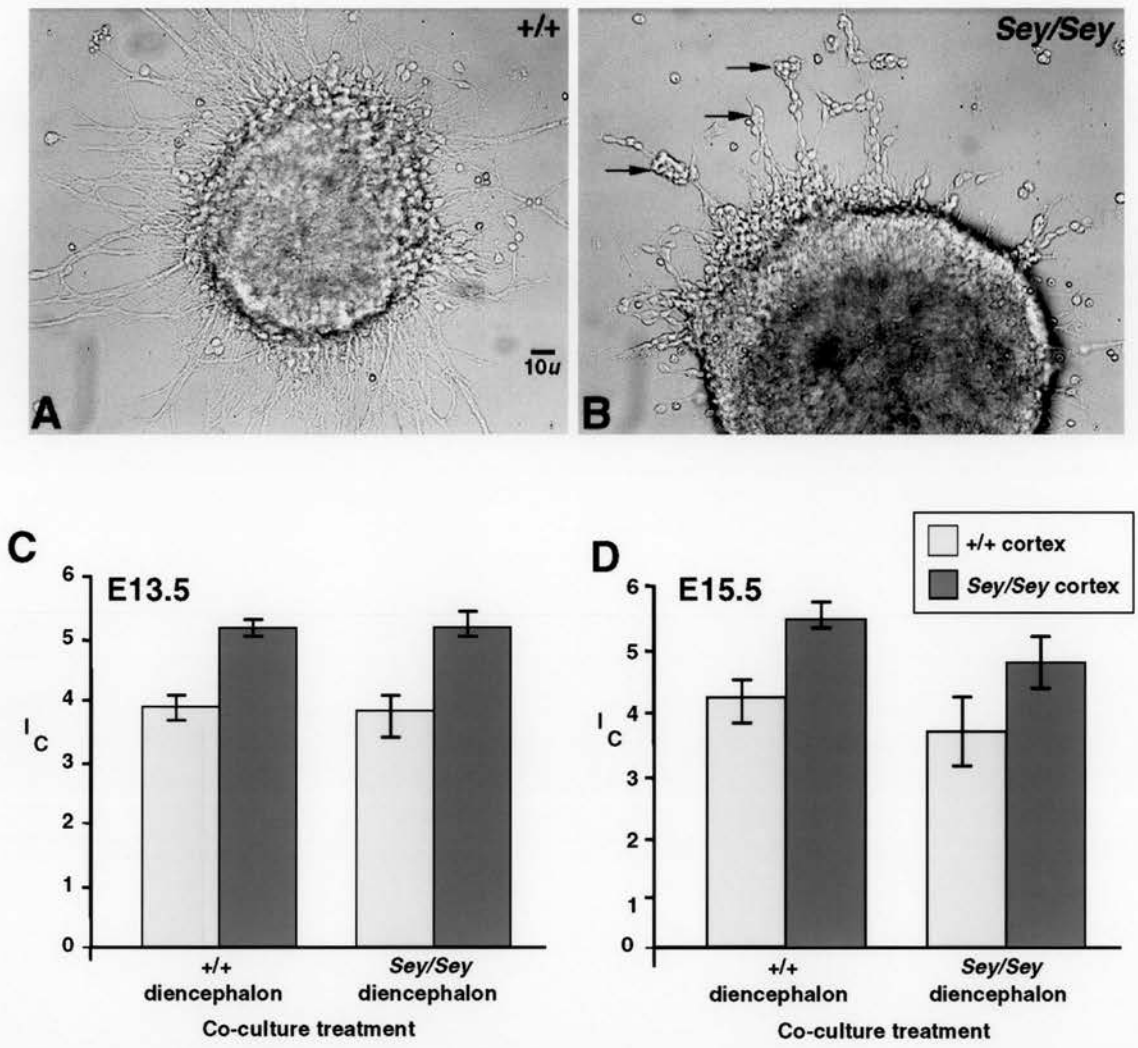

Figure 4.2 Cortical explant cultures

A,B. Differential interference contrast (DIC) images of (A) wildtype (+/+) and (B) *Sey/Sey* E15.5 cortical explant cultures after 24 hours co-cultured with wildtype diencephalon tissue.

A. Wildtype. The explant extends a network of processes and individual cells migrate outwards.

B. *Sey/Sey*. The explant extends processes and many cells which migrate out form clumps (arrows).

C,D. Histograms comparing the values for the cellular clumping measurement Ic in (C) E13.5 and (D) E15.5 wildtype and *Sey/Sey* cortical explants after 24 hours in culture. Bars show standard error. Cortical explants were subjected to co-culture treatment with either wildtype or *Sey/Sey* diencephalon. At each age and for each treatment *Sey/Sey* cortex shows significantly more clumping than wildtype. There is no significant effect of co-culture treatment or age on cell clumping.

+/+, wildtype. Scale bar in A, 10μm, also applies to B.

calculate I_C. As several factors were being tested for their effect on clumping (strain, treatment, position and age) an analysis of variance (ANOVA) was carried out on the resulting data; further details of the analysis are also described in the Appendix.

The ANOVA revealed that, at E13.5 and E15.5, clumping was significantly greater in migrating cells from *Sey/Sey* than wildtype cortical explants ($p<0.001$) (Fig. 4.2C,D). Averaged values for I_C (± S.E.) at E15.5 were 3.7± 0.3 for wildtype and 5.3 ± 0.2 for *Sey/Sey*. Furthermore, the analysis revealed no significant difference between co-culturing E15.5 explants (whether wildtype or *Sey/Sey*) with wildtype or *Sey/Sey* diencephalic tissue (Figure 4.2C,D). This demonstrates that the clumping phenotype of *Sey/Sey* cortical cells is not rescued by diffusible factors released by wildtype thalamus, and suggests that the adhesive properties of cortical cells are regulated independently of thalamic innervation.

BrdU labelling of *Sey/Sey* cortical cells has demonstrated that cells born at E13.5 acquire a relatively normal distribution in the cortical plate, whereas cells born at E16.5 remain within the VZ (Caric *et al.*, 1997). It was therefore interesting to investigate whether the clumping phenotype of *Sey/Sey* cortical cells *in vitro* was specific to the E15.5 cortex or also occurred in younger tissue. To address this question, I set up the explant system using both E13.5 and E15.5 cortex. However, the ANOVA revealed no significant difference in cell clumping between the two ages: clumping was again significantly greater at E13.5 in *Sey/Sey* ($I_C = 5.2 \pm 0.1$) than wildtype ($I_C = 3.9 \pm 0.2$) ($p < 0.001$) (Fig. 4.2C).

To assess whether cellular clumping was influenced by the anterior-posterior positional gradient of cortical development (Bayer & Altman, 1991), explants were set up using tissue from either the anterior or posterior third of the cortex at both E13.5 and E15.5. However, anterior-posterior position was found to have no significant effect on clumping.

4.2.2 A cell survival analysis

It is possible that the differences in cell clumping behaviour observed may be due to enhanced survival of *Sey/Sey* cells, if, for example, more wildtype cells migrating from the explant are undergoing cell death. To test this, a survival analysis was undertaken in which migrating cells were double labelled with fluorescent dyes for living and dead cells. Counts were performed on explants of each strain (wildtype and *Sey/Sey*), age (E13.5 and E15.5) and treatment (cultured alone, with wildtype diencephalon or with *Sey/Sey* diencephalon) described above. In addition, counts were made on explants which were cultured for either 24, 72 or 120 hours. For each age, explant cultures were set up using two separate brains

over two independent experiments; in each experiment counts were made on at least 10 randomly selected explants in each well.

Average cell survival figures are summarised in Table 4.1. ANOVA on the data collected after 24 hours in culture revealed no significant difference in cell survival between wildtype and *Sey/Sey* tissue at both E13.5 and E15.5. Treatment and age also had no significant effect on cell survival after 24 hours in culture. This suggests that, in this explant system, cell clumping after 24 hours is independent of cell survival and that the difference in clumping between wildtype and *Sey/Sey* cannot be attributed to differences in cell survival.

In addition, the cell survival data suggests that wildtype or *Sey/Sey* explants cultured for longer than 24 hours showed increased survival on co-culture with *Sey/Sey* diencephalon compared to wildtype diencephalon. This observation was not tested for significance.

		% survival (±S.E.)					
	Length of time in culture	**24 hours**		**72 hours**		**120 hours**	
	Age of dissected tissue	**E13.5**	**E15.5**	**E13.5**	**E15.5**	**E13.5**	**E15.5**
Genotype of cortex (strain)	**Co-culture treatment**						
+/+	**none**	65 (±3)	77 (±3)	29 (±7)	47 (±5)	35 (±9)	5 (±3)
Sey/Sey	**none**	72 (±7)	70 (±4)	42 (±9)	29 (±9)	33 (±6)	4 (±1)
+/+	**+/+ diencephalon**	62 (±4)	71 (±2)	54 (±5)	61 (±8)	52 (±8)	20 (±4)
Sey/Sey	**+/+ diencephalon**	68 (±5)	71 (±5)	53 (±5)	44 (±5)	42 (±3)	21 (±3)
+/+	***Sey/Sey* diencephalon**	61 (±3)	73 (±5)	62 (±9)	72 (±7)	60 (±6)	47 (±3)
Sey/Sey	***Sey/Sey* diencephalon**	73 (±4)	77 (±3)	61 (±7)	50 (±7)	51 (±4)	28 (±3)

Table 4.1. Survival of cells migrating from *Sey/Sey* and wildtype (+/+) cortical explants over time and with different co-culture conditions. The average number of cells surviving is given as a percentage of the total number of cells migrating from an explant. In each category the cells from at least 10 explants were counted in 2 separate experiments (20 explants in total) . ANOVA on the 24 hour data showed no significant effect of either strain, treatment or age on cell survival.

4.2.3 Analysis of clumping cells

Immunostaining of cells migrating from the explants was performed to evaluate the cell types involved in aberrant migration. Antibody TuJ1 to neuron-specific class III β-tubulin isotype stains the earliest born postmitotic neurons (Ferreira & Caceres, 1992) and revealed

that many cells migrating from both wildtype and *Sey/Sey* explants are TuJ1 positive and that some, but not all, cell clumps also contain TuJ1 positive cells (Fig.4.3). Staining with the antibody against phosphorylated histone H3 marks metaphase cells (Hendzel *et al.*, 1997; Hendzel *et al.*, 1998). This antibody revealed that, with the exception of one or two migrating cells, the vast majority of cell division is occurring within the explant body, in both wildtype and *Sey/Sey* (Fig. 4.4). Cell division occurs very rarely within clumping cells in *Sey/Sey* explants (Fig. 4.4E). Finally, RC2 antibody, a protein localised to radial glia (Edwards *et al.*, 1990), revealed cells with normal radial glial morphology extending from both wildtype and *Sey/Sey* explants (Fig. 4.5). In both strains, some cells appear to be migrating along radial glia. However, those cells which are clustering in *Sey/Sey* explants appear to have lost contact with the glial surface and have instead adhered to one another (Fig. 4.5C). In both wildtype and mutant explants the numbers of neuronal and glial cells were approximately the same (although no formal counts were performed).

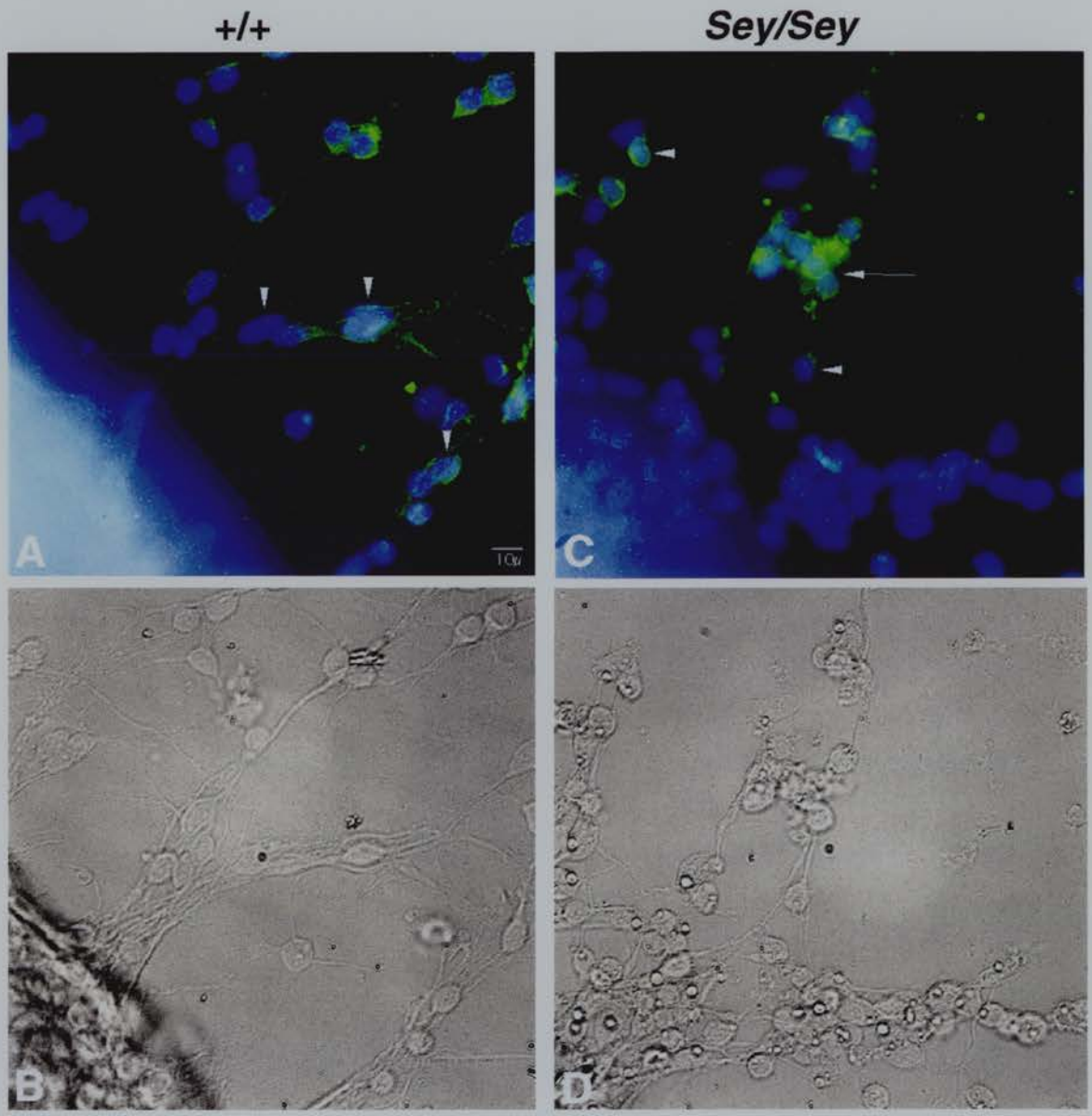

Figure 4.3 *TuJ1* expression in cortical explants

Wildtype (+/+) (A,B) and *Sey/Sey* (C,D) cortical explant cultures after 24 hours co-cultured with wildtype diencephalon.

A,C. Explants immunostained for TuJ1 (green) marking postmitotic neurons and counterstained with DAPI (blue).

A. Wildtype. A proportion of cells migrating from the explant are TuJ1 positive (arrowheads).

C. *Sey/Sey.* Individual TuJ1 positive cells migrate from the *Sey/Sey* explant (arrowheads). Some cell clumps also contain TuJ1 positive cells (arrows).

B,D. DIC images of the explants shown in (A,C).

+/+, wildtype. Scale bar in A, 10μm and applies to all images.

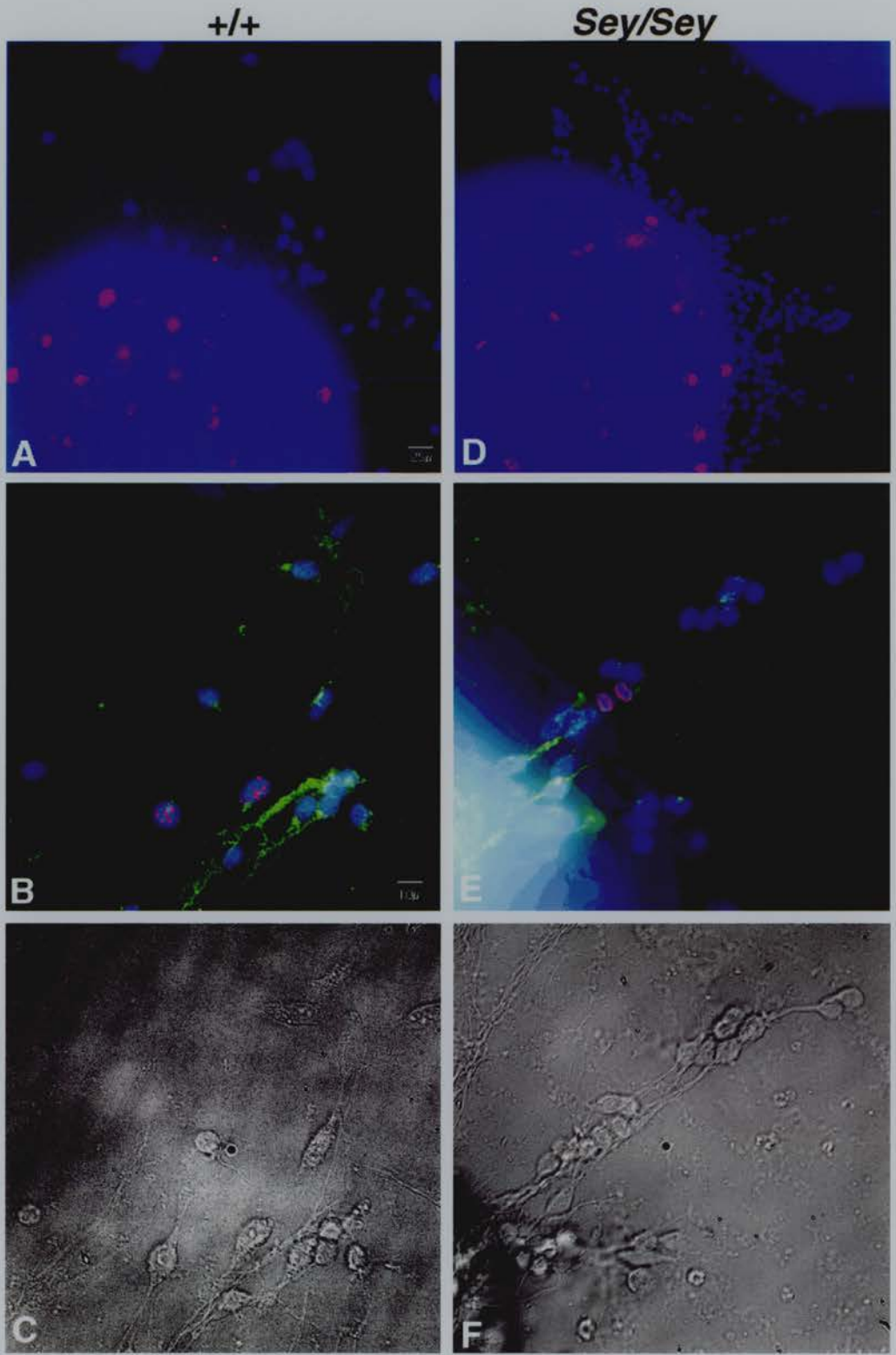

Figure 4.4 Cell division in cortical explants

Wildtype (+/+) (A-C) and *Sey/Sey* (D-E) cortical explant cultures after 24 hours co-cultured with wildtype diencephalon.

A,D. Explants imunostained for phosphorylated histone H3 marking metaphase cells (red) and nuclei counterstained with DAPI (blue). The majority of cell division occurs within the explant body in both wildtype (A) and *Sey/Sey* (D) explants.

B,E. Explants imunostained for phosphorylated histone H3 marking metaphase cells (red), neural cell adhesion molecule (NCAM, green) and nuclei counterstained with DAPI (blue). The majority of migrating cells, with one or two rare exceptions, are not dividing.

C,F. DIC images of the explants shown in B,E.

+/+, wildtype. Scale bars: A, 25μm and applies to D; B, 10μm and applies to C,E,F.

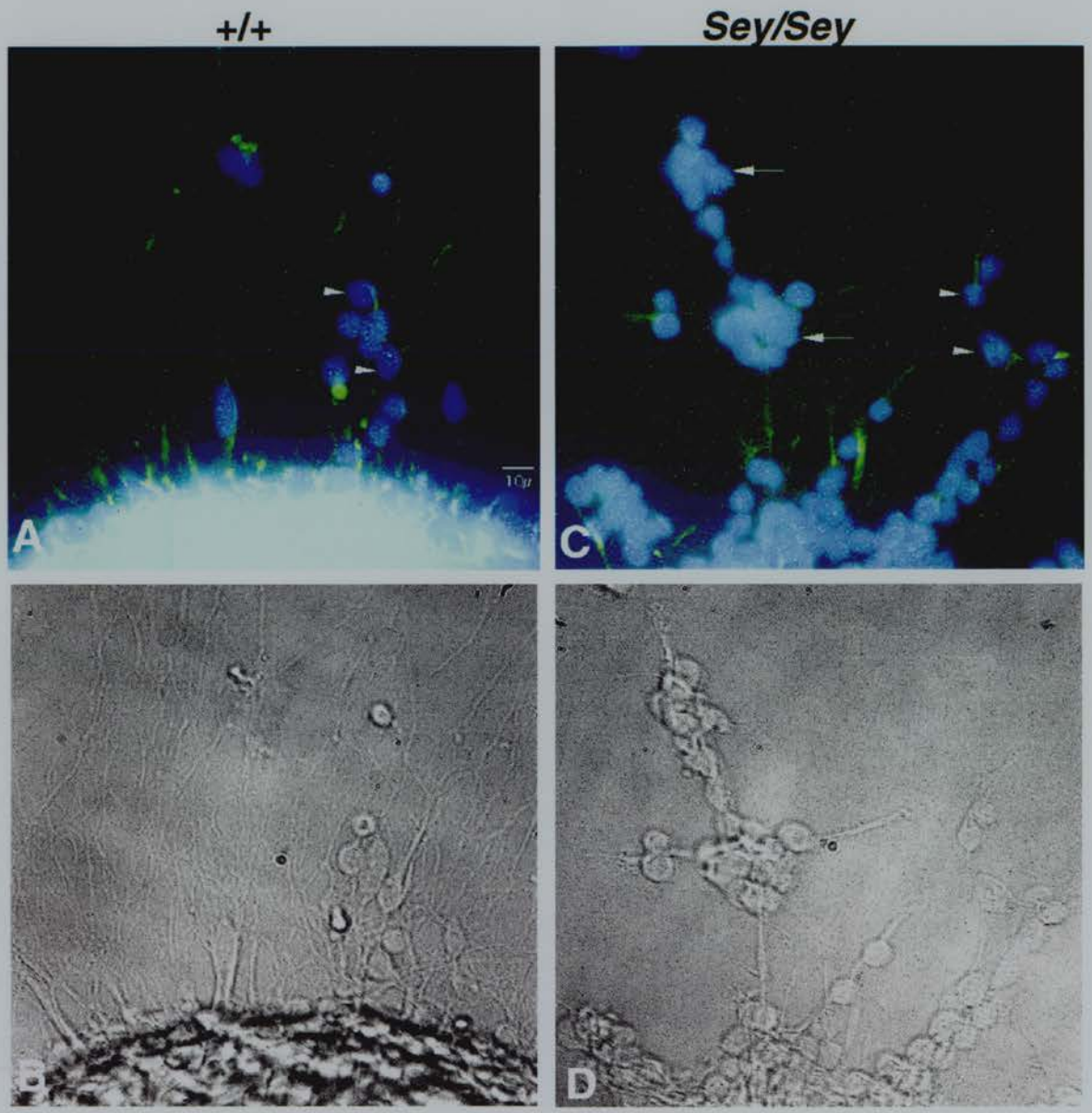

Figure 4.5 Radial glial-guided migration in cortical explants

Wildtype (+/+) (A,B) and *Sey/Sey* (C,D) cortical explant cultures after 24 hours co-cultured with wildtype diencephalon.

A,C. Explants imunostained for RC2 (green) marking radial glia and nuclei counterstained with DAPI (blue).

A. Wildtype. Radial glia extend from the explant and cells migrate along them (arrowheads).

C. *Sey/Sey*. Individual cells also migrate along radial glial from the *Sey/Sey* explant. In clumps (arrows) some cells appear to lose contact with the glial surface and adhere to each other.

B,D. DIC images of the explants shown in (A,C).

+/+, wildtype. Scale bar in A, 10μm, and applies to all images.

4.3 Discussion

Taken together, results presented in this chapter suggest that, in the absence of *Pax6*:

- migrating cortical cells exhibit preferential adhesion to each other rather than to radial glia *in vitro*, causing their aggregation into clumps;
- clumping cells are postmitotic and are undergoing neuronal differentiation.

This suggests that these clumps correspond to the cells of the expanded ventricular layers and ectopic SVZ clusters seen in the *Sey/Sey* cortex *in vivo*, which also express *TuJ1* (Caric *et al.*, 1997).

4.3.1 Validity of an *in vitro* explant system

In order for results obtained in an *in vitro* system to have real biological meaning, the system must mimic cellular events *in vivo*. In contrast to the experiments performed by Gotz *et al.* (1998) on disaggregated *Sey/Sey* cortical cells, this explant system maintains cell contacts, which are thought to be important in regulating aspects of cortical progenitor behaviour such as proliferation and specification (Davis & Temple, 1994; Bohner *et al.*, 1997). In these experiments, pieces of tissue cultured in serum-free medium extended radial glia and exhibited glial-guided neuronal migration, similar to the behaviour of migrating neurons *in vivo* (Rakic, 1972; Hatten, 1990; Misson *et al.*, 1991). Furthermore, differences in cellular behaviour between wildtype and *Sey/Sey* were reproduced: *Sey/Sey* cortical migratory cells aggregated in clusters analogous to the accumulation of cells seen in the *Sey/Sey* VZ. These observations support the validity of the system in representing events *in vivo* and demonstrate its potential for use in future experiments. For example, it would be of particular interest to test if the *Sey/Sey* migratory defect can be rescued by transfection with a *Pax6* expressing construct.

4.3.2 *Sey/Sey* cortical migratory phenotype is independent of thalamocortical innervation

It was proposed from my data in Chapter 3 that the absence of thalamocortical innervation in the *Sey/Sey* brain might contribute to the late-onset of *Sey/Sey* cortical defects. Here, I presented two observations suggesting that the altered adhesive properties of *Sey/Sey* cortical cells *in vitro* appear to be determined independently of the thalamus:

- the majority of thalamocortical innervation occurs from E14.5-E16.5, yet *Sey/Sey* cell clumping *in vitro* is apparent prior to this at E13.5;
- *Sey/Sey* cortical clumping phenotype is not rescued by co-culture with wildtype diencephalon.

This *in vitro* result suggests that the absence of thalamocortical innervation from the *Sey/Sey* cortex does not contribute to the *Sey/Sey* cortical phenotype *in vivo*. However, by co-

culturing cortical explants in the same well, but not in contact with, diencephalic tissue, I have only examined the role of long-range diffusible molecules released from the thalamus. I have not addressed the possibility that short-range diffusible molecules or contact-mediated cues provided by thalamic innervation are essential for cortical migration. This hypothesis could be tested with an *in vitro* system allowing innervation of *Sey/Sey* cortical explants with wildtype thalamus. In addition, preliminary data obtained during this study suggested that co-culture with *Sey/Sey* diencephalon does enhance survival of cortical cells more than wildtype diencephalon after several days in culture (Table 4.1). This implies that diffusible factors released by the *Sey/Sey* thalamus may influence aspects of cortical development, such as survival, other than cell adhesive properties. Thus the thalamus may still play a role in the *Sey/Sey* cortical defects, but is unlikely to be the primary cause of them.

4.3.3 *Sey/Sey* cortical neurons possess altered adhesive properties

Radial migration of neurons involves a highly regulated sequence of adhesive interactions between neurons, glia, and the extracellular matrix (ECM). The observations made in my explant system suggest that *Pax6* is specifically required to maintain normal neuronal cell-cell interactions during cortical migration. In the absence of Pax6 function, cells are still able to migrate on radial glia, suggesting that the neuronal-glial interaction is maintained. However, during migration, cells abnormally adhere to each other in clusters, suggesting they possess altered adhesive properties that enhance neuron-neuron (neurophilic) interactions. Two previous observations also support a role for Pax6 in regulating neuron-neuron adhesion:

- in contrast to controls, *Sey/Sey* cells transplanted into wildtype VZ are found in clusters in the cortical plate, suggesting that they have adhered together prior to or during migration (D. Price, personal communication);
- *Sey/Sey* cortical cells preferentially aggregate with each other rather than with wildtype cortical cells in cell association assays (Stoykova *et al.*, 1997).

A variety of molecules might mediate *Pax6* regulation of neuronal adhesion. For example, a recent study showed that cortical neurons lacking certain integrins, cell surface receptors which mediate cell-ECM and cell-cell interactions, reveal a phenotype highly reminiscent of *Pax6* null neurons (Anton *et al.*, 1999). Thus, antibodies blocking integrin $\alpha_3\beta_1$ function cause migrating cortical neurons to adhere to each other rather than radial glia in migration assays. *Integrin* α_3 is highly expressed in the cortical VZ and IZ and α_3 null mice lack cortical lamination. It has been proposed that downregulation of α_3 may trigger a switch from gliophilic to neurophilic adhesion (Anton *et al.*, 1999). This, and other neuronal adhesion molecules summarised in Table 1.2 are candidate downstream targets of *Pax6* in mediating neuronal interactions during migration.

4.3.4 A model for *Sey/Sey* cortical development

My *in vitro* data is particularly meaningful in relation to the cause of cortical defects in the *Sey/Sey* cortex. Previously, irregular cortical stratification has invariably been attributed to a defect in neuronal migration (Schmahl *et al.*, 1993; Stoykova *et al.*, 1996; Caric *et al.*, 1997). Cortical neurons born at E16.5 are unable to migrate past older cortical layers (Caric *et al.*, 1997) and differences in the number and morphology of *Sey/Sey* cortical radial glia (Gotz *et al.*, 1998) suggested this could be accounted for by a failure in glial-guided migration. However, several lines of evidence now suggest that *Sey/Sey* cells retain the capacity to undergo glial guided migration:

- *Sey/Sey* cells transplanted into a wildtype cortical environment are able to migrate to their correct position in the cortical plate (Caric *et al.*, 1997), demonstrating that the cells retain the capacity to migrate normally;
- Brain lipid-binding protein (BLBP), a marker induced in radial glia by attaching and migrating neurons (Feng *et al.*, 1994; Feng & Heintz,1995) is expressed normally by radial glia in *Sey/Sey* cortex (Gotz *et al.*, 1998), suggesting that neuronal-glial signalling still occurs normally;
- my data show that *Pax6* null cells have the ability to migrate normally on *Pax6* null radial glia *in vitro*, suggesting that the migratory block is removed by transplantation out of the *Sey/Sey* cortical environment.

Thus it seems that *Sey/Sey* cortical cells are capable of normal glial guided migration in most respects and that migratory defects *per se* are probably not the primary cause of the cortical phenotype. Instead, I propose that, before or during migration, increased neuron-neuron adhesion causes accumulation of neurons into clusters, and that this prevents migration of later born cortical neurons *in vivo*. It cannot be discounted that radial glia, which exhibit cell autonomous morphological defects in the *Sey/Sey* cortex (Gotz *et al.*, 1998), could also contribute to neuronal clumping; it is possible that glial cell surface properties or neuron-glial signalling are also important in instructing neurons to detach from glia (Anton *et al.*, 1996) and that these cues are presented prematurely during *Sey/Sey* glial-guided migration.

This hypothesis must, however, take into account the late-onset of cortical defects in *Sey/Sey*. Whereas defects in *Sey/Sey* cortical migration and morphology are only seen from E14.5 (Schmahl *et al.*, 1993; Caric *et al.*, 1997), clumping of *Sey/Sey* cells *in vitro* is seen earlier at E13.5, suggesting that neurons generated throughout neruogenesis have altered adhesive properties. I suggest that this paradox may be accounted for by the slow rate of neuron production during early neurogenesis (Miller, 1985; Caviness *et al.*, 1995). Neurons born

early are likely to encounter few other neurons as they migrate out to the cortical plate, and are therefore unlikely to form neuronal aggregates large enough to inhibit migration. Only when the rate of neuron production peaks during the final third of neurogenesis (E14.5-16.5), and the density of neurons becomes high enough to cause neuronal clumping, is a physical barrier created which impedes further neuronal migration. Furthermore, this mechanism would be exacerbated by the accelerated rate of progression through neurogenesis suggested by evidence presented in Chapter 2.

CHAPTER 5

A candidate gene expression analysis

5.1 Introduction

5.1.1 Identification of genes acting downstream of Pax6

Up to this point, I have presented experiments aiming to elucidate Pax6 function using cell biology assays. Identification of molecules acting downstream of Pax6 should give further insight into its functions during cortical development, and in the next two chapters I will describe the use of molecular techniques to approach this problem.

The paired and homeo-type DNA binding domains within Pax6 strongly suggests it acts in transcriptional regulation (Chalepakis *et al.*, 1991), yet its molecular function is unlikely to be simple. For example, in the hindbrain, the *Pax6* positive rhombic lip gives rise to both the cerebellar external granule layer (EGL) and precerebellar nuclei, and both exhibit migratory defects in the *Sey/Sey* brain (Engelkamp *et al.*, 1999). However, *Unc5h3* expression is lost from the mutant EGL whilst expression of this gene is maintained in remnants of the mutant pontine nucleus (Engelkamp *et al.*, 1999). This suggest that *Unc5h3* expression is regulated by Pax6, either directly or indirectly, in the EGL, but is independent of Pax6 in the precerebellar nuclei. An analogous process may occur in the cortex where *Pax6* is expressed in a heterogeneous collection of progenitor cell types comprising the cortical VZ (Gotz *et al.*, 1998). It is possible that within the progenitor population Pax6 regulates different molecular pathways in different subgroups of cells, at different times during development, or even in the same cell at the same time. Furthermore, Pax6 might either act alone, or in co-operation with other transcriptional regulators; interacting proteins within a transcriptional complex may be essential for modifying Pax6 function.

In an attempt to identify some of the genes acting downstream of *Pax6*, I used two separate methods:

1. Candidate gene analysis (Chapter 5);
2. Differential gene expression analysis by subtractive hybridisation (Chapter 6)

5.1.2 Candidate gene analysis

Based on evidence for the function of *Pax6* in controlling cell cycle progression, cell fate specification and cell adhesive properties, putative Pax6 target genes can be classified into the following categories:

- cell cycle components;
- signalling molecules/receptors, or their downstream pathways;
- cell fate determination molecules/regulators of spindle orientation;
- cell adhesion molecules;
- transcription factors.

Immunohistochemical expression analysis was performed for candidate genes in the last three categories.

Results presented in Chapter 2 suggest that *Pax6* plays a role in regulating cleavage orientation during asymmetric division. In this chapter, the possibility that Pax6 may also regulate the expression of cell fate determinants was addressed by analysing the expression of mammalian homologues of the asymmetrically localised *Drosophila* cell fate determinants, Numb and Prospero. The role of these genes in cortical development is outlined in the Introduction (and Figure 1.8). Briefly, mammalian *Numb* (*mNumb*) and *Numblike* (*Nbl*) were identified by sequence similarity to *Drosophila numb* and both can rescue neuronal cell fate transformations in the *Drosophila numb* mutant (Zhong *et al.*, 1996; Zhong *et al.*, 1997). The differential expression patterns of *mNumb* and *Nbl* in the developing cortex suggests they may have distinct functions during cortical development. *mNumb* is expressed throughout the cortex, and exhibits asymmetric localisation in cortical progenitors(Wakamatsu *et al.*, 1999; Zhong,1996), whilst Nbl is cytoplasmically distributed in differentiating cells of the cortical plate (Zhong *et al.*, 1997). It has been proposed that mNumb and Nbl proteins interact with Notch1 to influence cell fate during neurogenesis and neuronal differentiation, respectively (Zhong *et al.*, 1997; Wakamiatsu,1999). *Prox1*, the vertebrate homologue of *Drosophila prospero* has a dynamic developmental expression pattern in distinct precursor populations within the brain (Oliver *et al.*, 1993; Torii *et al.*, 1999). Its role, if any, in cortical development has not been determined.

Evidence presented in Chapter 4 supports a separate function for Pax6 in regulating cell adhesive properties. L1 and TAG-1 are members of the immunoglobulin superfamily of neural cell adhesion molecules (Moos *et al.*, 1988; Furley *et al.*, 1990) essential for axonal extension and guidance. L1 is primarily localised to the processes of developing neurons and is implicated in axonal guidance and fasciculation during embryonic brain development (reviewed in Brummendorf *et al.*, 1998). *L1* knockout mice exhibit defects in extension of neuronal processes (Demyanenko *et al.*, 1999) Recently, a Pax6 binding domain identified in the *L1* regulatory region was shown to be necessary for Pax6 driven expression *in vitro;* mice with a deletion of this domain lack *L1*-reporter expression in the telencephalon and

mesencephalon (Meech *et al.*, 1999). *TAG-1* is transiently expressed on the surface of subsets of neurons in the developing nervous system (Yamamoto *et al.*, 1986; Dodd *et al.*, 1988; Wolfer *et al.*, 1994) during axonal extension. TAG-1 can mediate both homophilic and heterophilic cellular interactions and has been shown to promote neurite outgrowth *in vitro* (Furley *et al.*, 1990; Stoeckli *et al.*, 1991; Felsenfeld *et al.*, 1994), a function requiring interaction with L1-type molecules and integrins (Felsenfeld *et al.*, 1994).

A series of genes have now been identified which, like *Pax6*, can drive ectopic eye formation in *Drosophila: sine oculis, eyes absent, dachsund, teashirt* and *eyegone*. These genes are thought to function in a complex regulatory network regulating *Drosophila* eye development (reviewed in Czerny *et al.*, 1999). Several mouse homologues of *sine oculis* (*Six* gene family; Oliver *et al.*, 1995) and *eyes absent* (*Eya* gene family; Xu *et al.*, 1997) have been identified, presenting the possibility that their regulatory interactions with *Pax6* could be conserved.

5.2 Results

The localisation of mNumb, Numblike, Prox1, L1 and TAG1 was examined in the cortex of the developing wild type and *Sey/Sey* brain at E10.5, 12.5 and 15.5. These stages correlate to the onset of neurogenesis, early neurogenesis and mid-neurogenesis respectively (Caviness *et al.*, 1995).

At E10.5 the developing telencephalic wall is comprised almost exclusively of proliferating neuroepithelial cells and Pax6 nuclear staining is evident in the majority of these cells in the wildtype embryo (Fig. 5.1B). The Pax6 antibody used in this study does not detect the truncated protein produced in the *Sey/Sey* mutant (Fig.5.1E). Cytoplasmic *Nbl* expression is detected in the emerging preplate or primordial plexiform layer (PPL) of the cortex in both wild type and *Sey/Sey* telencephalon (Fig. 5.1C,F). The preplate is formed by the first postmitotic cells migrating from the VZ (Marin-Padilla, 1998). Surprisingly, more Nbl positive cells are apparent in the *Sey/Sey* preplate compared to wild type (Fig. 5.1F). At E10.5 *mNumb* expression is detected throughout the neuroepithelium and no apparent differences between wildtype and *Sey/Sey* were seen; no cortical expression of *Prox1* or *TAG1* was found (data not shown).

By E12.5 the PPL is a well established layer and *Pax6* expression clearly defines the ventricular layer of the wildtype cortex (Fig.5.2B). In agreement with previous reports (Zhong *et al.*, 1997) Nbl staining is detected mainly in cells outside the ventricular zone in both wildtype and *Sey/Sey* (Fig. 5.2C,G). *Nbl* expression remains confined to postmitotic neurons in the developing PPL and, in contrast to findings at E10.5 and E15.5, wildtype and

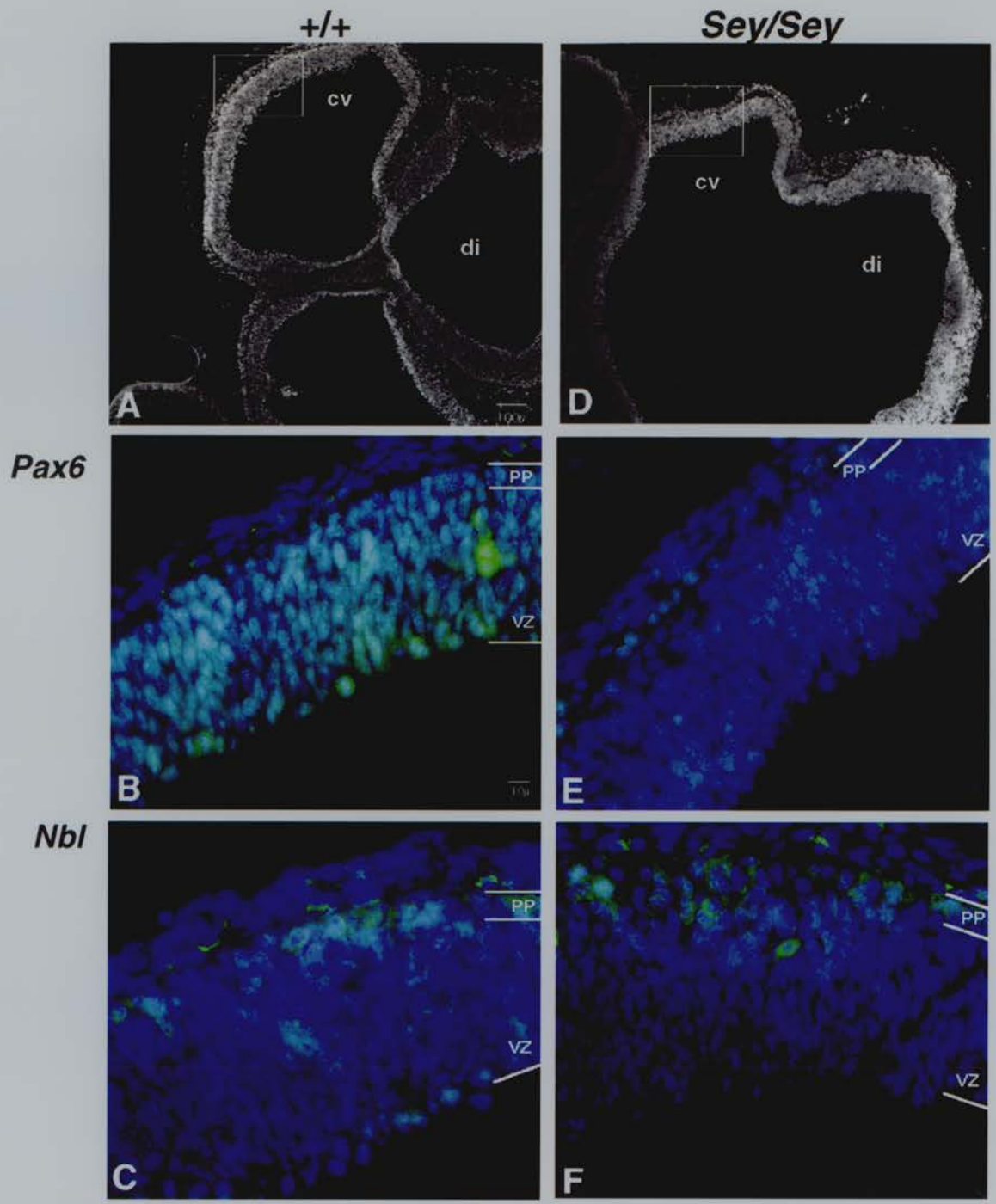

Figure 5.1 Expression analysis of *Pax6* and *Numblike* in wildtype and *Sey/Sey* E10.5 cortex

Coronal sections through E10.5 wildtype (+/+) (A-C) and *Sey/Sey* (D-F) brains. In all sections dorsal is to the right and in colour images nuclei are counterstained with DAPI (blue).

A. Low magnification image of wildtype coronal section stained with DAPI. Box shows the approximate area in the cerebral vesicle (cv) in which images (B,C) were taken.

B. Nuclear *Pax6* expression (green) in the wildtype ventricular zone (VZ).

C. Cytoplasmic *Numblike* (*Nbl*) expression (green) is detected in neurons of the preplate (PPL).

D. Low magnification image of *Sey/Sey* coronal section stained with DAPI in similar plane of section to (A). Box shows the approximate area in the cerebral vesicle (cv) in which images (E,F) were taken. The *Sey/Sey* cv shows altered morphology compared to wildtype.

E. The truncated protein produced in *Sey/Sey* is not recognised by the Pax6 antibody.

F. More Nbl-positive cells (green) are detected in the *Sey/Sey* PPL.

Scale bars: A, 100μm and also applies to D; B, 10μm and also applies to C,E,F. cv, cerebral vesicle; di, diencephalon; PPL, preplate; VZ ventricular zone.

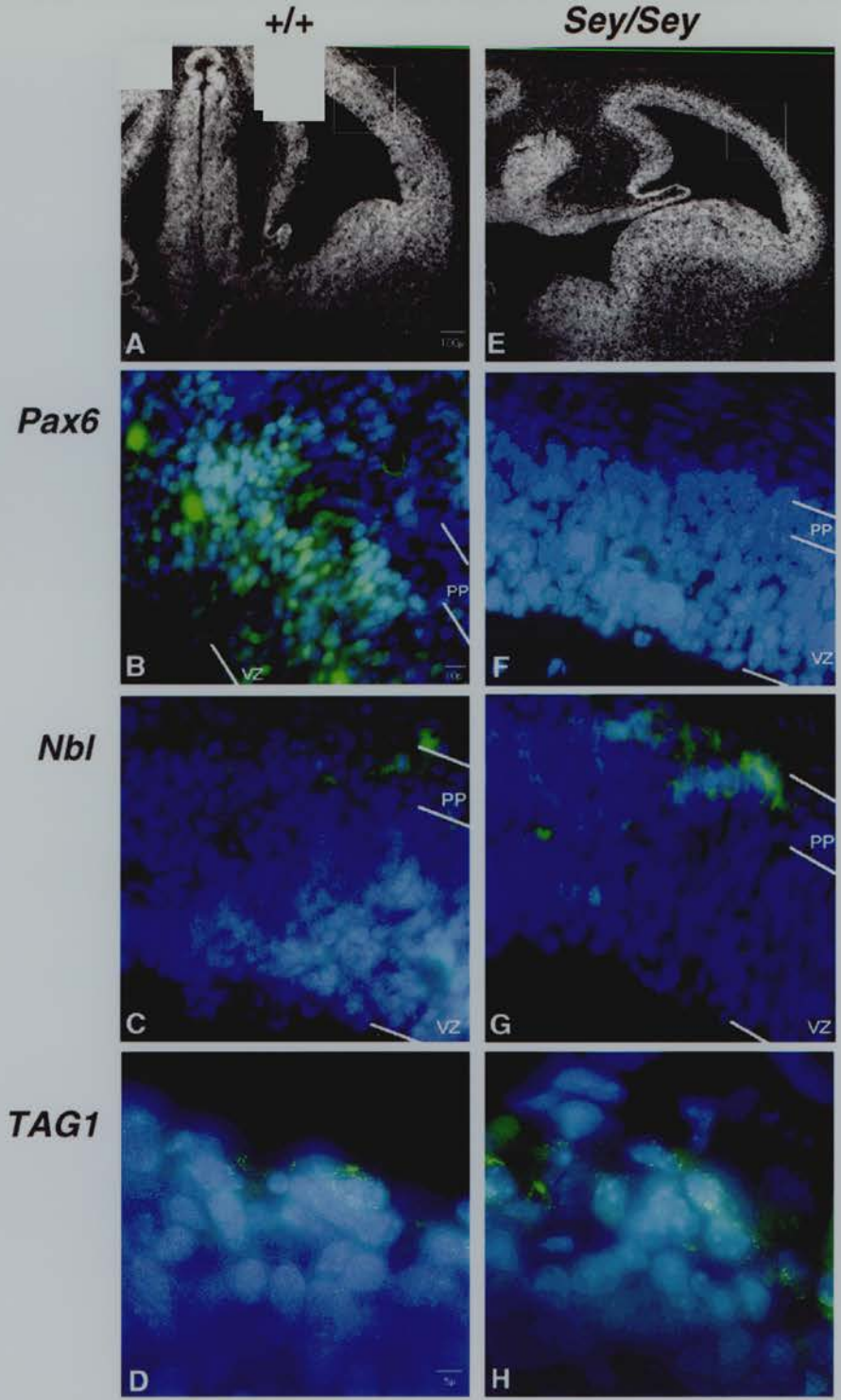

Figure 5.2 Expression analysis of *Pax6*, *Numblike* and *TAG1* in wildtype and *Sey/Sey* E12.5 cortex

Coronal sections through E12.5 wildtype (+/+) (A-D) and *Sey/Sey* (E-H) brains. In all sections dorsal is up and in colour images nuclei are counterstained with DAPI (blue).

A. Low magnification image of wildtype coronal section stained with DAPI. Box shows the approximate area in the cortex in which images (B-D) were taken.

B. Nuclear *Pax6* expression (green) in the wildtype ventricular zone (VZ).

C. Cytoplasmic *Numblike* (*Nbl*) expression (green) is detected in wildtype preplate (PP) neruons.

D. Higher power magnification of the PP reveals punctate *TAG1* expression (green) on the cell membranes of some neurons subset of neurons.

E. Low magnification image of *Sey/Sey* coronal section stained with DAPI in similar plane of section to (A). Box shows the approximate area in the cortex in which images (F-H) were taken.

F. No *Pax6* expression is detected in the *Sey/Sey* mutant cortex.

G.As in wildtype, Nbl-positive cells (green) are detected in the *Sey/Sey* PP. Unlike at E10.5, no increase in numbers of Nbl-positive cells is apparent.

H. Higher power magnification reveals more *TAG1*-positive neurons in the *Sey/Sey* PP compared to wildtype.

Scale bars: A, 100μm and also applies to E; B, 10μm and also applies to C,F,G; D, 5μm and also applies to H.

PP, preplate; VZ, ventricular zone.

Sey/Sey expression patterns are very similar. TAG-1 positive axons are also detectable in some differentiating neurons of the outer preplate in both wild type and *Sey/Sey* (Fig.5.2 D,H), although the number of TAG-1 positive axons appears greater in the *Sey/Sey* cortex compared to wildtype. *TAG-1* expression is localised to the cell membranes of axons and somata of specific populations of differentiating neurons during axon extension (Wolfer *et al.*, 1994) and appears as punctate spots on the cell membrane. As at E10.5, *mNumb* expression continues throughout the neuroepithelium without any apparent differences between wildtype and *Sey/Sey*. No cortical expression of *Prox1* was observed in either strain (data not shown).

At E15.5 the developing wildtype cortex has a well defined laminar structure broadly composed of proliferative layers (ventricular zone, VZ, and subventricular zone, SVZ), an intermediate layer (IZ) of radially migrating neurons and afferent and efferent axons and layers of differentiating neurons in the cortical plate (CP). *Pax6* expression is detected in the ventricular and subventricular zones of the wildtype cortex (Fig. 5.3B). Intense Nbl immunoreactivity is detectable in the IZ and moderate expression in the CP of both *Sey/Sey* and wild type (Fig. 5.3. C,H). However, in contrast to the compact laminar structure revealed by Nbl staining in wildtype (Fig.5.3C), the *Sey/Sey* IZ appears disordered (Fig5.3H), which may at least be partially explained by the loss of horizontally orientated thalamocortical and corticothalamic fibres, consistent with the absence of thalamocortical innervation reported in Chapter 3. In addition in the *Sey/Sey* cortex there was an apparent upregulation of *Nbl* in the CP relative to the level in the IZ in some sections (Fig.5.3H) which may be caused by secondary structural defects. In contrast, lower levels of *mNumb* expression are detectable in all layers of the wildtype cortex and no difference between levels nor pattern of expression are detectable in the *Sey/Sey* telencephalon (Fig.5.3D,I). I was unable to detect asymmetric crescents of mNumb protein in dividing cortical cells in several attempts, despite the addition of a signal amplification step using a biotinylated secondary antibody; this may be due to the fact that analysis was performed using a fluorescent rather than a confocal microscope.

The E15.5 wildtype cortex reveals intense TAG-1 staining on fibres of radial migrating neurons extending across the IZ (Fig. 5.3E); immunoreactivity is absent from VZ and SVZ. In comparison, TAG-1 staining in the *Sey/Sey* cortex shows a dramatically different pattern of cellular organisation (Fig. 5.3J): a punctate disorganised pattern of axons and neuron cell bodies in the IZ and the absence of radially aligned migrating cells. *L1* is expressed within the cortex mainly on neuronal axons and to a lesser extent on cell bodies (Godfraind *et al.*, 1988). In both wildtype and *Sey/Sey* staining is strongest in the concentration of axons in the

IZ (Fig. 5.4F,G), however the mutant exhibits a more compacted IZ and additional fingers of *L1* positive axons extend around clusters of SVZ tissue in the frontal lateral cortex. Furthermore, L1 reveals an absence of cortical innervation from subcortical areas in the *Sey/Sey* brain. Whereas L1 positive tracts are visible penetrating the cortex in wild type (Fig. 5.4F), no such innervation is visible in the *Sey/Sey* cortex (Fig. 5.4G).; these are probably thalamocortical axons (Fukuda *et al.*, 1999) and their absence in the mutant is discussed in Chapter 3.

Prox1 expression is still undetectable in the cortex at E15.5, however a discrete pattern of expression is apparent in the developing diencephalon and correlates with established regional forebrain boundaries (Puelles & Rubenstein,1993). In wild type embryos, this *Prox1* domain covers the dorsal thalamus and ventral pretectum (Fig. 5.4C). Interestingly, *Pax6* exhibits a reciprocal pattern of expression in ventral thalamus and dorsal pretectum (Fig. 5.4B). In the *Sey/Sey* diencephalon, the distinct dorsal expression boundaries of *Prox1* in dorsal thalamus and pretectum are lost (Fig. 5.4D), concordant with previous reports of reduced cell density and loss of morphological distinction between DT and pretectum in the mutant brain (Warren & Price, 1997).

A preliminary *in situ* hybridisation analysis of *Eya1, Eya2 , Eya3* and *Eya4* expression failed to reveal significant differences in expression between E15.5 wildtype and *Sey/Sey* brain (data not shown).

Figure 5.3 Expression analysis of *Pax6, Numblike, mNumb* and *TAG1* in wildtype and *Sey/Sey* E15.5 cortex

Sagittal sections through E15.5 wildtype (+/+) (A-E) and *Sey/Sey* (F-J) forebrain. In all sections dorsal is up and rostral is to the left. In colour images nuclei are counterstained with DAPI (blue).

A. Low magnification image of wildtype sagittal section stained with DAPI. Box shows the approximate area in the cortex in which images (B-D) were taken.

B. Nuclear *Pax6* expression (green) in the wildtype ventricular zone (VZ).

C. Strong cytoplasmic *Numblike* (*Nbl*) expression (green) is detected in the wildtype intermediate zone (IZ) and cortical plate (CP).

D. *mNumb* (green) is expressed on the cell membrane of cells in all layers of the wildtype cortex.

E. *TAG1* (green) is detected on axonal processes of radially aligned cells in the IZ.

F. Low magnification image of *Sey/Sey* sagittal section stained with DAPI in similar plane of section to (A). Box shows the approximate area in the cortex in which images (G-J) were taken.

G. No *Pax6* expression is detected in the *Sey/Sey* mutant cortex.

H. As in wildtype, *Nbl* is highly expressed by cells in the IZ and CP. *Nbl* expression appears higher in the mutant CP relative to wildtype and staining reveals the disorganised structure of the IZ.

I. *mNumb* is expressed in all layers of the *Sey/Sey* cortex and at the same level as in wildtype.

J. TAG1 is expressed in the *Sey/Sey* IZ. Expression is punctate and reveals a lack of radially aligned cells.

CP; cortical plate; IZ, intermediate zone; SVZ, subventricular zone; VZ ventricular zone.

Scale bars: A, 100μm and applies to F; B, 10μm and applies to C,-E,G-J.

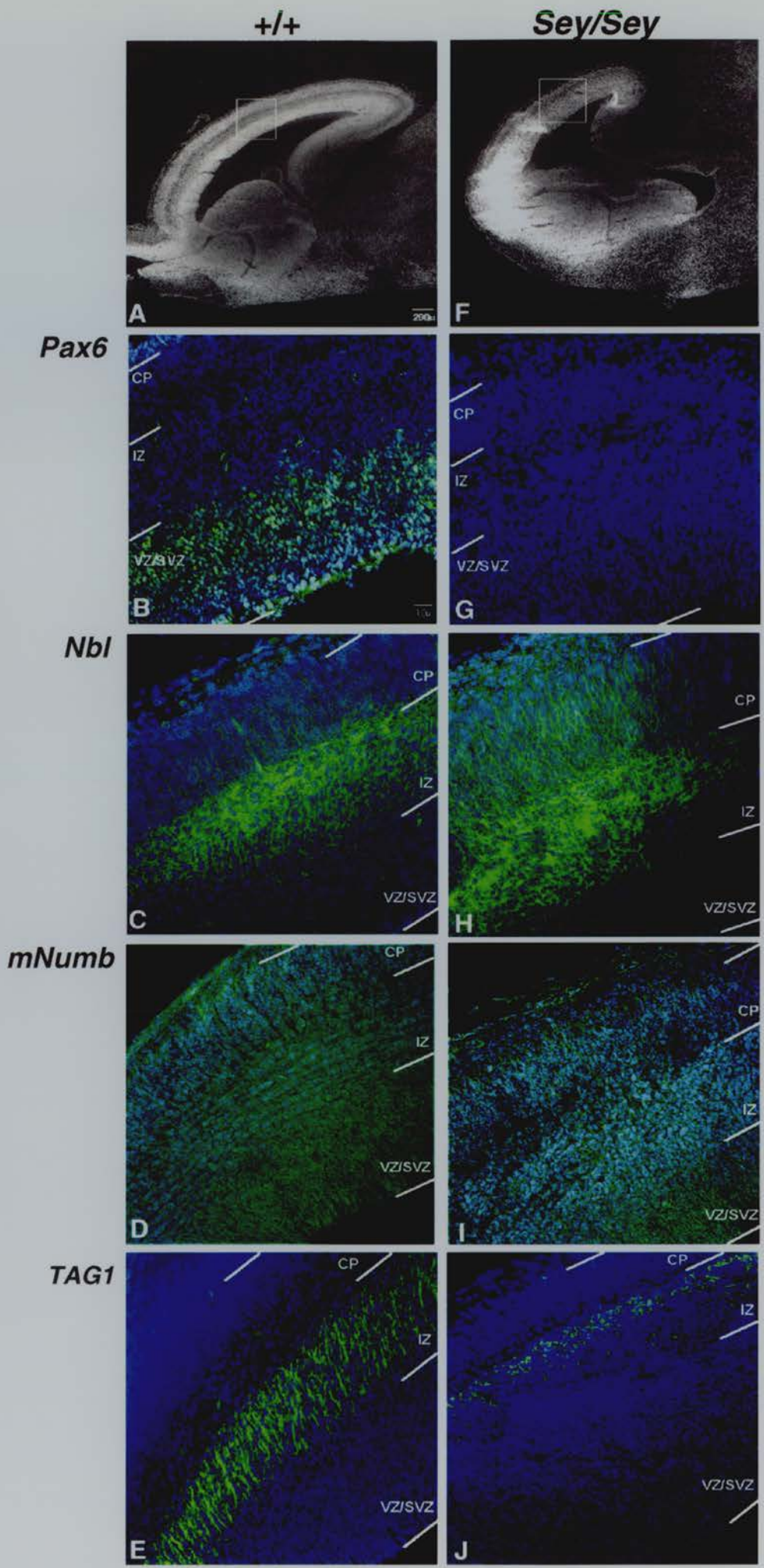
+/+
Sey/Sey
Pax6
Nbl
mNumb
TAG1
A
F
B
G
C
H
D
I
E
J
CP
IZ
VZ/SVZ

Figure 5.4 Expression analysis of *Pax6, Prox1* and *L1* in wildtype and *Sey/Sey* E15.5 forebrain

Sagittal sections through E15.5 wildtype (+/+) (A,B,C,E,F) and *Sey/Sey* (D,G) forebrain. In all sections dorsal is up and rostral is to the left. In colour images nuclei are counterstained with DAPI (blue).

A. Low magnification image of wildtype sagittal section stained with DAPI. Box shows the approximate area in the diencephalon in which images (B ,C) were taken. The same area in the *Sey/Sey* diencephalon is pictured in (D).

B. In wildtype *Pax6* (green) is expressed in the ventral thalamus (VT) and dorsal pretectum (PT).

C. *Prox1* (green) exhibits a reciprocal pattern of expression to *Pax6* in the wildtype dorsal thalamus (DT) and ventral pretectum.

D. In the *Sey/Sey* diencephalon there is loss of distinct dorsal boundaries of *Prox1* expression in the DT and PT compared to wildtype.

E. Low magnification image of wildtype lateral sagittal section stained with DAPI. Box shows the approximate area in the cortex in which image (F) was taken. The same area in the *Sey/Sey* cortex is pictured in (G).

F. In wildtype *L1* is strongly expressed in the intermediate zone (IZ). L1 positive thalamocortical tracts penetrate the cortex in wildtype (arrowheads)

G. In *Sey/Sey* the L1 positive region of expression in the IZ is thinner compared to wildtype. Fingers of L1 positive axons (arrows) extend around clusters of SVZ tissue.

CP; cortical plate; DT; dorsal thalamus; IZ, intermediate zone; PT, pretectum; VT, ventral thalamus.

Scale bars: A, 250μm and applies to E; B, 100μm and applies to C,D; F, 50μm and applies to G.

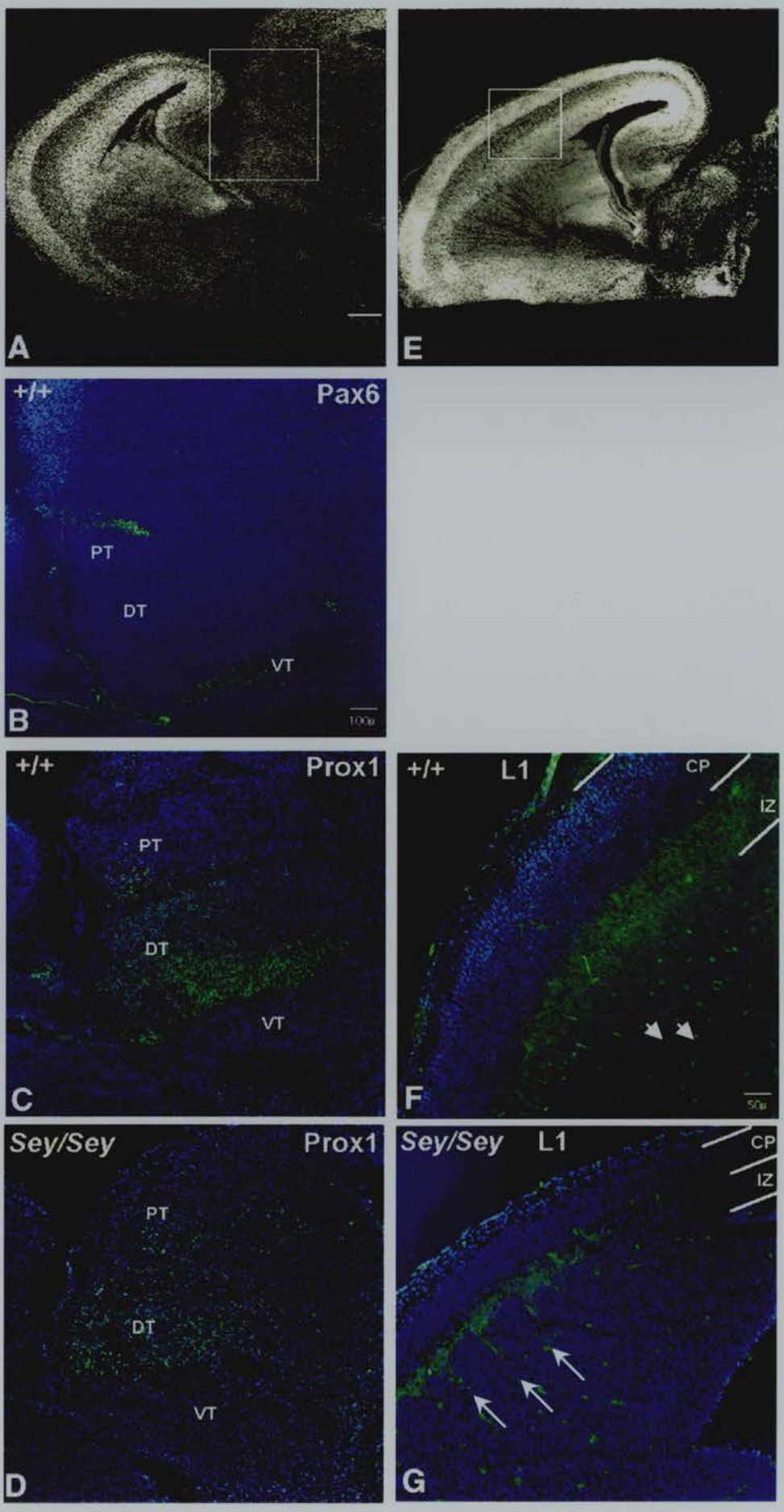
A
E
+/+
Pax6
PT
DT
VT
B
100μ
+/+
Prox1
PT
DT
VT
C
+/+
L1
CP
IZ
F
50μ
Sey/Sey
Prox1
PT
DT
VT
D
Sey/Sey
L1
CP
IZ
G

5.3 Discussion

Pax6 is expressed in the developing forebrain from E8.5 and developmental defects are apparent in the *Sey/Sey* forebrain as early as E9.5 (Mastick *et al.*, 1997). I suggested in Chapter 4 that late-onset cortical defects are the result of primary cellular defects (e.g. cell adhesion differences) acting from the early stages of cortical development. During gestation, these primary defects are compounded by secondary effects, (e.g. blocked migration) which combine to produce a more severe cortical phenotype. As a consequence, by E15.5 many genes which are not direct downstream targets of *Pax6* may be significantly altered in either their domain and/or level of expression. Thus at later stages of development, altered gene expression in the *Sey/Sey* cortex may correspond to either:

1. *Direct* effects

- Direct targets: Pax6 binds directly to the regulatory element of a specific set of genes to activate, repress or maintain expression;
- Downstream genes: genes acting downstream of Pax6 in the same genetic pathway but not as direct interacting targets of Pax6.

2. *Indirect* effects

- Secondary consequences: genes not in the same pathway as Pax6, but altered as a consequence of altered cell differentiation or cell behaviour;
- Tertiary consequences: altered cell behaviour results in morphological defects in an entire tissue or region, which is reflected in altered patterns (rather than levels) of gene expression throughout that region.

Distinguishing between direct and indirect effects can be difficult on the basis of expression analyses alone. For example, a reduced level of expression in a particular region could correspond to a direct downregulation of that gene, or, indirectly, to a reduced number of expressing cells in that area. Other biochemical screens are required to confirm direct regulatory interactions, for example, demonstration that Pax6 can bind promoter elements upstream of a candidate gene and that these elements are required for Pax6-mediated reporter gene expression.

The results of my candidate gene expression analysis reveal altered patterns, rather than levels of expression of *Numblike*, *L1* and *TAG-1* in the *Sey/Sey* cortex, suggesting that they are secondary or tertiary consequences of the loss of Pax6 function. The advantages and disadvantages of a 'candidate gene' approach for identifying gene targets will be discussed in Chapter 6.

However, the expression analysis also highlights three differences between wildtype and *Sey/Sey* cortex:

1. *An early increase in numbers of differentiating neurons*

At E10.5 my data suggest that numbers of early Nbl-positive postmitotic neurons in the preplate are increased. This is consistent with findings that numbers of proliferating cells are increased during early cortical development at E10.5 (Warren *et al.*, 1999) and that these divisions correspond to an increase in both proliferative (symmetric) and neurogenic (asymmetric) division (Chapter 2).

2. *Disrupted radial migration in the intermediate zone*

In agreement with accounts of disrupted migration of late-born neurons (Schmahl *et al.*, 1993; Caric *et al.*, 1997) and absence of thalamocortical axon innervation (Chapter 3), the altered organisation of the intermediate zone is particularly clear:

- TAG-1 staining reveals the absence of radially migrating neurons;
- L1 localisation shows the presence of ectopic clusters of SVZ tissue and the absence of cortical innervation from subcortical areas;
- Nbl localisation suggests disrupted tangential innervation in the IZ.

3. *Altered diencephalic regionalisation*

The pattern of *Prox1* staining in the *Sey/Sey* diencephalon highlights disrupted dorsal regional expression boundaries, consistent with earlier reports of abnormal diencephalic patterning (Stoykova *et al.*, 1997; Warren & Price, 1997). Interestingly, expression of *Prox1* has recently been proposed to define a transient population of restricted lineage precursors derived from multipotential stem cells (Torii *et al.*, 1999). Maintained *Prox1* expression in *Sey/Sey* therefore suggests that some degree of temporal control over cellular differentiation is maintained even if spatial restrictions have broken down. Absence of *Prox1* expression from the E15.5 developing cortex, when restricted lineage precursors are probably present (Williams & Price, 1995) suggests that *Prox1* expression is limited to a subset of precursor cells, or that other *Prox* family members are fulfilling this role in the cortex

CHAPTER 6

A differential gene expression analysis

6.1 Introduction

In parallel with the candidate gene approach (Chapter 5) to identify genes acting downstream of Pax6, cDNA libraries were constructed from wildtype and mutant telencephalon and common clones, representing genes expressed in both tissues, removed by subtractive hybridisation.

6.2 Results

6.2.1 Construction and characterisation of telencephalon cDNA libraries

Poly(A) RNA isolated from wildtype and *Sey/Sey* E15.5 telencephalic tissue was size selected and the largest fractions used to construct directional plasmid cDNA libraries. In order to avoid polylinker homology during subtractive hybridisation, both wildtype and *Sey/Sey* libraries were constructed in two different vectors, pSPORT1 and pSPORT2, which are identical except that they have inverted *NotI/SalI* restriction enzyme cloning sites. Initial characterisation of the unamplified libraries demonstrated that each contained from 0.56-1.3x10^6 independent clones (Table 6.1). It is estimated that a cDNA library containing 5x10^5 clones has >99% probability of containing rare transcripts (less than 10 copies per cell, (Ausubel *et al.*, 1994) therefore the libraries should contain a full representation of cellular transcripts. As the libraries were not constructed using a PCR-based strategy the representation of each gene in the library should reflect the relative abundance of its transcript in the brain. Insert sizes range from between 0.5-2.5 or 3kb (Table 6.1) suggesting that the libraries contains a proportion of full length transcripts. Of a sample of 24 clones sequenced from wildtype and *Sey/Sey* libraries in both vectors, 22 had a 3' poly(A) tail, demonstrating that the clones represent mRNA transcripts. 3 out of 60 clones randomly picked from all four libraries (5%) contained no insert.

In order to determine if the libraries were representative of the tissue from which they were derived, they were tested for the presence of cDNA clones representing β-*actin* and *stathmin/p19*, two genes known to be expressed in the developing brain at this stage (Tokunaga *et al.*, 1986; Schubart *et al.*, 1988). 12,500 clones were plated out and used to make duplicate colony lifts which were hybridised to cDNA probes. The β-*actin* cDNA probe hybridised to 45/12,500 (0.36%) of wildtype clones and 42/12,500 (0.34%) of *Sey/Sey* clones which is within the range of previous estimates of actin abundance (0.02- 4%; Ausubel *et al.*, 1994; Harrison *et al.*, 1995). *Stathmin* cDNA probe hybridised to 30/12,500 (0.25%) of

wildtype clones and 6/12,500 (0.05%) of *Sey/Sey* clones. Of 28 clones with inserts randomly picked and sequenced from wildtype and *Sey/Sey* libraries, 12 (43%) are novel or show homology to ESTs of unknown function and 16 show homology to known mammalian genes (Table 6.1). This data indicates that the libraries represent a good source of previously unidentified genes.

cDNA (from E15.5 telencephalon)	Vector	No. of independent clones	Insert size range in kb (no.of clones examined)	% of clones which are novel/show homology to ESTs of unknown function (no. of clones sequenced)	Examples of clones which show homology to mammalian genes
wildtype	pSport1	$7.8x10^5$	0.5-3 (12)	40% (10)	*α-tubulin*
wildtype	pSport2	$1.3x10^6$	0.7-3 (12)	67% (6)	homology to *NEDD8*, human developmentally down-regulated neural gene
Sey/Sey	pSport1	$5.6x10^5$	0.5-3 (18)	33% (6)	Mismatch repair protein
Sey/Sey	pSport2	$6.7x10^5$	0.5-2.5 (18)	33% (6)	*c-jun* oncogene
subtracted wildtype - *Sey/Sey*	pSport2	$4x10^3$	0.3-2.5 (320)	66% (44)	See table 6.3

Table 6.1 Summary of characteristics of cDNA libraries. Number of independent clones was estimated by plating dilutions of transformed bacteria. Insert sizes were estimated by *NotI/SalI* digestion of DNA from randomly selected colonies.

6.2.2 Generation and characterisation of a subtracted wildtype specific cDNA library

Subtraction of common clones from cDNA libraries greatly enriches for, and facilitates the identification of, novel tissue-specific genes (Harrison *et al.*, 1995). To enrich for genes upregulated by Pax6 in the developing cortex, the *Sey/Sey* telencephalon library was used to subtract common clones from the wildtype telencephalon library.

Following the subtraction strategy outlined in Figure 6.1, biotinylated RNA generated from the *Sey/Sey* library (driver) was hybridised at 130 fold excess to single-stranded DNA generated from the wildtype library (tracer). Common molecules in the two populations hybridise and (along with unbound biotinylated RNA) are removed by streptavidin binding. The remaining single stranded DNA was subjected to two more rounds of hybridisation with fresh driver RNA. The subtracted, single-stranded DNA was converted to double-stranded DNA and re-transformed to create a subtracted wildtype library. A control

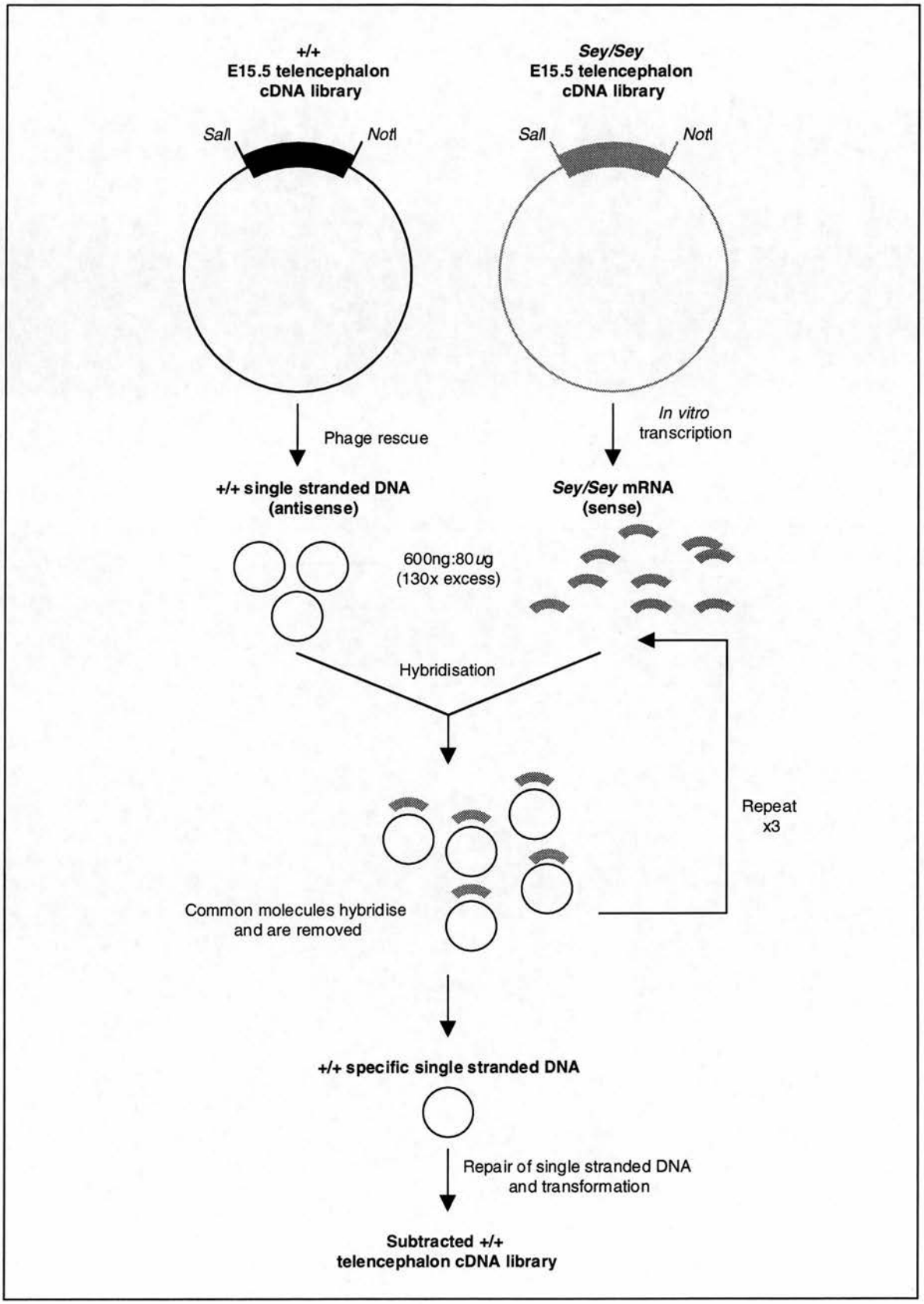

Figure 6.1 Flow digram showing the protocol used to generate the E15.5 wildtype subtracted telencephalon cDNA library

subtractive hybridisation was performed simultaneously without the addition of driver RNA. The size of the control wildtype library after recloning is approximately $6x10^5$ clones and the size of the subtracted library is $8x10^3$, demonstrating that over 98% of clones from the wildtype library were removed during the subtraction.

To assess the subtraction efficiency further, the relative abundance of molecules common to the two starting libraries was compared in the original wildtype library and the subtracted wildtype library. Aliquots of the wildtype, *Sey/Sey* and subtracted cDNA libraries were grown overnight and plasmid DNA isolated by maxiprep. 1μg of each was digested with *Not*I and *Sal*Ito release the inserts and size fractionated by gel electrophoresis. Southern blots of these gels were probed with β-*actin* and *stathmin/p19*. These genes are highly expressed in both wildtype and *Sey/Sey* libraries and should therefore be removed in the subtraction, and this is confirmed (Fig. 6.2).

A second indication of a successful subtractive hybridisation is enrichment of genes expressed only in the wildtype library. However, as yet, no genes are known to be expressed in wildtype and completely absent from *Sey/Sey* telencephalon which might be used as control probes. *Pax6* cannot be used as a non-functional form of the gene is expressed in *Sey/Sey* tissue. In subtractive hybridisations undertaken using identical protocols the successful enrichment of library-specific genes has been demonstrated (Harrison *et al.*, 1995; P. Rashbass & J. Moss, personal communication). Furthermore, the number of empty clones which, like wildtype specific genes, do not hybridise to the driver RNA population, increased from 5% in the original wildtype library to approximately 50% after the subtraction. Taken together these results are indicative of a successful subtraction and show that the final number of clones in the library that contained inserts is $4x10^3$.

6.2.3 Screening the subtracted cDNA library

The wildtype subtracted library should be enriched for genes expressed specifically in wildtype telencephalon that represent genes downstream of *Pax6*. To identify these genes, 700 individual clones (approximately 350 with inserts) were picked at random from the unamplified subtracted library. Half of these were used to make miniprep DNA, which was digested with *Not*I and *Sal*I to release the inserts and 500ng of each clone run out by gel electrophoresis on duplicate gels and Southern blotted. The other half were used in PCR reactions to amplify the cloned inserts and 500ng of the PCR products were dot blotted in triplicate.

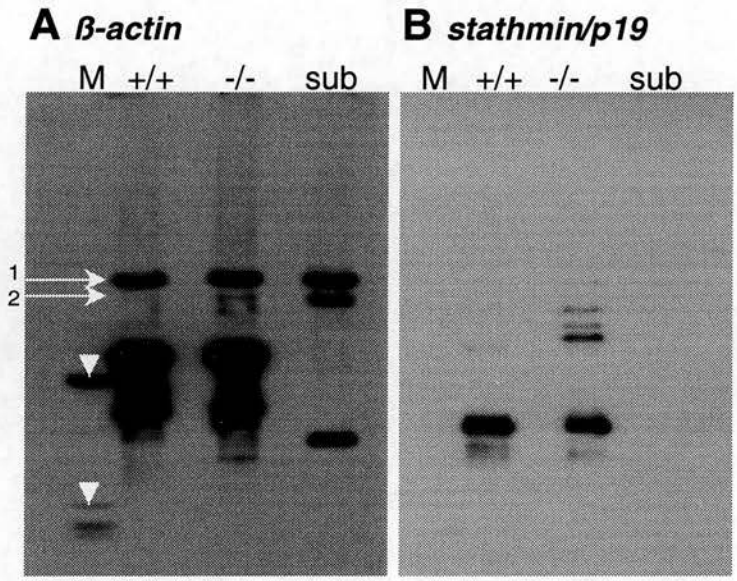

Figure 6.2 Southern blot analysis of the wildtype, *Sey/Sey* and subtracted E15.5 telencephalon cDNA libraries

NotI/SalI digests of DNA from the wildtype (+/+), *Sey/Sey* (-/-) and wildtype subtracted (sub) E15.5 telencephalon cDNA libraries probed with marker genes. Southern blots provide a 'fingerprint' reflecting the relative size and abundance of cDNA clones corresponding to that gene in each library.

A. *ß-actin* probe hybridises to many clones of different sizes in both wildtype and *Sey/Sey* libraries creating a smear. In the subtracted library the probe hybridises to a single band which corresponds to a single *ß-actin* clone. This demonstrates that the majority of *ß-actin* clones were removed in the subtractive hybridisation. The probe also shows cross-hybridisation to a single vector band in wildtype and *Sey/Sey* libraries (arrow 1). In the subtracted library two vector bands are seen (arrows 1 and 2) due to a vector rearrangement which occurred in some clones during the subtractive hybridisation. The *ß-actin* probe also exhibits cross-hybridisation to DNA in the marker lane (M; arrowheads).

B. *stathmin/p19* probe hybridises to several clones of different sizes in both wildtype and *Sey/Sey* libraries, creating a ladder of bands. In the subtracted library no hybridisation signal is seen demonstrating that all *stathmin/p19* clones were removed in the subtractive hybridisation.

M, markers; +/+, wildtype; -/-, *Sey/Sey*; sub, subtracted cDNA library.

Two screening strategies based on differential hybridisation were undertaken (Fig. 6.3); the results of these screens are summarised in Table 6.2. First, Southern blots and dot blots were hybridised with probes prepared from 300ng of insert DNA of the wildtype, *Sey/Sey* and subtracted libraries. Genes expressed at higher levels in wildtype tissue should hybridise more strongly to the wildtype compared to the *Sey/Sey* probes and, if enriched by the subtractive protocol, should also hybridise strongly to a probe from the subtracted library. This method has been used successfully to identify differentially expressed genes from subtracted eye cDNA libraries (P. Rashbass & J. Moss, personal communication). However, due to the nature of the complex probes used, small differences in hybridisation signal intensity proved difficult to detect using this method and no clones showed clear differential hybridisation.

On the assumption that brain-specific genes might represent developmentally important genes regulated by Pax6, a second strategy was devised to identify these within the subtracted library. In this method, duplicate Southern or dot blots were hybridised to probes prepared from E15.5 wildtype telencephalon and from adult liver. Of 350 clones with inserts screened by this second method, 50 (14%) clearly hybridised more strongly to brain than liver cDNA. Sequencing data obtained from the 3'end of 44 of these clones revealed that 11 (22%) correspond to known mammalian genes (Table 6.3) and the remaining 33 (66%) represent mammalian ESTs of unknown function or novel sequences. The first strand cDNA used to make the library is synthesised using an oligo d(T) primer and therefore these sequences will contain 3' untranslated region which exhibits less homology between species. Thus these numbers may over-represent the number of completely novel genes.

As a preliminary screen for clones with differential expression patterns in wildtype and *Sey/Sey* brain, 10 clones were selected: 5 with homology to known genes of interest, 3 with homology to ESTs of unknown function and 2 novel sequences (Table 6.3). Antisense digoxigenin labelled riboprobes were made and *in situ* hybridisation performed on 200µm vibratome sections of E15.5 wildtype and *Sey/Sey* whole head tissue. 9 out of 10 clones exhibited brain specific expression, confirming the initial screen with liver cDNA. Of these, 7 showed widespread non-differential brain expression with no apparent regional differences in staining intensity through the brain nor between wildtype and *Sey/Sey* brains, whilst 2 showed clear differences in expression pattern between wildtype and *Sey/Sey*.

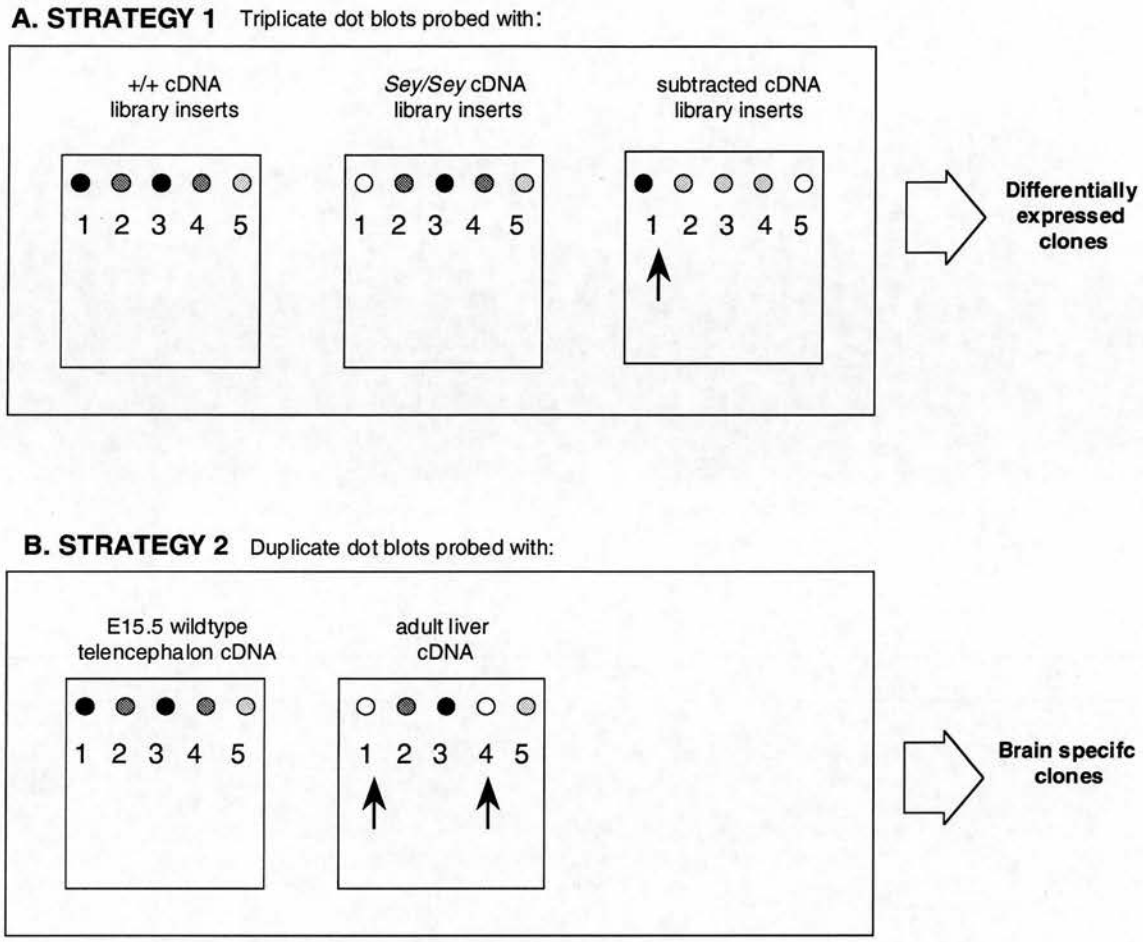

Figure 6.3 Screening strategies for the wildtype subtracted cDNA library

A. Strategy 1: triplicate dot blots of library clones are hybridised with probes prepared from the inserts of the wildtype, *Sey/Sey* and subtracted libraries. Genes expressed at higher levels in wildtype tissue and enriched in the subtraction should hybridise more strongly to wildtype and subtracted library probes compared to the *Sey/Sey* library probe (clone 1)

B. Strategy 2: duplicate dot blots of library clones are hybridised to probes prepared from E15.5 wildtype telencephalon and adult liver cDNA. Brain-specific genes hybridise to the telencephalon probe only (clones 1 and 4).

Screening step	Number of colonies screened	Results	Number selected for next stage
Differential hybridisation with probes prepared from the inserts of the wildtype, *Sey/Sey* and subtracted libraries	350 (9% of total library, 4000 clones)	No obvious difference in hybridisation intensity between different probes	N/A
Differential hybridisation with probes prepared from E15.5 wildtype telencephalon and adult liver	350	50 (14%) show clear stronger hybridisation to telencephalon cDNA probe	44
Sequencing from 3' end and homology searches	44	11 (33%) correspond to known mammalian genes 33 (66%) represent mammalian ESTs of unknown function or novel sequences	10 (5 with homology to known genes and 3 with homolgy to ESTs, 2 novel) (Table 6.3)
Riboprobe synthesis and *in situ* hybridisation to E15.5 whole head wildtype and *Sey/Sey* vibratome sections	10	9 (see Table 6.3 for details)	2 showing differential expression between wildtype and *Sey/Sey*.
In situ hybridisation analysis on E15.5 wildtype and *Sey/Sey* cryostat sections	2	2 exhibit reduced expression in regions of *Sey/Sey* brain (Figure 6.3)	

Table 6.2 Screening steps applied to clones in the wildtype subtracted cDNA library. The library contained a total of 4000 clones with inserts.

Clone number	Characterisation on basis of BLAST sequence homology searches	Brain specific expression?	Differential expression between wildtype and *Sey/Sey*?
S95	Mouse cDNA of unknown function	Y	N
S147	LIM domain binding protein-2 (LDB2)/ CLIM1	Y	Y
S180	Homology to human *E4BP4* (member of bZIP family of DNA-binding proteins)	Y	N
S225	Cylophilin-related protein	Y	N
S234	Mouse cDNA of unknown function	N	N
S266	Mouse cDNA of unknown function	Y	N
S461	Novel	Y	N
S462	Homology to POU domain protein	Y	N
S469	*LMO3/rhombotin 3*	Y	Y
S521	Novel	Y	N

Table 6.3. Results of screening subtracted library clones by *in situ* hybridisation to E15.5 whole head wildtype and *Sey/Sey* vibratome sections.

6.2.4 Identification of two differentially expressed genes

Sequencing and homology searches showed that the two differentially expressed clones correspond to LIM domain binding protein 2 (LDB2) and a putative novel member of the LIM only (LMO) family of LIM domain-containing proteins.

The first clone, S147, represents a cDNA clone of *LDB2*, a member of a gene family which mediates protein interactions during transcriptional regulation (Bach *et al.*, 1997). Of over 1000 nucleotides sequenced from the 5' end (Fig. 6.4), the clone exhibits 99% identity over 250 amino acids at the 5' end of *LDB2* (Fig. 6.5) and >99% nucleotide identity over the same region. Sequencing from the 3' end confirmed the sequence match and revealed a polyadenylation signal, suggesting that the clone is full length.

To analyse the expression differences of *LDB2* between wildtype and *Sey/Sey*, a brief *in situ* hybridisation analysis was carried out on E15.5 brain sections by Judy Fletcher at the MRC Human Genetics Unit (Fig. 6.8). In wildtype, *LDB2* is highly expressed in the cortical plate and shows a moderate level of expression in the ventral thalamus and differentiating striatum (Fig. 6.8E,G). In contrast, in the *Sey/Sey* brain the domain of cortical plate expression is significantly reduced in width and strength of expression and thalamic expression is highly reduced or absent (Fig. 6.8F,H).. Striatal expression is present in lateral sections(data not shown).

The second differentially expressed clone, S469, shows 100% identity on an amino acid level to the published mouse and human LMO3 protein sequence (Fig. 6.6 and 6.7). The *LMO* (LIM-only) gene family (also called *rhombotin* (*Rbtn*) and *Ttg* (*Translocated in T-cell leukaemia* gene) encode proteins with two tandem cysteine-rich LIM domains but no homeodomain (Boehm *et al.*, 1990). Little sequence data has been published 5' of the LIM domains for LMO3, whereas LMO1 and LMO2 have diverging 5' sequences outside the conserved domain. Coding sequence of clone S469 also extends 5' of this domain and shows little homology to LMO1 or LMO2. Therefore, although the complete amino acid identity to LMO3 strongly suggest that S469 is a larger clone of this gene, it is possible that it represents a new member of the *LMO* gene family. Therefore for this study the clone will be referred to as sLMO. In the wildtype brain *sLMO* expression is detected weakly in the cortical plate particularly in differentiating neurons of the rostral cortex (Fig. 6.8I). In the diencephalon a strongly positive domain is present in the dorsal thalamus (Fig. 6.8K).Strikingly, expression domains in the cortical plate and thalamus are absent from the *Sey/Sey* brain (Fig. 6.8J,L). *sLMO* expression also labels a distinct structure in the basal telencephalon - probably the differentiating cells of pallidum or posterior rhinencephalon - which appears more diffusely labelled in the wildtype telencephalon (Fig. 6.8 I-K). The same structure is labelled by R-cadherin in Stoykova *et al.*, (1996). Due to lack of time no further analysis of these clones was possible.

```
  1 GnnATAGTCnnTGACTATAnAAGAGCTTGACGTCGCATGCACGCGTACGTAAGCTTGGAT  60
 61 CCTCTAGAGTCGACCCACGCGTCCGCCCACGCGTCCGCGGACGCGTGGGTGCCTGCCTGC 120
121 CTCTGTGTGTGTCTGTGTGTGTGTGAGCGTATGTGCGTGCGTCTACTTTGTACTGTGAAG 180
181 AACACAGCCCATGTGCTCTGCATGGACGTTCCTGATACTCTATTAAGCTTGATTTTCGAC 240

241 AAGCAGGCAAGATGTCCAGCACACCACATGACCCCTTCTATTCTTCTCCTTTCGGCCCAT 300
  1           M  S  S  T  P  H  D  P  F  Y  S  S  P  F  G  P  F  17

301 TTTATAGGAGACATACACCATACATGGTACAGCCAGAGTACCGAATCTATGAGATGAACA 360
 18   Y  R  R  H  T  P  Y  M  V  Q  P  E  Y  R  I  Y  E  M  N  K  37

361 AGAGACTGCAGTCTCGTACAGAGGACAGTGACAACCTCTGGTGGGATGCGTTTGCCACTG 420
 38   R  L  Q  S  R  T  E  D  S  D  N  L  W  W  D  A  F  A  T  E  57

421 AATTTTTTGAAGATGATGCCACATTAACACTTTCATTTTGTTTGGAAGATGGACCAAAGC 480
 58   F  F  E  D  D  A  T  L  T  L  S  F  C  L  E  D  G  P  K  R  77

481 GATACACTATCGGCAGGACCCTCATTCCCCGTTATTTTAGCACCGTATTTGAAGGAGGGG 540
 78   Y  T  I  G  R  T  L  I  P  R  Y  F  S  T  V  F  E  G  G  V  97

541 TGACAGACCTGTACTACATCCTTAAACACTcaArGGAGTCATATcACAACTCATcCATcA 600
 98   T  D  L  Y  Y  I  L  K  H  S  ?  E  S  Y  H  N  S  S  I  T 117

601 cAGTAgACTGCGAcCAGTGTGCCATGGtCACACAGCATGGGAAGCCCATGtTTACCAAGG 660
118   V  D  C  D  Q  C  A  M  V  T  Q  H  G  K  P  M  F  T  K  V 137

661 TATGCACAGAArGCAGGCTGATCTTGGAATTCACATTTGATGACCTCATGAGAATAAAAA 720
138   C  T  E  ?  R  L  I  L  E  F  T  F  D  D  L  M  R  I  K  T 157

721 CGTGGCACTTTACCATTGnACAGTACAGGGAGCTGGTCCCCAGAAGCATACTAGCCATGC 780
158   W  H  F  T  I  ?  Q  Y  R  E  L  V  P  R  S  I  L  A  M  H 177

781 ACGCACAAGATCCTCAGGTCCTGGATCAGCTGTCCAAAAATATCACCAGGATGGGTCTCA 840
178   A  Q  D  P  Q  V  L  D  Q  L  S  K  N  I  T  R  M  G  L  T 197

841 CAAACTTCACCCTCAACTACCTCAGGTTGTGTGTAATACTGGAGCCAATGCAGGAACTGA 900
198   N  F  T  L  N  Y  L  R  L  C  V  I  L  E  P  M  Q  E  L  M 217

901 TGTCGAGACACAAAACCTACAACCTCAGTCCCCGAGACTGCCTGAAGACCTGTCTGTTTC 960
218   S  R  H  K  T  Y  N  L  S  P  R  D  C  L  K  T  C  L  F  H 237

961 ACAAGTGGCAGCGAATGGTGGCCCCGCCAGCAGAACCCACAAGG                1004
238   K  W  Q  R  M  V  A  P  P  A  E  P  T  R                  251
```

Figure 6.4 Consensus 5′ nucleotide sequence of subtracted library clone S147 and its predicted amino acid sequence. The start methionine in the amino acid sequence is numbered 1. Sequence was generated using three sequencing runs into the 5′ end and a consensus sequence was constructed using the Gel assemble program at HGMP; small case letters indicate positions of disparity between sequence runs.

```
S147    1 MSSTPHDPFYSSPFGPFYRRHTPYMVQPEYRIYEMNKRLQSRTEDSDNLW  50
          ||||||||||||||||||||||||||||||||||||||||||||||||||
LDB2    1 MSSTPHDPFYSSPFGPFYRRHTPYMVQPEYRIYEMNKRLQSRTEDSDNLW  50

S147   51 WDAFATEFFEDDATLTLSFCLEDGPKRYTIGRTLIPRYFSTVFEGGVTDL  100
          ||||||||||||||||||||||||||||||||||||||||||||||||||
LDB2   51 WDAFATEFFEDDATLTLSFCLEDGPKRYTIGRTLIPRYFSTVFEGGVTDL  100

S147  101 YYILKHSXESYHNSSITVDCDQCAMVTQHGKPMFTKVCTEXRLILEFTFD  150
          |||||||  ||||||||||||||||||||||||||||||  |||||||||
LDB2  101 YYILKHSKESYHNSSITVDCDQCAMVTQHGKPMFTKVCTEGRLILEFTFD  150

S147  151 DLMRIKTWHFTIXQYRELVPRSILAMHAQDPQVLDQLSKNITRMGLTNFT  200
          ||||||||||||  ||||||||||||||||||||||||||||||||||||
LDB2  151 DLMRIKTWHFTIRQYRELVPRSILAMHAQDPQVLDQLSKNITRMGLTNFT  200

S147  201 LNYLRLCVILEPMQELMSRHKTYNLSPRDCLKTCLFHKWQRMVAPPAEPTR 251
          |||||||||||||||||||||||||||||||||||||||||||||||||||
LDB2  201 LNYLRLCVILEPMQELMSRHKTYNLSPRDCLKTCLFQKWQRMVAPPAEPTR 251
```

Figure 6.5 Alignment of the predicted 5′ amino acid sequence of S147 with mouse LDB2/CLIM1 sequence. Sequences were aligned by BLAST on the Swissprot protein database. Vertical lines represent identical amino acids; S147 shows 99% identity to LDB2 over this region..

```
1   AGAGTCCGTTGCTTACAAGAGCTATGACGTCGCATGCACGCGTACGTAAGCTTGGATCCT  60
1     S  P  L  L  T  R  A  M  T  S  H  A  R  V  R  K  L  G  S  S  20

61  CTAGAGTCGACCCACGCGTCCGCCCACnCGTCCGCGGACGCGTGGGCGAAGCTGCAGCGA 120
21    R  V  D  P  R  V  R  P  ?  V  R  G  R  V  G  E  A  A  A  T  40

121 CTCAGGCACGCCTCAGTCAACTCATGCAGAAACAAGAGAAAAGTTTTGGCATACAAATGC 180
41    Q  A  R  L  S  Q  L  M  Q  K  Q  E  K  S  F  G  I  Q  M  L  60

181 TCTCAGTTCAGCCAGACACCAAGCCAAAAGGTTGTGCTGGCTGCAACCGAAAAATCAAGG 240
61    S  V  Q  P  D  T  K  P  K  G  C  A  G  C  N  R  K  I  K  D  80

241 ACCGGTATCTCCTAAAGGCACTGGACAAATACTGGCATGAGGaCTGCCTGAAGTGTGCCT 300
81    R  Y  L  L  K  A  L  D  K  Y  W  H  E  D  C  L  K  C  A  C 100

301 GCTGCGACTGCCGTTTGGgAGAGGTGGGcTCCACCCTGTACACGAAAGCTAACCTTATCC 360
101   C  D  C  R  L  G  E  V  G  S  T  L  Y  T  K  A  N  L  I  L 120

361 TTTGTCGCAGAGACTATCTGAGGCTGTTTGGTGTAACGGGAAACTGCGCTgCCTGTAGCA 420
121   C  R  R  D  Y  L  R  L  F  G  V  T  G  N  C  A  A  C  S  K 140

421 AGCTCATCCCTgCCTTTGAGATGGTGAtGcGTgCCAaGGATAATGTGTACCACcTGgAcT 480
141   L  I  P  A  F  E  M  V  M  R  A  K  D  N  V  Y  H  L  D  C 160

481 GCTTTGCcTGTCaGCTTTGCAATCAGAGATtTTGTGTCGGAGACAAATTTTTCTTAAAGA 540
161   F  A  C  Q  L  C  N  Q  R  F  C  V  G  D  K  F  F  L  K  N 180

541 ACAATaTGaTTCTTTGCCaGACAGAcTACGAGGAAgGCCTCATGAAAGAAgGcTATGCAC 600
181   N  M  I  L  C  Q  T  D  Y  E  E  G  L  M  K  E  G  Y  A  P 200

601 CCCAgGTCCGyTGAgCCCGCAGCAGCGTcTCCCcAACAATGCAAAgCAcTACATCCTTTT 660
201   Q  V  R  *                                                  203

661 ATCTTTTTTGcTCACGTGTATaTAAGAATCAATcGACACAGGAACCTGcTGAATAGGGTA 720
721 GCGgTAGGTGAGCAGGATGGCCATGTGGAGGAGAAGGTGGACTGCATCTGTATGTAGTGA 780
781 AATTGCCCCCGTTCAAGAGTTGAATGTTCATTATTAAAGAGAGAAGTAATGTAAAA     836
```

Figure 6.6 Consensus sequence of subtracted library clone S469 and its predicted amino acid sequence.
Sequence was generated using sequencing runs into the 5′ and 3′ ends and a consensus sequence was constructed using the Gel assemble program at HGMP; small case letters indicate positions of disparity between sequence runs.

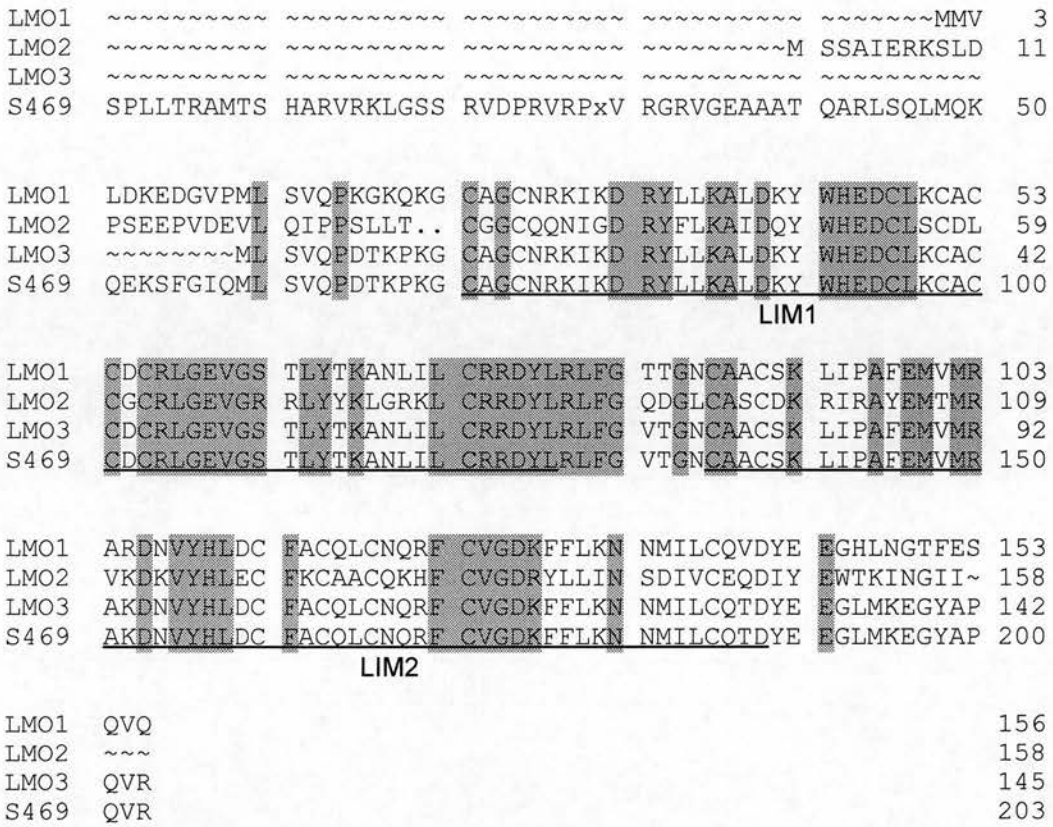

Figure 6.7 Alignment of the predicted amino acid sequence of S469 with mouse LMO1, LMO2 and LMO3 sequences. Shading shows conservation of amino acids between all four sequences and underlined sequence shows the two adjacent LIM domains (LIM1 & LIM2). S469 shows 100% amino acid identity to the published LMO3 sequence but has additional 5′ coding sequence.

Figure 6.8 Expression analysis of *Pax6*, *LDB2* and *sLMO* in wildtype and *Sey/Sey* E15.5 forebrain

Non-radioactive *in situ* hybridisation of *Pax6* (A-D), *LDB2* (E-H) and *sLMO* (I-L) on parasagittal sections. The left half of the page shows lateral sections through the telencephalon; the right half of the page shows sections in a more medial plane through the telencephalon and diencephalon. In all images dorsal is up and rostral is to the right.

A-D. *Pax6* expression

A. Wildtype. *Pax6* expression is detected in the ventricular zone (VZ) of the wildtype cortex (Ctx).

B. *Sey/Sey*. *Pax6* is expressed in the ventricular and subventricular layers (VZ/SVZ).

C. Wildtype. *Pax6* is expressed in the cortical VZ/SVZ, ventral thalamus (VT), pretectum (PT) and posterior entopeduncular nucleus (pep) in the hypothalamus.

D. *Sey/Sey*. In the mutant, *Pax6* expression is detected in the VZ/SVZ and VT. Expression in the PT and pep are not apparent in this section.

E-H. LDB2 expression

E. Wildtype. LDB2 is expressed in the cortical plate (CP) and developing striatum (St).

F. *Sey/Sey*. The domain of LDB2 expression in the *Sey/Sey* CP is reduced in width and strength; striatal expression is not detected in this section but is present in more lateral sections (data not shown).

G. Wildtype. Expression is detected in the CP and ventral thalamus (VT).

H. *Sey/Sey*. Expression is reduced in the CP and absent from the VT.

I-L. *sLMO* expression

I. Wildtype. Weak sLMO expression is detected in the CP, and stronger expression in the rostral cortex.

J. *Sey/Sey*. sLMO expression is absent from the *Sey/Sey* CP and rostral cortex. sLMO is expressed in a structure in the ventral telencephalon (arrow) which is probably the differentiating cells of the pallidum or posterior rhinencephalon. This structure is more diffusely labelled in wildtype lateral sections (arrow in (I)) and is labelled in wildtype (arrow in K) but not *Sey/Sey* (L) medial sections.

K. Wildtype. *sLMO* is expressed in the dorsal thalamus (DT) and pretectum.

L. *Sey/Sey*. Expression is lost from the mutant DT and PT.

Ctx, cortex; CP, cortical plate; DT, dorsal thalamus; IZ, intermediate zone; MZ, marginal zone; pep, posterior entopeduncular nucleus; PT, pretectum; St, striatum; SVZ, subventricular zone; VT, ventral thalamus; VZ, ventricular zone. Scale bar in A, 250µm and applies to all images.

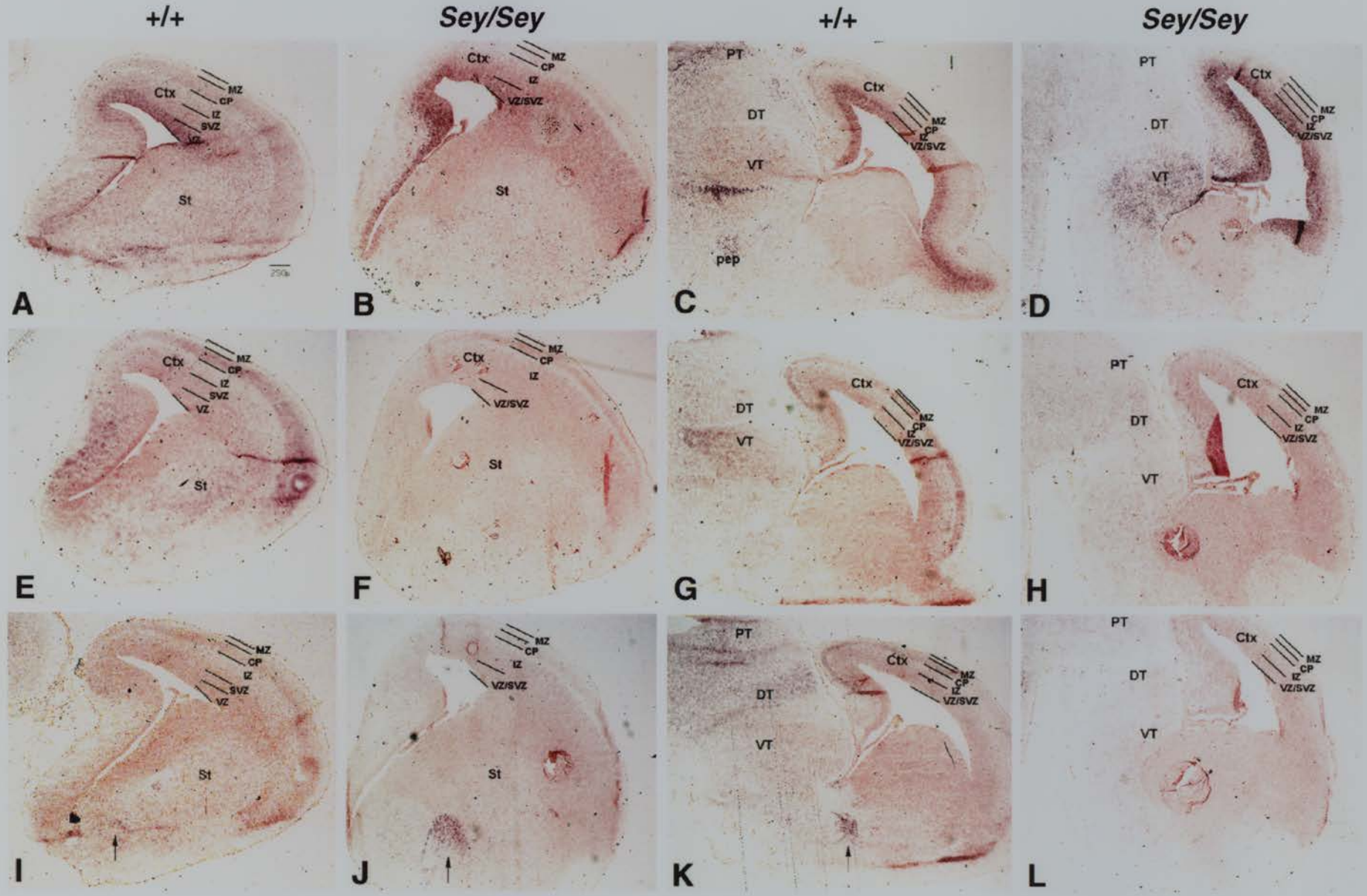
+/+
Sey/Sey
+/+
Sey/Sey
Pax6
LDB2
sLMO
A
B
C
D
E
F
G
H
I
J
K
L
Ctx
MZ
CP
IZ
SVZ
VZ
VZ/SVZ
St
PT
DT
VT
pep

6.3 Discussion

6.3.1 Experimental approaches to identifying genes downstream of *Pax6*

Identification of genes acting downstream of *Pax6* remains an elusive yet important step to understanding Pax6 function during cortical development. Previously, several methods have been used to identify candidate genes:

- genes showing co-localisation with *Pax6* e.g. *R-cadherin* (Stoykova *et al.*, 1997) ;
- genes expected to show altered expression based on the morphology or cellular phenotype of the *Pax6* mutant e.g. extracellular matrix component *tenascin C* (Gotz *et al.*, 1998);
- genes containing putative Pax6 binding domains in their regulatory regions e.g. *L1* (Chalepakis *et al.*, 1994).

However, such approaches are limited in their potential for target gene identification by:

- our incomplete understanding of the *Pax6* mutant phenotype;
- their basis on prior assumptions about the nature of likely targets;
- inherent prejudice towards known, well-characterised genes.

Adopting a 'candidate gene' approach is therefore likely to omit important downstream genes.

These problems can be partly overcome by differential gene expression analysis, which compares gene expression in two related tissues and facilitates the identification of genes expressed at different levels. Several techniques have emerged for analysing differential gene expression including differential display, representational difference analysis, subtractive hybridisation and microarray hybridisation. The most appropriate method will depend on the biological system and the questions being asked of it, however an effective screening strategy should incorporate the following elements:

- closely related tissues to ensure the only molecular differences between them are due to the gene of interest;
- an efficient method for isolating these differences;
- an effective screen to verify differential clones.

These factors will be briefly discussed in relation to the aims of this project.

Choice of tissue

In this study, E15.5 telencephalic tissue was chosen for the following reasons:

- wild-type, *Sey/Sey* heterozygote and *Sey/Sey* homozygote phenotypes can be distinguished at this stage;

- relatively large quantities of tissue can be obtained from only a few embryos and the tissue can be dissected out precisely and cleanly;
- *Pax6* is highly expressed in the telencephalon at this age.

However, utilisation of E15.5 tissue in the subtractive hybridisation makes it probable that a higher proportion of genes identified are the result of indirect effects of Pax6 (as discussed in Chapter 5). Even so, the primary actions of Pax6 probably extend throughout cortical development, therefore a screen at this stage may also yield direct targets of Pax6 regulation. Whether direct or indirect targets, novel genes identified from the telencephalon with distinct expression patterns in wildtype and *Sey/Sey* may serve as valuable markers in the continuing investigation of forebrain development and in understanding the *Sey/Sey* phenotype.

Subtractive hybridisation

My experimental strategy involved the construction of two high quality cDNA libraries from wildtype and mutant tissues. To facilitate the isolation of Pax6 regulated genes, the wildtype library was enriched for differentially expressed transcripts by subtractive hybridisation. Southern blot analysis demonstrated the successful removal of common molecules from the wildtype library and the subsequent isolation of two differentially expressed genes validates the effectiveness of this approach in isolating differentially expressed genes. The subtracted wildtype library therefore represents a valuable resource of candidate genes downstream of *Pax6*. The subtraction strategy is, however, limited to identification of genes expressed at an increased level in the target population. Using the wildtype cDNA library as the target population identified genes upregulated in the wildtype tissue, or requiring Pax6 for normal expression. Genes repressed by Pax6 would be identified using the *Sey/Sey* library as the target; as wildtype and *Sey/Sey* libraries were cloned into both driver and target vectors this experiment could be readily undertaken at a future date.

Screening strategy

The screening strategies in this study employed differential hybridisation using radioactively labelled 'complex' probes prepared from either the cDNA libraries or from total mRNA isolated from embryonic brain or adult liver tissue. Complex probes prepared from brain tissue may contain as many as 300,000 individual mRNA molecules in widely differing amounts (reviewed by Jordan, 1998). In contrast to hybridisation using gene-specific probes, in which there is a large excess of probe compared to target DNA, for differential hybridisation each individual sequence in the complex probe is present in small amounts compared to the target. In the experiments described in this chapter 300ng of complex probe was hybridised to 500ng of target DNA from each library clone. Under these

conditions the amount of probe hybridised to a given target should be proportional to the relative abundance of the corrresponding transcript in the tissue from which the probe was derived (Jordan, 1998). Thus, in theory, differential hybridisation of a target to complex probes prepared from different tissues should allow differences in gene expression between the tissues to be detected (Harrison *et al.*, 1995). However, the amount of each individual cDNA sequence labelled will be small and it may be difficult to quantify slight differences in the strength of hybridisation signals.

Screening for differentially expressed clones by comparative hybridisation with wildtype and *Sey/Sey* cDNA probes yielded no clear candidates. There are several possible explanations for this result:

- the majority of genes expressed in the *Sey/Sey* telencephalon are the same as those in the wildtype telencephalon. To date, all genes known to have reduced levels of expression in the *Sey/Sey* cortex are expressed in other areas of the telencephalon unaffected by *Pax6* (Stoykova *et al.*, 1997; Gotz *et al.*, 1998). Genes such as these should be enriched in the subtracted library, but will still hybridise to a *Sey/Sey* cDNA radioactive probe making them difficult to identify by this screening method.
- genes exhibiting strong differential expression were not represented in the sample of clones screened. In all, 350 clones with inserts (9% of the subtracted library) were screened. However, if Pax6 directly upregulates only a small number of genes, they might be excluded from this sample.
- Pax6 acts chiefly as a transcriptional repressor rather than a transcriptional activator; the subtraction only enriched for genes upregulated by Pax6 and would therefore not enrich for such genes. Performing the subtraction with the wildtype as driver and *Sey/Sey* as target populations would identify these putative targets.
- Pax6 direct targets are expressed at low levels and differential hybridisation and detection methods are not sufficiently sensitive to reveal these differences.

It is most probable that a combination of these explanations accounts for the lack of candidate targets identified by the first screen.

In a second screening approach, comparative hybridisation to embryonic brain and adult liver cDNA identified 50 clones representing a range of novel and previously characterised genes with brain specific expression. Furthermore, utilisation of an *in situ* hybridisation screen on vibratome sections led to the rapid identification of two differentially expressed genes. Significantly, this illustrates the importance of incorporating such a step into a screening strategy, especially when attempting to isolate developmental genes which may exhibit differential expression patterns rather than differential expression levels.

A preliminary screen of nearly 10% of clones in the wildtype subtracted library has already led to the isolation of two candidate genes downstream of Pax6 (with a further 40 requiring expression analysis). These results clearly demonstrate the efficacy of this experimental scheme for identification of genes in developmental pathways and the library's potential as a resource for identification of genes downstream of Pax6 in the future.

6.3.2 LDB2 and sLMO: mediators of transcriptional regulation

Two clones identified from the subtracted wildtype library, *LDB2* and *sLMO*, exhibit altered domains of expression in the *Sey/Sey* forebrain specifically in regions where they are co-expressed with *Pax6* or regions derived from *Pax6* positive domains. They therefore represent excellent candidate downstream genes. This information is particularly exciting given the emerging importance of the *LDB* and *LMO* gene families in mediating a range of protein interactions during transcriptional regulation.

Clone *sLMO* is a member of the LMO (LIM only) protein family, composed almost entirely of two tandem LIM domains (Boehm *et al.*, 1990; Boehm *et al.*, 1991). LIM domains are well characterised double zinc-finger protein motifs (reviewed in Dawid *et al.*, 1998). Four members of the *LMO* family have so far been characterised; *LMO1* and *LMO3* are highly homologous and exhibit specific partly overlapping expression patterns in the mouse forebrain (Foroni *et al.*, 1992; Hinks *et al.*, 1998); *LMO2* and *LMO4* are more distantly related and exhibit more widespread expression during development (Foroni *et al.*, 1992; Kenny *et al.*, 1998; Sugihura *et al.*, 1998). The LMO proteins are highly conserved between man and mouse (Foroni *et al.*, 1992) and have been implicated in cellular proliferation and differentiation. LMOs are thought to function as transcriptional cofactors, regulating gene expression by bringing together other components of transcriptional complexes (Wadman *et al.*, 1997; Visvader *et al.*, 1997). *LMO3* expression has been reported throughout the cortex but highest in the cortical plate, piriform cortex and caudate putamen (Hinks *et al.*, 1998); *sLMO* exhibits overlapping expression except that its cortical expression is restricted to the CP. This, and the additional 5′ coding sequence of the *sLMO* clone suggest it might be a novel member of the *LMO* gene family with a partially overlapping expression pattern, however this requires confirmation by isolating the full length cDNA and further sequence analysis.

The second gene identified from the subtracted library, *LIM-domain binding protein 2* (*LDB2*, also *cofactor of LIM homeodomain protein 1, CLIM1*), is a member of another family of proteins with similar function. LDB2 was identified in a screen for proteins interacting with the LIM domain of P-Lim/Lhx3 (Bach *et al.*, 1997), and shown to be highly homologous to a

previously reported protein, LDB1 (Agulnick *et al.*, 1996)/nuclear LIM interactor (NLI) (Jurata *et al.*, 1996). A third family member, LDB3, has been found in zebrafish (Toyama *et al.*, 1998) and all three LDB proteins are highly conserved.

Like LMOs, the LDBs are involved in mediating protein interactions in transcriptional complexes. LDB1 binds LIM domains via its C-terminal region and is able to form homodimers involving the N-terminal region (Fig. 6.9; Jurata *et al.*, 1997; Breen *et al.*, 1997) suggesting it could act as a bridge between two LIM proteins in a complex (Figure 6.9). For example, certain proteins containing both LIM and homeodomains bind DNA through their homeodomain and act as transcription factors (e.g. Lim, Lhx and Isl proteins). Studies of Lhx3 *in vitro* have shown that the protein is much more effective in DNA binding and transcriptional regulation after deletion of the LIM domains, suggesting that LIM domains exert a negative regulatory role (Bach *et al.*, 1997). LDB1 appears to act as an essential transcriptional cofactor: LIM domain binding by LDB1 overcomes the inhibitory action of LIM domains on transcription (Agulnick *et al.*, 1996; Bach *et al.*, 1997). Furthermore, LDB2 interacts with both LIM domain and homeodomain proteins (Bach *et al.*, 1997). Co-transfection of *LDB2* with either *Lhx3/P-Lim* or the homeobox gene *P-Otx* enhances transcriptional activation from a reporter construct *in vitro*, and transfection of all three together leads to strong synergistic activation (Bach *et al.*, 1997). This suggests that LDBs could enhance transcription by interacting with a wide range of LIM and homeodomain proteins.

LDBs and LMOs may also interact with each other. LDB1 has been isolated in a protein complex including LMO2 (Wadman *et al.*, 1997); interaction of the two proteins appears to repress cell differentiation during erythropoiesis (Visvader *et al.*, 1997). A recent finding that the more distantly related LMO4 also interacts with LDB1 and 2 (Kenny *et al.*, 1998; Sugihara *et al.*, 1998) suggests that the LMO-LDB interaction is conserved amongst members of the gene family and that these proteins often function together during transcriptional regulation. Remarkably, a *Drosophila* homologue of LDB1, Chip, has been identified which binds LIM domains (Morcillo *et al.*, 1997; Dawid *et al.*, 1998) and a *Drosophila* LMO protein (dLMO) found to be encoded by the *Beadex* gene (Milan *et al.*, 1998). A recent study suggests that both genes regulate activity of the LIM domain protein Apterous during *Drosophila* wing development (Milan *et al.*, 1998).

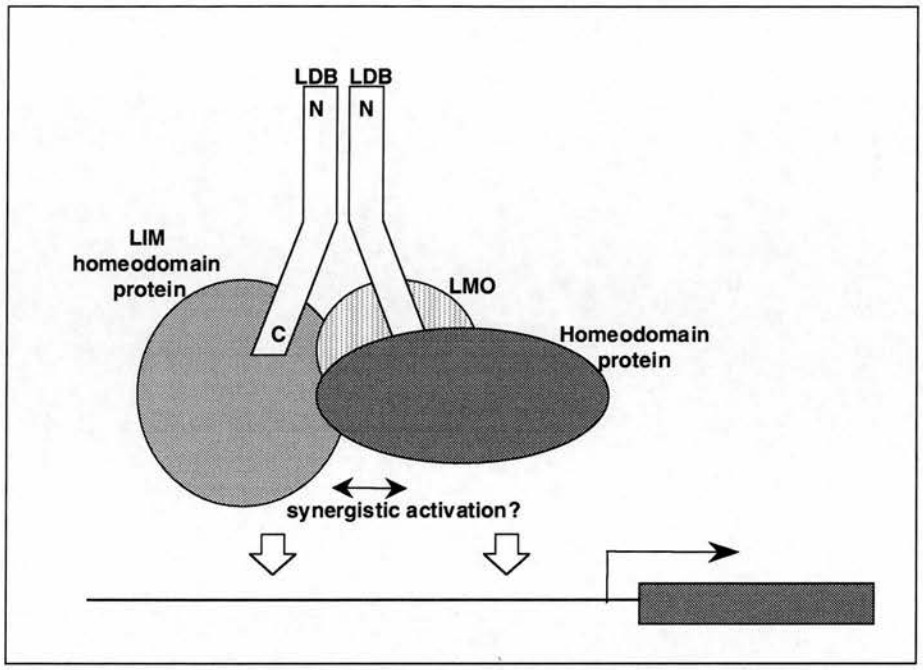

Figure 6.9 Summary of the putative protein-protein interactions involving LDBs and LMOs

Dimer formation via its N-terminal regions allows LDBs to mediate interactions between different LIM homeodomain and LMO proteins that bind to its C-terminal regions by way of their LIM domains. Other homeodomain proteins might also be recruited to such a complex, which can lead to synergistic transcriptional activation of target genes (adapted from Dawid et al., 1998).

In summary, current evidence suggests that LDBs and LMOs may function together to assemble a range of transcription factors into protein complexes which regulate transcription. These interactions are summarised in Figure 6.9. However, many of the protein interactions reported *in vitro* await functional confirmation *in vivo*.

The results presented in this chapter demonstrate that *LDB2* and *sLMO* are co-expressed in differentiating neurons in the cortical plate and expression of both is lost in the absence of *Pax6*. However, *Pax6* is expressed in the progenitors of these cells in the ventricular zone, so although they are acting downstream of Pax6, they are unlikely to be direct transcriptional targets. Loss of gene expression could either corresponds to:

- a direct effect of Pax6 (the genes are directly downstream of Pax6 but not direct interacting targets);
- an indirect effect (loss of Pax6 from the progenitor cell causes a change in cell types produced by the progenitor; for example, if neuron type 2 is specified rather than neuron type 1, all genes expressed in neuron type 1 will be absent although they are not directly downstream of Pax6).

Therefore, combined with the work discussed above, the following hypothesis can be put forward:

- *LDB2* and *sLMO* are upregulated, directly or indirectly, downstream of Pax6;
- LDB2 and sLMO interact to modulate the transcriptional activity of at least two classes of key developmental genes, LIM genes and homeobox genes;
- via these genes, neuron differentiation is regulated.

LDB2 is expressed from as early as E8.5 in regions of the developing telencephalon and diencephalon that broadly overlap with *Pax6* expression (Bach *et al.*, 1997; Grindley *et al.*, 1997; Mastick *et al.*, 1997) and could therefore function downstream of Pax6 throughout forebrain development. LMO and LDB interactions also occur in *Drosophila* wing development, which raises the interesting possibility that other related LMOs and LDBs might lie downstream of Pax6 homologues in the developing CNS of *Drosophila* and other organisms.

6.3.3 Pax6, LIM proteins and neuronal cell type specification

Recent investigations of Pax6 function in the developing neural tube highlights significant parallels with my results and suggest that Pax6 might function in specification of neuronal cell type via regulation of LIM genes in the cortex. In the ventral spinal cord and hindbrain, progenitor cells in the ventricular zone around the lumen generate neurons that differentiate into different subclasses according to their position along the dorsal-ventral axis. The

neuronal subtypes can be distinguished by their expression of a distinct combination of LIM domain genes (Tsuchida *et al.*, 1994; Appel *et al.*, 1995; Ericson *et al.*, 1997; Sharma *et al.*, 1998). Loss of *Pax6* expression from the neural tube results in dorsal to ventral transformation of progenitor identity such that distinct classes of neurons derived from these progenitors are lost or transformed to a more ventral fate in association with altered expression of LIM genes (Fig. 1.16; Ericson *et al.*, 1997; Osumi *et al.*, 1997) .

Pax6 has also been implicated in regulation of LIM gene expression in the diencephalon: *Lim1* expression is lost from neurons in a domain of dorsal prosomere 1 where it coincides with *Pax6* expression during early brain development (Mastick *et al.*, 1997) and *Lim1* expression is also disrupted during later development (N. Warren, personal communication). My results provide additional evidence that a similar mechanism may be operating in more rostral levels of the neural tube. In the absence of Pax6 function, a class of differentiating neurons normally generated by Pax6 positive progenitors and defined by expression of the LIM domain gene *sLMO* is reduced or absent from the forebrain.

These findings suggest the following model for Pax6 function in specifying neuronal cell type in the forebrain:

- the combination of LIM domain genes expressed by a neuron defines its identity;
- Pax6 is required to specify the identity of neurons generated by precursor cells as they divide in the VZ;
- neuron specification involves the activation of a genetic pathway in newly generated neurons, ultimately leading to LIM gene activation when neurons differentiate in the CP;
- in the absence of Pax6 function, neurons are misspecified, leading to alteration or loss of neuronal LIM gene expression.

In this model, LDB and sLMO function to modulate the transcriptional activity of LIM genes during neuron differentiation. In support of this idea, a recent paper showed that *Lhx9*, a novel LIM homeodomain gene transiently expressed in the cortical intermediate zone, interacts with both LDB1 and LDB2 (Retaux *et al.*, 1999; Bertuzzi *et al.*, 1999). Significantly, *LDB1* and *LDB2* are also highly expressed in the ventral neural tube (Bach *et al.*, 1997), thus LDBs could act as key downstream effectors of Pax6 by mediating LIM-protein neuronal specification in both spinal cord and forebrain. However, testing this hypothesis will necessitate a full characterisation of LIM gene and *LDB* expression in the developing brain, and analysis of alterations in expression and corresponding neuronal cell fate in the *Sey/Sey* forebrain.

CHAPTER 7

Discussion and future work

7.1 *Pax6* in the cortex

It is clear from the *Sey/Sey* mutant that the transcription factor *Pax6* is a key regulatory gene in cortical development. In my thesis I have described the results of experiments aiming to elucidate its functions. I have presented evidence that, in the *Sey* homozygote:

- Asymmetric division of cortical progenitors is increased, and interkinetic nuclear migration disrupted by mid-neurogenesis;
- Thalamic innervation is absent from the cortex;
- Neurons migrating from cortical explants *in vitro* exhibit clumping.

In vitro experiments presented in Chapter 4 suggest that diffusible factors released by wildtype or *Sey/Sey* thalamus do not rescue clumping of *Sey/Sey* cortical cells. However, it remains possible that the absence of thalamocortical innervation from the *Sey/Sey* brain may influence aspects of cortical development other than cell adhesive properties and contribute towards the cortical phenotype. I highlighted in the Introduction that abnormalities in forebrain patterning are apparent prior to the onset of cortical neurogenesis (Grindley *et al.*, 1997; Mastick *et al.*, 1997) and these early patterning defects may also play a role in late-onset cortical defects. These ideas are summarised in Figure 7.1.

In addition, I have described efforts to isolate genes acting downstream of Pax6. Construction of wildtype and *Sey/Sey* cDNA libraries and removal of common clones led to the identification of two transcriptional regulators which are expressed in differentiated neurons generated by *Pax6*-expressing progenitors and are absent from the *Sey/Sey* cortical plate. These are therefore putative genes acting in pathways downstream of Pax6.

On the basis of these findings and other previous work (Warren, *et al.*, 1997; Gotz *et al.*, 1998; Warren *et al.*, 1999) I have suggested that, during cortical development, Pax6 has several roles: in regulating progression through the cell cycle during neurogenesis, in cortical cell fate specification and in determining neuronal adhesive properties. I therefore propose that late onset cortical defects in *Sey/Sey* result from the compounding and cumulative effects of defects in these processes during neurogenesis, such that:

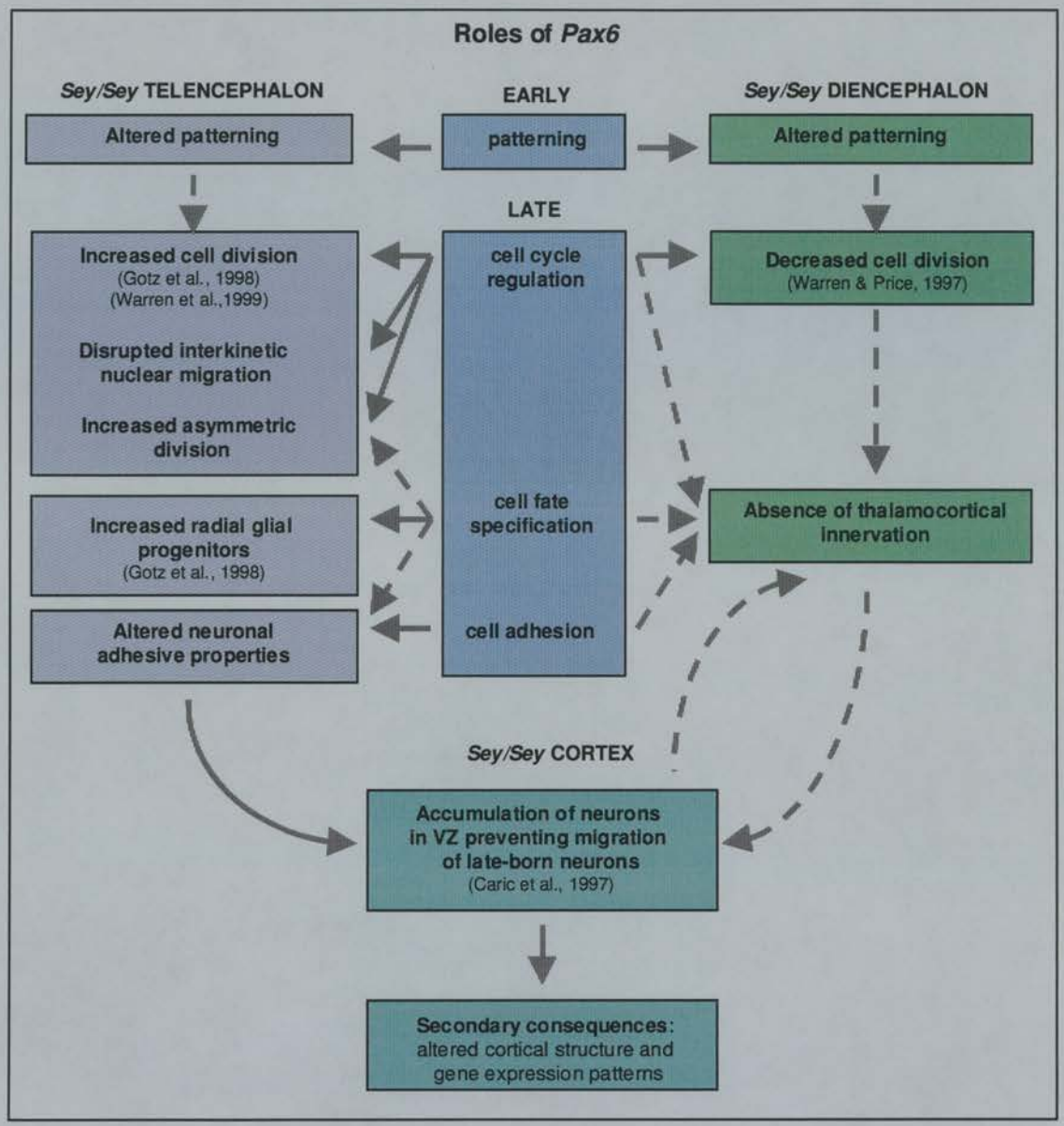

Figure 7.1 Summary of the putative roles of *Pax6* in the developing forebrain and their contribution towards abnormal cortical development in the *Sey/Sey* mouse.

I propose that Pax6 has roles both early in development, in forebrain patterning, and later, in cell cycle regulation, cell fate specification and regulation of cell adhesive properties (central panel). Developmental defects in the *Sey/Sey* telencephalon and diencephalon (right and left panels respectively) can be attributed to a failure in these processes. Together, these defects contribute towards abnormal cortical development.

- progression through the neurogenic cell cycle is accelerated, generating excess neurons;
- the increased numbers of neurons are (1) misspecified and (2) generated with altered adhesive properties that enhance neuron-neuron interactions;
- as neuron production peaks towards late neurogenesis, neurons clump together, creating a physical barrier to any further cell migration;

Thus post-mitotic neurons accumulate, and undergo differentiation, within the VZ/SVZ, creating an expanded ventricular layer and reduced CP.

7.2 Roles of *Pax6* in development

Although it is probable that Pax6 has diverse functions in the cortex, it is possible that it plays the same roles in its different CNS expression domains during development. For example, the spinal cord proliferative zone exhibits many similarities to the cortical VZ: both contain multipotent progenitor cells (reviewed in Lillien, 1998), and both exhibit crescents of asymmetrically localised mNumb in the chick (Wakamatsu *et al.*, 1999). Therefore similar mechanisms regulating progenitor development may operate in more caudal levels of the neural tube. It would be interesting to explore whether aspects of progenitor behaviour disrupted in the *Sey/Sey* cortex, such as proliferation and asymmetric division, are also affected in the *Sey/Sey* spinal cord and could account for disrupted cell fate specification. Similarly in the optic cup, *Pax6* is highly expressed in the presumptive neural retina (Walther & Gruss,1991; Grindley *et al.*, 1995), a layer of multipotent progenitors which give rise to diverse cell types of the adult retina. Foveal hypoplasia is a common feature of aniridia patients (*Pax6* heterozygotes), suggesting that *Pax6* is also required for development of the retinal progenitor population. However, this question is difficult to examine in the *Sey/Sey* homozygote, in which eye development arrests prior to retina formation.

In the cerebellum, altered neuronal adhesive properties might underlie migration defects in the external granule layer. The process of migration involves a series of interactions, including initial release of a neuron from surrounding cells, recognition and adhesion to the appropriate pathway (e.g. radial glia), initiation of cell movement, active translocation along the pathway, and arrest at the appropriate position. Evidence presented by Caric *et al.*, (1997) and data in Chapter 4 suggests that, in the cortex, *Sey/Sey* cells are intrinsically capable of all these steps, and I propose that cortical defects which have previously been classified as migratory problems are instead accounted for by differences in cell adhesion. Thus, neurons with altered adhesive properties are prevented from migrating when they encounter too many other 'sticky' neurons. *In vitro*, cerebellar EGL cells exhibit a neuronal phenotype similar to that seen in cortical explants: cells are capable of movement away from the explant, but are more tightly packed and more adherent to the substratum (Engelkamp *et al.*,

1999). This suggests that these cells too, have altered adhesive properties which prevent normal migration.

However, it is also clear that in some cases Pax6 performs different roles in different tissues. For example, progenitor proliferation rates are increased in the developing cortex, decreased in the diencephalon and unaltered in the cerebellum (Warren & Price, 1997; Gotz *et al.*, 1998; Engelkamp *et al.*, 1999; Warren *et al.*, 1999). This suggests that Pax6 regulates cell cycle progression in the forebrain, but not the hindbrain. I would therefore favour the conclusion that the roles of Pax6 are far from simple, and that it performs different functions in different tissues throughout development.

7.3 Future work

The broad scope of my investigations into the *Sey/Sey* cortical phenotype means that each analysis leaves room for further exploration. I have already mentioned areas in which these experiments might be extended in the discussion sections of the previous chapters. Here, I will briefly summarise some possible areas of future work to address my hypotheses:

1. *Analysis of Sey/Sey cortical cell cycle properties*

The role of Pax6 in regulating cell cycle progression could be explored by using time lapse imaging and cell cycle specific markers to determine the length of the cell cycle and its component phases. In addition, the promoter regions of genes involved in cell cycle regulation could be analysed for putative Pax6 binding sites.

2. *Analysis of the potential of Sey/Sey cortical progenitors to generate cortical cell fates*

The behaviour of progenitors may be investigated *in vitro* by monitoring the patterns of symmetric and asymmetric division and the cell types generated by dissociated cortical progenitors (Qian *et al.*, 1998). *In vivo*, progenitor divisions and the fate of progeny cells could be followed using time lapse imaging. It would also be interesting to examine the subcellular localisation of cell fate determinants such as Numb, and other putative regulators of spindle orientation and cell polarisation, in the *Sey/Sey* cortex.

3. *Analysis of the adhesive properties of Sey/Sey neurons*

The cortical explant system could be used to explore the nature of putative adhesive differences between wildtype and *Sey/Sey* neurons, For example, *Sey/Sey* and wildtype explants could be co-cultured adjacent to one another and examined for segregation of neurons of different genotype. An immunohistochemical analysis of candidate cell adhesion molecules e.g. integrin $\alpha_3\beta_1$, may reveal differences in gene expression between wildtype and

Sey/Sey cells. The question of cell-autonomy could also be addressed by rescue experiments: co-culture of *Sey/Sey* explants with wildtype cortical cells or transfection with a *Pax6*-expressing construct.

4. *Investigation of candidate downstream genes*

Continued analysis of the subtracted wildtype telencephalon library may identify other genes regulated directly or indirectly by Pax6. If a gene proves to be of particular interest, a targeted gene disruption using ES cells could be considered to further evaluate gene function and its contribution to the *Sey/Sey* phenotype.

5. *Analysis of the role of early Pax6 function in the Sey/Sey cortical phenotype*

The possible contribution of early forebrain patterning abnormalities to late-onset cortical defects also remains to be assessed. This could be approached using Cre/lox mediated site-specific recombination to target *Pax6* inactivation after early patterning has occurred normally.

CHAPTER 8

Material and Methods

8.1 Mice

All mouse embryos were derived from *Sey* ^{Ed} heterozygote crosses (also called Pax6 ^{SeyEd}; Roberts, 1967) maintained on an outbred CD1 background and were housed on a 12 hour light-12 hour dark cycle at the Biomedical Research Facility or Transgenic Unit at the Western General Hospital. The day of the vaginal plug following mating was designated E0.5. The mutation in *Sey* is G194X, which is predicted to result in a truncated non-functional protein lacking the homeodomain and C-terminal sequences (Hill *et al.*, 1991). Pregnant females were killed by cervical dislocation; embryos and tissues were dissected in ice cold sterile phosphate buffered saline (PBS) pH 7.4. (0.1M $NaH_2PO_4.H_2O$, 0.1M $Na_2HPO_4.7H_2O$ in H_2O).

8.2 Histology

8.2.1 Wax embedding and sectioning

E15.5 or E17.5 whole brains were fixed in 1% paraformaldehyde (PFA; BDH), 1% 5-sulfosalicylic acid (Sigma) in PBS for 3 hours at 4°C, washed 5x 5 minutes at room temperature and then overnight in PBS at 4°C, before dehydration by 1 hour changes in 30%, 50%, and 70% ethanol at room temperature. Embryos were then automatically processed in a Tissue-Tek VIP machine (Miles Inc.) through 45 minute changes of 85% and 95% ethanol, 2x 100% ethanol, 2x 100% xylene and 4x paraffin wax at 60°C. Embryos were oriented and embedded in fresh wax and 7µm sections were cut on a Wetzlar (Leitz) microtome by Allyson Ross. Sections were floated out on water at 40°C onto glass slides (Chance Propper) and left to dry at room temperature for 24 hours prior to any further analysis.

8.2.2 Cryostat embedding and sectioning

Sterile solutions were used for the embedding of tissues for *in situ* hybridisation. Tissues were fixed in 4% PFA, 4% sucrose at 4°C overnight, then washed 3x 5 minutes in 4% sucrose in PBS at room temperature. Tissues were embedded in melted 1.5% agar, 5% sucrose in PBS. Agar blocks were trimmed and transferred to 30% sucrose in PBS and left at 4°C until the blocks sank (usually 2 days). Blocks were rapidly frozen on dry ice and stored at -70°C for up to 6 months in a sealed container.

10μm sections were cut on a cryostat (Leica). Blocks were allowed to reach chamber temperature for 30 minutes prior to cutting. Sections were mounted on TESPA coated glass slides (below), allowed to air dry for at least one hour and stored in sealed boxes with silica gel at -20°C or below for up to 6 months.

TESPA slides: Glass slides were washed for 20 seconds each in 10% HCl in 70% ethanol, sterile dH_2O and 100% acetone (Fisher Scientific). Slides were air dried, then washed for 20 seconds each in 2% TESPA (3-aminuteopropyl-triethoxysilane, Sigma) and 2x 100% acetone. Slides were air dried and stored in a sealed box.

8.2.3 Haemotoxylin and eosin staining

Slides were dewaxed by placing in 2x 5 minute changes of xylene and rehydrated in 2x 5 minute changes of 100% ethanol followed by 5 minute changes in 90%, 70%, 50% and 30% ethanol. Slides were then washed for a few minutes in water, stained in haemotoxylin (Surgipath) for 4-5 minutes, washed in running water, differentiated in 1% HCl in 70% ethanol for a few seconds and washed again in running water. Slides were then transferred to lithium carbonate solution for a few seconds, washed in running water and stained in eosin (3 parts 1% aqueous eosin (Surgipath), 1 part 1% ethanol and 0.05% acetic acid) for 1-2 minutes. The slides were rinsed in water and then processed as follows: 1x 15 seconds 100% ethanol, 2x1 minute 100% ethanol, 2x5 minutes 100% xylene and mounted in DPX (BDH) with a glass coverslip (Chance Propper).

8.3 Immunohistochemistry

8.3.1 Antibodies

The following antibodies were used, listed with their supplier:

Antibody		Concentration used	Supplier (and reference)
L1	mouse IgG	1:100	Developmental Studies Hybridoma bank (Sweadner, 1983)
NCAM	mouse IgM	1:4000	Sigma
Numb	rabbit IgG	1:1000/2000	gift from W. Zhong & Y.N. Jan (Zhong *et al.*, 1996)
Numblike	rabbit IgG	1:1000/2000	gift from W. Zhong & Y.N. Jan (Zhong *et al.*, 1997)
Pax6	mouse IgG	1: 100	Developmental studies hybridoma bank (Kawakami *et al.*, 1997)
Phospho-histone H3	rabbit IgG	1:1000	Upstate biotechnology
Prox1	rabbit IgG	1:100	gift from G. Oliver
RC2	mouse IgM	1:100	Developmental Studies Hybridoma Bank (Misson *et al.*, 1988)
TAG-1	mouse IgM	1:100	gift from A. Furley (Furley *et al.*, 1990)
TuJ1	mouse IgG	1:400	Sigma

FITC and TRITC conjugated (anti donkey) secondary antibodies were from Jackson Immunolabs; all were used at 1:200.

8.3.2 Staining of cryostat sections

PBTS: For all antibodies except Numb and Numblike PBTS blocking solution was 0.1% heat inactivated sheep serum (Sigma), 0.01% Triton-X100 (Sigma) in PBS pH 7.4. For Numb and Numblike antibodies the blocking solution was 3% sheep serum, 0.1% Bovine Serum Albumin (Sigma), 0.1% Triton-X100 in PBS pH 7.4.

Cryostat sections were defrosted at room temperature for at least 30 minutes, washed for 5x 1-2 minutes in PBS and blocked in PBTS for 2 hours. 100-200µl of antibody diluted in PBTS was applied to the slides, which were incubated in a humidified chamber at 4°C overnight. Slides were then washed for 3x 5 minutes in PBS. 100-200µl of 2° antibody diluted in PBS was applied to the slides and they were incubated in a dark humidified chamber at room temperature for 1-2 hours. The slides were then mounted in Vectashield (Vector laboratories) containing 1µg/ml DAPI (4,6-diamidino-2-phenylindole, Molecular Probes) with a glass coverslip, sealed with clear nail varnish (Boots No.7) and stored in the dark at 4°C.

8.4 *In situ* hybridisation

8.4.1 Synthesis of riboprobes

Digoxigenin (DIG)-labelled anti-sense riboprobes were synthesised in a 50µl reaction containing: 32.75µl ddH_2O, 5µl transcription buffer ([1]Roche), 5µl 10x DIG reaction mix (Roche); 1µl linearised plasmid (1µg/µl, cut in RNase free reaction), 50 units RNase inhibitor (Roche), 100 units T7 RNA polymerase (Roche). The reaction was incubated at 37°C for 2 hours. RNA was precipitated by addition of 6.5µl 4M LiCl and 185µl ethanol, incubation at -70°C for 30 minutes and centrifugation at 13000 rpm for 10 minutes at 4°C. The pellet was washed with 50µl 70% ethanol at -20°C and dried for a minute at room temperature before resuspension in 100µl sterile dH_2O plus 40 units RNase inhibitor.

8.4.2 Solutions used for vibratome/cryostat and wholemount *in situ* protocols

BSA/gelatine mix: 2.2g (0.48% w/v) gelatine dissolved in 450ml PBS at 60°C, allowed to cool to room temperature and 70g (0.15% w/v) Bovine Serum Albumen added. Aliquots were stored at -20°C.

PBT: 0.1% Triton-X100 in PBS and autoclave

10x salt: 2M NaCl, 0.1M Tris HCl, 0.01M Tris base, 0.05M $NaH_2PO_4.H_2O$, 0.05M Na_2HPO_4, 0.05M EDTA in dH_2O and autoclave

Hybridisation solution: 1x salt (above), 50% ultrapure formamide (Gibco BRL), 50% dextran sulphate (Sigma), 1mg/ml yeast RNA (Roche), 1x Denhardt's (Sambrook *et al.*, 1989) in sterile dH_2O.

Wash solution A: 1X SSC (3M NaCl, 0.3M $Na_3C_6H_5O_7.2H_2O$, pH7.0), 50% formamide (Sigma), 0.1% Triton-X100

Wash solution B: 0.2X SSC, 50% formamide, 0.1% Triton-X100

10x TBST: 1.4M NaCl, 27mM KCl, 0.25M Tris HCl ph7.5, 1% Triton-X100

NTMT: 100mM NaCl, 100mM Tris HCl pH9.5, 50mM MgCl2, 0.1% Triton-X100

NBT/BCIP staining solution: 4.5µl NBT (4-Nitro blue tetrazolium chloride, Roche) , 3.5µl BCIP (X-phosphate/5-Bromo-4-chloro-3-indolyl-phosphate, Roche) in NTMT

[1] Roche was previously known as Boehringer Mannheim

8.4.3 *In situ* hybridisation to frozen cryostat sections

Hybridisation

Sections were defrosted at room temperature for at least 30 minutes. DIG riboprobe was diluted 1:200 in hybridisation buffer, mixed and denatured at 70°C for 5-10 minutes; 100µl was added to each slide and covered with a sterile coverslip. Slides were hybridised overnight at 65°C in a sealed perspex box on a paper towel soaked in 1x salts, 50% formamide.

Post-hybridisation washes and antibody staining

Slides were transferred to a glass Coplin jar, washed for 1x 15 minute in Wash Solution A at 65°C to float off coverslips, 2 x 30 minute in Wash Solution A at 65°C, 2x 30 minutes in 1x TBST at room temperature and then blocked in 1x TBST plus 10% heat inactivated sheep serum for 1 hour at room temperature. Anti-Digoxigenin Fab fragment conjugated to alkaline phosphate (Roche) was diluted 1:2000 in blocking solution, 100µl added to each slide and covered with a sterile coverslip. Slides were then incubated in a humidified chamber at 4°C overnight.

Post-antibody washes and staining

Slides were washed 5x 15 minutes in 1xTBST at room temperature, then 2x 10 minutes in NTMT. They were then incubated in freshly made up staining solution in the dark until the staining reaction had proceeded to the desired extent. The reaction was stopped by washing for 2x 10 minutes in NTMT. Slides were fixed in 4% PFA/0.1% glutaraldehyde (Sigma) for 20 minutes and stored in PBS at 4°C. Slides were processed as follows: 1 minute changes in 30%, 50%, 70%, 90%, 2x 100% ethanol, 2x5 minutes 100% xylene and mounted in DPX with a glass coverslip.

8.4.4 *In situ* hybridisation to vibratome sections

This protocol was adapted from (Christiansen *et al.*, 1995) and modified by Penny Rashbass and Dieter Engelkamp. Sections were stored, and all hybridisation steps were carried out in, sterile 6-well tissue culture plates (Nunc).

Vibratome sectioning

Tissue was fixed in 4% PFA overnight at 4°C, then washed 2x 5 minutes in PBS. 400µl 25% glutaraldehyde (Sigma) was added to 4 ml BSA/Gelatine mix and the tissue was quickly immersed and oriented appropriately. Blocks were allowed to set for at least 30 minutes before cutting 200µm sections on a vibratome in cold PBS. Sections were dehydrated by 5 minute changes in 25%, 50% and 75% methanol in PBT, 2x 5 minute in 100% methanol and were stored in 100% methanol at -20°C.

Hybridisation

Sections were rehydrated by 5 minute changes in 75%, 50% and 25% methanol in PBT, 2x 5 minutes in PBT, then bleached with 6% hydrogen peroxide (Sigma) in PBT for 10 minutes and washed for 3x 5minutes in PBT. This was replaced with hybridisation mix (up to 15 sections per well in 1-2ml of hyb mix) and sections were prehybridised overnight in a humidified chamber at 65°C. DIG riboprobe was diluted 1:200 in hybridisation buffer, mixed and denatured at 70°C for 5-10 minutes. Prehybridisation mix was replaced with hybridisation mix and sections hybridised overnight at 65°C.

Post-hybridisation washes and antibody staining

Sections were washed as follows: 2x 10 minutes Wash Solution A at 65°C, 2x30 minutes Wash Solution A at 65°C, 2x 30 minutes Wash Solution B at 65°C and 3x 10 minutes 1x TBST at room temperature. Sections were then blocked in 1x TBST plus 10% heat inactivated sheep serum for >3 hours at room temperature Blocking solution was replaced with Anti-Digoxigenin Fab fragment conjugated to alkaline phosphate diluted 1:2000 in 1% heat inactivated sheep serum in 1x TBST and sections were rocked at 4°C overnight.

Post-antibody washes and staining

Sections were washed 3x10 minutes in NTMT at room temperature on a slowly rotating shaker, transferred to glass staining dishes and incubated in freshly made up staining solution in the dark until the staining reaction had proceeded to the desired extent. The reaction was stopped by washing for 2x 10 minutes in NTMT and sections were washed in PBS (pH3-4)/1% Triton-X100 for at least 10 minutes at 4°C (or up to 3 days to bring down background staining). The sections were fixed in 4% PFA/0.1% glutaraldehyde for 20 minutes and stored in PBS at 4°C.

8.5 DiI labelling

Brains for DiI labelling were fixed and stored in 4% PFA in PBS at 4°C. Brains were washed 3x in PBS, cut in half sagittally with a razor blade and small crystals of DiI (1,1'-dioctadecyl-3,3,3',3'-tetramethylindo-carbocyanin perchlorate, Sigma) pushed into the tissue using a flame-pulled glass pipette. Brains were replaced in 4% PFA in PBS and incubated at 37°C for 2 weeks to speed the diffusion process. For sectioning, brains were washed 3x 5 minutes in PBS and embedded in 5% agarose (routine electrophoresis grade, Flowgen) in PBS. 250µm sections were cut on a vibratome and stored in PBS at 4°. Sections were viewed on glass slides.

8.6 Microexplant cultures

8.6.1 Culture system

Wildtype and *Sey/Sey* telencephalic vesicles were dissected and outer membranes removed under a dissecting microscope. The cortex was cut into strips and then into pieces of diameter 0.1-0.2mm using needles and sharpened wire. Diencephalon was dissected out using a scalpel. Tissue was cultured in chambered coverglass slides (Nunc) coated with 100µg/ml poly(L)lysine (Sigma) and 100µg/ml laminin (Sigma) at 37°C in 5% CO_2. Serum free medium was used: Dulbeccos modified Eagles medium (DMEM, 49%), F10 medium (49%), 1% N2 supplement (Sigma; 5µg/ml insulin, 5µg/ml transferrin, 20nM progesterone, 100 µM putrescine; 30nM selenium), 30µg/ml glutamate, 70µg/ml penicillin, 130µg/ml streptomycin.

8.6.2 Cell survival analysis

Explants were incubated in 250nM SYTO Blue and SYTOX Green fluorescent nucleic acid stains (Molecular Probes) in culture medium for 10 minutes at 37°C before analysis.

8.6.3 Explant immunohistochemistry

Cortical explant cultures were fixed in methanol:acetone (1:1, -20°C) for 20 minutes, washed for 2 x10 minutes in PBT (0.1% Triton-X100 in PBS) and treated as described for frozen sections in 8.3.2 except that washes were performed in PBT for at least 10 minutes each. Explants were stored in Vectashield containing 1µg/ml DAPI in the dark at 4°C.

8.7 Microscopy

Slides were analysed and images taken using a Photometrics CH250 CCD digital camera on a Zeiss Axioskop microscope or a Xillix Microimager 1400 CCD camera on Zeiss Axioplan II and Zeiss Axiovert 100 microscopes. Chroma P1 filter sets were used for fluorescent microscopy. Images were captured using either Smartcapture extensions (Digital Scientific, Cambridge) running in IPLab or scripts written by the charming Paul Perry at the MRC Human Genetics Unit.

8.8 General molecular biology methods

8.8.1 Bacterial cell culture and DNA isolation

8.8.1.1 Media and additives

Media were made by the medium preparation service at the MRC Human Genetics Unit and sterilised by autoclaving.

L-Broth and L-Agar

10g tryptone (Difco), 5g yeast extract (Difco), 10g NaCl and 2.46g $MgSO_4$ dissolved in 1 litre of dH_2O. L-agar was prepared by addition of 15g agar (Oxoid Ltd) to 1 litre of broth.

Additives

Additives to media when required were:

Ampicillin (Sigma), dissolved in dH_2O and added to media and agar to a final concentration of 50μg/ml.

X-Gal (5-Bromo-4-Chloro-3-Indolyl β-D- Galactopyranoside, Sigma), dissolved in dimethylformamide to 20 mg/ml and used at a final concentration of 40μg/ml.

IPTG (isopropylthio-β-D- galactosidase, Sigma) dissolved in dH_2O to 100mM and used at a final concentration of 0.5mM.

8.8.1.2 Growth and plating of bacteria

Bacteria grown from colonies were picked using a sterile toothpick dropped into L-Broth. Bacteria were grown at 37°C, those in liquid media in a shaker at approximately 250rpm. For plating, 100-200μl of suspended bacterial cells was placed on the surface of L-agar plates and spread evenly with a sterile bent glass rod. Plates were then inverted and incubated for 12-16 hours at 37°C. Bacterial plates were stored up to several weeks at 4°C.

8.8.1.3 Bacterial storage conditions

Long-term storage of bacterial cultures was in L-Broth with 15-20% glycerol at -70°C. For long term storage of bacterial colonies on Hybond-N+ (Amersham) membranes, the membrane was placed on a L-agar plate containing 15-20% glycerol for no more than 15 minutes. A second Hybond-N+ membrane was placed on top of the colonies, the two sandwiched between sheets of 3MM chromatography paper (Whatman) and stored pressed between two plastic plates at -70°C . Bacteria were revived from long term storage by incubation in L-Broth or on L-Agar at 37°C.

8.8.1.4 Electrotransformation of bacterial cells

DNA and electrocompetent cells were mixed on ice, transferred to an ice cold 0.1cm electrode gap Gene Pulser Cuvettes (BIORAD) and subjected to a pulse at 1.8V, 200Ω, 25μFD using a Gene Pulser (BIORAD). Immediately following electroporation, 1 ml of L-Broth was added and the cells incubated with shaking for 1 hour at 37°C. Dilutions of the bacterial cells were plated out to assess the transformation efficiency.

8.8.1.5 Plasmid DNA extraction

Small scale plasmid preparations were carried out using the Qiagen plasmid miniprep kit and large scale preparations using QIAprep Plasmid Maxi Kit (Qiagen), both following the manufacturers protocol.

8.8.2 Enzymatic manipulation of DNA

8.8.2.1 Purification of DNA

Phenol/Chloroform/Isoamyl alcohol purification

To separate DNA from contaminants, an equal volume of phenol:chloroform:isoamyl alcohol (25:24:1, Gibco-BRL) was added to the DNA solution. The mixture was vortexed for 30 seconds, centrifuged at 13000 rpm for 5 minutes and the upper aqueous phase removed to a clean tube. Where necessary, back extraction was performed: an equal volume of aqueous solution was added to the phenol:chloroform:isoamyl alcohol, vortexed and centrifuged as above and the two aqueous phases combined.

Two methods were used to concentrate DNA and remove salts:

1. *Ethanol precipitation*: 0.1x volume of 3M NaAc pH 5.5 or 0.5x volume of 7.5M NH_4OAc was added to the DNA solution, followed by 2x volume of 100% ethanol. The contents were mixed and chilled at -20°C for at least 30 minutes. DNA was pelleted by centrifugation at 13000rpm for 20 minutes, the pellet washed in 70% ethanol, briefly dried at 37°C or under vacuum and resuspended in the desired volume of dH_2O or TE.
2. *Microcon purification*: DNA was purified using a Microcon column (Amicon) following the manufacturers protocol.

8.8.2.2 Quantification of DNA and RNA

The concentration of nucleic acid solutions were determined by measuring their absorbance at 260nm in a spectrophotometer (Pharmacia). An absorbance reading of 1 corresponds to a concentration of 40μg/μl of RNA and 50μg/μl of DNA.

8.8.2.3 Restriction enzyme digestion of DNA

Digestion of DNA with restriction enzymes (Roche) was carried out in the buffer recommended by the manufacturer at 37°C. Up to 1µg of DNA was digested in a total volume of 20µl containing 1 unit of enzyme for 1 hour. Double digests with enzymes that required the same buffer were performed simultaneously.

8.8.3 DNA and RNA electrophoresis

Solutions

20x TAE : 1M Tris HCl, pH8.0; 20mM EDTA; 0.4M acetic acid, pH8.3.

10x DNA/RNA Loading Buffer: 0.25% bromophenol blue, 0.25% xylene cyanol FF, 30% glycerol (Fisher Scientific) in dH_2O

DNA molecules were separated according to their size on horizontal agarose gels by electrophoresis. 1-2% agarose (routine electrophoresis grade, Flowgen) was used depending on the size of fragments being analysed. All agarose gels were made with and run in 1x TAE and contained ethidium bromide (BIORAD) at a final concentration of 0.5µg/ml. When running RNA molecules (e.g. to determine whether riboprobe synthesis was successful) the tank, comb and gel tray were washed with 0.1% sodium dodecyl sulphate (SDS) and rinsed with sterile water. Loading buffer was added to the DNA sample to give a 1x final concentration. Gels were run at 20-100V to separate the DNA fragments which were subsequently visualised on a UV transilluminator and photographed using a video copy processor (Mitsubishi). 500ng of 1kb DNA ladder (Gibco BRL) was run on each gel to enable the size of DNA fragments to be determined.

8.8.4 Transfer of nucleic acids to membranes

8.8.4.1 Southern transfer

DNA was transferred from gels to nylon membranes by capillary blotting using a method adapted from Southern (1975). A large strip of 3MM chromatography paper was soaked in 0.4M NaOH and placed on a glass plate so that the ends of the paper were in a reservoir of solution, forming a wick. The gel was placed on top of the wick and a piece of nylon membrane (Hybond-N+, Amersham) and three pieces of 3MM chromatography paper soaked in 0.4M NaOH cut to the size of the gel were placed directly onto the gel ensuring no air was trapped. Saran wrap (Dow Chemical Company) was used to form a barrier around the gel and a weighted stack of paper towels was placed on top. Transfer of DNA by capillary action was complete after 16 hours and the membrane washed briefly in 2xSSC.

8.8.4.2 Dot blots

Dot blots were made using a dot blotting apparatus (BIORAD). A Hybond-N+ membrane and 3MM chromatography paper, prewetted in 2xSSC were sandwiched in the apparatus and 5µl of PCR reaction directly transferred onto the membrane. A vacuum was applied to the apparatus to draw through the solution and transfer the DNA to the membrane.

After Southern or dot blots membranes were left to air dry and DNA was bound to the filter by exposure to 1200µJoules of UV irradiation in a Stratalinker (Stratagene), or by baking at 80°C for 1hour.

8.8.5 Radiolabelling of DNA and hybridisation

8.8.5.1 Random prime labelling of DNA probes

Probes were labelled with [α-^{32}P]-dCTP (Amersham) by random priming from hexadeoxyribonucleotides with the Klenow fragment of *E.coli* DNA polymerase I (Feinberg & Vogelstein, 1984).

25-50ng of DNA was denatured by boiling at 100°C for 5 minutes and cooling on ice. Labelling was performed using the Random Prime DNA labelling kit (Roche). 1µl each of 0.5mM dATP, dGTP and dTTP (25µM final concentration), 2µl of reaction buffer, 1µl of Klenow enzyme, 2.5µl of 10µCi/µl [α-^{32}P]-dCTP and H_2O were added up to a final volume of 20µl. The reaction was incubated at 37°C for 1 hour. Unincorporated nucleotides were removed by running the sample through a Nick column (Pharmacia) following the manufacturers instructions. After elution the probe was denatured by heating to 100°C for 5 minutes before adding to the hybridisation solution.

8.8.5.2 Hybridisation of radioactive probes to membranes

Hybridisation

All hybridisations were carried out in glass bottles (Techne) incubated in a rotating oven (Techne) at 65°C. Membranes were prehybridised for at least 1 hour in 5mg/ml Marvel dried milk, 0.5M sodium pyrophosphate, 7% sodium dodecyl sulphate (SDS) in H_2O (Church & Gilbert, 1984) before addition of the probe and incubation overnight.

Post-hybridisation washes

Hybridisation solution was removed, filters rinsed once and then washed for 2x 30 minutes in 30mM sodium pyrophosphate, 0.1% SDS in H_2O at 65°C.

Autoradiography

Filters were placed in light-tight signal enhancing cassettes and exposed to X-OMAT X-ray film (Kodak) at -70°C for an appropriate exposure time determined by the radioactive signal intensity. Film was developed on an automatic X-ray film processor RGII (Fuji).

8.8.5.3 Removal of radioactive probes from membranes

For repeat use of blots, membranes were stripped of radioactivity. A boiling solution of 0.1% SDS was poured directly onto the membrane, the solution agitated until it cooled to room temperature, and the process repeated.

8.9 Isolation of RNA and cDNA synthesis

Tissue for RNA isolation was freshly dissected from embryos, snap frozen on dry ice and stored at -70°C. All manipulations were carried out using RNase free solutions, glass and plastic ware.

8.9.1 Isolation of poly(A) RNA

Frozen tissue was homogenised using a syringe by passing through a series of needles of decreasing size (bore size 19G, 21G, 23G and 25G). Poly(A)RNA was extracted directly from homogenised tissue using magnetic oligo$(dT)_{25}$ Dynabeads (Dynal) and solutions following the manufacturers protocol. Repeat isolations were performed on the same tissue to maximise extraction of RNA. RNA was concentrated by addition of 0.7 volume of 7.5M NH_4OAc and 1x volume of isopropanol and incubation at -70°C for at least 30 minutes. RNA was pelleted by centrifugation at 13000 rpm for 30 minutes, washed with 70% ethanol at -20°C, resuspended in sterile dH_2O water and stored at -70°C.

8.9.2 First strand cDNA synthesis

First strand cDNA synthesis from poly(A) RNA for use as probes was performed using an oligo(dT) primer (Gibco-BRL) and all other components supplied in the SuperScript Plasmid System for cDNA Synthesis and Plasmid Cloning (Gibco-BRL) following the manufacturers instructions.

8.10 cDNA library construction

cDNA plasmid libraries were constructed using the SuperScript Plasmid System for cDNA Synthesis and Plasmid Cloning (Gibco-BRL) essentially following the manufacturers protocol. Four libraries were made in total: two E15.5 wildtype telencephalon and two E15.5 *Sey/Sey* telencephalon libraries each in pSPORT1 or pSPORT2 plasmid vectors (Gibco-BRL).

First strand cDNA was synthesised from approximately 3µg wildtype or *Sey/Sey* poly(A) RNA using a primer-adapter containing 15 dT residues and a *Not*I restriction site (GCGGCCGCCC$(A)_{15}$) with SuperScript II reverse transcriptase for 1 hour at 37°C. Second strand cDNA was synthesised with *E. coli* DNA polymerase in the presence of *E. coli* DNA ligase and *E. coli* RNase H for 2 hours at 16°C. After this, and each subsequent enzyme step, a phenol:chloroform:isoamyl extraction was performed to remove any contaminating protein. The double-stranded cDNA was blunt ended with T4 DNA polymerase incubated at 5 minutes at 16°C and *Sal*I adapters were added using T4 DNA ligase and incubation for 16 hours at 16°C. The cDNA was digested with *Not*I and size fractionated using sephacryl 500 chromatography columns. Preliminary experiments done by Julie Moss confirmed that size selection of the different fractions was similar to that claimed by the manufacturers. The columns were used to select fragments larger than 500 base pairs and thus decrease the probability that *Sal*I adapters used in the library construction were incorporated in the final ligation. For both wildtype and *Sey/Sey* libraries 10ng of the largest cDNA fraction was separately ligated with 50ng of *Not*I-*Sal*I cut pSPORT1 and pSPORT2 vector using T4 DNA ligase for 3 hours at room temperature. Each ligation was ethanol precipitated, washed with 70% ethanol and resuspended in 5µl 0.5x TE (5mM Tris, 0.5mM EDTA, pH7.5).

Each ligation reaction was divided into 5 aliquots of 1µl and each aliquot electroporated into 40µl ElectroMAX DH12S cells (Gibco-BRL). The transformed cells were combined and serial dilutions plated on L-agar plus ampicillin and X-Gal/IPTG blue/white colour selection to determine the library size. To increase the number of clones in the libraries 10ng of the second largest fraction was ligated and electroporated as described above and the two combined to give the final libraries. 0.5 ml aliquots of $5x10^5$ clones of the unamplified libraries were stored at -70°C.

8.11 Generation of subtracted cDNA libraries

The subtracted cDNA library was generated broadly following the protocol supplied with the pSPORT2 vector (GIBCO BRL) using single stranded tracer DNA made from the pSPORT2 wildtype library and biotinylated RNA driver made from the pSPORT1 *Sey/Sey* library. Siliconised 1.5ml eppendorf tubes were used at all stages of the protocol and were prepared by rinsing tubes with Silicon Treatment Repelcote (BDH), air drying and autoclaving.

Preparation of single stranded tracer DNA

50ml of superbroth (35g tryptone, 20g yeast extract, 5g NaCl in 1 litre at pH7.5) plus ampicillin was inoculated with an unamplified aliquot of wildtype pSPORT2 library and incubated at 37°C in a shaking incubator until the OD_{600} had reached 0.15-0.2. 250µl M13K07 helper phage (>$1x10^{11}$ pfu/ml, Gibco-BRL, supplied with DH12S electrocompetent cells) was then added and incubation continued in the same conditions overnight. The culture was spun 2x 10 minutes at 9000 rpm to pellet bacteria and the supernatant divided into 2 x 20mls in siliconised Corex tubes. 40µl 1M $MgCl_2$, 200 units DNase I (Roche) and 20µl 10mg/ml RNase A (Sigma) was added to each 20mls, the solution covered with Parafilm and incubated for 30 minutes at 37°C. 5mls of 2.5M NaCl/20% PEG8000 was added, the solution incubated on ice for 1 hour and then spun at 9000rpm for 30 minutes. The supernatant was poured off, 100µl 0.5x TE added and the pellet resuspended by pipetting. The solution was transferred to an eppendorf tube and a further 100µl 0.5x TE added and mixed. 0.25 vol 2.5M NaCL/20% PEG8000 was added, the solution incubated on ice for 1 hour and centrifuged at 13000rpm for 15 minutes at 4°C. The supernatant was removed and the pellet resuspended by vigorous vortexing in 200µl 0.5x TE. 2µl 20mg/ml Proteinase K (Gibco-BRL) and 2µl 10% SDS was added and the solution was incubated at 45°C for 1 hour. Four phenol/chloroform extractions were performed and the DNA was precipitated with 7.5M NH_4OAc and 100% ethanol (as described above). The pellet was resuspended in 100µl 0.5x TE, quantified using a spectrophotometer and a small aliquot was examined by gel electrophoresis.

Blocking the pSPORT2 poly(T) region

5 µg of single stranded DNA (ssDNA), 1.5 µl Taq Polymerase buffer (Roche) and 1µg oligo poly(A) ($GCGGCCGCCC(A)_{15}$) were mixed together and made up into 15 µl with dH_2O. The reaction was incubated for 2 minutes at 90°C and then 30 minutes at 55°C. 1.5µl Taq Polymerase buffer, 1.5µl 10mM dTTP , 2.5 units of Taq Polymerase (Roche) and 11.5µl dH_2O were then added and the reaction incubated at 70°C for 20 minutes. 70µl 0.5x TE was added and the solution phenol/chloroform extracted and back extracted with 100µl 0.5xTE. DNA was precipitated with 7.5M NH_4OAc, 100% ethanol and 5µg yeast tRNA was added as a carrier to aid with nucleic acid precipitation. The pellet was resuspended in 20µl 0.5x TE.

Preparation of biotinylated driver RNA

Preparation of template DNA

Two unamplified aliquots of *Sey/Sey* driver pSPORT1 library were added to 2x 250mls L-Broth plus ampicillin and incubated at 37°C in a shaking incubator overnight. The DNA was then isolated by maxiprep. Four parallel 100µl restriction digests were set up, each

containing 5µg DNA, 10µl buffer and 2.5 units *Sal*I and incubated at 37°C for 2 hours, after which a further 2.5 units *Sal*I were added and incubated at 37°C for another 30 minutes. To this, 5µl 10% SDS and 1µl 10mg/ml Proteinase K were added and the reaction incubated at 37°C for 30 minutes. The solution was phenol/chloroform extracted, ethanol precipitated and the pellet resuspended in 10µl 0.5xTE.

In vitro transcription

10µl DNA template, 10µl 10mM Biotin-14-CTP (Roche), 5µl dNTP mix(10mM dATP, dUTP, dGTP, 5mM dCTP) 100 units T7 RNA Polymerase (Roche), 5µl 10x transcription buffer (supplied with T7 RNA Polymerase) and 50 units RNase inhibitor (Roche) were mixed, made up to 50µl with dH_2O and incubated at 37°C overnight. RNA was precipitated by addition of 6.5µl 4M LiCl, and 185µl 100% ethanol, incubation at -70°C for 30 minutes and centrifugation at 13000 rpm at 4°C for 10 minutes. The pellet was washed with 50µl 70% ethanol and dried very briefly before resuspension in 50µl dH_2O. LiCl precipitation was then repeated and the pellet resuspended to a final concentration of 4µg/µl to which 40 units RNase inhibitor was added.

Hybridisation

Solutions

Hybridisation buffer: 80% ultrapure formamide, 100mM HEPES pH7.6, 2mM EDTA, 0.2% SDS

Streptavidin Binding Buffer: 50mM HEPES pH7.6, 500mM NaCl, 2mM EDTA

The following hybridisations were set up in siliconised eppendorf tubes:

	RNA (0.2µg/µl)	ssDNA (4µg/µl)	Hyb buffer	sterile dH_2O	5M NaCl
Control (no driver RNA)	0	3µl	25µl	20µl	2µl
Subtraction	20µl	3µl	25µl	0	2µl

RNA or dH_2O was added to the buffer, heated to 65°C for 10 minutes, chilled on ice and then the ssDNA and NaCl added. Tubes were wrapped in Parafilm to prevent evaporation and incubated at 42°C shaking at 200rpm for 24 hours.

Removal of RNA:ssDNA hybrids

The hybridisation mix was transferred to an eppendorf tube containing 200µl Streptavidin Binding Buffer and mixed. 5µg Streptavidin (Gibco-BRL) was added, mixed by vortexing

Removal of RNA:ssDNA hybrids

The hybridisation mix was transferred to an eppendorf tube containing 200µl Streptavidin Binding Buffer and mixed. 5µg Streptavidin (Gibco-BRL) was added, mixed by vortexing and incubated at room temp for 5 minutes. The solution was extracted with 250µl phenol:chloroform:isoamyl alcohol and back extracted with 50µl Binding Buffer; extraction was then repeated on the supernatant a further two times. ssDNA was precipitated with 7.5M NH_4OAc, 100% ethanol and 5µg yeast tRNA as carrier and the pellet resuspended in 3µl 0.5x TE. Hybridisation and hybrid removal were repeated 2 times using the precipitated ssDNA and fresh driver RNA; subtracted ssDNA was resuspended in a final volume of 10µl 0.5x TE.

Conversion of single stranded to double stranded DNA

10µl ssDNA, 4µl ddH_2O, 4µl 5x Sequenase buffer (Amersham) and 2µl M13 forward sequencing primer (30ng/µl, Applied Biosystems) were mixed, incubated for 1 minute at 65°C and allowed to cool slowly to approximately 35°C. To this was added: 4µl 5x Sequenase buffer, 2µl dNTPs (10mM dATP, dCTP, dGTP, dTTP), 2 units Sequenase (Amersham) and 12µl ddH_2O, and the solution incubated at 37°C for 3 hours. 60µl 0.5xTE was added and DNA precipitated by addition of 7.5M NH_4OAc and 100% ethanol and incubation at -20°C overnight. The pellet was resuspended in 10µl 0.5x TE. To remove salt from the solution a 0.025µm drop dialysis filter (Millipore) was placed on a Petri dish of sterile water, the DNA solution pipetted onto the filter and left for 30 minutes. The solution was then removed and made up to 10µl. 2µl of DNA solution was electroporated into 40µl ElectroMAX DH12S cells (GIBCO BRL) and serial dilutions plated to assess the subtracted library size.

8.12 Library replica plating

Solutions

Denaturing solution: 0.5M NaOH, 1.5M NaCl

Neutralising solution: 1.5M NaCl, 0.5M Tris-HCl pH7.2, 0.001M EDTA

Library plating

For the wildtype and *Sey/Sey* telencephalon libraries, a single library aliquot of $5x10^5$ clones was diluted to 2ml with L-Broth, plated over 4 x 20x20cm squares of Hybond-N+ (Amersham) on 22 x 22cm L-Agar ampicillin plates (Nunc). For the subtracted library an entire aliquot (1ml) of electroporated cells corresponding to 1/5 of the total subtracted library ($1.6x10^3$ clones) was plated onto a single square of Hybond-N+ on an L-Agar

ampicillin plate. Plates were incubated at 37°C for 2 hours and then 30°C overnight until colonies were approximately 1mm in diameter.

Replica plating

Two replica filters of each master filter were made as follows:
Two 21x21cm 3MM chromatography paper squares and a 20x20cm square of Hybond-N+ were wetted in L-Broth and blotted dry in filter paper. Master and replica filters were labelled. Dry 3MM, wet 3MM, master membrane (colonies upwards), replica membrane, wet 3MM and dry 3MM were layered in that order, sandwiched between 2 large glass plates and an even heavy weight of approximately 65 kgs (me) was applied. The 3MM squares were removed and needle holes were pierced through master and replica membranes to orient replicas. Master and replica membranes were peeled apart carefully and each placed, colony side up, onto fresh L-Agar plates. Plates were incubated at 37°C, the master filter for 1hour or more until colonies had recovered and the replicas for 4-5hrs until colonies had reached 1-2mm in diameter. This process was then repeated to make the second replica filter.

Fixing DNA to membrane

Two trays were prepared containing 3MM paper soaked in (1) denaturing solution and (2) neutralising solution and replica filters were placed colony side up in the denaturing tray for 10 minutes. Filters were transferred to the neutralising tray for 10 minutes, then washed gently and very thoroughly in 2x SSC. The filters were air dried overnight and DNA fixed by exposure to 1200µJoules of UV irradiation in a Stratalinker (Stratagene), or by baking at 80°C for 1hour.

8.13 Library amplification and analysis

8.13.1 Library amplification

For the wildtype and *Sey/Sey* telencephalon libraries, a library aliquot of $5x10^5$ clones was diluted to 1 ml with L-Broth, incubated at 37°C for 30 minutes and plated over a 22x22cm L-Agar ampicillin plate. For the subtracted library a second 2µl aliquot of ligated DNA corresponding to 1/5 of the subtracted library ($1.6x10^3$ clones) was electroporated into 40µl ElectroMAX DH12S cells (GIBCO BRL) and plated onto a 22x22cm L-Agar ampicillin plate. Plates were incubated at 37°C overnight.

10 ml of L-broth plus 20% glycerol was spread over the plate and agitated on a shaker for 15 minutes at room temperature to loosen the colonies. The bacterial suspension was scraped gently off the agar and titred, in a similar manner as that done for the unamplified libraries.

The amplified libraries were stored in aliquots of $2.2x10^{11}$ (wildtype) , $4.1x10^{10}$ (*Sey/Sey*) and $5.3x10^{8}$ (subtracted) clones, each corresponding to several thousand copies of the unamplified libraries

8.13.2 Southern blot analysis

An aliquot of the amplified wildtype and *Sey/Sey* libraries was inoculated into 500 ml L-Broth plus ampicillin and grown overnight at 37°C. DNA was isolated by maxiprep, 1µg of each digested with *Not*I and *Sal*I to release the inserts, size fractionated by gel electrophoresis and the gels Southern blotted.

8.13.3 Preparation of probes

Gene specific probes were prepared from cloned mouse cDNA fragments by restriction digests. Either DNA fragments were run in low melting point agarose gel (Ultrapure LMP Agarose, Gibco-BRL) in 1x TAE, visualised on a UV transilluminator and excised using a sterile scalpel blade, or DNA fragments were run in a Flowgen agarose gel as described in section 8.8.3, excised from the gel and isolated from the agarose using the QIAEX gel extraction kit (Qiagen) following the manufacturers protocol.

The β-*actin* cDNA probe was a gift from Ruth Arkell; the *stathmin/p19* cDNA was isolated from a wildtype E15.5 telencephalon cDNA library.

Probes of whole library DNA were prepared by digesting 30 µg of amplified library DNA in 6 separate 50µl digests containing 2.5 units each of *Not*I and *Sal*I at 37°C overnight. These were combined and concentrated using a Microcon-30 column, run out by gel electrophoresis and isolated using DEAE-cellulose membrane (NA-45) following the protocol in Sambrook *et al.*, (1989). 300ng of whole library DNA or tissue cDNA was labelled for use as probes.

8.14 PCR Amplification of vector inserts from bacterial cultures

Amplification of pSPORT inserts direct from overnight bacterial cultures was performed in 96 well PCR plates (Costar). Each PCR reaction contained 2µl 10x PCR buffer (Perkin Elmer), 20pmol T7 primer, 20pmol SP6 primer, 1.5mM $MgCl_2$ (Perkin Elmer), 0.25mM dNTPs (Roche), 1µl bacterial culture, 1 unit AmpliTaq Gold (Perkin Elmer), 9.6µl dH_2O.

Reactions were overlaid with mineral oil (Sigma) and reactions carried out in a Tetrad MJ PTC225 PCR machine under the following conditions: initial denaturation at 94°C for 14

minutes 30x amplification cycles (94°C for 1', 50°C for 1', 72°C for 1') followed by a final extension of 72°C for 5'.

8.15 DNA sequencing

Double stranded DNA was sequenced by di-deoxy sequencing (Sanger *et al.*, 1977). 0.5-1µg of plasmid DNA was labelled using an ABI Prism dRhodamine cycle sequencing kit in a Tetrad MJ PTC200 PCR machine following the manufacturers instructions: 25 cycles at 96°C for 10'', 50°C for 5'', 60°C for 4'. Precipitated DNA was run by Agnes Gallagher on an Applied Biosystems 377A DNA sequencer.

Sequence analysis and editing was performed using the BLAST search facility (Altschul *et al.*, 1990) and (Genetics Computer Group) programmes (Devereux *et al.*, 1984) available through the HGMP computing service.

8.16 Oligonucleotides

Oligonucleotides were supplied by Genosys as precipitates and were resuspended in dH_2O. T7 and Q696 primers were used to PCR amplify inserts from, and sequence into, the pSPORT library clones. To sequence further into clone 147 primers were designed using the GCG Prime program at HGMP.

Primer	Sequence 5'→3'	Notes
Q696	GATTTAGGTGACACTATAG	
T7	TAATACGACTCACTATAGGG	
W762	TATGGACAGCGTAATCAGGTG	5'→3' internal primer for clone 147
W763	ATTCCCCGTTATTTTAGCACC	3'→5' internal primer for clone 147

References

Acampora, D., Mazan, S., Lallemand, Y., Avantaggiato, V., Maury, M., Simeone, A., and Brulet, P. (1995). Forebrain and midbrain regions are deleted in Otx2-/- mutants due to a defective anterior neuroectoderm specification during gastrulation. Development *121*, 3279-3290.

Adams, R.J. (1996). Metaphase spindles rotate in the neuroepithelium of rat cerebral cortex. J.Neurosci. *16*, 7610-7618.

Agulnick, A.D., Taira, M., Breen, J.J., Tanaka, T., Dawid, I.B., and Westphal, H. (1996). Interactions of the LIM-domain-binding factor Ldb1 with LIM homeodomain proteins. Nature *384*, 270-272.

Altschul, S.F., Gish, W., Miller, W., Myers, E.W., and Lipman, D.J. (1990). Basic local alignment search tool. J.Mol.Biol. *215*, 403-410.

Anderson, S.A., Qiu, M., Bulfone, A., Eisenstat, D.D., Meneses, J., Pedersen, R., and Rubenstein, J.L. (1997). Mutations of the homeobox genes Dlx-1 and Dlx-2 disrupt the striatal subventricular zone and differentiation of late born striatal neurons. Neuron *19*, 27-37.

Ang, S.L. and Rossant, J. (1994). HNF-3 beta is essential for node and notochord formation in mouse development. Cell *78*, 561-574.

Ang, S.L., Jin, O., Rhinn, M., Daigle, N., Stevenson, L., and Rossant, J. (1996). A targeted mouse Otx2 mutation leads to severe defects in gastrulation and formation of axial mesoderm and to deletion of rostral brain. Development *122*, 243-252.

Angevine, J.B.J. (1970). Time of neuron origin in the diencephalon of the mouse. An autoradiographic study. J.Comp.Neurol. *139*, 129-187.

Angevine, J.B.J. and Sidman, R.L. (1961). Autoradiographic study of cell migration during histogenesis of cerebral cortex in the mouse. Nature *192*, 766-768.

Anton, E.S., Cameron, R.S., and Rakic, P. (1996). Role of neuron-glial junctional domain proteins in the maintenance and termination of neuronal migration across the embryonic cerebral wall. J.Neurosci. *16*, 2283-2293.

Anton, E.S., Marchionni, M.A., Lee, K.F., and Rakic, P. (1997). Role of GGF/neuregulin signaling in interactions between migrating neurons and radial glia in the developing cerebral cortex. Development *124*, 3501-3510.

Anton, E.S., Kreidberg, J.A., and Rakic, P. (1999). Distinct functions of alpha3 and alpha(v) integrin receptors in neuronal migration and laminar organization of the cerebral cortex. Neuron *22*, 277-289.

Appel, B., Korzh, V., Glasgow, E., Thor, S., Edlund, T., Dawid, I.B., and Eisen, J.S. (1995). Motoneuron fate specification revealed by patterned LIM homeobox gene expression in embryonic zebrafish. Development *121*, 4117-4125.

Arimatsu, Y., Miyamoto, M., Nihonmatsu, I., Hirata, K., Uratani, Y., Hatanaka, Y., and Takiguchi-Hayashi, K. (1992). Early regional specification for a molecular neuronal phenotype in the rat neocortex. Proc.Natl.Acad.Sci.U.S.A. *89*, 8879-8883.

Arimatsu, Y., Ishida, M., Takiguchi-Hayashi, K., and Uratani, Y. (1999). Cerebral cortical specification by early potential restriction of progenitor cells and later phenotype control of postmitotic neurons. Development *126*, 629-638.

Artavanis-Tsakonas, S., Rand, M.D., and Lake, R.J. (1999). Notch signaling: cell fate control and signal integration in development. Science *284*, 770-776.

Ausubel, F.M., Brent, R., Kingston, R.E., Moore, D.D., Seidman, J.G., Smith, J.A., and Struhl, K. (1994). Current Protocols in Molecular Biology (Greene Publishing and Wiley Interscience,USA).

Ba-Charvet, K.T., von, B.Y., Guazzi, S., Boncinelli, E., and Godement, P. (1998). A potential role for the OTX2 homeoprotein in creating early 'highways' for axon extension in the rostral brain. Development *125*, 4273-4282.

Bach, I., Carriere, C., Ostendorff, H.P., Andersen, B., and Rosenfeld, M.G. (1997). A family of LIM domain-associated cofactors confer transcriptional synergism between LIM and Otx homeodomain proteins. Genes Dev. *11*, 1370-1380.

Bagnard, D., Lohrum, M., Uziel, D., Puschel, A.W., and Bolz, J. (1998). Semaphorins act as attractive and repulsive guidance signals during the development of cortical projections. Development *125*, 5043-5053.

Balling, R., Deutsch, U., and Gruss, P. (1988). undulated, a mutation affecting the development of the mouse skeleton, has a point mutation in the paired box of Pax 1. Cell *55*, 531-535.

Barbe, M.F. and Levitt, P. (1991). The early commitment of fetal neurons to the limbic cortex. J.Neurosci. *11*, 519-533.

Barth, K.A. and Wilson, S.W. (1995). Expression of zebrafish nk2.2 is influenced by sonic hedgehog/vertebrate hedgehog-1 and demarcates a zone of neuronal differentiation in the embryonic forebrain. Development *121*, 1755-1768.

Bayer, S.A. and Altman, J. (1991). Neocortical Development (New York: Raven Press).

Berry, M. and Rogers, A.W. (1965). The migration of neuroblasts in the developing cerebral cortex. J.Anat. *99*, 691-709.

Bertuzzi, S., Porter, F.D., Pitts, A., Kumar, M., Agulnick, A., Wassif, C., and Westphal, H. (1999). Characterization of Lhx9, a novel LIM/homeobox gene expressed by the pioneer neurons in the mouse cerebral cortex. Mech.Dev. *81*, 193-198.

Bicknese, A.R., Sheppard, A.M., O'Leary, D.D., and Pearlman, A.L. (1994). Thalamocortical axons extend along a chondroitin sulfate proteoglycan- enriched pathway coincident with the neocortical subplate and distinct from the efferent path. J.Neurosci. *14*, 3500-3510.

Blakemore, C. and Molnar, Z. (1990). Factors involved in the establishment of specific interconnections between thalamus and cerebral cortex. Cold Spring Harb.Symp.Quant.Biol. *55:491-504*, 491-504.

Blaschke, A.J., Staley, K., and Chun, J. (1996). Widespread programmed cell death in proliferative and postmitotic regions of the fetal cerebral cortex. Development *122*, 1165-1174.

Boehm, T., Foroni, L., Kennedy, M., and Rabbitts, T.H. (1990). The rhombotin gene belongs to a class of transcriptional regulators with a potential novel protein dimerisation motif. Oncogene *5*, 1103-1105.

Boehm, T., Foroni, L., Kaneko, Y., Perutz, M.F., and Rabbitts, T.H. (1991). The rhombotin family of cysteine-rich LIM-domain oncogenes: distinct members are involved in T-cell translocations to human chromosomes 11p15 and 11p13. Proc.Natl.Acad.Sci.U.S.A. *88*, 4367-4371.

Bohner, A.P., Akers, R.M., and McConnell, S.K. (1997). Induction of deep layer cortical neurons *in vitro*. Development *124*, 915-923.

Bonini, N.M., Leiserson, W.M., and Benzer, S. (1993). The eyes absent gene: genetic control of cell survival and differentiation in the developing Drosophila eye. Cell *72*, 379-395.

Bonini, N.M., Bui, Q.T., Gray-Board, G.L., and Warrick, J.M. (1997). The Drosophila eyes absent gene directs ectopic eye formation in a pathway conserved between flies and vertebrates. Development *124*, 4819-4826.

Bonni, A., Sun, Y., Nadal-Vicens, M., Bhatt, A., Frank, D.A., Rozovsky, I., Stahl, N., Yancopoulos, G.D., and Greenberg, M.E. (1997). Regulation of gliogenesis in the central nervous system by the JAK-STAT signaling pathway. Science *278*, 477-483.

Bopp, D., Burri, M., Baumgartner, S., Frigerio, G., and Noll, M. (1986). Conservation of a large protein domain in the segmentation gene paired and in functionally related genes of Drosophila. Cell *47*, 1033-1040.

Braisted, J.E. and O'Leary, D.D. (1995). Axons from the ventrobasal thalamic nucelus pioneer the thalamocortical pathway to rat neocortex. Soc.Neurosci.Abstr. *21*, 798

Braisted, J.E., Tuttle, R., and O'Leary, D.D. (1999). Thalamocortical axons are influenced by chemorepellent and chemoattractant activities localized to decision points along their path. Dev.Biol. *208*, 430-440.

Breen, J.J., Agulnick, A.D., Westphal, H., and Dawid, I.B. (1998). Interactions between LIM domains and the LIM domain-binding protein Ldb1. J.Biol.Chem. *273*, 4712-4717.

Briscoe, J., Sussel, L., Serup, P., Hartigan-O'Connor, D., Jessell, T.M., Rubenstein, J.L., and Ericson, J. (1999). Homeobox gene Nkx2.2 and specification of neuronal identity by graded Sonic hedgehog signalling. Nature *398*, 622-627.

Brummendorf, T., Kenwrick, S., and Rathjen, F.G. (1998). Neural cell recognition molecule L1: from cell biology to human hereditary brain malformations. Curr.Opin.Neurobiol. *8*, 87-97.

Buescher, M., Yeo, S.L., Udolph, G., Zavortink, M., Yang, X., Tear, G., and Chia, W. (1998). Binary sibling neuronal cell fate decisions in the Drosophila embryonic central nervous system are nonstochastic and require inscuteable- mediated asymmetry of ganglion mother cells. Genes Dev. *12*, 1858-1870.

Bulfone, A., Puelles, L., Porteus, M.H., Frohman, M.A., Martin, G.R., and Rubenstein, J.L. (1993). Spatially restricted expression of Dlx-1, Dlx-2 (Tes-1), Gbx-2, and Wnt- 3 in the embryonic day 12.5 mouse forebrain defines potential transverse and longitudinal segmental boundaries. J.Neurosci. *13*, 3155-3172.

Bulfone, A., Smiga, S.M., Shimamura, K., Peterson, A., Puelles, L., and Rubenstein, J.L. (1995). T-brain-1: a homolog of Brachyury whose expression defines molecularly distinct domains within the cerebral cortex. Neuron *15*, 63-78.

Burrill, J.D., Moran, L., Goulding, M.D., and Saueressig, H. (1997). PAX2 is expressed in multiple spinal cord interneurons, including a population of EN1+ interneurons that require PAX6 for their development. Development *124*, 4493-4503.

Burrows, R.C., Wancio, D., Levitt, P., and Lillien, L. (1997). Response diversity and the timing of progenitor cell maturation are regulated by developmental changes in EGFR expression in the cortex. Neuron *19*, 251-267.

Callaerts, P., Halder, G., and Gehring, W.J. (1997). PAX-6 in development and evolution. Annu.Rev.Neurosci. *20:483-532*, 483-532.

Callaerts, P., Munoz-Marmol, A.M., Glardon, S., Castillo, E., Sun, H., Li, W.H., Gehring, W.J., and Salo, E. (1999). Isolation and expression of a Pax-6 gene in the regenerating and intact Planarian Dugesia(G)tigrina. Proc.Natl.Acad.Sci.U.S.A. *96*, 558-563.

Caric, D., Gooday, D., Hill, R.E., McConnell, S.K., and Price, D.J. (1997). Determination of the migratory capacity of embryonic cortical cells lacking the transcription factor Pax-6. Development *124*, 5087-5096.

Casarosa, S., Fode, C., and Guillemot, F. (1999). Mash1 regulates neurogenesis in the ventral telencephalon. Development *126*, 525-534.

Catalano, S.M., Robertson, R.T., and Killackey, H.P. (1991). Early ingrowth of thalamocortical afferents to the neocortex of the prenatal rat. Proc.Natl.Acad.Sci.U.S.A. *88*, 2999-3003.

Catalano, S.M., Messersmith, E.K., Goodman, C.S., Shatz, C.J., and Chedotal, A. (1998). Many major CNS axon projections develop normally in the absence of semaphorin III. Mol.Cell Neurosci. *11*, 173-182.

Caviness, V.S.J. (1982). Neocortical histogenesis in normal and reeler mice: a developmental study based upon [3H]thymidine autoradiography. Brain Res. *256*, 293-302.

Caviness, V.S.J., Takahashi, T., and Nowakowski, R.S. (1995). Numbers, time and neocortical neuronogenesis: a general developmental and evolutionary model. Trends Neurosci. *18*, 379-383.

Caviness, V.S.J., Takahashi, T., and Nowakowski, R.S. (1999). The G1 restriction point as critical regulator of neocortical neuronogenesis. Neurochem.Res. *24*, 497-506.

Chae, T., Kwon, Y.T., Bronson, R., Dikkes, P., Li, E., and Tsai, L.H. (1997). Mice lacking p35, a neuronal specific activator of Cdk5, display cortical lamination defects, seizures, and adult lethality. Neuron *18*, 29-42.

Chalepakis, G., Fritsch, R., Fickenscher, H., Deutsch, U., Goulding, M., and Gruss, P. (1991). The molecular basis of the undulated/Pax-1 mutation. Cell *66*, 873-884.

Chalepakis, G., Wijnholds, J., Giese, P., Schachner, M., and Gruss, P. (1994). Characterization of Pax-6 and Hoxa-1 binding to the promoter region of the neural cell adhesion molecule L1. DNA Cell Biol. *13*, 891-900.

Chen, R., Amoui, M., Zhang, Z., and Mardon, G. (1997). Dachshund and eyes absent proteins form a complex and function synergistically to induce ectopic eye development in Drosophila.Cell *91*, 893-903.

Chenn, A. and McConnell, S.K. (1995). Cleavage orientation and the asymmetric inheritance of Notch1 immunoreactivity in mammalian neurogenesis. Cell *82*, 631-641.

Chenn, A., Braisted, J.E., McConnell, S.K., and O'Leary, D.D.M. (1997). Development of the Cerebral Cortex: Mechanisms controlling cell fate, laminar and areal patterning and axonal connectivity. In Molecular and Cellular Approaches to Neural Development. W.M. Cowan, T.M. Jessell, and S.L. Zipursky, eds. (Oxford: Oxford University Press), pp. 440-473.

Chenn, A., Zhang, Y.A., Chang, B.T., and McConnell, S.K. (1998). Intrinsic polarity of mammalian neuroepithelial cells. Mol.Cell Neurosci. *11*, 183-193.

Cheyette, B.N., Green, P.J., Martin, K., Garren, H., Hartenstein, V., and Zipursky, S.L. (1994). The Drosophila sine oculis locus encodes a homeodomain-containing protein required for the development of the entire visual system. Neuron *12*, 977-996.

Chiang, C., Litingtung, Y., Lee, E., Young, K.E., Corden, J.L., Westphal, H., and Beachy, P.A. (1996). Cyclopia and defective axial patterning in mice lacking Sonic hedgehog gene function. Nature *383*, 407-413.

Chisholm, A.D. and Horvitz, H.R. (1995). Patterning of the Caenorhabditis elegans head region by the Pax-6 family member vab-3. Nature *377*, 52-55.

Cho, E.A. and Dressler, G.R. (1998). TCF-4 binds beta-catenin and is expressed in distinct regions of the embryonic brain and limbs. Mech.Dev. *77*, 9-18.

Chow, R.L., Altmann, C.R., Lang, R.A., and Hemmati-Brivanlou, A. (1999). Pax6 induces ectopic eyes in a vertebrate. Development *126*, 4213-4222.

Christiansen, J.H., Dennis, C.L., Wicking, C.A., Monkley, S.J., Wilkinson, D.G., and Wainwright, B.J. (1995). Murine Wnt-11 and Wnt-12 have temporally and spatially restricted expression patterns during embryonic development. Mech.Dev. *51*, 341-350.

Church, G.M. and Gilbert, W. (1984). Genomic sequencing. Proc.Natl.Acad.Sci.U.S.A. *81*, 1991-1995.

Cvekl, A. and Piatigorsky, J. (1996). Lens development and crystallin gene expression: many roles for Pax-6. Bioessays *18*, 621-630.

Czerny, T. and Busslinger, M. (1995). DNA-binding and transactivation properties of Pax-6: three amino acids in the paired domain are responsible for the different sequence recognition of Pax-6 and BSAP (Pax-5). Mol.Cell Biol. *15*, 2858-2871.

Czerny, T., Halder, G., Kloter, U., Souabni, A., Gehring, W.J., and Busslinger, M. (1999). twin of eyeless, a second Pax-6 gene of Drosophila, acts upstream of eyeless in the control of eye development. Mol.Cell *3*, 297-307.

D'Arcangelo, G., Miao, G.G., Chen, S.C., Soares, H.D., Morgan, J.I., and Curran, T. (1995). A protein related to extracellular matrix proteins deleted in the mouse mutant reeler . Nature *374*, 719-723.

Dale, J.K., Vesque, C., Lints, T.J., Sampath, T.K., Furley, A., Dodd, J., and Placzek, M. (1997). Cooperation of BMP7 and SHH in the induction of forebrain ventral midline cells by prechordal mesoderm. Cell *90*, 257-269.

Davis, A.A. and Temple, S. (1994). A self-renewing multipotential stem cell in embryonic rat cerebral cortex. Nature *372*, 263-266.

Dawid, I.B., Breen, J.J., and Toyama, R. (1998). LIM domains: multiple roles as adapters and functional modifiers in protein interactions. Trends Genet. *14*, 156-162.

De, C.J. and O'Leary, D.D. (1992). Growth and targeting of subplate axons and establishment of major cortical pathways [published erratum appears in J Neurosci 1993 Mar;13(3):following table of contents]. J.Neurosci. *12*, 1194-1211.

De, C.J., Lopez-Mascaraque, L., and Valverde, F. (1996). Dynamics of cell migration from the lateral ganglionic eminence in the rat. J.Neurosci. *16*, 6146-6156.

Dehay, C., Giroud, P., Berland, M., Smart, I., and Kennedy, H. (1993). Modulation of the cell cycle contributes to the parcellation of the primate visual cortex. Nature *366*, 464-466.

Dellovade, T.L., Pfaff, D.W., and Schwanzel-Fukuda, M. (1998). Olfactory bulb development is altered in small-eye (Sey) mice. J.Comp.Neurol. *402*, 402-418.

Demyanenko, G.P., Tsai, A.Y., and Maness, P.F. (1999). Abnormalities in neuronal process extension, hippocampal development, and the ventricular system of L1 knockout mice. J.Neurosci. *19*, 4907-4920.

Devereux, J., Haeberli, P., and Smithies, O. (1984). A comprehensive set of sequence analysis programs for the VAX. Nucleic.Acids.Res. *12*, 387-395.

Dodd, J., Morton, S.B., Karagogeos, D., Yamamoto, M., and Jessell, T.M. (1988). Spatial regulation of axonal glycoprotein expression on subsets of embryonic spinal neurons. Neuron *1*, 105-116.

Doe, C.Q., Chu-LaGraff, Q., Wright, D.M., and Scott, M.P. (1991). The prospero gene specifies cell fates in the Drosophila central nervous system. Cell *65*, 451-464.

Dressler, G.R., Deutsch, U., Chowdhury, K., Nornes, H.O., and Gruss, P. (1990). Pax2, a new murine paired-box-containing gene and its expression in the developing excretory system. Development *109*, 787-795.

Eagleson, K.L., Lillien, L., Chan, A.V., and Levitt, P. (1997). Mechanisms specifying area fate in cortex include cell-cycle-dependent decisions and the capacity of progenitors to express phenotype memory. Development *124*, 1623-1630.

Echelard, Y., Epstein, D.J., St-Jacques, B., Shen, L., Mohler, J., McMahon, J.A., and McMahon, A.P. (1993). Sonic hedgehog, a member of a family of putative signaling molecules, is implicated in the regulation of CNS polarity. Cell *75*, 1417-1430.

Edmondson, J.C. and Hatten, M.E. (1987). Glial-guided granule neuron migration *in vitro*: a high-resolution time- lapse video microscopic study. J.Neurosci. *7*, 1928-1934.

Edwards, M.A., Yamamoto, M., and Caviness, V.S.J. (1990). Organization of radial glia and related cells in the developing murine CNS. An analysis based upon a new monoclonal antibody marker. Neuroscience *36*, 121-144.

Ekker, S.C., Ungar, A.R., Greenstein, P., von, K.D., Porter, J.A., Moon, R.T., and Beachy, P.A. (1995). Patterning activities of vertebrate hedgehog proteins in the developing eye and brain. Curr.Biol. *5* , 944-955.

Emerling, D.E. and Lander, A.D. (1996). Inhibitors and promoters of thalamic neuron adhesion and outgrowth in embryonic neocortex: functional association with chondroitin sulfate. Neuron *17*, 1089-1100.

Engelkamp, D., Rashbass, P., Seawright, A., and van Heyningen.V. (1999). Role of Pax6 in development of the cerebellar system. Development *126*, 3585-3596.

Epstein, D.J., Vekemans, M., and Gros, P. (1991). Splotch (Sp2H), a mutation affecting development of the mouse neural tube, shows a deletion within the paired homeodomain of Pax-3. Cell *67*, 767-774.

Epstein, J.A., Glaser, T., Cai, J., Jepeal, L., Walton, D.S., and Maas, R.L. (1994). Two independent and interactive DNA-binding subdomains of the Pax6 paired domain are regulated by alternative splicing. Genes Dev. *8*, 2022-2034.

Ericson, J., Muhr, J., Placzek, M., Lints, T., Jessell, T.M., and Edlund, T. (1995). Sonic hedgehog induces the differentiation of ventral forebrain neurons: a common signal for ventral patterning within the neural tube [published erratum appears in Cell 1995 Jul 14;82(1):following 165]. Cell *81*, 747-756.

Ericson, J., Morton, S., Kawakami, A., Roelink, H., and Jessell, T.M. (1996). Two critical periods of Sonic Hedgehog signaling required for the specification of motor neuron identity. Cell *87*, 661-673.

Ericson, J., Rashbass, P., Schedl, A., Brenner-Morton, S., Kawakami, A., van, H.V., Jessell, T.M., and Briscoe, J. (1997). Pax6 controls progenitor cell identity and neuronal fate in response to graded Shh signaling. Cell *90*, 169-180.

Erzurumlu, R.S. and Jhaveri, S. (1992). Emergence of connectivity in the embryonic rat parietal cortex. Cereb.Cortex. *2*, 336-352.

Favor, J., Sandulache, R., Neuhauser-Klaus, A., Pretsch, W., Chatterjee, B., Senft, E., Wurst, W., Blanquet, V., Grimes, P., Sporle, R., and Schughart, K. (1996). The mouse Pax2(1Neu) mutation is identical to a human PAX2 mutation in a family with renal-coloboma syndrome and results in developmental defects of the brain, ear, eye, and kidney. Proc.Natl.Acad.Sci.U.S.A. *93*, 13870-13875.

Feinberg, A.P. and Vogelstein, B. (1984). "A technique for radiolabeling DNA restriction endonuclease fragments to high specific activity". Addendum. Anal.Biochem. *137*, 266-267.

Felsenfeld, D.P., Hynes, M.A., Skoler, K.M., Furley, A.J., and Jessell, T.M. (1994). TAG-1 can mediate homophilic binding, but neurite outgrowth on TAG-1 requires an L1-like molecule and beta 1 integrins. Neuron *12*, 675-690.

Feng, L., Hatten, M.E., and Heintz, N. (1994). Brain lipid-binding protein (BLBP): a novel signaling system in the developing mammalian CNS. Neuron *12*, 895-908.

Feng, L. and Heintz, N. (1995). Differentiating neurons activate transcription of the brain lipid- binding protein gene in radial glia through a novel regulatory element. Development *121*, 1719-1730.

Ferreira, A. and Caceres, A. (1992). Expression of the class III beta-tubulin isotype in developing neurons in culture. J.Neurosci.Res. *32*, 516-529.

Figdor, M.C. and Stern, C.D. (1993). Segmental organization of embryonic diencephalon. Nature *363*, 630-634.

Filosa, S., Rivera-Perez, J.A., Gomez, A.P., Gansmuller, A., Sasaki, H., Behringer, R.R., and Ang, S.L. (1997). Goosecoid and HNF-3beta genetically interact to regulate neural tube patterning during mouse embryogenesis. Development *124*, 2843-2854.

Fishell, G., Mason, C.A., and Hatten, M.E. (1993). Dispersion of neural progenitors within the germinal zones of the forebrain [published erratum appears in Nature 1993 May 20;363(6426):286] . Nature *362*, 636-638.

Fishell, G. (1997). Regionalization in the mammalian telencephalon. Curr.Opin.Neurobiol. *7*, 62-69.

Foroni, L., Boehm, T., White, L., Forster, A., Sherrington, P., Liao, X.B., Brannan, C.I., Jenkins, N.A., Copeland, N.G., and Rabbitts, T.H. (1992). The rhombotin gene family encode related LIM-domain proteins whose differing expression suggests multiple roles in mouse development. J.Mol.Biol. *226*, 747-761.

Fox, J.W., Lamperti, E.D., Eksioglu, Y.Z., Hong, S.E., Feng, Y., Graham, D.A., Scheffer, I.E., Dobyns, W.B., Hirsch, B.A., Radtke, R.A., Berkovic, S.F., Huttenlocher, P.R., and Walsh, C.A. (1998). Mutations in filamin 1 prevent migration of cerebral cortical neurons in human periventricular heterotopia. Neuron *21*, 1315-1325.

Francis, F., Koulakoff, A., Boucher, D., Chafey, P., Schaar, B., Vinet, M.C., Friocourt, G., McDonnell, N., Reiner, O., Kahn, A., McConnell, S.K., Berwald-Netter, Y., Denoulet, P., and Chelly, J. (1999). Doublecortin is a developmentally regulated, microtubule-associated protein expressed in migrating and differentiating neurons Neuron *23* , 247-256.

Frantz, G.D., Weimann, J.M., Levin, M.E., and McConnell, S.K. (1994). Otx1 and Otx2 define layers and regions in developing cerebral cortex and cerebellum. J.Neurosci. *14*, 5725-5740.

Frantz, G.D. and McConnell, S.K. (1996). Restriction of late cerebral cortical progenitors to an upper-layer fate. Neuron *17*, 55-61.

Franz, T. (1994). Extra-toes (Xt) homozygous mutant mice demonstrate a role for the Gli-3 gene in the development of the forebrain. Acta Anat.(Basel.) *150*, 38-44.

Freund, C., Horsford, D.J., and McInnes, R.R. (1996). Transcription factor genes and the developing eye: a genetic perspective. Hum.Mol.Genet. *5 Spec No:1471-88*, 1471-1488.

Frise, E., Knoblich, J.A., Younger-Shepherd, S., Jan, L.Y., and Jan, Y.N. (1996). The Drosophila Numb protein inhibits signaling of the Notch receptor during cell-cell interaction in sensory organ lineage. Proc.Natl.Acad.Sci.U.S.A. *93*, 11925-11932.

Frotscher, M. (1998). Cajal-Retzius cells, Reelin, and the formation of layers. Curr.Opin.Neurobiol. *8*, 570-575.

Fujiwara, M., Uchida, T., Osumi-Yamashita, N., and Eto, K. (1994). Uchida rat (rSey): a new mutant rat with craniofacial abnormalities resembling those of the mouse Sey mutant. Differentiation. *57*, 31-38.

Fukuda, T., Kawano, H., Ohyama, K., Li, H.P., Takeda, Y., Oohira, A., and Kawamura, K. (1997). Immunohistochemical localization of neurocan and L1 in the formation of thalamocortical pathway of developing rats. J.Comp.Neurol. *382*, 141-152.

Furley, A.J., Morton, S.B., Manalo, D., Karagogeos, D., Dodd, J., and Jessell, T.M. (1990). The axonal glycoprotein TAG-1 is an immunoglobulin superfamily member with neurite outgrowth-promoting activity. Cell *61*, 157-170.

Furuta, Y., Piston, D.W., and Hogan, B.L. (1997). Bone morphogenetic proteins (BMPs) as regulators of dorsal forebrain development. Development *124*, 2203-2212.

Gao, P.P., Yue, Y., Zhang, J.H., Cerretti, D.P., Levitt, P., and Zhou, R. (1998). Regulation of thalamic neurite outgrowth by the Eph ligand ephrin-A5: implications in the development of thalamocortical projections. Proc.Natl.Acad.Sci.U.S.A. *95*, 5329-5334.

Gehring, W.J. and Ikeo, K. (1999). Pax 6: mastering eye morphogenesis and eye evolution. Trends Genet. *15*, 371-377.

Georges-Labouesse, E., Mark, M., Messaddeq, N., and Gansmuller, A. (1998). Essential role of alpha 6 integrins in cortical and retinal lamination. Curr.Biol. *8*, 983-986.

Ghosh, A. and Shatz, C.J. (1992). Pathfinding and target selection by developing geniculocortical axons. J.Neurosci. *12*, 39-55.

Ghosh, A. and Greenberg, M.E. (1995). Distinct roles for bFGF and NT-3 in the regulation of cortical neurogenesis . Neuron *15*, 89-103.

Glardon, S., Callaerts, P., Halder, G., and Gehring, W.J. (1997). Conservation of Pax-6 in a lower chordate, the ascidian Phallusia mammillata. Development *124*, 817-825.

Glardon, S., Holland, L.Z., Gehring, W.J., and Holland, N.D. (1998). Isolation and developmental expression of the amphioxus Pax-6 gene (AmphiPax-6): insights into eye and photoreceptor evolution. Development *125*, 2701-2710.

Glaser, T., Walton, D.S., and Maas, R.L. (1992). Genomic structure, evolutionary conservation and aniridia mutations in the human PAX6 gene. Nat.Genet. *2*, 232-239.

Glaser, T., Jepeal, L., Edwards, J.G., Young, S.R., Favor, J., and Maas, R.L. (1994). PAX6 gene dosage effect in a family with congenital cataracts, aniridia, anophthalmia and central nervous system defects [published erratum appears in Nat Genet 1994 Oct;8(2):203]. Nat.Genet. *7*, 463-471.

Gleeson, J.G., Lin, P.T., Flanagan, L.A., and Walsh, C.A. (1999). Doublecortin is a microtubule-associated protein and is expressed widely by migrating neurons . Neuron *23*, 257-271.

Godfraind, C., Schachner, M., and Goffinet, A.M. (1988). Immunohistological localization of cell adhesion molecules L1, J1, N- CAM and their common carbohydrate L2 in the embryonic cortex of normal and reeler mice. Brain Res. *470*, 99-111.

Goffinet, A.M. (1997). Developmental neurobiology. Unscrambling a disabled brain [news; comment]. Nature *389*, 668-669.

Goodman, C.S. and Doe, C.Q. (1993). Embryonic development of the Drosophila central nervous system. In The Development of Drosophila melanogaster. M. Bate and A.

Martinez-Arias, eds. (Cold Spring Harbour, New York: Cold Spring Harbour Laboratory Press), pp. 1091-1131.

Gotz, M., Stoykova, A., and Gruss, P. (1998). Pax6 controls radial glia differentiation in the cerebral cortex. Neuron *21*, 1031-1044.

Goulding, M.D., Lumsden, A., and Gruss, P. (1993). Signals from the notochord and floor plate regulate the region-specific expression of two Pax genes in the developing spinal cord. Development *117*, 1001-1016.

Grindley, J.C., Davidson, D.R., and Hill, R.E. (1995). The role of Pax-6 in eye and nasal development. Development *121*, 1433-1442.

Grove, E.A., Williams, B.P., Li, D.Q., Hajihosseini, M., Friedrich, A., and Price, J. (1993). Multiple restricted lineages in the embryonic rat cerebral cortex. Development *117*, 553-561.

Grove, E.A., Tole, S., Limon, J., Yip, L., and Ragsdale, C.W. (1998). The hem of the embryonic cerebral cortex is defined by the expression of multiple Wnt genes and is compromised in Gli3-deficient mice. Development *125*, 2315-2325.

Grumet, M., Hoffman, S., Crossin, K.L., and Edelman, G.M. (1985). Cytotactin, an extracellular matrix protein of neural and non-neural tissues that mediates glia-neuron interaction. Proc.Natl.Acad.Sci.U.S.A. *82*, 8075-8079.

Hadjantonakis, A.K., Gertsenstein, M., Ikawa, M., Okabe, M., and Nagy, A. (1998). Generating green fluorescent mice by germline transmission of green fluorescent ES cells. Mech.Dev. *76*, 79-90.

Halder, G., Callaerts, P., and Gehring, W.J. (1995). Induction of ectopic eyes by targeted expression of the eyeless gene in Drosophila . Science *267*, 1788-1792.

Hammerschmidt, M., Bitgood, M.J., and McMahon, A.P. (1996). Protein kinase A is a common negative regulator of Hedgehog signaling in the vertebrate embryo. Genes Dev. *10*, 647-658.

Harrison, S.M., Dunwoodie, S.L., Arkell, R.M., Lehrach, H., and Beddington, R.S. (1995). Isolation of novel tissue-specific genes from cDNA libraries representing the individual tissue constituents of the gastrulating mouse embryo. Development *121*, 2479-2489.

Hatten, M.E. (1990). Riding the glial monorail: a common mechanism for glial-guided neuronal migration in different regions of the developing mammalian brain. Trends Neurosci. *13*, 179-184.

Hatten, M.E. and Mason, C.A. (1990). Mechanisms of glial-guided neuronal migration *in vitro* and *in vivo*. Experientia *46*, 907-916.

Helwig, U., Imai, K., Schmahl, W., Thomas, B.E., Varnum, D.S., Nadeau, J.H., and Balling, R. (1995). Interaction between undulated and Patch leads to an extreme form of spina bifida in double-mutant mice. Nat.Genet. *11*, 60-63.

Hendzel, M.J., Wei, Y., Mancini, M.A., Van, H.A., Ranalli, T., Brinkley, B.R., Bazett-Jones, D.P., and Allis, C.D. (1997). Mitosis-specific phosphorylation of histone H3 initiates primarily within pericentromeric heterochromatin during G2 and spreads in an ordered fashion coincident with mitotic chromosome condensation. Chromosoma *106*, 348-360.

Hendzel, M.J., Nishioka, W.K., Raymond, Y., Allis, C.D., Bazett-Jones, D.P., and Th (1998). Chromatin condensation is not associated with apoptosis. J.Biol.Chem. *273*, 24470-24478.

Hill, R.E., Jones, P.F., Rees, A.R., Sime, C.M., Justice, M.J., Copeland, N.G., Jenkins, N.A., Graham, E., and Davidson, D.R. (1989). A new family of mouse homeo box-containing genes: molecular structure, chromosomal location, and developmental expression of Hox-7.1. Genes Dev. *3*, 26-37.

Hill, R.E., Favor, J., Hogan, B.L., Ton, C.C., Saunders, G.F., Hanson, I.M., Prosser, J., Jordan, T., Hastie, N.D., and van, H.V. (1991). Mouse small eye results from mutations in a paired-like homeobox- containing gene [published erratum appears in Nature 1992 Feb 20;355(6362):750]. Nature *354*, 522-525.

Hinks, G.L., Shah, B., French, S.J., Campos, L.S., Staley, K., Hughes, J., and Sofroniew, M.V. (1997). Expression of LIM protein genes Lmo1, Lmo2, and Lmo3 in adult mouse hippocampus and other forebrain regions: differential regulation by seizure activity. J.Neurosci. *17*, 5549-5559.

Hirotsune, S., Takahara, T., Sasaki, N., Hirose, K., Yoshiki, A., Ohashi, T., Kusakabe, M., Murakami, Y., Muramatsu, M., and Watanabe, S. (1995). The reeler gene encodes a protein with an EGF-like motif expressed by pioneer neurons . Nat.Genet. *10*, 77-83.

Hogan, B.L., Hirst, E.M., Horsburgh, G., and Hetherington, C.M. (1988). Small eye (Sey): a mouse model for the genetic analysis of craniofacial abnormalities. Development *103 Suppl:115-9*, 115-119.

Hohl-Abrahao, J.C. and Creutzfeldt, O.D. (1991). Topographical mapping of the thalamocortical projections in rodents and comparison with that in primates. Exp.Brain Res. *87*, 283-294.

Hopker, V.H., Shewan, D., Tessier-Lavigne, M., Poo, M., and Holt, C. (1999). Growth-cone attraction to netrin-1 is converted to repulsion by laminin- 1. Nature *401*, 69-73.

Horvitz, H.R. and Herskowitz, I. (1992). Mechanisms of asymmetric cell division: two Bs or not two Bs, that is the question. Cell *68*, 237-255.

Howell, B.W., Hawkes, R., Soriano, P., and Cooper, J.A. (1997). Neuronal position in the developing brain is regulated by mouse disabled-1 . Nature *389*, 733-737.

Jang, C.-C. (1999). Two Pax genes, eye gone and eyeless, act in parallel in determining Drosophila eye development. Development *in press*,

Johe, K.K., Hazel, T.G., Muller, T., Dugich-Djordjevic, M.M., and McKay, R.D. (1996). Single factors direct the differentiation of stem cells from the fetal and adult central nervous system. Genes Dev. *10*, 3129-3140.

Jones, E.G. (1985). The thalamus (New York: Plenum).

Jordan, B.R. (1998). Large-scale expression measurement by hybridization methods: from high-density membranes to 'DNA chips'. J. Biochem. (Tokyo) *124*, 251-258.

Jordan, T., Hanson, I., Zaletayev, D., Hodgson, S., Prosser, J., Seawright, A., Hastie, N., and van, H.V. (1992). The human PAX6 gene is mutated in two patients with aniridia. Nat.Genet. *1*, 328-332.

Jurata, L.W., Kenny, D.A., and Gill, G.N. (1996). Nuclear LIM interactor, a rhombotin and LIM homeodomain interacting protein, is expressed early in neuronal development. Proc.Natl.Acad.Sci.U.S.A. *93*, 11693-11698.

Jurata, L.W. and Gill, G.N. (1997). Functional analysis of the nuclear LIM domain interactor NLI. Mol.Cell Biol. *17*, 5688-5698.

Kammandel, B., Chowdhury, K., Stoykova, A., Aparicio, S., Brenner, S., and Gruss, P. (1999). Distinct cis-essential modules direct the time-space pattern of the Pax6 gene activity. Dev.Biol. *205*, 79-97.

Kaufmann, M.H. and Bard, J.B.L. (1999) Anatomical Basis of Mouse Development (San Diego: Academic Press)

Kawakami, A., Kimura-Kawakami, M., Nomura, T., and Fujisawa, H. (1997). Distributions of PAX6 and PAX7 proteins suggest their involvement in both early and late phases of chick brain development. Mech.Dev. *66*, 119-130.

Kawano, H., Fukuda, T., Kubo, K., Horie, M., Uyemura, K., Takeuchi, K., Osumi, N., Eto, K., and Kawamura, K. (1999). Pax-6 is required for thalamocortical pathway formation in fetal rats. J.Comp.Neurol. *408*, 147-160.

Kenny, D.A., Jurata, L.W., Saga, Y., and Gill, G.N. (1998). Identification and characterization of LMO4, an LMO gene with a novel pattern of expression during embryogenesis. Proc.Natl.Acad.Sci.U.S.A. *95*, 11257-11262.

Kilpatrick, T.J. and Bartlett, P.F. (1995). Cloned multipotential precursors from the mouse cerebrum require FGF-2, whereas glial restricted precursors are stimulated with either FGF-2 or EGF. J.Neurosci. *15*, 3653-3661.

Kimura, S., Hara, Y., Pineau, T., Fernandez-Salguero, P., Fox, C.H., Ward, J.M., and Gonzalez, F.J. (1996). The T/ebp null mouse: thyroid-specific enhancer-binding protein is essential for the organogenesis of the thyroid, lung, ventral forebrain, and pituitary. Genes Dev. *10*, 60-69.

Kinnunen, A., Niemi, M., Kinnunen, T., Kaksonen, M., Nolo, R., and Rauvala, H. (1999). Heparan sulphate and HB-GAM (heparin-binding growth-associated molecule) in the development of the thalamocortical pathway of rat brain. Eur.J.Neurosci. *11*, 491-502.

Knoblich, J.A., Jan, L.Y., and Jan, Y.N. (1995). Asymmetric segregation of Numb and Prospero during cell division. Nature *377*, 624-627.

Kohtz, J.D., Baker, D.P., Corte, G., and Fishell, G. (1998). Regionalization within the mammalian telencephalon is mediated by changes in responsiveness to Sonic Hedgehog. Development *125*, 5079-5089.

Komuro, H. and Rakic, P. (1992). Selective role of N-type calcium channels in neuronal migration. Science *257*, 806-809.

Komuro, H. and Rakic, P. (1996). Intracellular Ca2+ fluctuations modulate the rate of neuronal migration. Neuron *17*, 275-285.

Kornack, D.R. and Rakic, P. (1995). Radial and horizontal deployment of clonally related cells in the primate neocortex: relationship to distinct mitotic lineages. Neuron *15*, 311-321.

Krauss, S., Johansen, T., Korzh, V., Moens, U., Ericson, J.U., and Fjose, A. (1991). Zebrafish pax[zf-a]: a paired box-containing gene expressed in the neural tube. EMBO J. *10*, 3609-3619.

Kraut, R., Chia, W., Jan, L.Y., Jan, Y.N., and Knoblich, J.A. (1996). Role of inscuteable in orienting asymmetric cell divisions in Drosophila. Nature *383*, 50-55.

Kraut, R. and Campos-Ortega, J.A. (1996). inscuteable, a neural precursor gene of Drosophila, encodes a candidate for a cytoskeleton adaptor protein. Dev.Biol. *174*, 65-81.

Kuchinke, U., Grawe, F., and Knust, E. (1998). Control of spindle orientation in Drosophila by the Par-3-related PDZ- domain protein Bazooka. Curr.Biol. *8*, 1357-1365.

Kuhn, R., Schwenk, F., Aguet, M., Rajewsky, K. (1995). Inducible gene targeting in mice. Science *269*,1427-9.

Lambert, d.R. and Goffinet, A.M. (1998). A new view of early cortical development. Biochem.Pharmacol. *56*, 1403-1409.

Levitt, P., Barbe, M.F., and Eagleson, K.L. (1997). Patterning and specification of the cerebral cortex. Annu.Rev.Neurosci. *20:1-24*, 1-24.

Li, H.S., Yang, J.M., Jacobson, R.D., Pasko, D., and Sundin, O. (1994). Pax-6 is first expressed in a region of ectoderm anterior to the early neural plate: implications for stepwise determination of the lens. Dev.Biol. *162*, 181-194.

Liem, K.F.J., Tremml, G., Roelink, H., and Jessell, T.M. (1995). Dorsal differentiation of neural plate cells induced by BMP-mediated signals from epidermal ectoderm. Cell *82*, 969-979.

Liem, K.F.J., Tremml, G., and Jessell, T.M. (1997). A role for the roof plate and its resident TGFbeta-related proteins in neuronal patterning in the dorsal spinal cord. Cell *91*, 127-138.

Liesi, P., Seppala, I., and Trenkner, E. (1992). Neuronal migration in cerebellar microcultures is inhibited by antibodies against a neurite outgrowth domain of laminin. J.Neurosci.Res. *33*, 170-176.

Lillien, L. (1998). Neural progenitors and stem cells: mechanisms of progenitor heterogeneity. Curr.Opin.Neurobiol. *8*, 37-44.

Loosli, F., Kmita-Cunisse, M., and Gehring, W.J. (1996). Isolation of a Pax-6 homolog from the ribbonworm Lineus sanguineus. Proc.Natl.Acad.Sci.U.S.A. *93*, 2658-2663.

Lotto, R.B. and Price, D.J. (1995). The stimulation of thalamic neurite outgrowth by cortex-derived growth factors *in vitro*: the influence of cortical age and activity. Eur.J.Neurosci. *7*, 318-328.

Lotto, R.B. and Price, D.J. (1996). Effects of subcortical structures on the growth of cortical neurites *in vitro*. Neuroreport. *7*, 1185-1188.

Lotto, R.B., Aitkenhead, A., and Price, D.J. (1999). Effects of the thalamus on the development of cerebral cortical efferents *in vitro*. J.Neurobiol. *39*, 186-196.

Luskin, M.B., Pearlman, A.L., and Sanes, J.R. (1988). Cell lineage in the cerebral cortex of the mouse studied *in vivo* and *in vitro* with a recombinant retrovirus. Neuron *1*, 635-647.

Macdonald, R., Xu, Q., Barth, K.A., Mikkola, I., Holder, N., Fjose, A., Krauss, S., and Wilson, S.W. (1994). Regulatory gene expression boundaries demarcate sites of neuronal differentiation in the embryonic zebrafish forebrain. Neuron *13*, 1039-1053.

Macdonald, R., Barth, K.A., Xu, Q., Holder, N., Mikkola, I., and Wilson, S.W. (1995). Midline signalling is required for Pax gene regulation and patterning of the eyes. Development *121*, 3267-3278.

Macdonald, R. and Wilson, S.W. (1996). Pax proteins and eye development. Curr.Opin.Neurobiol. *6*, 49-56.

Mansouri, A., Stoykova, A., Torres, M., and Gruss, P. (1996). Dysgenesis of cephalic neural crest derivatives in Pax7-/- mutant mice. Development *122*, 831-838.

Mansouri, A., Hallonet, M., and Gruss, P. (1996). Pax genes and their roles in cell differentiation and development. Curr.Opin.Cell Biol. *8*, 851-857.

Mardon, G., Solomon, N.M., and Rubin, G.M. (1994). dachshund encodes a nuclear protein required for normal eye and leg development in Drosophila. Development *120*, 3473-3486.

Marin-Padilla, M. (1998). Cajal-Retzius cells and the development of the neocortex. Trends Neurosci. *21*, 64-71.

Marmur, R., Mabie, P.C., Gokhan, S., Song, Q., Kessler, J.A., and Mehler, M.F. (1998). Isolation and developmental characterization of cerebral cortical multipotent progenitors. Dev.Biol. *204*, 577-591.

Mastick, G.S., Davis, N.M., Andrew, G.L., and Easter, S.S.J. (1997). Pax-6 functions in boundary formation and axon guidance in the embryonic mouse forebrain. Development *124*, 1985-1997.

Matsuo, I., Kuratani, S., Kimura, C., Takeda, N., and Aizawa, S. (1995). Mouse Otx2 functions in the formation and patterning of rostral head. Genes Dev. *9*, 2646-2658.

Matsuo, T., Osumi-Yamashita, N., Noji, S., Ohuchi, H., Koyama, E., Myokai, F., Matsuo, N., Taniguchi, S., Doi, H., and Iseki, S. (1993). A mutation in the Pax-6 gene in rat small eye is associated with impaired migration of midbrain crest cells. Nat.Genet. *3*, 299-304.

McConnell, S.K. (1988). Fates of visual cortical neurons in the ferret after isochronic and heterochronic transplantation. J.Neurosci. *8*, 945-974.

McConnell, S.K. and Kaznowski, C.E. (1991). Cell cycle dependence of laminar determination in developing neocortex. Science *254*, 282-285.

Meech, R., Kallunki, P., Edelman, G.M., and Jones, F.S. (1999). A binding site for homeodomain and Pax proteins is necessary for L1 cell adhesion molecule gene expression by Pax-6 and bone morphogenetic proteins. Proc.Natl.Acad.Sci.U.S.A. *96*, 2420-2425.

Metin, C. and Godement, P. (1996). The ganglionic eminence may be an intermediate target for corticofugal and thalamocortical axons. J.Neurosci. *16*, 3219-3235.

Metin, C., Deleglise, D., Serafini, T., Kennedy, T.E., and Tessier-Lavigne, M. (1997). A role for netrin-1 in the guidance of cortical efferents. Development *124*, 5063-5074.

Meyers, E.N., Lewandoski, M., and Martin, G.R. (1998). An Fgf8 mutant allelic series generated by Cre- and Flp-mediated recombination. Nat.Genet. *18*, 136-141.

Milan, M., Diaz-Benjumea, F.J., and Cohen, S.M. (1998). Beadex encodes an LMO protein that regulates Apterous LIM-homeodomain activity in Drosophila wing development: a model for LMO oncogene function. Genes Dev. *12*, 2912-2920.

Miller, B., Chou, L., and Finlay, B.L. (1993). The early development of thalamocortical and corticothalamic projections. J.Comp.Neurol. *335*, 16-41.

Miller, M.W. (1985). Cogeneration of retrogradely labeled corticocortical projection and GABA-immunoreactive local circuit neurons in cerebral cortex. Brain Res. *355*, 187-192.

Misson, J.P., Takahashi, T., and Caviness, V.S.J. (1991a). Ontogeny of radial and other astroglial cells in murine cerebral cortex. Glia *4*, 138-148.

Misson, J.P., Austin, C.P., Takahashi, T., Cepko, C.L., and Caviness, V.S.J. (1991b). The alignment of migrating neural cells in relation to the murine neopallial radial glial fiber system. Cereb.Cortex. *1*, 221-229.

Misson, J.P., Edwards, M.A., Yamamoto, M., and Caviness, V.S.J. (1988). Identification of radial glial cells within the developing murine central nervous system: studies based upon a new immunohistochemical marker. Brain Res.Dev.Brain Res. *44*, 95-108.

Miyashita-Lin, E.M., Hevner, R., Wassarman, K.M., Martinez, S., and Rubenstein, J.L. (1999). Early neocortical regionalization in the absence of thalamic innervation. Science *285*, 906-909.

Molnar, Z. and Blakemore, C. (1995). How do thalamic axons find their way to the cortex? Trends Neurosci. *18*, 389-397.

Molnar, Z., Adams, R., and Blakemore, C. (1998a). Mechanisms underlying the early establishment of thalamocortical connections in the rat. J.Neurosci. *18*, 5723-5745.

Molnar, Z., Adams, R., Goffinet, A.M., and Blakemore, C. (1998b). The role of the first postmitotic cortical cells in the development of thalamocortical innervation in the reeler mouse. J.Neurosci. *18*, 5746-5765.

Molnar, Z. and Blakemore, C. (1999). Development of signals influencing the growth and termination of thalamocortical axons in organotypic culture. Exp.Neurol. *156*, 363-393.

Moos, M., Tacke, R., Scherer, H., Teplow, D., Fruh, K., and Schachner, M. (1988). Neural adhesion molecule L1 as a member of the immunoglobulin superfamily with binding domains similar to fibronectin. Nature *334*, 701-703.

Morcillo, P., Rosen, C., Baylies, M.K., and Dorsett, D. (1997). Chip, a widely expressed chromosomal protein required for segmentation and activity of a remote wing margin enhancer in Drosophila. Genes Dev. *11*, 2729-2740.

Noctor, S.C., Palmer, S.L., Hasling, T., and Juliano, S.L. (1999). Interference with the development of early generated neocortex results in disruption of radial glia and abnormal formation of neocortical layers. Cereb.Cortex. *9*, 121-136.

Nornes, H.O., Dressler, G.R., Knapik, E.W., Deutsch, U., and Gruss, P. (1990). Spatially and temporally restricted expression of Pax2 during murine neurogenesis. Development *109*, 797-809.

Nornes, S., Clarkson, M., Mikkola, I., Pedersen, M., Bardsley, A., Martinez, J.P., Krauss, S., and Johansen, T. (1998). Zebrafish contains two pax6 genes involved in eye development. Mech.Dev. *77*, 185-196.

O'Leary, D.D. (1989). Do cortical areas emerge from a protocortex? Trends Neurosci. *12*, 400-406.

O'Leary, D.D., Schlaggar, B.L., and Stanfield, B.B. (1992). The specification of sensory cortex: lessons from cortical transplantation. Exp.Neurol. *115*, 121-126.

O'Leary, D.D., Borngasser, D.J., Fox, K., and Schlaggar, B.L. (1995). Plasticity in the development of neocortical areas. Ciba.Found.Symp. *193:214-30; discussion 251-7*, 214-230.

O'Leary, D.D. and Wilkinson, D.G. (1999). Eph receptors and ephrins in neural development. Curr.Opin.Neurobiol. *9*, 65-73.

O'Rourke, N.A., Chenn, A., and McConnell, S.K. (1997). Postmitotic neurons migrate tangentially in the cortical ventricular zone. Development *124*, 997-1005.

Ogawa, M., Miyata, T., Nakajima, K., Yagyu, K., Seike, M., Ikenaka, K., Yamamoto, H., and Mikoshiba, K. (1995). The reeler gene-associated antigen on Cajal-Retzius neurons is a crucial molecule for laminar organization of cortical neurons. Neuron *14*, 899-912.

Ohshima, T., Ward, J.M., Huh, C.G., Longenecker, G., Veeranna, Pant, H.C., Brady, R.O., Martin, L.J., and Kulkarni, A.B. (1996). Targeted disruption of the cyclin-dependent kinase 5 gene results in abnormal corticogenesis, neuronal pathology and perinatal death. Proc.Natl.Acad.Sci.U.S.A. *93*, 11173-11178.

Oliver, G., Sosa-Pineda, B., Geisendorf, S., Spana, E.P., Doe, C.Q., and Gruss, P. (1993). Prox 1, a prospero-related homeobox gene expressed during mouse development. Mech.Dev. *44*, 3-16.

Oliver, G., Mailhos, A., Wehr, R., Copeland, N.G., Jenkins, N.A., and Gruss, P. (1995). Six3, a murine homologue of the sine oculis gene, demarcates the most anterior border of the developing neural plate and is expressed during eye development. Development *121*, 4045-4055.

Oohira, A., Matsui, F., Watanabe, E., Kushima, Y., and Maeda, N. (1994). Developmentally regulated expression of a brain specific species of chondroitin sulfate proteoglycan, neurocan, identified with a monoclonal antibody IG2 in the rat cerebrum. Neuroscience *60*, 145-157.

Osumi, N., Hirota, A., Ohuchi, H., Nakafuku, M., Iimura, T., Kuratani, S., Fujiwara, M., Noji, S., and Eto, K. (1997). Pax-6 is involved in the specification of hindbrain motor neuron subtype. Development *124*, 2961-2972.

Pan, D. and Rubin, G.M. (1998). Targeted expression of teashirt induces ectopic eyes in Drosophila. Proc.Natl.Acad.Sci.U.S.A. *95*, 15508-15512.

Patil, N., Cox, D.R., Bhat, D., Faham, M., Myers, R.M., and Peterson, A.S. (1995). A potassium channel mutation in weaver mice implicates membrane excitability in granule cell differentiation . Nat.Genet. *11*, 126-129.

Pellegrini, M., Mansouri, A., Simeone, A., Boncinelli, E., and Gruss, P. (1996). Dentate gyrus formation requires Emx2. Development *122*, 3893-3898.

Peters, H., Neubuser, A., Kratochwil, K., and Balling, R. (1998). Pax9-deficient mice lack pharyngeal pouch derivatives and teeth and exhibit craniofacial and limb abnormalities. Genes Dev. *12*, 2735-2747.

Pignoni, F., Hu, B., Zavitz, K.H., Xiao, J., Garrity, P.A., and Zipursky, S.L. (1997). The eye-specification proteins So and Eya form a complex and regulate multiple steps in Drosophila eye development [published erratum appears in Cell 1998 Feb 20;92(4):following 585]. Cell *91*, 881-891.

Pituello, F., Yamada, G., and Gruss, P. (1995). Activin A inhibits Pax-6 expression and perturbs cell differentiation in the developing spinal cord *in vitro*. Proc.Natl.Acad.Sci.U.S.A. *92*, 6952-6956.

Pituello, F., Medevielle, F., Foulquier, F., and Duprat, A.M. (1999). Activation of Pax6 depends on somitogenesis in the chick embryo cervical spinal cord. Development *126*, 587-596.

Plachov, D., Chowdhury, K., Walther, C., Simon, D., Guenet, J.L., and Gruss, P. (1990). Pax8, a murine paired box gene expressed in the developing excretory system and thyroid gland. Development *110*, 643-651.

Platt, K.A., Michaud, J., and Joyner, A.L. (1997). Expression of the mouse Gli and Ptc genes is adjacent to embryonic sources of hedgehog signals suggesting a conservation of pathways between flies and mice. Mech.Dev. *62*, 121-135.

Plaza, S., Dozier, C., and Saule, S. (1993). Quail Pax-6 (Pax-QNR) encodes a transcription factor able to bind and trans-activate its own promoter. Cell Growth Differ. *4*, 1041-1050.

Plaza, S., Turque, N., Dozier, C., Bailly, M., and Saule, S. (1995). C-Myb acts as transcriptional activator of the quail PAX6 (PAX-QNR) promoter through two different mechanisms. Oncogene *10*, 329-340.

Plaza, S., Hennemann, H., Saule, S., and Dozier, C. (1999). Evidence that POU factor brn-3B regulates expression of Pax-6 in neuroretina cells. J.Neurobiol. *41*, 349-358.

Polleux, F., Dehay, C., Moraillon, B., and Kennedy, H. (1997). Regulation of neuroblast cell-cycle kinetics plays a crucial role in the generation of unique features of neocortical areas. J.Neurosci. *17*, 7763-7783.

Porter, F.D., Drago, J., Xu, Y., Cheema, S.S., Wassif, C., Huang, S.P., Lee, E., Grinberg, A., Massalas, J.S., Bodine, D., Alt, F., and Westphal, H. (1997). Lhx2, a LIM homeobox gene, is required for eye, forebrain, and definitive erythrocyte development. Development *124*, 2935-2944.

Price, D.J. and Lotto, R.B. (1996). Influences of the thalamus on the survival of subplate and cortical plate cells in cultured embryonic mouse brain. J.Neurosci. *16*, 3247-3255.

Price, J. and Thurlow, L. (1988). Cell lineage in the rat cerebral cortex: a study using retroviral- mediated gene transfer. Development *104*, 473-482.

Price, M., Lazzaro, D., Pohl, T., Mattei, M.G., Ruther, U., Olivo, J.C., Duboule, D., and Di, L.R. (1992). Regional expression of the homeobox gene Nkx-2.2 in the developing mammalian forebrain. Neuron *8* , 241-255.

Puelles, L. and Rubenstein, J.L. (1993). Expression patterns of homeobox and other putative regulatory genes in the embryonic mouse forebrain suggest a neuromeric organization. Trends Neurosci. *16*, 472-479.

Puschel, A.W., Adams, R.H., and Betz, H. (1996). The sensory innervation of the mouse spinal cord may be patterned by differential expression of and differential responsiveness to semaphorins. Mol.Cell Neurosci. *7*, 419-431.

Qian, X., Davis, A.A., Goderie, S.K., and Temple, S. (1997). FGF2 concentration regulates the generation of neurons and glia from multipotent cortical stem cells. Neuron *18*, 81-93.

Qian, X., Goderie, S.K., Shen, Q., Stern, J.H., and Temple, S. (1998). Intrinsic programs of patterned cell lineages in isolated vertebrate CNS ventricular zone cells. Development *125*, 3143-3152.

Qiu, M., Bulfone, A., Martinez, S., Meneses, J.J., Shimamura, K., Pedersen, R.A., and Rubenstein, J.L. (1995). Null mutation of Dlx-2 results in abnormal morphogenesis of proximal first and second branchial arch derivatives and abnormal differentiation in the forebrain. Genes Dev. *9* , 2523-2538.

Qiu, M., Anderson, S., Chen, S., Meneses, J.J., Hevner, R., Kuwana, E., Pedersen, R.A., and Rubenstein, J.L. (1996). Mutation of the Emx-1 homeobox gene disrupts the corpus callosum. Dev.Biol. *178*, 174-178.

Qiu, M., Bulfone, A., Ghattas, I., Meneses, J.J., Christensen, L., Sharpe, P.T., Presley, R., Pedersen, R.A., and Rubenstein, J.L. (1997). Role of the Dlx homeobox genes in proximodistal patterning of the branchial arches: mutations of Dlx-1, Dlx-2, and Dlx-1 and -2 alter morphogenesis of proximal skeletal and soft tissue structures derived from the first and second arches. Dev.Biol. *185*, 165-184.

Quinn, J.C., West, J.D., and Hill, R.E. (1996). Multiple functions for Pax6 in mouse eye and nasal development. Genes Dev. *10*, 435-446.

Quiring, R., Walldorf, U., Kloter, U., and Gehring, W.J. (1994). Homology of the eyeless gene of Drosophila to the Small eye gene in mice and Aniridia in humans . Science *265*, 785-789.

Rakic, P. (1972). Mode of cell migration to the superficial layers of fetal monkey neocortex. J.Comp.Neurol. *145*, 61-83.

Rakic, P. (1974). Neurons in rhesus monkey visual cortex: systematic relation between time of origin and eventual disposition. Science *183*, 425-427.

Rakic, P., Cameron, R.S., and Komuro, H. (1994). Recognition, adhesion, transmembrane signaling and cell motility in guided neuronal migration. Curr.Opin.Neurobiol. *4*, 63-69.

Rakic, P. and Caviness, V.S.J. (1995). Cortical development: view from neurological mutants two decades later. Neuron *14*, 1101-1104.

Reid, C.B., Liang, I., and Walsh, C. (1995). Systematic widespread clonal organization in cerebral cortex. Neuron *15*, 299-310.

Reid, C.B., Tavazoie, S.F., and Walsh, C.A. (1997). Clonal dispersion and evidence for asymmetric cell division in ferret cortex. Development *124*, 2441-2450.

Rennie, S., Lotto, R.B., and Price, D.J. (1994). Growth-promoting interactions between the murine neocortex and thalamus in organotypic co-cultures. Neuroscience *61*, 547-564.

Retaux, S., Rogard, M., Bach, I., Failli, V., and Besson, M.J. (1999). Lhx9: a novel LIM-homeodomain gene expressed in the developing forebrain. J.Neurosci. *19*, 783-793.

Rhinn, M., Dierich, A., Shawlot, W., Behringer, R.R., Le, M.M., and Ang, S.L. (1998). Sequential roles for Otx2 in visceral endoderm and neuroectoderm for forebrain and midbrain induction and specification. Development *125*, 845-856.

Rhyu, M.S. and Knoblich, J.A. (1995). Spindle orientation and asymmetric cell fate. Cell *82*, 523-526.

Richards, L.J., Koester, S.E., Tuttle, R., and O'Leary, D.D. (1997). Directed growth of early cortical axons is influenced by a chemoattractant released from an intermediate target. J.Neurosci. *17*, 2445-2458.

Rio, C., Rieff, H.I., Qi, P., Khurana, T.S., and Corfas, G. (1997). Neuregulin and erbB receptors play a critical role in neuronal migration [published erratum appears in Neuron 1997 Dec;19(6):1349]. Neuron *19*, 39-50.

Rivera-Perez, J.A., Mallo, M., Gendron-Maguire, M., Gridley, T., and Behringer, R.R. (1995). Goosecoid is not an essential component of the mouse gastrula organizer but is required for craniofacial and rib development. Development *121*, 3005-3012.

Roach, S.A. (1968). Theory of random clumping. (London: Methuen)

Roberts, R.C. (1967). Small-eyes, a new dominant mutation in the mouse. Genetic Re.Camb. *9*, 121-122.

Roelink, H., Augsburger, A., Heemskerk, J., Korzh, V., Norlin, S., Ruiz, Tanabe, Y., Placzek, M., Edlund, T., and Jessell, T.M. (1994). Floor plate and motor neuron induction by vhh-1, a vertebrate homolog of hedgehog expressed by the notochord. Cell *76*, 761-775.

Roelink, H., Porter, J.A., Chiang, C., Tanabe, Y., Chang, D.T., Beachy, P.A., and Jessell, T.M. (1995). Floor plate and motor neuron induction by different concentrations of the amino-terminal cleavage product of sonic hedgehog autoproteolysis. Cell *81*, 445-455.

Rubenstein, J.L., Martinez, S., Shimamura, K., and Puelles, L. (1994). The embryonic vertebrate forebrain: the prosomeric model. Science *266*, 578-580.

Rubenstein, J.L. and Shimamura, K. (1997). Regulation of patterning and differentiation in the embryonic vertebrate forebrain. In Molecular and Cellular Approaches to Neural Development. W.M. Cowan, T.M. Jessell, and S.L. Zipursky, eds. (Oxford: Oxford University Press), pp. 356-390.

Rubenstein, J.L. and Beachy, P.A. (1998). Patterning of the embryonic forebrain. Curr.Opin.Neurobiol. *8*, 18-26.

Rubenstein, J.L., Anderson, S., Shi, L., Miyashita-Lin, E., Bulfone, A., and Hevner, R. (1999). Genetic control of cortical regionalization and connectivity . Cereb.Cortex. *9*, 524-532.

Sadler, T.W.ed. (1985). Langman's Medical Embryology (Baltimore: Williams & Wilkins).

Sambrook, J., Fritsch, E.F., and Maniatis, T. (1989). Molecular Cloning: A Laboratory Manual (Cold Spring Harbor Laboratory Press).

Sanger, F., Nicklen, S., and Coulson, A.R. (1977). DNA sequencing with chain-terminating inhibitors. Proc.Natl.Acad.Sci.U.S.A. *74*, 5463-5467.

Sauer, F.C. (1935). Mitosis in the neural tube. J.Comp.Neurol. *62*, 377-405.

Schedl, A., Ross, A., Lee, M., Engelkamp, D., Rashbass, P., van, H.V., and Hastie, N.D. (1996). Influence of PAX6 gene dosage on development: overexpression causes severe eye abnormalities. Cell *86*, 71-82.

Schlaggar, B.L. and O'Leary, D.D. (1991). Potential of visual cortex to develop an array of functional units unique to somatosensory cortex. Science *252*, 1556-1560.

Schmahl, W., Knoedlseder, M., Favor, J., and Davidson, D. (1993). Defects of neuronal migration and the pathogenesis of cortical malformations are associated with Small eye (Sey) in the mouse, a point mutation at the Pax-6-locus. Acta Neuropathol.(Berl.) *86*, 126-135.

Schubart, U.K. (1988). Expression of phosphoprotein p19 in brain, testis, and neuroendocrine tumor cells. Developmental regulation in rat brain. J.Biol.Chem. *263*, 12156-12160.

Serafini, T., Colamarino, S.A., Leonardo, E.D., Wang, H., Beddington, R., Skarnes, W.C., and Tessier-Lavigne, M. (1996). Netrin-1 is required for commissural axon guidance in the developing vertebrate nervous system. Cell *87*, 1001-1014.

Serikaku, M.A. and O'Tousa, J.E. (1994). sine oculis is a homeobox gene required for Drosophila visual system development. Genetics *138*, 1137-1150.

Sharma, K., Sheng, H.Z., Lettieri, K., Li, H., Karavanov, A., Potter, S., Westphal, H., and Pfaff, S.L. (1998). LIM homeodomain factors Lhx3 and Lhx4 assign subtype identities for motor neurons. Cell *95*, 817-828.

Sheldon, M., Rice, D.S., D'Arcangelo, G., Yoneshima, H., Nakajima, K., Mikoshiba, K., Howell, B.W., Cooper, J.A., Goldowitz, D., and Curran, T. (1997). Scrambler and yotari disrupt the disabled gene and produce a reeler- like phenotype in mice . Nature *389*, 730-733.

Shen, Q., Qian, X., Capela, A., and Temple, S. (1998). Stem cells in the embryonic cerebral cortex: their role in histogenesis and patterning. J.Neurobiol. *36*, 162-174.

Shen, W. and Mardon, G. (1997). Ectopic eye development in Drosophila induced by directed dachshund expression. Development *124*, 45-52.

Shimamura, K., Hartigan, D.J., Martinez, S., Puelles, L., and Rubenstein, J.L. (1995). Longitudinal organization of the anterior neural plate and neural tube. Development *121*, 3923-3933.

Shimamura, K., Martinez, S., Puelles, L., and Rubenstein, J.L. (1997). Patterns of gene expression in the neural plate and neural tube subdivide the embryonic forebrain into transverse and longitudinal domains. Dev.Neurosci. *19*, 88-96.

Shimamura, K. and Rubenstein, J.L. (1997). Inductive interactions direct early regionalization of the mouse forebrain. Development *124*, 2709-2718.

Simeone, A., Acampora, D., Gulisano, M., Stornaiuolo, A., and Boncinelli, E. (1992a). Nested expression domains of four homeobox genes in developing rostral brain . Nature *358*, 687-690.

Simeone, A., Gulisano, M., Acampora, D., Stornaiuolo, A., Rambaldi, M., and Boncinelli, E. (1992b). Two vertebrate homeobox genes related to the Drosophila empty spiracles gene are expressed in the embryonic cerebral cortex. EMBO J. *11*, 2541-2550.

Simeone, A. (1998). Otx1 and Otx2 in the development and evolution of the mammalian brain. EMBO J. *17*, 6790-6798.

Skeath, J.B. and Doe, C.Q. (1998). Sanpodo and Notch act in opposition to Numb to distinguish sibling neuron fates in the Drosophila CNS. Development *125*, 1857-1865.

Soriano, E., Alvarado-Mallart, R.M., Dumesnil, N., Del, R.J., and Sotelo, C. (1997). Cajal-Retzius cells regulate the radial glia phenotype in the adult and developing cerebellum and alter granule cell migration. Neuron *18*, 563-577.

Sosa-Pineda, B., Chowdhury, K., Torres, M., Oliver, G., and Gruss, P. (1997). The Pax4 gene is essential for differentiation of insulin-producing beta cells in the mammalian pancreas. Nature *386*, 399-402.

Southern, E.M. (1975). Detection of specific sequences among DNA fragments separated by gel electrophoresis. J.Mol.Biol. *98* , 503-517.

Spana, E.P. and Doe, C.Q. (1995). The prospero transcription factor is asymmetrically localized to the cell cortex during neuroblast mitosis in Drosophila. Development *121*, 3187-3195.

St-Onge, L., Sosa-Pineda, B., Chowdhury, K., Mansouri, A., and Gruss, P. (1997). Pax6 is required for differentiation of glucagon-producing alpha-cells in mouse pancreas. Nature *387*, 406-409.

Stoeckli, E.T., Kuhn, T.B., Duc, C.O., Ruegg, M.A., and Sonderegger, P. (1991). The axonally secreted protein axonin-1 is a potent substratum for neurite growth. J.Cell Biol. *112*, 449-455.

Stoykova, A. and Gruss, P. (1994). Roles of Pax-genes in developing and adult brain as suggested by expression patterns. J.Neurosci. *14*, 1395-1412.

Stoykova, A., Fritsch, R., Walther, C., and Gruss, P. (1996). Forebrain patterning defects in Small eye mutant mice. Development *122*, 3453-3465.

Stoykova, A., Gotz, M., Gruss, P., and Price, J. (1997). Pax6-dependent regulation of adhesive patterning, R-cadherin expression and boundary formation in developing forebrain. Development *124*, 3765-3777.

Suda, Y., Matsuo, I., and Aizawa, S. (1997). Cooperation between Otx1 and Otx2 genes in developmental patterning of rostral brain. Mech.Dev. *69*, 125-141.

Sugihara, T.M., Bach, I., Kioussi, C., Rosenfeld, M.G., and Andersen, B. (1998). Mouse deformed epidermal autoregulatory factor 1 recruits a LIM domain factor, LMO-4, and CLIM coregulators. Proc.Natl.Acad.Sci.U.S.A. *95*, 15418-15423.

Sun, T., Pringle, N.P., Hardy, A.P., Richardson, W.D., and Smith, H.K. (1998). Pax6 Influences the Time and Site of Origin of Glial Precursors in the Ventral Neural Tube. Mol.Cell Neurosci. *12*, 228-239.

Sussel, L., Marin, O., Kimura, S., and Rubenstein, J.L. (1999). Loss of Nkx2.1 homeobox gene function results in a ventral to dorsal molecular respecification within the basal telencephalon: evidence for a transformation of the pallidum into the striatum. Development *126*, 3359-3370.

Sweadner, K.J. (1983). Post-translational modification and evoked release of two large surface proteins of sympathetic neurons. J.Neurosci. *3*, 2504-2517.

Takahashi, T., Nowakowski, R.S., and Caviness, V.S.J. (1995a). The cell cycle of the pseudostratified ventricular epithelium of the embryonic murine cerebral wall. J.Neurosci. *15*, 6046-6057.

Takahashi, T., Nowakowski, R.S., and Caviness, V.S.J. (1995b). Early ontogeny of the secondary proliferative population of the embryonic murine cerebral wall. J.Neurosci. *15*, 6058-6068

Takahashi, T., Nowakowski, R.S., and Caviness, V.S.J. (1996). Interkinetic and migratory behavior of a cohort of neocortical neurons arising in the early embryonic murine cerebral wall. J.Neurosci. *16*, 5762-5776.

Tan, S.S. and Breen, S. (1993). Radial mosaicism and tangential cell dispersion both contribute to mouse neocortical development . Nature *362*, 638-640.

Tan, S.S., Faulkner-Jones, B., Breen, S.J., Walsh, M., Bertram, J.F., and Reese, B.E. (1995). Cell dispersion patterns in different cortical regions studied with an X-inactivated transgenic marker. Development *121*, 1029-1039.

Tanabe, Y. and Jessell, T.M. (1996). Diversity and pattern in the developing spinal cord [published erratum appears in Science 1997 Apr 4;276(5309):21]. Science *274*, 1115-1123.

Tassabehji, M., Read, A.P., Newton, V.E., Patton, M., Gruss, P., Harris, R., and Strachan, T. (1993). Mutations in the PAX3 gene causing Waardenburg syndrome type 1 and type 2. Nat.Genet. *3*, 26-30.

Temple, S. and Qian, X. (1995). bFGF, neurotrophins, and the control or cortical neurogenesis [comment]. Neuron *15*, 249-252.

Temple, S. and Qian, X. (1996). Vertebrate neural progenitor cells: subtypes and regulation. Curr.Opin.Neurobiol. *6*, 11-17.

Tessier-Lavigne, M. and Goodman, C.S. (1996). The molecular biology of axon guidance. Science *274*, 1123-1133.

Theil, T., Alvarez-Bolado, G., Walter, A., and Ruther, U. (1999). Gli3 is required for Emx gene expression during dorsal telencephalon development. Development *126*, 3561-3571.

Thomaidou, D., Mione, M.C., Cavanagh, J.F., and Parnavelas, J.G. (1997). Apoptosis and its relation to the cell cycle in the developing cerebral cortex. J.Neurosci. *17*, 1075-1085.

Tokunaga, K., Taniguchi, H., Yoda, K., Shimizu, M., and Sakiyama, S. (1986). Nucleotide sequence of a full-length cDNA for mouse cytoskeletal beta- actin mRNA. Nucleic.Acids.Res. *14*, 2829

Tomarev, S.I., Callaerts, P., Kos, L., Zinovieva, R., Halder, G., Gehring, W., and Piatigorsky, J. (1997). Squid Pax-6 and eye development . Proc.Natl.Acad.Sci.U.S.A. *94*, 2421-2426.

Ton, C.C., Miwa, H., and Saunders, G.F. (1992). Small eye (Sey): cloning and characterization of the murine homolog of the human aniridia gene. Genomics *13*, 251-256.

Torii, M., Matsuzaki, F., Osumi, N., Kaibuchi, K., Nakamura, S., Casarosa, S., Guillemot, F., and Nakafuku, M. (1999). Transcription factors Mash-1 and Prox-1 delineate early steps in differentiation of neural stem cells in the developing central nervous system. Development *126*, 443-456.

Torres, M., Gomez-Pardo, E., Dressler, G.R., and Gruss, P. (1995). Pax-2 controls multiple steps of urogenital development. Development *121*, 4057-4065.

Torres, M., Gomez-Pardo, E., and Gruss, P. (1996). Pax2 contributes to inner ear patterning and optic nerve trajectory. Development *122*, 3381-3391.

Toyama, R., Kobayashi, M., Tomita, T., and Dawid, I.B. (1998). Expression of LIM-domain binding protein (ldb) genes during zebrafish embryogenesis. Mech.Dev. *71*, 197-200.

Trommsdorff, M., Gotthardt, M., Hiesberger, T., Shelton, J., Stockinger, W., Nimpf, J., Hammer, R.E., Richardson, J.A., and Herz, J. (1999). Reeler/Disabled-like disruption of neuronal migration in knockout mice lacking the VLDL receptor and ApoE receptor 2. Cell *97*, 689-701.

Tropepe, V., Sibilia, M., Ciruna, B.G., Rossant, J., Wagner, E.F., and van, d.K. (1999). Distinct neural stem cells proliferate in response to EGF and FGF in the developing mouse telencephalon. Dev.Biol. *208*, 166-188.

Tsuchida, T., Ensini, M., Morton, S.B., Baldassare, M., Edlund, T., Jessell, T.M., and Pfaff, S.L. (1994). Topographic organization of embryonic motor neurons defined by expression of LIM homeobox genes . Cell *79*, 957-970.

Turque, N., Plaza, S., Radvanyi, F., Carriere, C., and Saule, S. (1994). Pax-QNR/Pax-6, a paired box- and homeobox-containing gene expressed in neurons, is also expressed in pancreatic endocrine cells. Mol.Endocrinol. *8*, 929-938.

Tuttle, R., Nakagawa, Y., Johnson, J.E., and O'Leary, D.D. (1999). Defects in thalamocortical axon pathfinding correlate with altered cell domains in Mash-1-deficient mice. Development *126*, 1903-1916.

Urbanek, P., Wang, Z.Q., Fetka, I., Wagner, E.F., and Busslinger, M. (1994). Complete block of early B cell differentiation and altered patterning of the posterior midbrain in mice lacking Pax5/BSAP . Cell *79*, 901-912.

Vaessin, H., Grell, E., Wolff, E., Bier, E., Jan, L.Y., and Jan, Y.N. (1991). prospero is expressed in neuronal precursors and encodes a nuclear protein that is involved in the control of axonal outgrowth in Drosophila. Cell *67*, 941-953.

Verdi, J.M., Schmandt, R., Bashirullah, A., Jacob, S., Salvino, R., Craig, C.G., Program, A.E., Lipshitz, H.D., and McGlade, C.J. (1996). Mammalian NUMB is an evolutionarily conserved signaling adapter protein that specifies cell fate. Curr.Biol. *6*, 1134-1145.

Verdi, J.M., Bashirullah, A., Goldhawk, D.E., Kubu, C.J., Jamali, M., Meakin, S.O., and Lipshitz, H.D. (1999). Distinct human NUMB isoforms regulate differentiation vs. proliferation in the neuronal lineage. Proc.Natl.Acad.Sci.U.S.A. *96*, 10472-10476.

Visvader, J.E., Mao, X., Fujiwara, Y., Hahm, K., and Orkin, S.H. (1997). The LIM-domain binding protein Ldb1 and its partner LMO2 act as negative regulators of erythroid differentiation. Proc.Natl.Acad.Sci.U.S.A. *94*, 13707-13712.

Wadman, I.A., Osada, H., Grutz, G.G., Agulnick, A.D., Westphal, H., Forster, A., and Rabbitts, T.H. (1997). The LIM-only protein Lmo2 is a bridging molecule assembling an erythroid, DNA-binding complex which includes the TAL1, E47, GATA-1 and Ldb1/NLI proteins. EMBO J. *16*, 3145-3157.

Wakamatsu, Y., Maynard, T.M., Jones, S.U., and Weston, J.A. (1999). NUMB localizes in the basal cortex of mitotic avian neuroepithelial cells and modulates neuronal differentiation by binding to NOTCH-1 . Neuron *23*, 71-81.

Wallin, J., Wilting, J., Koseki, H., Fritsch, R., Christ, B., and Balling, R. (1994). The role of Pax-1 in axial skeleton development. Development *120*, 1109-1121.

Walsh, C. and Cepko, C.L. (1988). Clonally related cortical cells show several migration patterns. Science *241*, 1342-1345.

Walsh, C. and Cepko, C.L. (1992). Widespread dispersion of neuronal clones across functional regions of the cerebral cortex . Science *255*, 434-440.

Walsh, C. and Cepko, C.L. (1993). Clonal dispersion in proliferative layers of developing cerebral cortex . Nature *362*, 632-635.

Walther, C., Guenet, J.L., Simon, D., Deutsch, U., Jostes, B., Goulding, M.D., Plachov, D., Balling, R., and Gruss, P. (1991). Pax: a murine multigene family of paired box-containing genes. Genomics *11*, 424-434.

Walther, C. and Gruss, P. (1991). Pax-6, a murine paired box gene, is expressed in the developing CNS. Development *113*, 1435-1449.

Warren, N. and Price, D.J. (1997). Roles of Pax-6 in murine diencephalic development. Development *124*, 1573-1582.

Warren, N., Caric, D., Pratt, T., Clausen, J.A., Asavaritikrai, P., Mason, J.O., Hill, R.E., and Price, D.J. (1999). The transcription factor, Pax6, is required for cell proliferation and differentiation in the developing cerebral cortex . Cereb.Cortex. *9*, 627-635.

Weinstein, D.C., Ruiz, Chen, W.S., Hoodless, P., Prezioso, V.R., Jessell, T.M., and Darnell, J.E.J. (1994). The winged-helix transcription factor HNF-3 beta is required for notochord development in the mouse embryo. Cell *78*, 575-588.

Williams, B.P. and Price, J. (1995). Evidence for multiple precursor cell types in the embryonic rat cerebral cortex. Neuron *14*, 1181-1188.

Williams, B.P., Park, J.K., Alberta, J.A., Muhlebach, S.G., Hwang, G.Y., Roberts, T.M., and Stiles, C.D. (1997). A PDGF-regulated immediate early gene response initiates neuronal differentiation in ventricular zone progenitor cells. Neuron *18*, 553-562.

Williams, B.P.ed. (1995). Gray's Anatomy (New York: Churchill Livingstone).

Williams, S.C., Altmann, C.R., Chow, R.L., Hemmati-Brivanlou, A., and Lang, R.A. (1998). A highly conserved lens transcriptional control element from the Pax-6 gene. Mech.Dev. *73*, 225-229.

Wolfer, D.P., Henehan-Beatty, A., Stoeckli, E.T., Sonderegger, P., and Lipp, H.P. (1994). Distribution of TAG-1/axonin-1 in fibre tracts and migratory streams of the developing mouse nervous system. J.Comp.Neurol. *345*, 1-32.

Wolpert, L., Beddington, R., Brockes, J., Jessell, T., Lawrence, P. and Meyerowitz, E. (1998) Principles of Development (Current Biology: London).

Xu, P.X., Woo, I., Her, H., Beier, D.R., and Maas, R.L. (1997). Mouse Eya homologues of the Drosophila eyes absent gene require Pax6 for expression in lens and nasal placode. Development *124*, 219-231.

Xu, P.X., Zhang, X., Heaney, S., Yoon, A., Michelson, A.M., and Maas, R.L. (1999). Regulation of Pax6 expression is conserved between mice and flies. Development *126*, 383-395.

Xu, W., Rould, M.A., Jun, S., Desplan, C., and Pabo, C.O. (1995). Crystal structure of a paired domain-DNA complex at 2.5 A resolution reveals structural basis for Pax developmental mutations. Cell *80*, 639-650.

Xu, Y., Baldassare, M., Fisher, P., Rathbun, G., Oltz, E.M., Yancopoulos, G.D., Jessell, T.M., and Alt, F.W. (1993). LH-2: a LIM/homeodomain gene expressed in developing lymphocytes and neural cells. Proc.Natl.Acad.Sci.U.S.A. *90*, 227-231.

Xu, Z.P. and Saunders, G.F. (1997). Transcriptional regulation of the human PAX6 gene promoter. J.Biol.Chem. *272*, 3430-3436.

Xuan, S., Baptista, C.A., Balas, G., Tao, W., Soares, V.C., and Lai, E. (1995). Winged helix transcription factor BF-1 is essential for the development of the cerebral hemispheres. Neuron *14*, 1141-1152.

Yamada, G., Mansouri, A., Torres, M., Stuart, E.T., Blum, M., Schultz, M., De, R.E., and Gruss, P. (1995). Targeted mutation of the murine goosecoid gene results in craniofacial defects and neonatal death. Development *121*, 2917-2922.

Yamamoto, M., Boyer, A.M., Crandall, J.E., Edwards, M., and Tanaka, H. (1986). Distribution of stage-specific neurite-associated proteins in the developing murine nervous system recognized by a monoclonal antibody. J.Neurosci. *6*, 3576-3594.

Ye, W., Shimamura, K., Rubenstein, J.L., Hynes, M.A., and Rosenthal, A. (1998). FGF and Shh signals control dopaminergic and serotonergic cell fate in the anterior neural plate. Cell *93*, 755-766.

Yoshida, M., Suda, Y., Matsuo, I., Miyamoto, N., Takeda, N., Kuratani, S., and Aizawa, S. (1997). Emx1 and Emx2 functions in development of dorsal telencephalon. Development *124*, 101-111.

Zhang, Y. and Emmons, S.W. (1995). Specification of sense-organ identity by a Caenorhabditis elegans Pax-6 homologue. Nature *377*, 55-59.

Zhang, Z. and Galileo, D.S. (1998). Retroviral transfer of antisense integrin alpha6 or alpha8 sequences results in laminar redistribution or clonal cell death in developing brain. J.Neurosci. *18*, 6928-6938.

Zheng, C., Heintz, N., and Hatten, M.E. (1996). CNS gene encoding astrotactin, which supports neuronal migration along glial fibers. Science *272*, 417-419.

Zhong, W.M., Feder, J.N., Jiang, M.M., Jan, L.Y., and Jan, Y.N. (1996). Asymmetric localization of a mammalian numb homolog during mouse cortical neurogenesis. Neuron *17*, 43-53.

Zhong, W.M., Jiang, M.M., Weinmaster, G., Jan, L.Y., and Jan, Y.N. (1997). Differential expression of mammalian Numb, Numblike and Notch1 suggests distinct roles during mouse cortical neurogenesis. Development *124*, 1887-1897.

Zhu, Y., Li, H., Zhou, L., Wu, J.Y., and Rao, Y. (1999). Cellular and molecular guidance of GABAergic neuronal migration from an extracortical origin to the neocortex. Neuron *23*, 473-485.

Appendix

Analysis of cell clumping data

Author: A.D.Carothers

Introduction

What is commonly referred to as "clumping" of cells is a phenomenon that depends both on the *spatial density* of the cells and on the *scale* of the observations. In addition there may be *real* factors tending to affect the degree of clumping - for example, attraction or repulsion - which are of practical interest. It follows that we need a measure of clumping that minimizes the effects of the former factors. The following is one possible procedure. No doubt others could be devised, but it is doubtful that they would lead to essentially different conclusions.

(i). Define and measure the target area, A.
(ii). Count the total number of cells, N, within A.
(iii). Count the number of isolated non-touching cells, N_0, within A.
(iv). Compute $I_C = -\log[X/(X+1)]/\log(2)$, where

$$X = \frac{p}{1-p}\cdot\frac{1-R}{R}, \qquad p = \frac{N_0}{N}, \qquad R = exp(-4\pi r^2 N/A)$$

and r denotes the 'average' radius of a cell. Note that R is the expected proportion of isolated cells under the null hypothesis that cells are randomly distributed (Roach, 1968). Hence, I_C takes the value 0 if $N_0 = N$ (all cells are isolated), the value ∞ if $N_0 = 0$ (all cells are in clumps of two or more), and the value 1 if $N_0 = NR$ (proportion of isolated cells is equal to that expected under the null hypothesis that cells are randomly distributed). It can also be shown that under the null hypothesis $Var(I_C) \propto 1/(NR(1 - R))$. For a wide range of values of R, $R(1 - R)$ is reasonably constant and $Var(I_C)$ depends only on N. Note that the expected numbers under the null hypothesis are calculated on the assumption that all cells are circular and of equal radius. Although the results are fairly robust to this assumption, extreme deviations would require an alternative approach e.g. simulation. This would be the case if cells were very non-circular or varied widely in size and/or shape.

Experimental data

Each of two treatments (*wildtype diencephalon, Sey diencephalon*) was applied to each of two sources of embryonic brain tissue (*anterior, posterior*) from each of two strains of mice

(*wildtype, Sey*) at each of two ages (*13.5, 15.5* days), giving a total of $2 \times 2 \times 2 \times 2 = 16$ combinations of factors. For each combination measurements were taken on 5 explants on each of three different days (referred to as 'cultures'), giving a total of $16 \times 5 \times 3 = 240$ observations. Measurements were made by defining a series of concentric 'rings' of equal width surrounding each explant, measuring their area, and counting the numbers of touching and non-touching cells within each ring (Fig. 4.1). There was wide variation in the number of cell-containing rings surrounding explants (range 1-7, mean 3.83, SD 1.34). In some cases, it was possible to measure explants only over a 90° or 180° sector because their centre was located close to the edge of the image. However, the clumping index defined above should not be biased as a result of this. From a set of 20 randomly-selected cells, the mean cell area, πr^2, was estimated as 129.7 pixels for the purpose of calculating R (see above).

Analysis of data

Analysis of variance was applied, using the MINITAB 'GLM' module, with all 4 main factors (*treatment, position, strain, age*) fully crossed, with *culture* nested within main factors, and with *explant* nested within *culture*. The response variable (I_c) was weighted by N. The summary output is shown below and the conclusions can be summarized as follows: (1) there was a significantly (P=0.011) greater variation between *cultures* than between *explants* within *cultures;* hence, the between-*culture* variation was used as a basis for testing the significance of all main effects and their interactions; (2) with the exception of the difference between *strains*, which was highly significant (P< 0.0001), none of the other main effects nor any of the 2-, 3- or 4- way interactions was significant at the P=0.05 level. The analysis was repeated for the *13.5* day and *15.5* day data separately, with essentially the same conclusion - that only the *strain* difference was statistically significant (P<0.0001, in both analyses). Between-*culture* variation was significant at the 5% level at *13.5* days (P=0.028), but not at *15.5* days (P=0.073). The analysis was also repeated for each *strain* separately. There were no significant effects of *treatment, position* or *age* for either *strain*. However, the between-*culture* variation was significantly greater for the *Sey* strain than for the *wt* strain (128.84 vs 47.28, $F_{16,16} = 2.73$, P=0.026).

Analysis of Variance: Summary of Results

```
General Linear Model
Factor                  Type Levels Values
Age                     fixed      2 135 155
Pos                     fixed      2 A P
Str                     fixed      2 S W
Tre                     fixed      2 SD WD
Cult(Age Pos Str Tre)   fixed     48 1 2 3 1 2 3 1 2 3 1 2 3 1 2 3 1 2 3 1 2 3 1
                                     2 3 1 2 3 1 2 3 1 2 3 1 2 3 1 2 3 1 2 3 1 2
                                     3 1 2 3

Analysis of Variance for C2, using Adjusted SS for Tests

Source                  DF     Seq SS     Adj SS     Adj MS       F      P
Age                      1      26.08       0.02       0.02    0.00  0.986
Pos                      1       2.26      99.71      99.71    1.99  0.160
Str                      1    4087.01    3452.73    3452.73   68.91  0.000
Tre                      1      23.25       3.55       3.55    0.07  0.790
-------------------------------------------------------------------------
Age*Pos                  1       4.05      37.70      37.70    0.75  0.387
Age*Str                  1      25.84      34.49      34.49    0.69  0.408
Age*Tre                  1       1.71       4.10       4.10    0.08  0.775
Pos*Str                  1      41.63      51.88      51.88    1.04  0.310
Pos*Tre                  1      86.28       0.59       0.59    0.01  0.914
Str*Tre                  1      93.63     100.79     100.79    2.01  0.158
Age*Pos*Str              1     105.80      85.19      85.19    1.70  0.194
Age*Pos*Tre              1     144.18       4.81       4.81    0.10  0.757
Age*Str*Tre              1      17.50      60.63      60.63    1.21  0.273
Pos*Str*Tre              1      24.97      66.85      66.85    1.33  0.250
Age*Pos*Str*Tre          1     161.21     167.32     167.32    3.34  0.069
Cult(Age Pos Str Tre)   32    2818.01    2818.01      88.06    1.76  0.011
-------------------------------------------------------------------------
Error                  192    9620.82    9620.82      50.11
Total                  239   17284.23
```

Validation of model

Analysis of variance requires the assumption that the underlying response variable, weighted if necessary, is Normally distributed with uniform variance around the fitted model. This was tested by examination of the residuals (weighted by $\sqrt{N}$), which was satisfactory. This justifies the rather complicated transformation of X used in defining I_c. The model also assumes that the response variable is insensitive to the number of concentric rings used to compute I_c for each explant. This was tested by fitting the number of rings as a covariate in the analysis of variance (essentially what is being tested is whether there was any linear trend between I_c and the number of rings, after fitting the remaining terms of the model). The effect was found to be non-significant ($P>0.5$). Finally, the weighted residuals were found to show no trend in mean or variance with either $R(1-R)$ or N, indicating that the weighting used was appropriate.